I. PEREPECHKO

LOW-TEMPERATURE PROPERTIES OF POLYMERS

LOW-TEMPERATURE PROPERTIES OF POLYMERS

I. PEREPECHKO
Moscow Automotive Engineering Institute

Translated from the Russian by
A. BEKNAZAROV

MIR PUBLISHERS
Moscow

PERGAMON PRESS
Oxford · New York · Toronto · Sydney · Paris · Frankfurt

U.K.	Pergamon Press Ltd., Headington Hill Hall, Oxford OX3 OBW, England
U.S.A.	Pergamon Press Inc., Maxwell House, Fairview Park, Elmsford, New York 10523, U.S.A.
CANADA	Pergamon of Canada, Suite 104, 150 Consumers Road, Willowdale, Ontario, M2J 1P9, Canada
AUSTRALIA	Pergamon Press (Aust.) Pty. Ltd., PO Box 544, Potts Point, N.S.W. 2011, Australia
FRANCE	Pergamon Press SARL, 24 rue des Ecoles, 75240 Paris, Cedex 05, France
FEDERAL REPUBLIC OF GERMANY	Pergamon Press GmbH, 6242 Kronberg-Taunus, Hammerweg 6, Federal Republic of Germany

---

© Издательство «Химия», 1977

© English translation, Mir Publishers, 1980

All Rights Reserved. No part of this publication may be reproduced, stored in a retrieval system or transmitted in any form or by any means: electronic, electrostatic, magnetic tape, mechanical photocopying, recording or otherwise, without permission in writing from the copyright holder

First edition 1980

British Library Cataloging in Publication Data

Perepechko, Igor' Ivanovich
Low-temperature properties of polymers.
1. Polymers and polymerization—Thermal properties
2. Low temperatures
I. Title
547'.84 QD381 80-40137

ISBN 0 08 025301 6

Translated from 'Svoistva polimerov pri nizkikh temperaturakh' published by Khimiya Publishers, Moscow, 1977

PREFACE

One of the features of the vigorous development of a number of branches of modern technology in recent years has been the ever increasing interest in the properties of polymeric materials at low temperatures, including the liquid-helium temperature. The investigation of polymers at low temperatures is of great importance for an understanding of a number of the most important problems in the physics and physical chemistry of polymers.

In spite of a large number of publications devoted to the study of the physical properties of polymers in the cryogenic (low-temperature) region, it is sometimes difficult, even for the specialist, to obtain information on the most important properties of polymers at very low temperatures. This is because the data on the individual properties of polymers are scattered throughout the scientific journals and are sometimes difficult to compare.

The purpose of this book is to systematize the available material and to delineate the principal trends in the investigation of those closely interrelated properties—thermal (heat capacity, thermal conductivity, thermal expansion), acoustical, dielectric, viscoelastic, etc.—which govern the entire set of important physical properties of polymers at low temperatures. An attempt is made to show how the chemical constitution and the supermolecular structure influence the physical properties of polymers in the low-temperature region.

All the chapters of this book, except the last two, are organized according to the same plan. Each chapter, devoted to a single physical property, consists of three sections. First, the theory of the property under discussion and the related physical phenomena are briefly considered. This is followed by a description of methods of investigation of these properties and phenomena at low temperatures. Finally, systematized data from experimental investigations are presented.

The last three chapters are concerned mainly with studies of the properties of polymers at low temperatures which have been carried out in recent years by the author and his collaborators P.D. Golub and V.E. Sorokin.

The author wishes to express his sincere gratitude to L.A. Kvacheva, O.V. Startsev, and E.B. Voloshinov for their help in preparing the manuscript.

CHAPTER 1

HEAT CAPACITY OF POLYMERS AT LOW TEMPERATURES

1.1. BASIC CONCEPTS OF THE HEAT CAPACITY OF SOLIDS

Heat capacity is one of the most important thermal characteristics of substances. Most frequently the heat capacity of a system is considered at constant volume, C_v, which is substantially dependent on temperature.

The molar heat capacity of a solid at constant volume, C_v, is defined by the expression

$$C_v = \left(\frac{\partial U_m}{\partial T} \right)_v \tag{1.1}$$

where U_m is the internal energy of 1 mole of substance; T is the temperature; v is the molar volume.

We know that a solid consists of atoms which oscillate about an equilibrium position. In the classical approximation, the atoms of a solid may be regarded as harmonic oscillators. This means that the oscillating atoms experience forces of interaction that obey Hooke's law, i.e., the forces that are proportional to the relative departure of the atoms from their mean equilibrium positions.

We know that the average energy of a simple one-dimensional harmonic oscillator, $\bar{E}_1$, depends only on temperature:

$$\bar{E}_1 = kT \tag{1.2}$$

where $k = 1.38 \times 10^{-23}$ J/K is the Boltzmann constant.

The Boltzmann constant is defined as the ratio $k = R/N_0$, where R is the universal gas constant [$R = 8.31$ J/(mole·K)], and N_0 is Avogadro's number ($N_0 = 6.023 \times 10^{23}$ mole^{-1}). One mole of a solid substance can be treated as a system of $3N_0$ simple one-dimensional harmonic oscillators. The internal energy of such a system is given by

$$U_m = 3N_0kT = 3RT \tag{1.3}$$

From expression (1.1) it follows that the molar heat capacity of a solid is

$$C_v = 3R \approx 0.025 \text{ kJ/(mole}\cdot\text{K)} \tag{1.4}$$

Expression (1.4) is the well-known Dulong-Petit law, which is in good agreement with the values of C_v found experimentally for many solids over a wide range of temperatures, up to quite high temperatures.

It has, however, been found that at low temperatures the heat capacity of solids depends on temperature, which contradicts the Dulong-Petit law, and that with a considerable decrease of temperature, when $T \to 0$, the heat capacity of non-metallic solids varies proportionately to T^3. This result cannot be explained within the framework of the classical theory. One of the first to pay attention to this was Einstein (1, 2).

Einstein's Theory. Einstein attempted to account for a sharp decrease in the heat capacity of solids at low temperatures (at $T \to 0$) by proceeding from a simple model. In order to explain thermal properties at low temperatures, Einstein suggested that the crystal lattice of a solid containing N vibrating atoms be regarded as a system of $3N$ independent one-dimensional harmonic oscillators, each with the same characteristic vibrational frequency, ν. The Einstein harmonic oscillators differ from classical harmonic oscillators, since while a classical harmonic oscillator can have any vibration amplitude and, hence, any energy, Einstein's quantum harmonic oscillators can have only strictly defined, discrete energy values. The magnitude of this energy is given by the Planck formula:

$$E = nh\nu \tag{1.5}$$

where $n = 0, 1, 2, \ldots$ (positive integers); h is Planck's constant ($h \approx 6.62 \times 10^{-34}$ J · s); ν is the frequency.

Formula (1.5) is sometimes written in the form:

$$E = n\hbar\omega \tag{1.6}$$

where $\omega = 2\pi\nu$ is the circular frequency; $\hbar = h/2\pi$.

Thus, a quantum harmonic oscillator can have only quantized energy values which differ by the value of n. In accordance with quantum theory, the average energy of a harmonic oscillator can be represented in the following form:

$$\bar{E}_1 = \frac{\sum\limits_{n=0}^{\infty} n\hbar\omega e^{-\frac{n\hbar\omega}{kT}}}{\sum\limits_{n=0}^{\infty} e^{-\frac{n\hbar\omega}{kT}}} = \frac{\hbar\omega\left(e^{-\frac{\hbar\omega}{kT}} + 2e^{-2\frac{\hbar\omega}{kT}} + \ldots\right)}{\left(1 + e^{-\frac{\hbar\omega}{kT}} + e^{-\frac{2\hbar\omega}{kT}} + \ldots\right)} \tag{1.7}$$

Expression (1.7) can be transformed so that

$$\bar{E}_1 = \frac{\hbar\omega}{e^{\frac{\hbar\omega}{kT}} - 1} \tag{1.8}$$

A comparison of expressions (1.8) and (1.2) shows that the average energies of quantum and classical harmonic oscillators are substantially different. Note that expression (1.8) is more general. From this expression we can derive, as a special case, an expression for the average energy of a classical harmonic oscillator. Indeed, at high temperatures, when $kT \gg \hbar\omega$, the denominator in expression (1.8) can be expanded into a series:

$$e^{\frac{\hbar\omega}{kT}} - 1 = 1 + \frac{\hbar\omega}{kT} + \ldots - 1 \approx \frac{\hbar\omega}{kT}$$

Thus, at high temperatures expression (1.8) has the form

$$\bar{E}_1 \approx kT$$

The heat capacity of a system of N identical quantum harmonic oscillators can be written thus:

$$C = \frac{\partial U}{\partial T} = \frac{\partial (N\bar{E}_1)}{\partial T} = Nk\left(\frac{\hbar\omega}{kT}\right)^2 \frac{e^{\frac{\hbar\omega}{kT}}}{\left(e^{\frac{\hbar\omega}{kT}} - 1\right)^2} \tag{1.9}$$

Expression (1.9) can also be written in a somewhat different form if one makes use of the concept of the characteristic Einstein temperature θ_E, which is defined by the equation

$$\theta_E = \hbar\omega/k \tag{1.10}$$

For most solids the characteristic temperature, θ_E, is equal to about 100-300 K. From formula (1.10) it follows that at $T = 300$ K the characteristic frequency $\nu = \omega/2\pi = kT/h \approx 5 \times 10^{12}$ Hz. This frequency approximately corresponds to the vibrational frequency of individual atoms. In view of formula (1.10), the expression for heat capacity (1.9) can be written as follows:

$$C = Nk\left(\frac{\theta_E}{T}\right)^2 \frac{e^{\theta_E/T}}{\left(e^{\theta_E/T} - 1\right)^2} = NkE\left(\frac{\theta_E}{T}\right) \tag{1.11}$$

where $E\left(\frac{\theta_E}{T}\right)$ is the Einstein function defined as

$$E\left(\frac{\theta_E}{T}\right) = \left(\frac{\theta_E}{T}\right)^2 \frac{e^{\theta_E/T}}{\left(e^{\theta_E/T} - 1\right)^2} \tag{1.11a}$$

Formula (1.11) describes well the temperature dependence of the heat capacity of some solids.

In the case of low temperatures, when $T \to 0$ ($kT \ll \hbar\omega$) and $T \ll \theta_E$, from formula (1.11) it follows that

$$C \approx Nk\left(\frac{\theta_E}{T}\right)^2 e^{-\theta_E/T} \tag{1.12}$$

It is obvious that the largest contribution to the temperature dependence of heat capacity at $T \to 0$, according to the Einstein theory, is made by the exponential factor. From formula (1.12) we see that at low temperatures the heat capacity must decrease according to the exponential law. Numerous experimental data, however, indicate that the heat capacity of the crystal lattice of most solids at $T \to 0$ varies proportionately to T^3. This fact has been accounted for in the Debye theory.

Debye's Theory of the Heat Capacities of Solids. The Einstein postulate that all atoms may be regarded as harmonic oscillators vibrating with the same frequency would have been satisfactory if each atom had vibrated independently of its neighbours. In actual fact, the atoms of a solid are so firmly bound with one another that most probably they vibrate as an entity. Debye proposed that a solid be treated as an elastic continuum and derived an expression for vibrational frequencies that would be present in such a system. The discrete nature of the crystal lattice and its atomic structure were taken into account only by way of limiting the number of possible vibrational frequencies in the lattice to the $3N$ degrees of freedom of the N atoms making up the crystal lattice. Debye suggested that the acoustical spectrum of a solid be regarded as the spectrum of an isotropic elastic continuum, but that the number of independent elastic waves that arise as a result of the oscillations of N lattice atoms be assumed to be equal to $3N$. It is known that in an isotropic elastic continuum for each wave vector $\bar{k}$ there correspond one longitudinal wave and two transverse waves with speeds independent of the direction of their propagation.

The internal energy in Debye's theory is defined by the following expression:

$$U = \frac{3k^4T^4}{2\pi^2\hbar^3\bar{c}^3} \int_0^{x_m} \frac{x^3\,dx}{e^x - 1} \tag{1.13}$$

where $\bar{c}$ is the average velocity of elastic waves; $x_m = \hbar\omega_m/kT$ (here ω_m is the upper boundary maximum frequency of lattice vibrations, which is governed by the condition that the number of possible lattice vibrations is equal to $3N$).

From Debye's theory it follows that

$$\omega_m = \bar{c}\sqrt[3]{6\pi^2\frac{N}{V}} \tag{1.14}$$

where N is the number of atoms in volume V; $\bar{c}$ is the average speed of elastic waves in an isotropic elastic solid.

$$\bar{c}=\left[\frac{1}{3}\left(\frac{2}{c_t^3}+\frac{1}{c_l^3}\right)\right]^{-1/3} \tag{1.15}$$

in which expression the quantities c_t and c_l are the average speeds of transverse and longitudinal elastic waves, respectively.

We now introduce the notation

$$\hbar\omega_m/k=\theta_D \tag{1.16}$$

The parameter θ_D is called the Debye characteristic temperature and plays an important part in the consideration of the thermal properties of a solid. From expressions (1.14) through (1.16) it follows that

$$\theta_D=\frac{h}{k}\left(\frac{3N}{4\pi V}\right)^{1/3}\left[\frac{1}{3}\left(\frac{2}{c_t^3}+\frac{1}{c_l^3}\right)\right]^{-1/3} \tag{1.17}$$

Differentiating the expression for the internal energy with respect to temperature, we obtain the following expression for heat capacity at constant volume (3, 4):

$$C_v=9N_1k\left(\frac{T}{\theta_D}\right)^3\int\limits_0^{x_m}\frac{e^x x^4\,dx}{(e^x-1)^2} \tag{1.18}$$

where $N_1=N/V$ is the number of atoms in unit volume.

The expression for heat capacity can be written in a different form:

$$C_v=3N_1kD\left(\frac{\theta_D}{T}\right) \tag{1.19}$$

where $D\left(\frac{\theta_D}{T}\right)$ is the Debye function equal to

$$D\left(\frac{\theta_D}{T}\right)=3\left(\frac{T}{\theta_D}\right)^3\int\limits_0^{\frac{\theta_D}{T}}\frac{\left(\frac{\theta_D}{T}\right)^4 e^{\theta_D/T}}{\left(e^{\theta_D/T}-1\right)^2}\,d\left(\frac{\theta_D}{T}\right) \tag{1.20}$$

The Debye function cannot be calculated accurately and therefore use is made of various approximations. Approximate methods of calculation are considerably simplified in the case of high ($T\gg\theta_D$) and very low ($T\ll\theta_D$) temperatures.

At $T\gg\theta_D$ ($x_m\ll 1$), from expression (1.18) we have

$$C_v\approx 3R \tag{1.21}$$

which is in good accord with the Dulong-Petit law.

At very low temperatures, when $T\ll\theta_D$ (at $T<\theta_D/12$), from expression (1.18) we can obtain, with an accuracy of up to

1 per cent, the following expression for heat capacity:

$$C_v = \frac{12\pi^4 N_0 k}{5}\left(\frac{T}{\theta_D}\right)^3 = \frac{12}{5}\pi^4 R\left(\frac{T}{\theta_D}\right)^3 \qquad (1.22)$$

This formula is the well-known Debye cube law. It agrees well with experimental data for a large number of solids. The question of the limits of applicability of Debye's equation has not, however, been resolved completely. In fact, formula (1.22) is in good agreement with experimental data not at $T < \theta_D/12$ but at much lower temperatures (5). The heat capacity of real solids is usually described well by Debye's equation only at $T \leqslant \theta_D/50$ and sometimes at $T \leqslant \theta_D/100$. For polymers the Debye T-cube law holds, as a rule, only in a very narrow range of temperatures only a few degrees above 0 K.

The good agreement between Debye's theory and experimental data at very low temperatures is ascribed to the fact that at $T \to 0$ K the crystal lattice experiences oscillations of sufficiently long wavelength, much larger than the lattice parameters.

It should be noted that Debye's theory has a number of shortcomings. For instance, it assumes that all the elastic waves in the lattice travel at the same speed. The dispersion law used in the derivation of relation (1.22) has the form $\omega = \bar{c}k$, where $k = 2\pi/\lambda$ is the wavenumber. Thus, Debye's theory disregards the dispersion (frequency dependence) of the speed of elastic waves. In accordance with this, in Debye's theory it is assumed that the limiting maximum frequency ω_m for all the waves excited in the lattice is the same, which does not conform with the actual picture observed in real solids. Moreover, the Debye theory ignores the complex nature of the interaction between the atoms and molecules of which the solid is composed.

Thus, the Debye theory is concerned with the complicated motion of the mass centres of the interlinked N elements of the lattice. This complex motion (lattice oscillations) is assumed to be equivalent to the motion of $3N$ independent one-dimensional harmonic oscillators. The coordinates of these oscillators are called the normal coordinates and their oscillations are known as the normal vibrations. The internal energy and heat capacity of a solid are additively composed of the contributions from individual normal vibrational modes. To calculate the heat capacity (to derive the formula describing the dependence of heat capacity on temperature), it is necessary to know the frequency spectrum of normal vibrations. This spectrum can be computed theoretically by making use of the so-called secular equation. In the case of a simple lattice, the solution of the secular equation contains three frequency branches (acoustical branches) which correspond to three possible independent orientations of the vector of polarization of lattice waves, i.e., to three types of elastic waves excited in the lattice (two transverse waves and one longitudinal wave). The simplicity of the Debye equation results from a number of simplifications made in its derivation.

The atomic structure of solids has been taken into considerably greater account in the theory of heat capacity proposed by Born and von Kármán (6). In this theory, a solid is regarded as a lattice consisting of point masses interconnected by springs. Born and von Kármán not only considered the action of central forces but also made an attempt to take into account the forces operating between atoms at greater distances. They showed that in the case of the simplest model, which is a one-dimensional chain with central forces acting between the nearest neighbouring atoms (nearest-neighbour forces), the Debye assumption that no dispersion of the speeds of elastic waves is present is not valid. The Born-Kármán theory takes into account that the maximum frequency ω_m (the cutoff frequency of the spectrum of normal vibrations) must be different for each elastic wave in each direction. The theory allows the calculation of the theoretical dependence of heat capacity if the model of interatomic forces is known. In a number of simple cases theoretical computations are in good agreement with the results of experimental investigations. But calculation of the frequency spectrum, which must be known if one wishes to derive a general formula for heat capacity appears to be a very difficult task. For this to be done, one has to know all the force constants and the interaction potential between atoms. Even then the solution of the secular equation is found to be rather involved. Besides, in real solids one has to deal with complex lattices. If the unit cell of such a lattice consists of n structural elements, one must add to the acoustical branches that result from the solution of the secular equation $3(n-1)$ optical branches, which under certain conditions are separated from one another and from the acoustical branches by energy gaps. All this considerably complicates the calculation of the spectrum of normal vibrations.

In view of this, the Debye theory is used most frequently in the study of the thermal properties of solids at low temperatures.

In Debye's theory it is assumed that the energy of each normal mode of vibration, E_i, is quantized:

$$E_i = n_i \hbar \omega_i \tag{1.23}$$

where n_i are whole numbers.

Thus, each normal mode of vibration (or each elastic wave) may be treated in the Debye theory like a quasi-particle characterized by strictly defined, discrete values (quanta) of energy. From the standpoint of quantum theory, normal lattice vibrations (the Debye elastic waves) may be regarded as quasi-particles which are energy quanta of the field of elastic vibrations, that is, phonons. Thus, in the quantum theory of heat capacity, lattice oscillations are treated as the phonon gas, which also leads to the Debye equation.

By analogy with the kinetic theory of gases, solid-state quantum theory deals with such concepts as the mean free path, the interaction of phonons, etc. The concept of the elastic waves in the lattice being quasi-particles (phonons), a concept which appeared as the result of the development of the Debye theory of heat capacity, has proved fruitful and is widely used in modern solid-state physics. It will be shown later that many phenomena that appear in polymers at low temperatures are phononic in nature.

1.2. BASIC CONCEPTS OF THE HEAT CAPACITY OF POLYMERS

According to Debye's theory, formula (1.22) should be valid for solids at $T < \theta_D/12$. The results of experimental investigations of the heat capacities of polymers at low temperatures (7) show, however, that, even with this condition being fulfilled, above 5-10 K the Debye equation fails to describe the temperature dependence of C_v even qualitatively. This is associated with the neglect in the Debye theory of the anisotropy of the forces of interatomic interaction in polymeric chains. One of the first theories of heat capacity that could be used to describe the thermal properties of polymers has been proposed by Tarasov (8).

The Tarasov Theory. Tarasov (8-12) applied the basic propositions of Debye's theory, which holds for an isotropic elastic continuum (a three-dimensional continuum), to one-dimensional and two-dimensional continuous media.

In the Debye approximation for a three-dimensional lattice the distribution function of natural frequencies, $\varphi(\nu)$, may be written in the form:

$$\varphi(\nu) = 9N\nu_m^{-3}\nu^2 \tag{1.24}$$

Thus, the distribution function of the frequencies of normal vibrations in a three-dimensional lattice is directly proportional to the square of the frequency ν. The number ds_3 of natural vibrations of a lattice or a three-dimensional continuum in the frequency range ν to $\nu + d\nu$ is given by the expression

$$ds_3 = \varphi(\nu)\,d\nu = 9N\nu_m^{-3}\nu^2 d\nu \tag{1.25}$$

Tarasov found that in the case of a two-dimensional continuum, i.e., a planar or surface network of atoms (a vibrating membrane can be used as an analogy), the number of natural vibrations, ds_2, between frequencies ν and $\nu + d\nu$ will be equal to

$$ds_2 = 6N\nu_m^{-2}\nu d\nu \tag{1.26}$$

With a one-dimensional continuum, i.e., an elastic rod, which represents, to a certain extent, an oscillating chain of atoms in the Tarasov theory, the number of natural vibrations between frequencies ν and $\nu + d\nu$ equals

$$ds_1 = 3N\nu_m^{-1}\, d\nu \tag{1.27}$$

In Debye's theory, the number of natural vibrations in the lattice is brought into agreement with the total number of vibrational degrees of freedom ($3N$) of a system consisting of N one-dimensional harmonic oscillators by using the relation

$$\int_0^{\nu_m} \varphi(\nu)\, d\nu = 3N \tag{1.28}$$

where $\varphi(\nu)$ is defined by expression (1.24).

Hence, for a three-dimensional continuum

$$\int_0^{\nu_m} ds_3 = 3N \tag{1.28a}$$

By analogy, in the Tarasov theory we also have

$$\int_0^{\nu_{1m}} ds_1 = 3N \quad \text{and} \quad \int_0^{\nu_{2m}} ds_2 = 3N$$

In this case, $3N$ is the total number of vibrational degrees of freedom for a chain or layer.

In a general case, expressions (1.25) through (1.27) may be written in the following form:

$$ds_m = 3mN\nu_m^{-m}\nu^{m-1}\, d\nu \tag{1.29}$$

where ds_m is the total number of natural modes of vibration in the interval $d\nu$ for an m-dimensional continuum ($m = 3$ in the case of a lattice; $m = 2$ for a layer; and $m = 1$ for a chain).

Using formula (1.29) and expression (1.8) for the average energy of a quantum harmonic oscillator, $\bar{E}_1$, we obtain for the total vibrational energy of the m-dimensional continuum:

$$U_m = \int_0^{\nu_m} \bar{E}_1\, ds_m \tag{1.30}$$

In turn, the vibrational heat capacity of the m-dimensional continuum is equal to

$$C_m = \frac{\partial U_m}{\partial T} = \frac{\partial}{\partial T} \int_0^{\nu_m} \bar{E}_1 \, ds_m \qquad (1.31)$$

Substituting expression (1.8) into formulas (1.30) and (1.31) and taking cognizance of relation (1.16), we obtain an equation for vibrational energy (8):

$$U_m = 3mR \frac{T^{(m+1)}}{\theta_m^m} \int_0^{\nu_m} \frac{x^m \, dx}{e^x - 1} \qquad (1.32)$$

Making use of expression (1.32) for the case of $m = 3$ (a three-dimensional continuum), Tarasov derived the usual expressions (1.18) through (1.20), which follow from the Debye theory.

For the case of $m = 2$ (a two-dimensional continuum) the following expression obtains for the heat capacity:

$$C_v = 3N_1 k D_2 \left(\frac{\theta_2}{T} \right) \qquad (1.33)$$

where $D_2\,(\theta_2/T)$ is the Debye two-dimensional function. This function is defined as

$$D_2 \left(\frac{\theta_2}{T} \right) = 2 \left(\frac{T}{\theta_2} \right)^2 \int_0^{\theta_2/T} \frac{\left(\frac{\theta_D}{T} \right)^3 e^{\frac{\theta_D}{T}}}{\left(e^{\theta_D/T} - 1 \right)^2} \, d \left(\frac{\theta_2}{T} \right) \qquad (1.34)$$

For a one-dimensional continuum ($m = 1$)

$$C_v = 3N_1 k D_1 \left(\frac{\theta_1}{T} \right) \qquad (1.35)$$

where θ_1 is the characteristic temperature (for $m = 1$); $D_1\,(\theta_1/T)$ is the Debye one-dimensional function.

$$D_1 \left(\frac{\theta_1}{T} \right) = \frac{T}{\theta_1} \int_0^{\theta_1/T} \frac{\left(\frac{\theta_1}{T} \right)^2 e^{\theta_1/T}}{\left(e^{\theta_1/T} - 1 \right)^2} \, d \left(\frac{\theta_1}{T} \right) \qquad (1.36)$$

Using the approximate values of the integrals at $\theta_m/T \gg 1$, the equations for the heat capacities of chains, layers, and lattices can be represented in the form (8):

$$C_1 = \pi^2 R \left(\frac{T}{\theta_1} \right) \qquad (1.37)$$

$$C_2 = 43.272 R \left(\frac{T}{\theta_2} \right)^2 \qquad (1.38)$$

$$C_3 = \frac{12}{5} \pi^4 R \left(\frac{T}{\theta_3} \right)^3 \qquad (1.39)$$

The characteristic temperatures θ_1 and θ_2 are connected with the Debye temperature $\theta_D = \theta_3$ by the relations $\theta_1 = 1.5\,\theta_3$ and $\theta_2 = 1.125\,\theta_3$.

Equations (1.37) and (1.38) have been specifically derived for describing the temperature dependence of the heat capacities of solids whose structures are built of chains or layers of very strongly bonded atoms, with, say, the bonds of principal valences. This is on the condition that the interaction between chains or between layers themselves is weaker (for example, the interaction due to van der Waals forces). This version of the heat-capacity theory proposed by Tarasov has come to be known as the theory of non-interacting chains or layers.

An essential feature of the equations given above, (1.33), (1.35) and (1.37), (1.38), is that they are intended for the calculation of the heat capacities of solids having a lamellar or chain (as in the case of polyethylene) structure, in which the forces of interaction between layers or chains are several orders of magnitude lower than in the plane of the layers or along the chains. In the region of very low temperatures, at which the effect of the weak forces of interaction between layers or chains is manifested, the lengths of Debye waves (elastic waves arising in the lattice due to the thermal vibrations of atoms) are still sufficiently great as compared with the distances between the structural elements of the lattice. Here the distribution function of the natural vibrational frequencies of the lattice, $\varphi(\nu)$, (the spectrum distribution density) is proportional to ν^2 and is defined by expression (1.24). Therefore, the heat capacity of solids possessing a lamellar or chain structure at very low temperatures obeys the Debye T-cube law (the Debye third power law).

As the temperature rises there will come a time when the interaction between layers or chains begins to play a secondary role. The frequency distribution in the vibrational spectrum of such solids degenerates more and more into the frequency distributions typical for a monomolecular layer or a one-dimensional chain.

This change in the character of the temperature dependence of heat capacity has been considered in a more systematic way by Tarasov in a theory of heat capacity which takes into account the interaction of chains and layers. In order to take into account all the intermediate conditions, in addition to the limiting cases of the weak interaction, which may be neglected as compared with the interaction inside the chains and layers, Tarasov assumed that in a situation of interacting chains not all the $3N$ modes of vibration, whose frequencies are in the range from ν_m to 0, are distributed by the law of the linear continuum [Eq. (1.27)]; only a certain number ($3N_1$), corresponding to the frequencies between ν_m and ν_1, are. Then for a one-dimensional continuum we obtain instead of Eq. (1.27):

$$ds'_1 = 3N_1 (\nu_m - \nu_1)^{-1} d\nu \tag{1.40}$$

In this case, instead of expressions (1.28) and (1.28a), we must write:

$$\int_{\nu_1}^{\nu_m} ds'_1 = 3N_1 \tag{1.41}$$

The parameter ν_1 is the limiting vibrational frequency of an atom of a given chain in the force field of surrounding chains. Here it is assumed that the vibrations, to which there correspond frequencies lower than ν_1 (i.e., from 0 to ν_1), are distributed not by the law of the linear continuum [Eq. (1.40)] but by the Debye law for a three-dimensional continuum, which in this particular case takes the form:

$$ds_3 = 9N_2\nu_1^{-3}\nu^2 d\nu \tag{1.42}$$

Obviously, the total number of atoms in the system under consideration is $N = N_1 + N_2$. It follows that the total number of vibrational degrees of freedom of N_2 atoms for which relation (1.42) holds true is determined by the following expression:

$$\int_{0}^{\nu_1} ds_3 = 3N_2 \tag{1.43}$$

Tarasov (8) gives the following expression for the vibrational energy, $U_{1(3)}$, of interacting chains:

$$U_{1(3)} = \frac{3N}{\nu_m} \int_0^{\nu_m} \frac{h\nu}{e^{\frac{h\nu}{kT}} - 1} d\nu + \frac{9N}{\nu_1^2 \nu_m} \int_0^{\nu_1} \frac{(h\nu)^3}{e^{\frac{h\nu}{kT}} - 1} d\nu \tag{1.44}$$

Making the substitutions $h\nu/kT = x$ and $h\nu_1/k = \theta_1$ in Eq. (1.44), we obtain the following formula for the heat capacity of interacting chains:

$$C_{1(3)} = \overline{D}_1\left(\frac{\theta_1}{T}\right) - \frac{\theta_3}{\theta_1}\left[\overline{D}_1\left(\frac{\theta_3}{T}\right) - \overline{D}_3\left(\frac{\theta_3}{T}\right)\right] \tag{1.45}$$

where $\overline{D}_1$ is the heat-capacity function of a linear continuum for non-interacting chains; $\overline{D}_3$ is the ordinary heat-capacity function.

The expression for the heat capacity of interacting layers, $C_{2(3)}$, is deduced in an analogous way:

$$C_{2(3)} = \overline{D}_2\left(\frac{\theta_2}{T}\right) - \left(\frac{\theta_3}{\theta_2}\right)^2 \left[\overline{D}_2\left(\frac{\theta_3}{T}\right) - \overline{D}_3\left(\frac{\theta_3}{T}\right)\right] \tag{1.46}$$

where $\overline{D}_2$ is the heat-capacity function of non-interacting layers.

From Eqs. (1.45) and (1.46) it follows that the temperature dependence of the heat capacity of a system consisting of interacting layers or interacting chains can be expressed in terms of the characteristic temperatures θ_1 and θ_2 that determine the spectrum of "internal" vibrations of the chains or layers. In calculations, use is also made of the characteristic temperature θ_3 which takes into account the interaction of these vibrations.

At very low temperatures Eqs. (1.45) and (1.46) lead to a cubic dependence of heat capacity on temperature. Indeed, at $T \rightarrow 0$

$$\bar{D}_1\left(\frac{\theta}{T}\right)=\pi^2 R\left(\frac{T}{\theta}\right) \qquad (1.47)$$

$$\bar{D}_2\left(\frac{\theta}{T}\right)=43.272 R\left(\frac{T}{\theta}\right)^2 \qquad (1.48)$$

$$\bar{D}_3\left(\frac{\theta}{T}\right)=\frac{12}{5}\pi^4 R\left(\frac{T}{\theta}\right)^3 \qquad (1.49)$$

Substituting expressions (1.47) through (1.49) into Eqs. (1.45) and (1.46), we get:

$$\underset{T\rightarrow 0}{C_{1(3)}}=\frac{\theta_3}{\theta_1}\cdot\frac{12}{5}\pi^4 R\left(\frac{T}{\theta_3}\right)^3=\frac{12}{5}\pi^4 R\left(\frac{T}{\theta_{1,3}}\right)^3 \qquad (1.50)$$

$$\underset{T\rightarrow 0}{C_{2(3)}}=\left(\frac{\theta_3}{\theta_2}\right)^2\cdot\frac{12}{5}\pi^4 R\left(\frac{T}{\theta_3}\right)^3=\frac{12}{5}\pi^4 R\left(\frac{T}{\theta_{2,3}}\right)^3 \qquad (1.51)$$

where

$$\theta_{1,3}=\theta_1^{1/3}\theta_3^{2/3} \quad \text{and} \quad \theta_{2,3}=\theta_3^{1/3}\theta_2^{2/3}$$

From the equations given above it follows that with a substantial difference between the characteristic temperatures, when $\theta_1/\theta_3 \gg 1$ (or when $\theta_2/\theta_3 \gg 1$) there may exist such a temperature region in which C_v is proportional to T (for chains) and C_v is proportional to T^2 (for layers), since the bracketed differences in Eqs. (1.45) and (1.46) are then sufficiently small. When the temperature is even lower, we see a departure from the dependences $C_v \propto T$ and $C_v \propto T^2$, respectively, and the heat capacity begins to be dependent on temperature according to the T-cube law. Evidently, when the ratio θ_3/θ_1 changes from 0 to 1, there are possible all kinds of dependences of heat capacity on temperature that lie between the functions $C_1 \propto T$ (for the case of non-interacting chains) and the Debye law $C \propto T^3$.

One can hardly expect, however, that the temperature dependence of heat capacity can be fully described by the above equations which take into account the presence of linear or two-dimensional structures with a weak or strong interaction. Just as in the case of the use of the ordinary Debye equation, the spectrum of normal vibrations of a continuum is sometimes combined with one or more vibration frequencies of side groups. Tarasov (8) noted in 1950 that the temperature dependence of the heat capacity of organic polymers can be described by combining the relations derived by him, (1.45) and (1.46) or (1.33) and (1.35), with the Einstein functions for the characteristic frequencies of side groups.

Wunderlich (13) and later Tucker and Rees (14) made use of the Tarasov theory for describing the temperature dependence of the heat capacity of a number of polymers and showed that this theory is in good agreement with experimental data. Later, however, Baur (7) noted that it remained unclear to what extent this agreement derives from the correctness of the choice of the physical model, since the Tarasov theory, while enabling sufficiently accurate calculations of the spectrum of valence vibrations in the low-frequency region, disregards the spectrum of deformation vibrations.

The Tarasov theory has also been criticized by Lifshitz (15).

The Lifshitz Theory. Lifshitz (15, 16) focused his attention on the fact that Tarasov had ignored some important points arising from the unusual law of dispersion of elastic flexural waves in the limiting case of non-interacting chains and layers. Lifshitz (15) considered anew the question of the dispersion law for the long-wave part of the vibrational spectrum of a lamellar crystal as a whole, using an approximation which, as well as the equations of the theory of elasticity of a strongly anisotropic body, also takes into account the transverse rigidity of atomic layers or chains.

In the case of crystalline structures, which are systems of weakly interlinked lamellae or chains, dispersion laws other than the Debye and Tarasov theories were used for elastic waves. For waves that propagate in non-interacting chains the following relations were applied:

$$\omega_3 = ck_z \text{ (longitudinal waves)} \tag{1.52}$$

$$\omega_{1,3} = \gamma k_z^2 \text{ (flexural waves)} \tag{1.53}$$

where the z axis coincides with the chain axis; c is the velocity of elastic waves; k_z is the projection of the wave vector onto the z axis; $\gamma = a\bar{v}/\pi$ (a is the interatomic distance in the chain; $\bar{v}$ is the "transverse rigidity" of the chain, a dimensionless parameter).

Taking into account the contributions of both longitudinal and flexural waves to the energy, Lifshitz obtained an expression for the heat capacity of non-interacting chains:

$$C_1 = Nk\gamma_1 \left(\frac{T}{\theta_1}\right)^{1/2} \left[1 + \gamma_2 \left(\frac{T}{\theta_1}\right)^{1/2}\right] \tag{1.54}$$

where $\gamma_1 \approx (2.3/\sqrt{\bar{v}})$; $\gamma_2 \approx \sqrt{\bar{v}}$; θ_1 is the "longitudinal" Debye temperature.

At low temperatures, when $T \ll \theta$, the heat capacity is equal to

$$C_1 = Nk\gamma_1 \left(\frac{T}{\theta_1}\right)^{1/2} \tag{1.55}$$

Thus, unlike Tarasov, who predicts for this case a linear dependence of heat capacity on temperature [Eq. (1.37)], Lifshitz found that C_1 is proportional to $\sqrt{T}$. For the case of non-interacting layers at $T \ll \theta$ he uses the following relation (15):

$$C_2 = \frac{Nk\pi}{12} \frac{T(a')^2}{\hbar\gamma} \propto Nk\frac{T}{\theta_2} \tag{1.56}$$

where $(a')^2$ is the area of a unit cell in the plane of the layer; $\gamma = c\,a'$; $\theta_2 = \pi\hbar c/ka'$.

Thus, in the case of interacting layers as well the Lifshitz theory leads to dramatically different results as compared with the Tarasov theory [see Eq. (1.38)].

In order to describe real chain and lamellar structures an attempt has been made (15) to take into account the interaction between chains (or layers). For this purpose, use was made of the law of dispersion of elastic waves in a crystal (17) in which the interaction forces acting in one direction are strongly different from the forces that act in the other two directions. It was assumed that the crystal has an axial symmetry. This is characteristic of crystals of the hexagonal system.

For interacting chains Lifshitz (15) derived the following expressions for heat capacity:

$$C = A\left(\frac{T}{\theta}\right)^3 \quad \text{at} \quad T \ll \eta^2\theta \tag{1.57}$$

$$C = B\left(\frac{T}{\theta}\right)^{5/2} \quad \text{at} \quad \eta^2\theta \ll T \ll \theta\sqrt{\frac{G}{E}}\,(G \ll E) \tag{1.58}$$

where A and B are coefficients expressed in terms of the elastic moduli of the crystal and the "transverse" rigidity of the chains (15); $\eta^2 = G/E$ (G is the shear modulus and E is Young's modulus along the z axis).

For the heat capacity of structures with interacting layers Lifshitz (15) derived the equations:

$$C = A_1\left(\frac{T}{\theta}\right)^3 \quad \text{at} \quad T < \eta_1^2\theta \tag{1.59}$$

$$C = B_1\left(\frac{T}{\theta}\right)^2 \quad \text{at} \quad \eta_1^2\theta \ll T \ll \theta\sqrt{\frac{G}{E_1}} \tag{1.60}$$

where A and B are coefficients which are functions of the elastic moduli of the crystal and of the "transverse rigidity" of the layers; $\eta^2 = G/E_1$ (E_1 is Young's modulus in the plane of the layer).

Equations (1.54) through (1.60) clearly have not been used for describing the temperature dependence of the heat capacity of polymers since even qualitatively they are not confirmed by experiment.

It should be noted that neither the Lifshitz nor the Tarasov theory takes into account many of the special features of polymers.

The Hecht-Stockmayer theory (18), which takes intermolecular interaction into account in the calculation of the vibrational spectrum of polymers is to a considerable extent free from the shortcomings mentioned above. For the purpose of calculations, Hecht and Stockmayer took a simple tetragonal lattice, which they used as a model of a polymeric crystal formed of chains arranged in parallel (Fig. 1.1). It was assumed that all the chain links have the same mass m and that the distance between the links is c along the chain and $a=b$ at right angles to the chain. The interaction between the chains was determined with the aid of the force constant α, which takes account of the interaction between the nearest neighbours in the x and y directions (at right angles to the chain axis) and also of the force constant β, which takes account of the interaction between neighbouring atoms (the valence forces) in the z direction (along the main chains). The interaction between other neighbouring links was described by introducing the force constants 2γ and $2\gamma'$, which take into account the influence of the links along the diagonal in the planes xz and yz (2γ) and also in the plane xy ($2\gamma'$) (see Fig. 1.1). Finally, the force constant $\varkappa$ takes account of the deformation of valence angles.

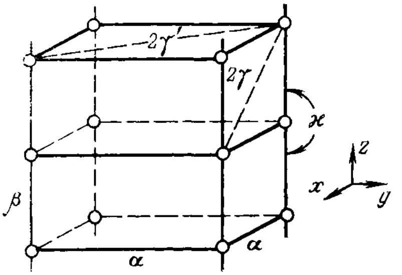

FIG. 1.1. The Stockmayer-Hecht model of a polymer crystal (18), taking into account various force constants. Polymeric chains are arranged along the z axis.

For numerical calculations Hecht and Stockmayer made use of the following reduced values of the dimensionless force constants: $\alpha_r = 0.03968$; $\beta_r = 0.992$; $\varkappa_r = 0.0992$; $\gamma_r = \gamma'_e = 0.002$.

The ratio $\beta/\alpha = 25$ reflects the fact that the valence bonds play a substantially greater role than the bonds arising from the van der Waals forces between adjacent chains. The ratio $\varkappa/\beta = 0.1$ is a good approximation for paraffins. For all the force constants used in the Hecht-Stockmayer model the inequality $\beta > \varkappa > \alpha \gg \gg \gamma = \gamma'$ holds true.

Hecht and Stockmayer (18) considered the equations of motion of a polymeric crystal, taking account of all the force constants given above. They arrived at an approximate solution of the secular equation for a simple lattice and showed that there correspond to this equation three acoustical branches, two of which coincide (they degenerate). The branches that degenerate characterize the natural vibrations at which the chain links are displaced perpendicular to the direction of the chain (deformation vibrations). The third acoustical branch defines natural vibrations at which the links are displaced along the chain (valence vibrations). Hecht and Stockmayer deduced an expression for the distribution function of natural vibrational frequencies and examined the manner in which it changes in the limiting case of low temperatures.

For heat capacity at constant volume these authors obtained the following expression:

$$C_v = 3R \int_{\nu=0}^{\nu=1} f(x)\, dI(\nu) \tag{1.61}$$

where $f(x) = x^2e^x/(e^x - 1)^2$; $x = (T_m/T)_\nu$ (T_m is the characteristic temperature, $T_m = h\nu_m/k$); $I(\nu)$ is the reduced integral distribution function of normal vibration frequencies.

To calculate heat capacity using Eq. (1.61) it is necessary to perform a graphical integration of this equation. Such calculations have been carried out by Hecht and Stockmayer, who tabulated values of $C_v/3R$ as a function of the parameters T/T_m and θ_D/T. From Eq. (1.61) we see that the dependence $C_v \propto T^3$ will hold true only in a very narrow temperature range near 0 K. At higher temperatures C_v is proportional to T^2. It is interesting that, according to the Hecht-Stockmayer theory, the dependence $C_v \propto T^2$ is possible not only for lamellar structures.

The model proposed by Hecht and Stockmayer is a highly simplified model which by no means reflects fully the structure of a real polymer. Nonetheless it takes into account two most important features of polymers: the anisotropy of polymeric chains, which is defined by the inequality $\beta/\alpha \gg 1$, and chain flexibility, which is represented by the force constant $\varkappa$. It should be noted that the Hecht-Stockmayer model can be used for quantitative calculations only when the chains of a polymer are straightened. If the structure of a polymer is such that its chains form many gauche conformations or are helices (these two cases are most frequently encountered), the theory does not fit heat capacity values arrived at through experiment.

1.3. METHODS OF MEASURING HEAT CAPACITY

The measurement of heat capacity is based on the use of the formula

$$C = \lim_{\Delta T \to 0} \left(\frac{\Delta Q}{\Delta T}\right) \tag{1.62}$$

Thus, for heat-capacity measurements to be made a strictly specified quantity of heat must be applied to the test sample, whose mass is known, and the associated change in the temperature of the sample is then determined.

Such a direct method of measuring heat capacity at low temperatures was first used by Nernst (19, 20) and Eucken (21), in order to design precision vacuum low-temperature calorimeters. These instruments served as the basis for the development of modern calorimeters intended for measuring the heat capacity of polymers at low temperatures. One of the difficulties encountered in heat-capacity measurements at low temperatures is associated with the fact that the heat given off by the heater in the calorimeter is consumed not only for heating the sample but also for heating the calorimeter itself and is partly lost to the surroundings. In this connection, the heat capacity found by direct measurements is equal to

$$C_{\text{exp}} = C_0 + C$$

where C is the heat capacity of the test sample and C_0 is the heat capacity of the calorimeter.

One of the basic problems of low-temperature calorimetry is the decrease of the quantity C_0 as compared with the heat capacity of the samples being investigated.

As a rule, adiabatic calorimeters are employed for measuring the heat capacity of polymers at low temperatures. A schematic representation of such a calorimeter is given in Fig. 1.2. The polymer whose heat capacity is to be measured is placed in a metallic container, inside which there is an electric heater and a thermometer (ordinarily, resistance thermometers are used). The container with the sample, the heater and the thermometer is in fact a calorimeter. The calorimeter is suspended by thin filaments of a material of low thermal conductivity inside another hermetic vessel

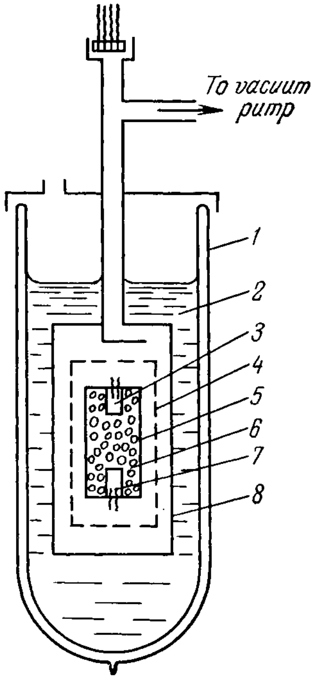

FIG. 1.2. Schematic representation of a low-temperature calorimeter:

1—Dewar vessel; 2—condensed gas (cooling agent); 3—electric heater; 4—adiabatic jacket; 5—calorimetric vessel; 6—sample; 7—thermometer; 8—evacuated jacket.

in which a vacuum of the order of 10^{-3} Pa is created. Between the walls of this vessel and the calorimeter there is one more intermediate jacket on which are placed the heater and thermocouples intended for regulating and controlling the temperature inside the jacket. The vacuum vessel together with the calorimeter and the intermediate jacket is placed in a Dewar vessel filled with liquid helium. The helium-filled Dewar vessel is in turn put in a Dewar vessel filled with liquid nitrogen.

Before the measurements are started a small amount of gaseous helium is introduced into the vacuum vessel to improve the heat exchange between the polymer sample and the coolant (liquid helium). After the sample has acquired the desired temperature the gaseous helium is pumped from the vacuum vessel. Then the electric heater of the calorimeter is supplied with voltage and a current is passed through the heater for a specific period of time. Knowing the current and voltage in the heater and the time for which the current is passed through the heater, it is easy to calculate the amount of heat released by the heater. Having measured the temperature change ΔT in the test sample, one can find its heat capacity.

It has already been said above that the consumption of heat for heating the calorimeter and the heat losses (both of which are determined by the heat capacity of the calorimeter, C_0) considerably limit the accuracy of calorimetric measurements. To improve the accuracy of calorimetric measurements one has either to accurately account for heat losses (to accurately determine C_0) or reduce them to such an extent that they can be disregarded ($C_0 \ll C$). This has led to the development of two methods of low-temperature calorimetry. The first method is as follows. The intermediate jacket, the temperature of which can be controlled, is made in such a way that it has a heat capacity sufficient for maintaining a constant temperature throughout the experiment. The instruments based on this principle have come to be known as isothermal calorimeters. The second method relies on the temperature of the intermediate jacket being automatically maintained equal to the temperature of the calorimeter. In this case the heat exchange between the calorimeter and the surroundings will be minimal. The intermediate jacket in this case is called adiabatic and the instruments based on this principle are called abiabatic calorimeters. A typical instrument of this type is the calorimeter designed by Furukawa (22).

To measure the specific heat capacity of polymers at low temperatures, use is made, as a rule, of adiabatic calorimeters. The special features of calorimetric measurements at low temperatures are described in the literature (22-36).

In order to reduce the heat capacity of the calorimeter, C_0, during low-temperature measurements, the sample of a solid itself is sometimes used as the calorimeter. In such a case, the heater and the resistance thermometer are inserted into the sample. This type of calorimeter has been used for measuring the heat capacity of polymers by Passaglia and Kevorkian (37). They reduced the heat capacity of the calorimeter by a factor of 17, lowering it to 5 per cent of the total heat capacity.

It should be noted that the experimentally determined quantity in calorimetric measurements is the specific heat capacity at constant pressure, C_p. In theoretical calculations, however, use is most frequently made of the heat capacity at constant volume, C_v. These two parameters are interrelated as follows:

$$C_p - C_v = Tv\,\beta^2/\varkappa \tag{1.63}$$

in which relation β is the thermal volume expansion coefficient which is equal to

$$\beta = \frac{1}{v}\left(\frac{\partial v}{\partial T}\right)_p \tag{1.64}$$

and $\varkappa$ is the isothermal compressibility, defined by the expression

$$\varkappa = -\frac{1}{v}\left(\frac{\partial v}{\partial p}\right)_T \tag{1.65}$$

At low temperatures, when $T \rightarrow 0$, β also decreases and the difference $C_p - C_v$ becomes negligibly small as compared with C_v. Therefore, at low temperatures the heat capacities of polymers, C_p and C_v, may be assumed to be roughly equal.

1.4. THE HEAT CAPACITY OF POLYMERS

The thermal characteristics of polymers near the temperature 0 K, unlike those of low-molecular-mass substances, have been little studied. The majority of experimental data on specific heat capacity of polymers at low temperatures refer to the temperature range, the lower limit of which corresponds to the temperature of liquid hydrogen (about 20 K) and the upper limit to room temperature. This temperature range turns out to be sufficient for the calculation from the measured values of specific heat capacity of the main thermochemical parameters of polymers (enthalpy, entropy). These are of great technical value. Incidentally, of importance for the elucidation of the mechanism of the heat capacity of polymers are measurements carried out at lower temperatures. The measurement of heat capacity of polymers in the temperature range from 1 to 20 K is of the greatest interest for the comparison of experimental evidence with results of theoretical calculations and also for the elucidation of those specific features of polymers which distinguish them from low-molecular-mass solids.

Attempts to extrapolate the values of specific heat capacity of polymers measured at 20 K to lower temperatures do not, as a rule, lead to consistent results. Typical in this regard is the history of measurements of the heat capacity of polytetrafluoroethylene. In 1952 Furukawa and his coworkers (38) measured the heat capacity of this polymer in the temperature range 15-365 K and, using the Debye function, extrapolated the results obtained to the region of helium temperatures down to 0 K. A comparison with the values of heat capacity obtained by direct calorimetric measurements (39, 40) has shown that the error due to extrapolation is 200 per cent. Such a considerable difference in the value of heat capacity does not, as a rule, lead to very large errors in calculations of entropy, which is why extrapolation is sometimes used to determine the thermochemical parameters of polymers. But to obtain reliable information on molecular motion and the vibrational spectrum of a polymer requires more precise values of heat capacity, which can be obtained only from direct calorimetric measurements at helium temperatures.

One of the difficulties in the measurement of specific heat capacity at low temperatures is the very low thermal conductivity of polymers. This explains why a prolonged period of time is required for the setting up of a thermal equilibrium in the sample, something which considerably complicates the experiments. Usually, in order to eliminate this difficulty, use is made of a large number of small pieces of the polymer to be tested, while in order to improve the thermal contact use is made of a thermal exchange gas (as a rule, helium). But in this case, new complications arise, associated with the absorption of heat by the exchange gas.

The comparatively small amount of experimental data on the specific heat capacity of polymers at low temperatures is also due to the considerable difficulties that arise in a theoretical interpretation of the results obtained. Indeed, at a first approximation it can be assumed (7) that the heat capacity of polymers in the solid state is given by:

$$C = C_1 + C_2 + C_3 \tag{1.66}$$

where C_1 is the heat capacity due to lattice vibrations (this contribution to heat capacity is greatest at low temperatures); C_2 is the heat capacity due to characteristic vibrations, including the independent motion of individual groups in a repeating unit of the polymer; C_3 is the heat capacity due to the presence of defects.

The elucidation of the role of these contributions to the heat capacity of polymers even in the region of low temperatures, where the situation is substantially simplified, presents considerable difficulties. In this connection, the use of sophisticated models, such as the Hecht-Stockmayer model (18) and the Genensky-

Newell model (41), are hardly of great interest, considering the scarcity of experimental data. More important at present is the comparison of experimental values of the heat capacity of polymers at low temperatures with the simplest, though rather approximate, models, such as the Debye and Tarasov models. In this connection, one of the tasks is to establish the limits of applicability of the Debye theory to polymers. At first glance, the use of the Debye theory for describing the behaviour of the heat capacity of polymers seems to be unjustified since this theory does not take into account the main feature of polymeric chains—their one-dimensional structure. In actual fact, during the propagation of long Debye waves (when low-frequency vibrations are excited) polymeric chains interact with one another as a result of the presence of the forces of interchain interaction. As a result, in the polymer there arise three-dimensional vibrations, which are described by the Debye theory.

In the case of the propagation of short Debye waves (when high-frequency vibrations are excited) the principal role in the spectrum is played by the vibrations directed along the skeleton of the polymeric chain. Obviously, it is in this case that the one-dimensional nature of the polymeric chain is manifested. The simplest continuum model, which takes into account both the three- and one-dimensional nature of the polymer, is the Tarasov model.

Nevertheless, neither the Debye nor the Tarasov model can provide an exact picture of the behaviour of the heat capacity of polymers since they ignore the dispersion of Debye waves. From the Debye theory it follows that the dependence $C \propto T^3$ must be observed at $T < \theta_D/12$; because of dispersion, however, this dependence is observed at $T < \theta_D/30$ or at even lower temperatures. It should be noted that the presence of dispersion may greatly distort the form of the dependence of heat capacity on temperature. Thus, while the Debye theory predicts that C/T^3 = constant, the presence of dispersion must lead to an increase in the quantity C/T^3 with temperature. According to the Tarasov theory (for a one-dimensional and a two-dimensional continuum) the quantity C/T^3 must decrease with rise of temperature. In the case of dispersion the quantity C/T^3 can remain constant even at relatively high temperatures.

Thus, the analysis of the temperature dependence of heat capacity at very low temperatures gives one access to important information on the nature of polymers and the methodology of a theoretical description of this class of substances.

The temperature dependence of the heat capacity of polymers at very low temperatures shows some specificity. It is essential that the heat capacities of amorphous and crystalline polymers differ considerably at low temperatures. The heat capacity of amorphous polymers at low temperatures is, as a rule, higher than the heat capacity of partly crystalline (especially, strongly crystallized) polymers. It would be of interest to find out how the low-temperature heat capacity of a polymer is changed when its degree of crystallinity is altered. However, the only crystalline polymer that has been studied to a sufficient extent is polyethylene.

We shall see below that the differences in the temperature dependence of the heat capacity of amorphous and crystalline polymers are not accidental. Typical in this respect is polyethylene.

1.4.1. THE HEAT CAPACITY OF CRYSTALLINE POLYMERS

Polyethylene. This polymer is the most convenient subject for the study of heat capacity at low temperatures, given that it has a simple chemical structure—its formula is $(—CH_2—)_n$—and there are no bulky side groups, the motion of which can make a considerable contribution to low-temperature heat capacity.

In order to compare the available experimental data with the results of theoretical calculations one must know the molar heat capacity of the polymer. By the molar heat capacity of a polymer is meant the heat capacity per 1 mole of the repeating unit. It is believed (42) that in a polymer having a structure of type (A) the gram-mole is the molecular mass of the group (A) expressed in grams, while in polymers with a structure of type (AB) it is the molecular mass of the group (AB) expressed in grams. The correctness of this definition is confirmed by the fact that at high temperatures Dulong-Petit law holds true: for substances of type A the heat capacity C at high temperatures tends to 0.025 kJ/(mole·K) and for polymers of type AB it tends to 0.050 kJ/(mole·K).

Since the repeating unit of polyethylene is the methylene group CH_2, it is natural that all data on the molar heat capacity of this polymer refer to the mass $m = 14.03$ g. Polyethylene is a partly crystalline polymer which forms an orthorhombic cell upon crystallization. The density of completely crystalline polyethylene is $\rho = 0.999$ Mg/m^3 (43, 44), and tha tof completely amorphous polyethylene is $\rho = 0.8525$ Mg/m^3 (45).

Among the first scientists to study the heat capacity of polyethylene at low temperatures were Sochava and Trapeznikova (46). Using an adiabatic vacuum calorimeter, they measured the specific heat C_p of polyethylene in the temperature range 58 to 273 K. It was found that if the experimental data are represented in the form

$$C = AT^m \tag{1.67}$$

(where A is a constant), then in the temperature range 58 to 95 K the value of m changes continuously from a value greater than unity to a value equal to 0.89. In the range 95-185 K the value of m remains constant and equal to 0.89, and at temperatures 185 K and higher m increases. Since $m = 1$ according to the Tarasov theory and $m = 0.5$ according to Lifshitz, it was concluded (46) that the Tarasov model is in better agreement with experimental results.

Later, Sochava (47) investigated the behaviour of the heat capacity of polyethylene at lower temperatures (from 17 to 60 K) and found that in the temperature range studied the value of m changes from 2.15 (17 K) to 1.1 (60 K). From this it follows that in this region the dependence of heat capacity on temperature is in contradiction to the Debye theory and that the chain interaction cannot be ignored in a theoretical analysis. Sochava and Trapeznikova (46, 47) indicated neither the density nor the degree of crystallinity of the polyethylene investigated, which is why a theoretical interpretation of these experimental data cannot be unambiguous.

This shortcoming has been considerably eliminated by Dainton and coworkers (48), who studied polyethylene samples of different crystallinity over a temperature range of 20-30 K. A detailed analysis of the available literature on the heat capacity of polyethylene at low temperatures has been carried out by Wunderlich (49, 50). This author has systematized the experimental values of C_p for polyethylene at temperatures from 1 to 420 K and calculated the enthalpy and entropy of the polymer; he has also calculated C_p for completely amorphous and completely crystalline samples. It was found that from 1 to 100 K the specific heat C_p of amorphous and completely crystalline samples of polyethylene is practically the same and only at $T > 100$ K does the specific heat of the amorphous sample begin to exceed the C_p value of the crystalline sample. From the experimental data reported by Wunderlich (49) it follows that at temperatures from 1 to 5 K the heat capacity of polyethylene strictly follows Debye's cube law. The Debye characteristic temperature calculated from experimental values of heat capacity is $\theta_D = 231$ K. It seems strange that the specific heat of polyethylene in the helium-temperature region does not depend on the degree of crystallinity equal to

$$\lambda = \frac{\rho - \rho_{am}}{\rho_{cr} - \rho_{am}} \qquad (1.68)$$

where ρ is the density of the given polymer; ρ_{cr} and ρ_{am} are, respectively, the densities of crystalline and fully amorphous samples of the given polymer.

In this connection, Tucker and Rees (14) and later Rees (33) once again considered the problem of the effect of the degree of crystallinity on the heat capacity of polyethylene in the helium-temperature region. Using the results of investigations carried out by them (14, 33, 40) over the temperature range 1 to 30 K and also the experimental data obtained by other authors (48, 51), they showed that the heat capacity of polyethylene depends on crystallinity not only in the region of relatively high temperatures (above 110 K) but also in the helium region. Figure 1.3 shows the temperature dependence of the specific heat capacity of completely amorphous and completely crystalline polyethylene. The

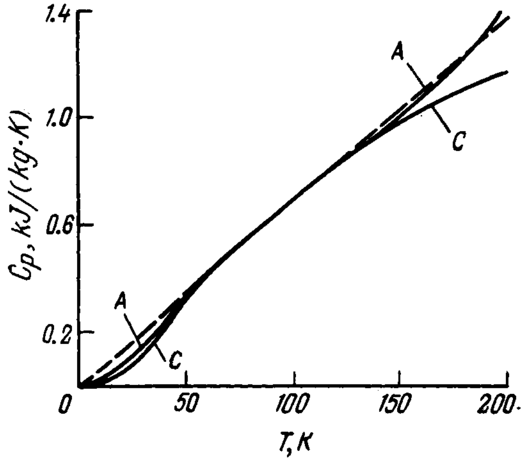

FIG. 1.3. The specific heat of a completely crystalline (C) and amorphous (A) polyethylene. The dashed line is a continuation of the linear dependence of heat capacity, which is valid for the temperature range 50 to 100 K.

values of C_p were obtained by extrapolation of experimental data on specific heat to $\lambda = 0$ (amorphous polyethylene) and to $\lambda = 1$ (crystalline polyethylene). From Fig. 1.3 it is seen that in the region of low (1-50 K) and of relatively high (110 K and higher) temperatures the heat capacities of amorphous and crystalline polyethylene are different. In both temperature ranges the heat capacity of amorphous polyethylene exceeds the corresponding values for crystalline polyethylene. The temperature range from 50 to 100 K is characteristic. Here the heat capacities of amorphous and crystalline polyethylene coincide and, what is more interesting, depend linearly on temperature, as predicted by the Tarasov theory. Moreover, the curves of $C_p = f(T)$ have the same slope in this region, which indicates that the characteristic temperature θ_1 in the Tarasov theory is independent of the density of polyethylene. This fact is an indication that in this temperature region there predominate in the vibrational spectrum of polyethylene one-dimensional vibrations, which at a first approximation are independent of the forces of interchain interaction (and, hence, of the density of the polymer) and are determined purely by the forces of intrachain interaction.

From Fig. 1.3 it can be seen that there exist two regions in which the heat capacities of amorphous and crystalline polyethylene differ. The high-temperature end of the $C_p = f(T)$ curve is associated with the transition of the amorphous regions of polyethylene from the glassy to the high-elastic (rubbery) state.

The dependence of C_p on the degree of crystallinity below 50 K is due to two factors: (1) in this region a considerable contribution to the acoustic spectrum of polyethylene is made by three-dimensional vibrations which are sensitive to the forces of interchain interaction and, hence, to the density of the polymer as well; (2) a considerable contribution can also be made by non-acoustic low-frequency vibrations which are caused by the presence of disordered amorphous regions.

In the temperature range 1-50 K the heat capacity of polyethylene is linearly dependent on the degree of crystallinity (14). This dependence is most strongly manifested at 5 K and becomes weaker with increase or decrease of temperature (Fig. 1.4). Whereas the weakening of the dependence of C_p on the degree of crystallinity with rise of temperature from 5 to 50 K may be explained by an increase in the frequency of normal vibrations and by the subsequent transition to relatively high-frequency one-dimensional vibrations, the reason for the decrease of this dependence with fall of temperature below 5 K is not quite so clear. While the heat capacity of partly crystalline polyethylene obeys Debye's cube law only up to 5 K (49, 50), the heat capacity of completely crystalline polyethylene obeys it up to 9 K. For completely crystalline polyethylene from 0 to 9 K the following relation holds:

$$C_{\mathrm{cr}} = 110.4 \times 10^{-3} T^3 \ \mathrm{J/(kmole \cdot K^4)} \tag{1.69}$$

If, using relation (1.69), we calculate, by means of Debye's formula (1.22), the characteristic temperature θ_D of fully crystalline polyethylene, it will be found to be equal to 260 K.

For a hypothetically completely amorphous polyethylene sample the temperature dependence of heat capacity at temperatures from 0 to 6 K may be represented in the form:

$$C_{\mathrm{am}} = 0.359 \times 10^{-3} T^3 + 45.45 \times 10^{-3} E(\theta_E/T) \ [\mathrm{kJ/(kmole \cdot K)}] \tag{1.70}$$

where $E(\theta_E/T)$ is the characteristic Einstein function with the Einstein characteristic temperature $\theta_E = 23$ K.

For analysing the behaviour of heat capacity at low temperatures use is often made of the plot of C/T^3 against T. Figure 1.5 shows such a plot for completely amorphous and completely crystalline polyethylene. The results were obtained by extrapolating to values of the degree of crystallinity equal, respectively, to 0 and 100 per cent. From this figure it can be seen that the quantity C/T^3 for crystalline polyethylene below 10 K is independent of temperature, whereas for amorphous polyethylene a “hump” near 5 K is observed. Thus, the temperature dependence of the heat capacity of amorphous polyethylene differs qualitatively from the same dependence for the fully crystalline polymer. The difference is that even in the region of very low temperatures (1-5 K) the heat capacity of amorphous polyethylene cannot be fully described with the aid of the simple Debye formula (1.22). The heat capacity calculated from formula (1.22) is only a part of the heat capacity of amorphous polyethylene at very low temperatures. The remaining, “excess”, or “super-Debye” part of heat capacity can be described by using one or more characteristic Einstein functions. The “super-Debye” at capacity at low temperatures is also a characteristic feature of other amorphous solids (52).

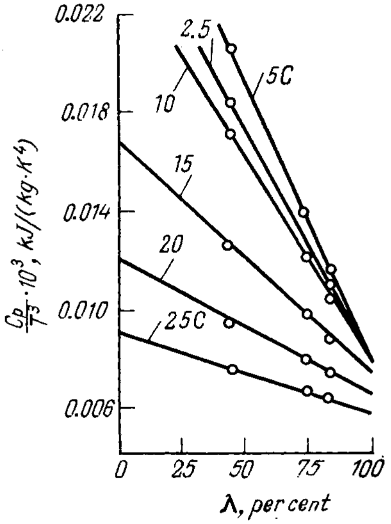

FIG. 1.4. The specific heat of polyethylene against the degree of crystallinity λ at various temperatures.

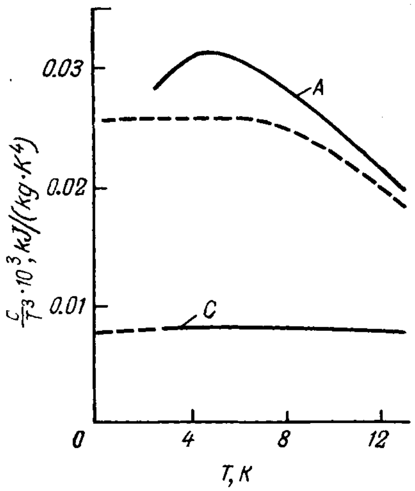

FIG. 1.5. The parameter C/T^3 agains temperature for completely cryst talline (C) and completely amorphous (A) polyethylene. The dasheline represents the data calculated according to the Tarasov theory.d

Experimental values for the heat capacity of fully crystalline polyethylene obtained by extrapolation have been used for the calculation of its vibrational spectrum. For such an analysis it is necessary to know the value of C_v, which is usually calculated by formula (1.63) from the experimentally obtained values of C_p. The difference between the values of C_v and C_p for polyethylene has to be taken into account, beginning from 70 K. Wunderlich (50) carried out a detailed comparison of experimental values for the heat capacity of fully crystalline polyethylene with the results of calculations based on various theories (10, 18, 53). The relevant data are listed in Table 1.1.

TABLE 1.1. *Experimental and Theoretically Calculated Values of the Heat Capacity C_v/R of Polyethylene*

T, K	Experiment	Tarasov theory	Shimanouchi calculations (53)	Hecht-Stockmayer theory
1	0.000019	0.000019	0.0057	0.000054
2	0.000152	0.000152	0.0548	0.000336
3	0.000515	0.000514	0.0958	0.000944
4	0.001219	0.001218	0.1255	0.001961
5	0.002382	0.002377	0.1501	0.003525
10	0.0162	0.0190	0.251	0.0234
20	0.1129	0.1234	0.406	0.1125
30	0.2548	0.2728	0.541	0.235
40	0.4045	0.4208	0.674	0.364
50	0.564	0.561	0.800	0.489
60	0.703	0.692	0.914	0.609
70	0.828	0.817	1.014	0.724
80	0.939	0.932	1.103	0.833
90	1.042	1.038	1.182	0.938
100	1.136	1.134	1.252	1.037
150	1.525	1.494	1.537	1.463
200	1.878	1.774	1.805	1.817
300	2.700	2.462	2.498	2.605

Shimanouchi, Tasumi, and Miyazawa (53) proceeded from the complete spectrum of normal vibrations of an isolated polymeric chain, calculated by themselves. In calculations that were made on the basis of the Tarasov theory for interacting chains $2N$ moles of vibrators were taken into account. The following relation was derived between the Debye temperature θ_D and the characteristic temperatures θ_1 and θ_3:

$$\theta_D^3 = \theta_1\theta_3^2 = 8.18 \times 10^6 \text{ K}^3; \quad \theta_1 = 550 \text{ K}; \quad \theta_3 = 123 \text{ K}$$

From Table 1.1 it follows that at low temperatures (1-150 K) the temperature dependence of the heat capacity of fully crystalline polyethylene is better described by the Tarasov theory. Nevertheless, Gotlib and Sochava (54) maintain that the Tarasov model has no theoretical backing since it takes into account only valence vibrations, while for a real polymeric chain in the given temperature range, according to these authors (54, 55), the principal role is played by skeletal torsional and deformation vibrations.

Gotlib and Sochava calculated anew the heat capacity of crystalline polyethylene over the temperature range 60-180 K. The calculation of the vibrational spectrum of a long regular polymeric chain, which is regarded as a one-dimensional crystal with a complex unit cell, has been made (54) on the basis of the Born-von Kármán method. Out-of-plane skeletal torsional vibrations, in-plane skeletal deformation vibrations and external deformation or rocking vibrations of CH_2 groups were examined for polyethylene. The heat capacity was calculated by numerical integration from the formula

$$C=\sum_{l=1}^{m}\int_{\nu_{l(\min)}}^{\nu_{l(\max)}}\frac{\left(\frac{h\nu}{kT}\right)^2 e^{\frac{h\nu}{kT}}}{\left(e^{\frac{h\nu}{kT}}-1\right)^2}G_l(\nu)\,d\nu \qquad (1.71)$$

where $G_l(\nu)$ is the density of the frequency spectrum; $\nu_{l(\min)}$ and $\nu_{l(\max)}$ are the minimal and maximal values of frequency in the lth branch; m is the number of branches.

The authors have succeeded in arriving at a satisfactory agreement with experimental data in the temperature range 60 to 180 K. Such calculations cannot be extended to the region of lower temperatures since no account is taken of three-dimensional lattice vibrations.

Tucker and Rees (14, 33) employed the modified Tarasov theory for the calculation of heat capacity. The Tarasov equations were used separately (for interacting chains) for longitudinal and transverse vibrations. Using the characteristic temperatures $\theta_{1L} = 1655$ K and $\theta_{3L} = 223$ K for longitudinal vibrations and $\theta_{1T} = 707$ K and $\theta_{3T} = 134$ K for transverse vibrations, they calculated the values of heat capacity for polyethylene. Their results differed from the experimental data by not more than 10 per cent.

An attempt has been made (33) to describe the heat capacity of completely amorphous polyethylene (with account taken of the small number of non-acoustic vibrations of very low frequency) with the aid of an analogous model. In this case, $\theta_{1L} = 1655$ K, $\theta_{3L} = 123$ K, $\theta_{1T} = 707$ K, and $\theta_{3T} = 74$ K.

Polytetrafluoroethylene (Teflon). Polytetrafluoroethylene $(\text{—}CF_2\text{—})_n$ is a widely used, partly crystalline polymer. The molecular mass of the repeat unit is 50.01. During synthesis polytetrafluoroethylene is produced in an almost completely crystalline form. In processing (when subjected to melting, annealing, quenching, and hydrostatic pressure) it becomes, however, partly amorphous. According to the data obtained by Kilian (56), the density of fully amorphous polytetrafluoroethylene is $\rho_{am} = 2.00$ Mg/m^3, and that of the completely crystalline polymer is $\rho_{cr} = 2.30$ Mg/m^3.

Among the first scientists to study the behaviour of the heat capacity of polytetrafluoroethylene at low temperatures were Furukawa, McCoskey and King (38). The heat capacity was measured with the aid of an adiabatic vacuum calorimeter in the temperature range 15-365 K. Four types of polytetrafluoroethylene samples were investigated: a powdered sample (which had not been treated after being synthesized), a molten sample, an annealed sample, and a quenched sample. The results of the investigation are presented in Fig. 1.6. In the low-temperature region the heat capacities of the various samples practically coincide; above 150 K the most crystalline (powdered) sample has the lowest heat capacity. This difference is associated with the unfreezing, above 150 K, of the segmental motion in the amorphous regions, i.e., with their transition from the glassy to the rubbery state. The dependence $C_p = f(T)$ given in Fig. 1.6 for the temperature range 0-15 K derives from the extrapolation of the experimental data obtained at temperatures from 15 to 30 K with the aid of the Debye function.

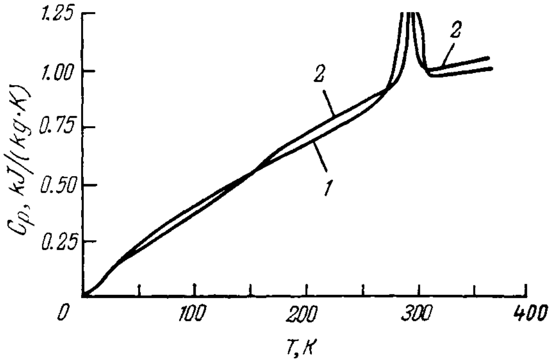

FIG. 1.6. The specific heat of polytetrafluoroethylene:

1—sample not treated after synthesis; 2—sample subjected to melting, annealing or quenching.

Rees and Tucker (40) have shown experimentally that such extrapolation is unsuccessful and leads to too small values of heat capacity. They obtained experimentally the values of heat capacity for polytetrafluoroethylene ($\rho = 2.16$ Mg/m^3) at temperatures ranging from 1 to 4.5 K and demonstrated that the heat-capacity values extrapolated by Furukawa to the temperature range 1 to 4 K are about twice as low as the values of C_p obtained by them. The results obtained by Rees and Tucker (40) are given in Fig. 1.7. From this figure it follows that the dependence $C_p \propto T^3$ is valid for polytetrafluoroethylene only at temperatures not exceeding 4 K. In this temperature range the following relation holds true (40):

$$C_p = (4.54 \pm 0.45) \times 10^{-5}\, T^3 \text{ [kJ/(kg·K)]} \qquad (1.72)$$

Expression (1.72) is in good agreement with the dependence

$$C_p = 4 \times 10^{-5} T^3 \text{ [kJ/(kg·K)]} \qquad (1.73)$$

obtained earlier by Noer, Dempsey, and Gordon (39).

The characteristic Debye temperature of polytetrafluoroethylene calculated by formulas (1.72) and (1.22) is 96 K. This is much lower than the Debye temperature of completely crystalline polyethylene (231 K). Such shifting of the upper limit of the Debye vibrational spectrum to lower frequencies may have been caused by the considerably greater bulkiness of CF_2 groups as compared with the methylene groups and also by the presence of weaker intramolecular forces. A considerable shifting of the vibrational spectrum to low frequencies in going from polyethylene to polytetrafluoroethylene leads to the disappearance of the energy gap between the acoustical and optical vibrations. In this connection, we would naturally expect that the heat capacity of polytetrafluoroethylene would be substantially higher than that of polyethylene. Indeed, at helium temperatures the C_p value of polytetrafluoroethylene is about 20 times greater than the corresponding value for polyethylene. With rise of temperature this difference diminishes and at 300 K the heat capacities of both polymers differ only by a factor of 2.

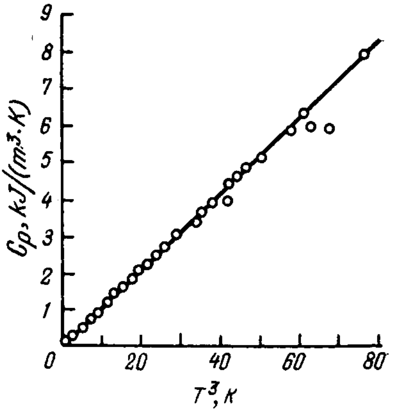

FIG. 1.7. The specific heat of polytetrafluoroethylene (ρ = 2.16 Mg/m³) at low temperatures.

A detailed analysis of the frequency spectrum of polytetrafluoroethylene has been carried out by Gotlib and Sochava (54). They compared polytetrafluoroethylene with polyethylene, assuming that the carbon skeleton in both polymers forms a planar zig-zag (which is a rather crude approximation for polytetrafluoroethylene, whose molecules in fact form a helix). They used the force constants found with the aid of infrared spectroscopy and calculated the vibrational spectrum of polytetrafluoroethylene. They studied the out-of-plane skeletal torsional, in-plane skeletal deformation and external deformation vibrations of the CF_2 groups. Analogous modes of vibration were also considered in an analysis of the frequency spectrum of polyethylene. Since the mass of the fluorine atom is greater than that of the hydrogen atom, other vibrational branches were also taken into account since they make a substantial contribution to the heat capacity of polytetrafluoroethylene: torsional, deformation scissoring (or bending) and wagging modes of vibration of CF_2 groups. Computations show that the vibrational heat capacity of polytetrafluoroethylene calculated on the basis of a set of force constants taken from spectroscopic data is in good agreement with experimental values in the temperature range 50-200 K. Gotlib and Sochava point out that the linear dependence of C_p on temperature observed at low temperatures may have resulted from the superposition of the contributions (which vary in a non-linear fashion with temperature) introduced by various branches of the entire low-frequency vibrational spectrum of the polymeric chain.

Roinishvili, Tavkhelidze, and Akopian, while discussing the results of their measurements of the heat capacity of amorphous and crystalline polyethylene terephthalate (60) in the temperature range 10-300 K, came to the conclusion that a comparison of experimental and theoretical data is not invariably justified. They noted that in the dependence $C = AT^m$ it is essential that $C = 0$ at $T = 0$, for which reason one should not compare portions of the $C = f(T)$ curve with the equation $C = A/T^m$ if the portion chosen is not extrapolated to 0 K. This also applies, to a certain extent, to the theoretically calculated portions of the curves plotted by Gotlib and Sochava (54), which at $T \to 0$ lead to heat-capacity values different from zero.

Other Crystalline Polymers. The heat capacity of other crystalline polymers have been little studied. In general, no experimental data are available on the effect of the degree of crystallinity on the behaviour of the heat capacity of crystalline polymers at low temperatures. Measurements have usually been carried out at not very low temperatures.

Rees and Tucker (40) investigated the heat capacity of *polytrifluorochloroethylene* $[-CF_2CFCl-]_n$ (the molecular mass of the repeat unit is 116.47), which has a density of $\rho = 2.114$ Mg/m^3, at temperatures ranging from 1 to 4.5 K. It has been found (40) that in this temperature range the heat capacity of polytrifluorochloroethylene is linearly dependent on T^3 (Fig. 1.8). The Debye temperature calculated from formula (1.22) is $\theta_D = 67$ K. At helium temperatures the heat capacity of polytrifluorochloroethylene is almost 3 times as high as the corresponding values for polytetrafluoroethylene. The higher values of the heat capacity of polytrifluorochloroethylene are possibly due to the low degree of crystallinity of the sample investigated.

The heat capacity of *polypropylene* $[-CH_2CHCH_3-]_n$ (the molecular mass of the repeat unit is 42.08) has been studied by Dainton, Evans, Hoare and Melia (48). They investigated samples of atactic (degree of crystallinity 16 per cent) and isotactic (48 per cent) polypropylene in the temperature range 20 to 30 K. It was found that the heat capacity of the more amorphous atactic polypropylene is somewhat higher than that of its isotactic counterpart. This difference could not be detected by Passaglia and Kevorkian (37, 58) in the temperature range 90-240 K. The heat capacity of atactic polypropylene, at 20 K, is 3.6 times greater than that of amorphous polyethylene. This cannot be explained by the contribution of the restricted rotation of the methyl groups to the heat capacity of polypropylene. The classical rotation of methyl groups at such low temperatures is impossible since the energy of the thermal motion of methyl groups at $T < 40$ K is lower than the potential energy barrier that hinders their rotation.

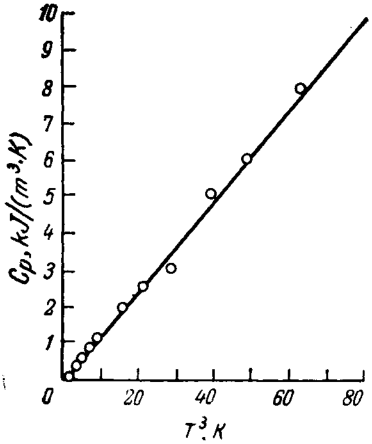

FIG. 1.8. The specific heat of polytrifluorochloroethylene ($\rho = 2.114$ Mg/m³) at low temperatures.

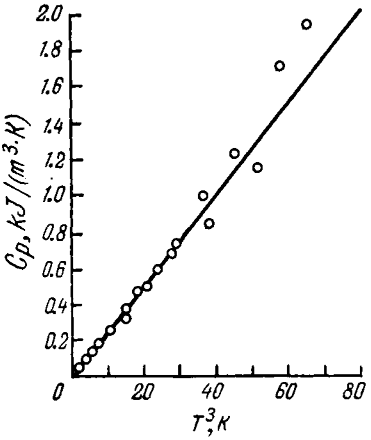

FIG. 1.9. The specific heat of Nylon 6,6 ($\rho = 1.14$ Mg/m³) at low temperatures.

The heat capacity of *nylon* (apparently, Nylon 6,6, polyhexamethylene) has been measured by Rees and Tucker (40) at temperatures from 1 to 4.5 K. For this polymer ($\rho = 1.14$ Mg/m³) the heat capacity has been found to depend on temperature between 1 and 3.5 K according to the T-cube law (Fig. 1.9). The heat capacity of Nylon 6 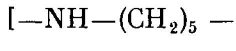 $[-NH-(CH_2)_5-\underset{\underset{O}{\|}}{C}-]_n$ and Nylon 7 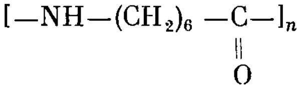 $[-NH-(CH_2)_6-\underset{\underset{O}{\|}}{C}-]_n$ have been studied (59) at temperatures from 70 K upwards. In the entire temperature range investigated the values of C_p for Nylon 7 exceed those for Nylon 6.

The heat capacity of *polyformaldehyde* or *polyoxymethylene* $[-CH_2O-]_n$ has been studied (48) in the temperature range

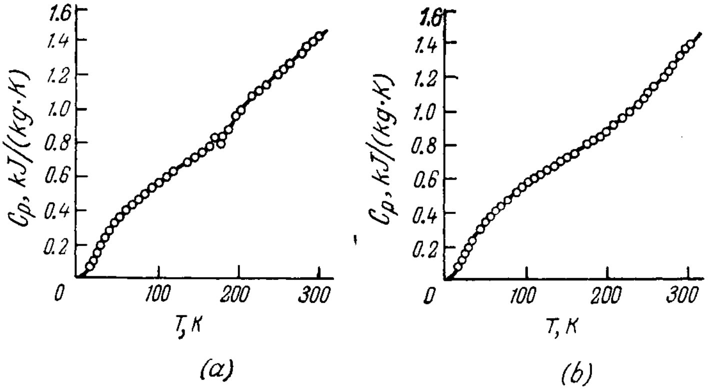

FIG. 1.10. The temperature dependence of specific heat: *a*—polyformaldehyde Delrin-1500); *b*—a trioxan-based polymer.

20-300 K. The measurements were carried out on a polymer produced by the polymerization of formaldehyde (Delrin) and on a powdered material produced by the polymerization of trioxane. The latter polymer had a high degree of crystallinity and its glass-transition temperature could not be found from calorimetric measurements, while with Delrin glass transition took place at 190 K (Fig. 1.10). Over the entire temperature range studied the polymer produced from trioxane has a lower heat capacity. Using the Debye function, Dainton (48) calculated the characteristic temperatures of both polymers ($\theta_D = 140$ K for Delrin, and $\theta_D = 129$ K for the trioxane-based polymer). In the range 20-80 K the heat capacity of Delrin is close to that of amorphous polyethylene.

1.4.2. THE HEAT CAPACITY OF AMORPHOUS POLYMERS

The main feature of the heat capacity of amorphous polymers at low temperatures is the departure of its temperature dependence from Debye's cube law. Whereas for crystalline polymers at temperatures from 1 to 4 K the heat capacity obeys, as a rule, Debye's law, in the case of amorphous polymers there is observed, down to the lowest temperatures, a fundamental difference between the temperature dependence of heat capacity and the behaviour predicted by the Debye theory. This is manifested in that even at very low temperatures the relation $C/T^3 = \text{const}$, which follows from the Debye theory, does not hold for amorphous polymers. It has already been said that for completely amorphous polyethylene a hump is observed on the plot of $C/T^3 = f(T)$ near 5 K. The departure from the dependence $C/T^3 = \text{const}$ at low temperatures is a distinctive feature of many amorphous materials, both organic and inorganic.

A similar change in heat capacity is observed with amorphous SiO_2 (61, 62), GeO_2, and selenium (63) at $T < 1$ K. This effect is ascribed to the presence of a small number of low-frequency optical vibrations due to the specificity of the amorphous state. For example, the heat capacity of completely amorphous polyethylene at low temperatures can be described by combining the frequency spectrum based on the Tarasov theory with a small number (0.17 per cent of repeat units) of vibrations with a characteristic temperature of 23 K.

Thus, typical of amorphous substances is the "super-Debye", "excess" heat capacity. This contribution to heat capacity becomes especially noticeable if the Debye part, found from supersonic measurements (see Chapter 9) extrapolated to 0 K, is subtracted from the experimentally found values of heat capacity. The results of such calculations for polymethyl methacrylate and polystyrene are given in Fig. 1.11. From a comparison of the curves shown in Fig. 1.11 it becomes clear that, apart from the contribution of acoustic vibrations, the contribution from non-acoustic vibrations becomes substantial near the temperature of liquid helium. A remarkable feature is that the value of C/T^3 below 1.5 K falls off and tends to a limiting value predicted on the basis of supersonic measurements (33, 52). This result should be treated cautiously since the values of the velocity of longitudinal and transverse waves are measured (52) at temperatures $T > 120$ K and then extrapolated to 0 K. Nevertheless, for polymethyl methacrylate, just as for polystyrene, there exists a non-acoustic, "super-Debye" contribution to heat capacity at helium temperatures.

A physical interpretation of the super-Debye contribution to low-temperature heat capacity is far from clear and can hardly be made on the basis of calorimetric measurements alone. General principles tell us that the excess heat capacity must be due to the small number of vibrations with discrete low frequencies. In amorphous SiO_2 these vibrations are active in terms of Raman scattering, which shows them as optical modes of vibration.

One possible physical interpretation is Rosenstock's idea (64) that low-frequency vibrational modes may be due to the presence of inner cavities or voids in the disordered structure. The vibrating kinetic units that are present inside or on the surface of these cavities are bound weakly with the lattice and therefore vibrate independently and with a low frequency. This model presupposes that the extra heat capacity can be detected in partly crystalline or completely amorphous polymers. Using the Rosenstock model, we can represent the heat capacity of an amorphous polymer as the sum of the Debye acoustic contribution and the super-Debye heat capacity due to independently vibrating oscillators. The frequency of the vibrations and the number of such oscillators can be found by using Einstein's theory of heat capacity.

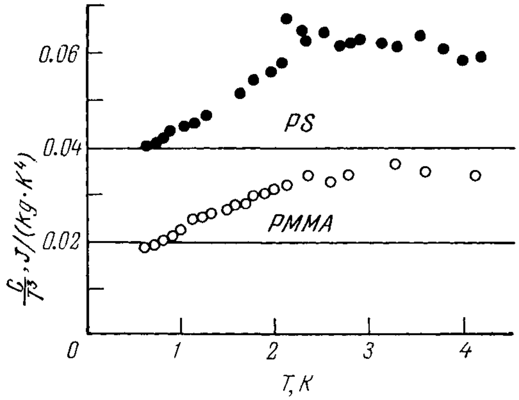

FIG. 1.11. Dependence of the parameter C/T^3 on temperature for polystyrene (●) and polymethyl methacrylate (○) (33). The solid lines represent the Debye contribution to heat capacity.

The nature of these oscillators has not yet been elucidated. Rees (33), for example, thinks that their role may be played by side groups. In the case of polymethyl methacrylate and amorphous polyethylene, methyl groups can play the role of oscillators (such groups in amorphous polyethylene play the role of branchings); as regards polystyrene, the situation is more complicated. The side groups in polystyrene are bulky phenyl groups which may be larger in size than the inner voids that are dealt with in the Rosenstock theory. A comparison of the characteristic frequencies shows that the mass of the vibrating kinetic unit of polystyrene is not much greater than in the case of polymethyl methacrylate and polyethylene (33). According to Rees (33), the role of Einstein oscillators in polystyrene can be played by the end groups or branchings.

Let us consider in more detail the low-temperature heat capacity of amorphous polymers.

Polymethyl Methacrylate. The molecular mass of the repeat unit in polymethyl methacrylate is 100.12. The majority of heat-capacity measurements have been carried out on atactic polymethyl methacrylate, which differs in glass-transition temperature ($T_g = 375$ K) from the isotactic ($T_g = 320$ K) and syndiotactic ($T_g = 395$ K) stereoisomers.

Sochava and Trapeznikova (42) measured the heat capacity of polymethyl methacrylate in the temperature range 60-260 K for the purpose of studying the retarded internal rotation. Two strongly extended humps were observed on the curve of C versus T. One of them lies in the range 60-130 K with an inflection point at 100 K, and the second, in the region of 130-180 K with a point of inflection at 150 K. It has been supposed (42) that the excess heat capacity in the range 60-130 K must have been caused by the excitation of torsional vibrations of the CH_3 groups. The spread of the hump could possibly be associated with the different modes of vibrations of the CH_3 groups. Based on their measurements, Sochava and Trapeznikova (42) believe that at a lower temperature the restricted rotation about the C_3 axis in the methyl group attached directly to the main chain is unfrozen. This conclusion has been found to be incorrect (see Chapter 5).

In order to separate out the contribution of lattice vibrations to the heat capacity of polymethyl methacrylate, Sochava and Trapeznikova calculated the part of heat capacity due to the retarded rotation of the CH_3 groups. The potential energy barrier for the CH_3 group attached to the main chain ($U = 3.34$ kJ/mole) was selected so that the calculated heat capacity was at a maximum at 100 K. The height of the potential barrier that hinders the rotation of the CH_3 group contained in the ester group was found to be equal to 16.72 kJ/mole. By subtracting this heat capacity due to the motion of the methyl groups from experimental data it was possible to determine the heat capacity due to the lattice vibrations alone. It was found that the acoustic part of heat capacity is well described by the Tarasov theory for non-interacting chains, with $\theta_D = 167.7$ K.

According to this theory, the heat capacity of polymethyl methacrylate at 50-100 K is linearly dependent on temperature. Later, Sochava (65) measured the heat capacity of this polymer at lower temperatures (16-60 K) and found that above 40 K the temperature dependence of the heat capacity is almost linear. The low-temperature heat capacity of polymethyl methacrylate has been extensively studied by a number of workers (33, 39, 48, 52, 66, 67). Below 4 K the heat capacity of the polymer can no longer be described by the Debye theory because the super-Debye part of the heat capacity manifests itself at these low temperatures as well. The physical interpretation of this non-acoustic contribution to the heat capacity presents certain difficulties because of the complex structure of the repeat unit.

Choy, Hunt, and Salinger, who studied polymethyl methacrylate in the temperature range 0.5-4.3 K, have shown (66) that the dependence $C/T^3 = f(T)$ does not remain constant at these temperatures (Fig. 1.12). Above 2 K the experimental values of heat capacity are nearly twice as high as the values calculated according to Debye's theory. Below 2 K the heat capacity of polymethyl methacrylate approaches the values predicted by this theory at $\theta_D = 115$ K. The excess super-Debye part of the heat capacity can be described with the aid of two Einstein vibrations with the characteristic temperatures 4.9 and 17.5 K. The fractions of the Einstein characteristic vibrations are, respectively, 0.014 per cent and 1 per cent of the total number of vibrations. The main difficulty lies in identifying the Einstein linear harmonic oscillators with real oscillating kinetic units. It is assumed that the harmonic oscillators described by the Einstein function are due to the vibrating side groups located near the voids or inner cavities in the polymer (66). The side groups in polymethyl methacrylate are methyl groups but they cannot undergo classical rotation near the temperature of liquid helium and one may only assume that their torsional vibrations take place as a result of the tunnel effect (67). Rees (33) has shown that the acoustic contribution to the heat capacity of polymethyl methacrylate can be described by the Tarasov model which takes into account the presence of one- and three-dimensional longitudinal and transverse vibrations.

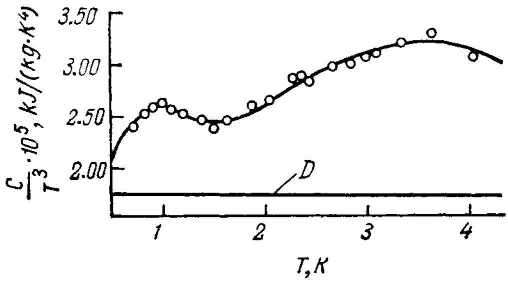

FIG. 1.12. Dependence of the parameter C/T^3 for polymethyl methacrylate at very low temperatures; D is the Debye contribution to heat capacity.

Polystyrene. The molar heat capacity of polystyrene is usually referred to 104.15 g of the polymer. Amorphous atactic polystyrene has been studied by many investigators (33, 42, 48, 52, 65-67).

The heat capacity of polystyrene has been measured at temperatures from 0.8 to 540 K. The most interesting result obtained from studies of polystyrene is that its heat capacity cannot be described with the aid of Debye's theory even at very low temperatures (about 1 K) (Fig. 1.13).

It has been shown (66) that the temperature dependence of the heat capacity of the polymer at very low temperatures can be depicted by combining Debye's theory at $\theta_D = 115$ K with two Einstein modes with the characteristic temperatures 5.5 and 16 K. The Einstein harmonic oscillators are, respectively, 0.038 and 1.8 per cent of the total number of oscillators. Just as with polymethyl methacrylate, the question of the nature of the vibrating kinetic units, expressed in terms of the Einstein harmonic oscillators, remains open. One would think that these vibrations may be linked with the side groups, but in polystyrene these side groups are very bulky phenyl groups. The motion of these groups near the temperature of liquid helium is hardly probable. A different viewpoint has been advanced by Zoller, Fehl, and Dillinger (68).

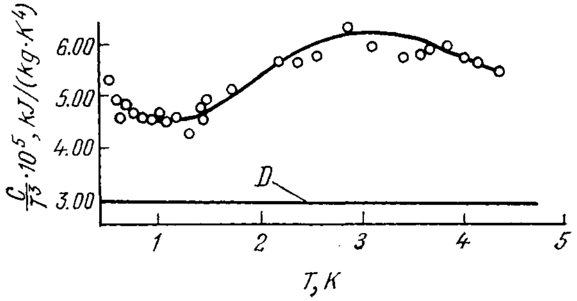

FIG. 1.13. Dependence of the parameter C/T^3 for polystyrene at very low temperatures; D is the Debye contribution to heat capacity.

These authors measured the heat capacity of samples of polystyrene which had been produced by various methods and which had different molecular masses, and also the heat capacity of α-substituted and *ortho*-substituted derivatives. They also studied polystyrene cross-linked with divinylbenzene. They found that the temperature dependence of the specific heat can be represented in the form:

$$C = AT^3 + f(T) \tag{1.74}$$

Thus, the experimental values of specific heat exceed the values calculated by Debye's theory. If it is assumed (68) that the "super-Debye" part of the heat capacity is due to the presence of Einstein one-dimensional oscillators in the polymer, then the following formula results from expression (1.74):

$$C = AT^3 + \frac{B\left(\frac{\theta_E}{T}\right)^2 \exp\left(\frac{\theta_E}{T}\right)}{\left[\exp\left(\frac{\theta_E}{T}\right) - 1\right]^2} \qquad (1.75)$$

where C is the specific heat; A, B, and θ_E are the parameters determined from experimental data.

If we denote the number of one-dimensional Einstein oscillators per 1 g of polymer by n_E, then from a comparison of expressions (1.75) and (1.11) it follows that $B = kn_E$, where k is the Boltzmann constant. Introducing the parameter r, which is defined as the ratio of the number of repeat units per 1 g of polymer, to the number n_E, we get:

$$r = \frac{N_0}{\mu_0 n_E} = \frac{N_0 k}{\mu_0 B} \qquad (1.76)$$

where N_0 is Avogadro's number and μ_0 is the molecular mass of the repeat unit.

The parameters A, B, θ_E, and r were chosen so that the values calculated from formula (1.75) best fitted the experimental data (68). This fitting is usually accomplished by computer. It has been found, unexpectedly, that the temperature dependence of the super-Debye heat capacity of polystyrene can be described by using a single Einstein function with a single value of θ_E. The characteristic Einstein temperature was found to be the same for all the polystyrene samples investigated (68). The parameter r varies but slightly from sample to sample (Table 1.2). This parameter is too large (n_E is too small) for the existence of Einstein harmonic oscillators to be linked with the vibrations of the phenyl groups. If we are to assume that each repeat unit makes a contribution to the heat capacity corresponding to one Einstein oscillator, it is necessary that r be equal to unity. The parameters A, B, and θ_E are almost independent of the presence of *ortho-* or *para-*substituents in the phenyl groups, while from dielectric and dynamic mechanical investigations it is known that these substituents have a retarding effect on the motion of phenyl groups. It is obvious that phenyl groups cannot be likened to Einstein harmonic oscillators.

One mechanism which might account for the Einstein contribution to the heat capacity is as follows (69). Even amorphous polymers possess, to a certain extent, a one-dimensional order. Since the interaction between atoms in the chain (due to covalent bonds) is considerably stronger than the van der Waals interaction between chains, it has been supposed (68, 69) that the units of isolated polymer chains may be regarded as one-dimensional Einstein oscillators.

TABLE 1.2. *Comparison of the Results of Calculation by Eq. (1.75) with Experimental Data (68)*

Polymer	Molecular mass	A, J/(kg·K^4)	B, J/(kg·K)	θ_E, K	$n_E \cdot 10^{-17}$, kg^{-1}	r
Polystyrene (PS)	33,600	0.0479	1.91	16.7	1.38	42
	34,400	0.0483	2.42	17.2	1.75	33
	349,000	0.0522	1.47	15.6	1.06	54
	365,000	0.0507	2.09	16.6	1.51	38
PS+0.01% DVB	—	0.047	2.66	15.8	1.93	—
PS+1% DVB	—	0.0528	1.85	17.3	1.34	—
PS+5% DVB	—	0.0500	2.08	16.7	1.51	—
PS+20% DVB	—	0.0427	2.43	16.2	1.76	—
PS+40% DVB	—	0.0347	2.70	17.1	1.96	—
Poly-*o*-methylstyrene	—	0.0458	2.72	14.8	1.97	26
Poly-*o*-chlorostyrene	—	0.0466	2.52	15.0	1.83	24
Poly-α-methylstyrene	—	0.0429	1.73	17	1.25	41

This model (68, 69) deals with a linear chain with different masses M and m ($M > m$), which are at a distance d from one another. It is presumed that only nearest neighbours interact with one another, this interaction being characterized by the elastic constant β. The normal vibrations of such a chain can be calculated. The dispersion equation $\omega(k) = 0$, where k is the wave vector, is split into two branches. One of these branches is optical and has the following frequencies:

$$\omega = \omega_0 = \left[2\beta\left(\frac{1}{M} + \frac{1}{m}\right)\right]^{1/2} \quad \text{at} \quad k \to 0 \tag{1.77}$$

$$\omega = \left(\frac{2\beta}{m}\right)^{1/2} \quad \text{at} \quad k \to \pi/2d \tag{1.78}$$

For the acoustical branch at small k values we may write (3):

$$\omega = d\left(\frac{2\beta}{M+m}\right)^{1/2} k \tag{1.79}$$

Considering that for a chain having N masses (consisting of $N/2$ repeat units if it is taken into account that a repeat unit contains one mass M and one mass m), the possible values of k_l are equal to

$$k_l = \frac{\pi}{Nd}\, l \tag{1.80}$$

(where $l = 1, 2, \ldots, N$), then we obtain the following expression for the allowed frequencies of the acoustical branch:

$$\omega_1 = \frac{\pi}{N}[2\beta/(M+m)^{1/2}] \tag{1.81}$$

$$\omega_2 \propto 2\omega_1 \tag{1.82}$$

Eliminating the elastic constant β from Eqs. (1.77) and (1.81), we obtain:

$$\omega_1 = [\pi\,(Mm)^{1/2}/(M+m)]\,\frac{\omega_0}{N} \tag{1.83}$$

As the temperature is raised from 0 K the allowed frequencies are first excited in the acoustical branch. If the chain consists of a large number of masses ($N > 10^8$), the allowed frequencies constitute a continuous series (i.e., they are typical of a linear continuum) and the heat capacity depends linearly on temperature. If the number of masses in the chain is not very large, we obtain a series of discrete frequency values and the heat capacity may be represented as the sum of Einstein contributions with different characteristic temperatures.

With a relatively small number of masses ($N = 10^2$-10^3) in the temperature range 1-4 K only one or two Einstein modes are excited.

Using such a model, we can calculate the frequency ω_1. In order to estimate the quantity ω_0 we can use the measured values of infrared absorption (1000 cm^{-1}). For unsubstituted polystyrene the mass M can be identified with the mass of the element of the repeat unit

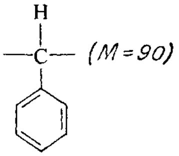

and m with the mass of the CH_2 group (the second element of the repeat unit). In this case, $m = 14$. Substituting these values into expression (1.83), we get:

$$\omega_1 \approx 10^3/N \tag{1.84}$$

For polystyrene (68) the characteristic Einstein temperature $\theta_E \approx$ 15-18 K. The respective values of ω_E range from 10 to 13 cm^{-1}. Substituting the values of $\omega_E = \omega_1$ into formula (1.84), we find that N ranges from 75 to 100. This means that there are 35-50 repeat units of polystyrene per one Einstein oscillator. This number is in good agreement with the parameter r (see Table 1.2), which is the ratio of the number of repeat units per 1 g to the number of Einstein oscillators per 1 g of the polymer.

The next higher frequency ω_2 is excited at 4 K and its contribution to the heat capacity is less than 1 per cent.

It may seem strange at first glance that the number $N/2$ of repeating units per one Einstein harmonic oscillator is 35-50, while one macromolecule of polystyrene contains 35-350 repeating units (depending on the molecular mass). This contradiction becomes understandable, however, if we take into account that the molecular mass of the portion of the polystyrene chain between the neighbouring nodes of the spatial entanglement network is 33-45, according to the results of acoustic measurements (70). It is interesting that the length of the chain element per one Einstein oscillator does not depend on the content of divinylbenzene (DVB) in cross-linked polystyrene. This is an indication that the boundary conditions that arise during the cross-linking have no effect on the vibrations of relatively small units of the main polymeric chain since the neighbouring chains become linked via benzene rings. In radiation-induced cross-linking the specific heat is sharply reduced, which is in good accord with Debye's theory (68) since adjacent chains are united as a result of the formation of covalent bonds between the carbon atoms situated in various chains. In such a system, no one-dimensional vibrations are possible and, instead, ordinary lattice vibrations are excited.

It is customarily believed (33, 52, 68) that the presence of excess super-Debye heat capacity at low temperatures, defined by the Einstein contribution to C_v, is a characteristic feature of amorphous substances, both organic and inorganic. It is supposed that this is associated with the presence of ordered regions in amorphous substances (these might be the units of the chain or small ordered but uncrystallized regions in amorphous polymers, or perhaps analogous regions and "microcrystallites" in inorganic glasses which cannot be detected by X-ray analysis). The vibrational spectrum of such ordered aggregates is discrete, and the lowest allowed frequency is excited at helium temperatures. This exerts a considerable effect on the low-temperature specific heat and thermal conductivity of such systems.

There also exist other points of view (71-73) on the nature of the super-Debye low-temperature heat capacity in polymers. One possible explanation for the mechanism of the super-Debye heat capacity (71) is that the increase in the heat capacity of amorphous solids at low temperatures as compared with crystals (and, hence, the increase in the low-frequency density of phononic states) may be explained by the interaction between longitudinal and transverse quasi-rotonic phonons. This interaction leads to the appearance of an extra frequency, the spread of the crystal density of the states and to its corresponding increase at low temperatures.

Sometimes, the super-Debye part of the heat capacity of amorphous polymers near 0 K is linearly dependent on temperature. For instance, the temperature dependence of the heat capacity of a polycarbonate below 4 K (74) is expressed by the relation

$$C = a_1 T + a_2 T^3 \tag{1.85}$$

where a_1 and a_2 are constants [for a polycarbonate $a_1 = 0.0038$ J/(kg·K^2) and $a_2 = 0.0410$ J/(kg·K^4)].

Such a change in heat capacity can be depicted theoretically with the aid of a macroscopic model proposed by Baltes (75) for describing the analogous dependence of the low-temperature heat capacity of amorphous SiO_2 and GeO_2. This model treats an amorphous body as consisting of homogeneous granules with a diameter d of the order of 10 Å; the shape and volume of the granules are random functions. The wave equation for each granule is solved with mixed boundary conditions. Since the wavelength of thermal vibrations is not small as compared with d, the normal vibrations are strongly perturbed, which leads to a non-zero value of the density of the states at zero frequency and, hence, to the linear dependence of the super-Debye heat capacity.

This model reminds one, to a certain extent, of the modern conceptions of the presence of ordered regions in amorphous polymers (70, 76-78).

CHAPTER 2

THERMAL CONDUCTIVITY OF POLYMERS AT LOW TEMPERATURES

2.1. BASIC CONCEPTS OF THE THERMAL CONDUCTIVITY OF DIELECTRICS

We understand by heat conduction in solids the heat flow from hotter regions of a solid to colder regions, as a result of which the temperatures become equal. Thermal conduction arises only if the temperature in some part of a solid differs from the temperatures of the other parts of the same solid. Let us consider a long thin rod. Suppose that the temperatures at the ends of this rod are T_1 and T_2 and the length of the rod is $l = x$; then a temperature gradient $\partial T/\partial x$ develops in the rod, which results in the appearance of a heat flow along the rod.

The basic law of heat conduction is the Fourier law:

$$q = -\varkappa \,\mathrm{grad}\, T \tag{2.1}$$

where $\vec{q}$ is the density vector of the heat flux (which is numerically equal to the energy transferred via the cross-sectional area of the specimen per unit time); $\varkappa$ is the thermal conductivity.

Heat conduction is an energy-transfer process. Like other energy-transfer processes, heat conduction is substantially relaxational in nature. Indeed, if the temperature in an element of a solid is changed in some way, the presence of a temperature gradient will lead to the generation of a heat flux which will exist until the temperature gradient becomes equal to zero as a result of the "diffusion" of energy from the sites with a higher temperature. If a constant temperature gradient is maintained artificially, a stationary, or steady-state, heat flux, constant in time, will develop in the solid.

According to the mechanism of heat transfer, all solids can be divided into three large groups: (1) nonmetals, in which heat transfer takes place as a result of lattice vibrations; (2) metals, in which electrons play the principal role in heat conduction; (3) alloys and other poorly conducting substances, whose thermal conductivity is due to a combination of these two factors.

Let us consider the thermal conductivity of solids belonging to the first group, i.e., the thermal conductivity of dielectric materials, since the majority of polymeric materials are dielectrics. We shall first confine ourselves to a consideration of crystalline dielectrics. If the crystal lattice is regarded as a set of harmonic oscillators, in which the normal vibrations are independent of one another and the vibration amplitudes depend on temperature, then no thermal resistance will be present in such a lattice. Besides, because of the independence of the modes of vibrations and the absence of any interaction between them, the energy of each vibration remains unchanged and no equilibrium energy distribution can take place in such a system.

Debye (79) made an attempt to take into account the interaction of the lattice waves and employed the formula taken from the kinetic theory of gases for the determination of thermal conductivity:

$$\varkappa = \frac{1}{3} C_v \bar{c} l \tag{2.2}$$

where C_v is the heat capacity per unit volume; $\bar{c}$ is the average velocity of sound; l is the mean free path of phonons.

The quantity $\tau = l/\bar{c}$ represents the time it takes for a lattice vibration excited above the equilibrium value to regain the equilibrium value. Thus, τ represents the lifetime of the phonon.

At relatively high temperatures $C_v = \text{const}$ (as follows from the Dulong-Petit law) and the sound velocity in the Debye approximation is also taken to be essentially independent of temperature, and therefore, since l is proportional to $1/T$, the thermal conductivity must be inversely proportional to the temperature T. As the temperature decreases the mean free path of phonons, l, increases and at sufficiently low temperatures l is determined by crystal size. Further decreases in temperature no longer affect the value of l, which remains constant under these conditions. In this region the thermal conductivity $\varkappa$ is proportional to C_v and, since at low temperatures C_v is proportional to T^3, it follows that $\varkappa$ too depends on temperature according to the same law.

It has been shown that finite values of $\varkappa$ cannot be obtained from the theory of the elastic continuum. Thermal conductivity can be explained only by turning to the dynamic lattice theory with account taken of anharmonicity phenomena.

According to the results obtained by Peierls (80), it follows from the dynamic lattice theory that thermal conductivity depends on temperature in different ways in different temperature regions.

In the region of relatively high temperatures ($T \gg \theta_D$) the mean free path l is proportional to T^{-1} and $\varkappa$ is proportional to T^{-1}. At low temperatures, when $T \ll \theta_D$ the mean free path and thermal conductivity are both proportional to $e^{\theta_D/aT}$ (where a is a constant; according to Peierls, $a \approx 2$). In the region of very low temperatures (at $T \to 0$ K) $l = \text{const}$ and $\varkappa$ is proportional to T^3.

Such a dependence of thermal conductivity on temperature is in satisfactory agreement with experimental data.

The development of a rigorous theory of heat conduction, which would allow us to calculate thermal conductivity as a function of temperature, is one of the most important problems of solid-state physics; the construction of such a theory is beset with formidable mathematical difficulties. In solving this problem use is often made of assumptions which require special verification.

Here we shall limit ourselves to a qualitative consideration of the matter, enough to give one an insight into the mechanism of heat conduction in dielectrics at low temperatures. The theory of heat conduction in dielectric crystals is developed in the following way.

To describe the energy flux the concept of phonons is used. It is assumed that in a periodic volume V, which contains N atoms, there exist $3N$ thermal vibrations, corresponding to the same number of waves. Each wave is characterized by the wave vector $\bar{k}$ and three polarization vectors $\bar{e}_s$. If the wave transfers an energy E_s^k, then its group velocity is given by

$$v_s^k = \frac{\partial \omega_s^k}{\partial k} \tag{2.3}$$

The density of the energy flux transferred by such a wave is

$$q_s^k = \frac{E_s^k}{V} v_s^k \tag{2.4}$$

The density of the heat flux transferred within the crystal with the aid of all the lattice vibrations is deduced by summation of expression (2.4) over all the vibrations:

$$q = \frac{1}{V} \sum_{ks} E_s^k v_s^k \tag{2.5}$$

Usually, the energy values of separate waves satisfy a particular distribution of waves among the energies. In order to calculate the heat flux use has to be made of the concept of the average energy $\bar{E}_s^k = E(\omega_s^k T)$.

In a quantum-mechanical treatment of lattice vibrations, instead of lattice waves one deals with phonons, characterized by the frequency ω_s^k, the pseudo-momentum $\hbar k$ and by the polarization s. The lattice vibrations are taken as a phonon gas which obeys the Bose-Einstein statistics. The phonon gas is characterized by the distribution function $\overline{N}_s^k$ which determines the number of particles in a given state. In this case, instead of the average energy $\overline{E}_s^k = E(\omega_s^k T)$, use is made of the concept of the average occupation numbers representing the distribution function $\overline{N}_s^k$.

In thermal equilibrium

$$(\overline{N}_s^k)_T = (e^{\hbar\omega_s^k/kT} - 1)^{-1} \qquad (2.6)$$

In the case of steady-state heat conduction a temperature gradient leads to small departures from the average occupation numbers $\overline{N}_s^k$ corresponding to the distribution in thermal equilibrium:

$$\overline{N}_s^k = (\overline{N}_s^k)_T + n_s^k \qquad (2.7)$$

where $\overline{N}_s^k$ is the non-equilibrium distribution function; $(N_s^k)_T$ is the distribution function corresponding to the state of thermal equilibrium; n_s^k is a minor addition which takes account of the departure of the distribution function from the equilibrium value.

A contribution to the heat transfer and, hence, to the heat flux, is made only by the term n_s^k, which represents the departure from the thermal equilibrium.

The heat flux density in this case is given by

$$q = \frac{1}{V} \sum_{k,\, s} \hbar\omega_s^k n_s^k v_s^k \qquad (2.8)$$

The main task is to determine the values of n_s^k; they must be proportional to the temperature gradient. In this case, one can derive expressions for the thermal conductivity. To solve this problem, the Boltzmann kinetic equation is used.

The change in the distribution function $\left.\frac{\partial \overline{N}_s^k}{\partial t}\right|_1$ in the neighbourhood of a particular point is caused by the external temperature field, and is compensated for by the collision of phonons with one another and also with other particles. Since the steady state $\overline{N}_s^k$ is constant over time, it follows that

$$\left.\frac{\partial \overline{N}_s^k}{\partial t}\right|_1 - \left.\frac{\partial \overline{N}_s^k}{\partial t}\right|_2 = 0 \qquad (2.9)$$

The first term takes account of the variation of the distribution function due to the convection of phonons, and the second the change caused by the collision between phonons (also by the interaction between phonons and lattice defects).

Expression (2.9) is a complex integro-differential equation. Its form and structure depend on the type of phonon interaction and its solution is beset with considerable mathematical difficulties. However there are various methods for solving it (81-83).

In solving the kinetic equation the Hamiltonian operator (or simply the Hamiltonian) H is written in the form

$$H = H_0 + \Phi_3 \tag{2.10}$$

where H_0 is the harmonic part of the Hamiltonian, which depends on the kinetic energy and the quadratic terms of the potential energy.

The potential energy of the lattice Φ, which is a function only of the coordinates of atomic nuclei and is a sum of the energy of the Coulomb interaction between nuclei and electrons and the kinetic energy of electrons, can be expanded into a power series in the degrees of displacements of nuclei from the equilibrium position. In this case

$$\Phi = \Phi_0 + \Phi_1 + \Phi_2 + \Phi_3 + \ldots \tag{2.11}$$

The term Φ_0 is the potential energy of the crystal in the equilibrium state. With an appropriate choice of the coordinate origin Φ_0 can be made equal to zero. If Φ is expanded into a series about the equilibrium position, the linear term Φ_1 also becomes zero. If we neglect the higher terms in the expansion and retain the quadratic (with respect to displacements from the equilibrium position) term Φ_2, we obtain the so-called harmonic approximation. The coefficients in Φ_2 determine the forces that act on the structural units of the lattice for small departures from the equilibrium position. It is in the harmonic approximation precisely that the Debye theory of heat capacity is valid. In this approximation the heat capacity of the lattice cannot be explained.

With large departures of particles from their equilibrium positions (in cases of high elastic stresses or high temperatures) higher (as compared with Φ_2) terms of the series must be taken into account in expression (2.11). If the terms Φ_3 and Φ_4 (or, at the very least, only Φ_3) are retained in expression (2.11), then we can describe the thermal conductivity of a dielectric crystal. It is exactly such anharmonic terms of the expansion series (2.11) that are contained in the Hamiltonian (2.10) for the crystal lattice in calculations of thermal conductivity. The nonlinear anharmonic terms in the expansion of the potential energy determine the nature of the interaction of phonons. If the Hamiltonian (2.10) contains the term Φ_3, it means that three-phonon processes are involved. An example of such a process is the interaction of two phonons with energies $h\nu_1$ and $h\nu_2$ and the pseudo-momenta $\hbar k_1$ and $\hbar k_2$. This gives rise to a third phonon of energy $h\nu$ and quasi-momentum $\hbar k$. A variant of the three-phonon interaction, in which one phonon is split into two phonons, is also possible.

Two types of phonon processes are possible. In one of these, the interaction of phonons occurs in such a way that the pseudo-momentum of a system of interacting phonons is not changed. This case is described by the following relation between the wave vectors of the interacting phonons:

$$\bar{K}_1 + \bar{K}_2 + \bar{K} = 0 \tag{2.12}$$

Evidently, the total momentum of all the phonons that arise in a dielectric crystal cannot be changed. Such phonon processes have come to be known as "Normal" or N-processes. "Normal" processes lead only to the redistribution of momentum and energy between the interacting phonons. Here the heat flux corresponding to the total pseudo-momentum of the phonons must not be attenuated. The additional factor responsible for this is that the heat transfer in a dielectric crystal is associated with the change in the number of phonons. When only the "Normal" processes are considered, the kinetic equation has no solution and the thermal resistance of crystals turns to zero. This is equivalent to the thermal conductivity becoming infinitely large. Hence, the "Normal" processes alone cannot lead to a finite value of the thermal conductivity of dielectrics.

In order to have thermal resistance, processes in which the total momentum of phonons is changed are required. If in a three-phonon interaction there is fulfilled the condition

$$\bar{K}_1 + \bar{K}_2 + \bar{K} = 2\pi\bar{b} \tag{2.13}$$

(where $\bar{b}$ is one of the vectors of the reciprocal lattice), the total pseudo-momentum of all the interacting phonons does not remain constant. The direction of the wave vectors in such an interaction is changed from what one would expect from the ordinary law of conservation of momentum. Therefore, the processes of phonon interaction, in which the law of conservation of pseudo-momentum is not fulfilled, are known as U-processes or "Umklapp" processes. (We have already spoken about the pseudo-momentum of phonons.) This is associated with the fact that the quantity $\hbar k$ is not, strictly speaking, the momentum of the lattice vibration. Therefore, strictly speaking, expressions (2.12) and (2.13) are not laws of conservation.

The mechanism of heat conduction in a dielectric crystal at low temperatures consists in the long-wave phonons, whose energy is insufficient for the development of "Umklapp" processes, giving rise, as the result of collisions (the "Normal" processes), to non-equilibrium (excited) phonons of high energy. The collisions of such phonons occur, according to expression (2.13), with a change in the quasi-momentum of the interacting phonons (the "Umklapp" processes). The "Umklapp" processes lead to the appearance of a finite value of thermal conductivity and of a non-zero thermal resistance of dielectric crystals. It is primarily the "Umklapp" processes that govern the course of the temperature dependence of thermal conductivity. At very low temperatures (at $T \to 0$ K) the "Umklapp" processes are unfrozen, since the energy of non-equilibrium phonons is no longer sufficient for the occurrence of these processes. As the temperature mounts the "Umklapp" processes are unfrozen for those branches of the spectrum which first appear at the boundary of the Brillouin zone. Therefore, for transverse acoustic modes the "Umklapp" processes may occur at lower temperatures (82) than for longitudinal modes.

This leads to an increase in the coefficient a in the expression for thermal conductivity ($\varkappa \propto e^{\theta_D/aT}$) and to the narrowing of the range in which $\varkappa$ is exponentially dependent on temperature.

If the term Φ_4 in the expansion of the potential energy [formula (2.11)] is retained, this means that four-phonon processes must be considered.

The status of the theory of the thermal conductivity of dielectrics is such that one can only roughly estimate the nature of the temperature dependence of $\varkappa$ while taking account of the particular mechanisms of phonon processes.

For an ideal lattice, in particular for the face-centred cubic lattice, Leibfried and Schloemann (84) deduced the following expression, using the variational method of solving the kinetic equation:

$$\varkappa = \frac{3\,(4)^{1/3}\,k^3 V_0^{1/3} M \theta_D^3}{10\pi^3 \hbar^3 \gamma^2 T} \tag{2.14}$$

where γ is the Grüneisen constant; V_0 is the atomic volume ($V_0 = V/N$); M is the mass.

Expression (2.14) is valid for relatively high temperatures ($T > \theta_D$). At low temperatures ($T < \theta_D$), when heat conduction is governed by the "Umklapp" processes, the thermal conductivity is given by the relation

$$\varkappa \propto \left(\frac{\theta_D}{T}\right) e^{\theta_D/aT} \tag{2.15}$$

With further decrease of temperature, when the "Umklapp" processes are found to be unfrozen and the mean free path is considerably increased, the major role is played by the scattering of phonons at the boundaries of crystallites or at the external boundaries of the specimen. In this case the thermal conductivity is given by

$$\varkappa = \frac{1}{3} C_v \bar{c} l = \frac{4\pi k^4 T^3}{h^3 \bar{c}^2}\, l \int\limits_0^x \frac{x^4 e^x}{(e^x - 1)^2}\, dx \tag{2.16}$$

where for C_v use is made of expression (1.18); $l = L\alpha^2$ (where L is the average distance between the boundaries of crystallites and α is a specific angle).

When phonons are scattered at the outer boundaries of crystallites the mean free path has the order of the smallest linear size of the specimen.

Apart from the "Umklapp" processes and phonon scattering, at the boundaries of crystallites (or at the outer boundaries of the specimen) there occur other types of phonon scattering as well, which lead to a finite thermal resistance. Phonon scattering may occur on lattice defects, which is analogous to Rayleigh scattering (81, 83, 85). The most thoroughly studied is the effect of point defects on thermal conductivity, i.e., substitution atoms, impurities, vacancies, and also of atoms residing between the lattice points of the crystal. If the role of the point defect is played by an atom of another substance, then not only is the mass changed but also the forces that bind it to other atoms. This results in a local change in the elastic properties of a dielectric crystal.

When long-wave acoustic phonons (low-frequency lattice vibrations) arise in the crystal, a sufficiently large number of neighbouring atoms vibrate together as a whole. These atoms are all characterized by an equal departure from their equilibrium positions. The neighbouring atoms vibrate together with the point defect, which behaves as a very small region with a different density (if the defect is a foreign atom with a mass differing from the mass of the atoms of a given element) or as a microregion with altered elastic properties. While colliding with such regions, the phonons experience elastic scattering, changing the direction of motion. At low temperatures the scattering of phonons on point defects may appear to be the principal mechanism leading to thermal resistance. Callaway (86) has shown that in such cases the principal role is played by the "Normal" processes.

A distinctive feature of Rayleigh scattering of phonons on point defects is that it manifests itself at long wavelengths. With shorter-wave phonons, whose wavelength is smaller than the radius of inhomogeneity, there may occur the phenomenon of resonance scattering of phonons on inhomogeneous inclusions (geometric resonance). A particular feature of geometric resonance (87) is that its contribution to low-temperature thermal conductivity does not depend on the relation between the elastic properties of the substance under study and those of the inclusion, but is determined by the geometric dimensions of the inclusions. For example, in a study of NaCl (88) containing colloidal particles of silver, there was detected, in the temperature range 0.2 to 2 K, a wide valley on the thermal conductivity—temperature curve.

Using these measurements, Wagner (88) succeeded in estimating the radius of the colloidal silver particles.

If the inclusions are molecules consisting of several atoms, then at low temperatures in such molecules the excitation of vibrations is possible (83). This will give rise to molecular resonance phonon scattering and to the corresponding contribution to thermal conductivity.

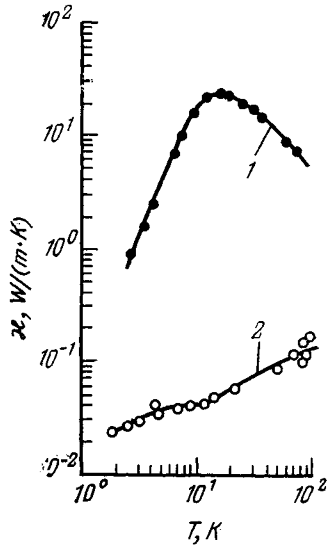

FIG. 2.1. Thermal conductivity $\varkappa$ of selenium as a function of temperature:

1—crystalline sample; 2—amorphous sample.

If the vibrational frequencies of the impurity atoms or molecules lie above the frequency band of the phonon spectrum of the main dielectric crystal, the so-called local vibrational modes (bound states) are generated. Bound states arise in those cases where there are light impurities or impurities with force constants considerably higher than those in the crystal. Phonon scattering on local modes of vibration occurs as a result of the occurrence of three-phonon processes. The scattering process consists of the following. When two lattice phonons, which always have low frequencies as compared with local modes, interact with each other, a local vibration is excited (the two phonons are absorbed) and two phonons are then emitted. A detailed analysis of the scattering of phonons on local modes of vibration has been carried out by Wagner (88).

Consideration of the thermal conductivity of amorphous solids presents considerable difficulties that arise out of the absence of translational symmetry in the arrangement of atoms, i.e., of the long-range order. By virtue of even this difference between amorphous solids and crystals the mechanism of heat transfer in amorphous solids might be expected to be different from that in crystals.

Indeed, the available experimental data (89) indicate that the temperature dependence of the thermal conductivity for amorphous solids is qualitatively different from the dependence $\varkappa = f(T)$ for crystalline solids. This becomes especially prominent if we compare the dependences $\varkappa = f(T)$ for a substance which can be produced in both the amorphous and the crystalline state (Fig. 2.1).

In contrast to the thermal conductivity of crystalline bodies, the thermal conductivity of amorphous substances has no low-temperature maximum and, as a rule, it increases with rise of temperature. The slope of the $\varkappa = f(T)$ curve may change in this case and at high temperatures the thermal conductivity tend to a constant limit. All this leads one to believe that a qualitatively different mechanism of heat conduction takes place in amorphous solids.

In dealing with the thermal conductivity of amorphous solids one often makes use of the Debye formula (2.2). The main task here is to determine the mean free path of phonons. By using the known experimental data one can occasionally estimate the magnitude of the mean free path l with the aid of formula (2.2). According to these estimates, the value of l is in good agreement with the sizes of the structural units in amorphous solids. For instance, Kittel (90) has shown that the mean free path in amorphous quartz glass is close to the sizes of the structural unit characteristic of this material. Indeed, the mean free path of phonons, l, in quartz glass at room temperature is equal to 8 Å, whereas the dimensions of the tetrahedral cell of silicon dioxide are 7 Å. Klemens, who analysed the temperature dependence of thermal conductivity, also came to the conclusion that it is associated with the regions of short-range order in quartz glass (81, 91).

The random, disordered arrangement of atoms in an amorphous solid is responsible for the fact that its elastic properties change from point to point. If an elastic wave propagates in such a solid, it may, in certain cases, undergo scattering, just as is the case in a medium with random inhomogeneities. Hence, the scattering of phonons may be expected to result from the change in their velocity from one point of the amorphous solid to another.

Employing a mathematical apparatus analogous to the one used for describing the propagation of radio waves in an irregularly refracting medium, Ziman examined the problem of the scattering of Debye elastic waves in an amorphous substance (92). The line of his reasoning is as follows. Suppose that a plane monochromatic wave strikes a layer of an amorphous substance which is a disordered medium of thickness x_0. Having passed through the layer of thickness x, on the surface of the layer the wave will be characterized by a random distribution of phases. Assuming that for each point of the layer there corresponds a definite local velocity of elastic waves, c, which differs from the average velocity c_0 by an amount δc, we can calculate the mean square of the phase shift on the layer surface. The change of the phase $d\varphi$ of the wave that has travelled the path dx may be represented in the form

$$d\varphi = \frac{2\pi}{\lambda} \cdot \frac{\delta c}{c_0}\, dx \tag{2.17}$$

where λ is the wavelength of the propagating wave.

Further, a very important assumption is made, that the quantity δc is not entirely accidental and near each point of the layer there is a small distance L over which δc changes but only slightly. The parameter L has come to be called the correlation length. It must be of the same order as the average size of the structural unit of the amorphous solid. Thus, the correlation length may be compared with the sizes of the regions in which a short-range order is retained. Ziman postulated that the correlation function of the values of δc at points a distance R apart, has the following form

$$\frac{\langle \delta c\,(r+R) \cdot \delta c\,(r) \rangle}{(\overline{\delta c})^2} = e^{-R^2/L^2} \tag{2.18}$$

Further it is necessary to calculate the mean square of the phase shift $\overline{\varphi}^2$ on the layer surface that has been crossed by the wave:

$$\overline{\varphi}^2 = 4\pi^{5/2} \frac{L\,(\overline{\delta c})^2}{\lambda^2 c_0^2}\, x_0 \tag{2.19}$$

If the length of the propagating wave $\lambda \gg L$, then the expression for the mean free path may be presented in the form

$$l_1 = \frac{x_0}{\pi \overline{\varphi}^2} = \frac{1}{4}\pi^{-7/2} \frac{c_0^2 \lambda^2}{(\overline{\delta c})^2 L} \tag{2.20}$$

If $\lambda \ll L$, then the mean free path is given by

$$l_2 = \pi^{-5/2} \frac{c_0^2}{(\overline{\delta c})^2} L \tag{2.21}$$

From formulas (2.20) and (2.21) it follows that in the case of long waves, when the wavelength λ is much larger than the elastic correlation length, the mean free path l is proportional to λ^2. In a case where $\lambda \ll L$, the mean free path is independent of the wavelength and is a constant quantity. In this case, inside the correlation region of L the wave propagates without being scattered, but it is strongly refracted at the boundaries of the region. It should be noted that the values of L and $c_0^2/(\overline{\delta c})^2$ are difficult to compute on the basis of conceptual models, and therefore the quantity l in formula (2.2) proves to be a fitting parameter. This shortcoming is not eliminated either when use is made of the following relation:

$$l_1/l_2 = \pi\,(Lk)^{-2} \tag{2.22}$$

(where $k = 2\pi/\lambda$ is the wavenumber), despite the fact that the value of l_2 can be determined from high-temperature measurements.

2.2. METHODS OF MEASURING THE THERMAL CONDUCTIVITY OF POLYMERS

Various methods have been used to study the thermal conductivity of polymers at low temperatures (93-96). Methods presently in use can be divided into two groups (107). One group includes techniques based on the use of steady-state thermal conditions, and the second comprises methods in which the regularities of the nonsteady-state thermal regime are employed. The first is the more common. In this case, in order to determine the thermal conductivity, it is necessary to induce and measure the heat flux that passes through the specimen and also to measure the temperature difference between two isothermal surfaces in the specimen. With static methods, which are employed for measuring the thermal conductivity of polymers, use is commonly made of flat, relatively thin, or cylindrical specimens. To find $\varkappa$ in each particular case, the thermal conductivity equation with specified boundary conditions is solved. In the simplest case of a flat specimen whose surfaces have constant temperatures thermal conductivity is given by

$$\varkappa = \frac{Qx}{S\,(T_1 - T_2)\,t} \tag{2.23}$$

where Q is the amount of heat passing in time t through the specimen with surface temperatures T_1 and T_2; x is the thickness of the specimen; S is the surface area of the specimen through which the heat flow takes place.

To create a heat flux through the specimen, use is made either of electric heaters or of the heat evolved through a phase transition.

Measuring thermal conductivity in polymers at low temperatures involves serious experimental difficulties. This is clearly associated with the fact that at present no polymer can be found, the thermal conductivity of which can be measured continuously at temperatures ranging from the temperature of liquid helium (4.2 K) to room temperature. As a rule, measurements of $\varkappa$ are conducted at $T < 25$ K (94, 95, 97, 98) or at $T < 4.2$ K (40, 96, 99, 100). At these temperatures the thermal conductivity of polymers is measured on long cylindrical specimens. Beginning from the temperature of liquid nitrogen up to room temperature, as well as at higher temperatures, $\varkappa$ is measured on flat specimens (101, 102). The difference is mainly associated with large radiation losses of the specimen at high temperatures, while at low temperatures these losses are very small. Thus, a gap has appeared in the experimental findings for the thermal conductivity of polymers between 25 and 77 K. One of the difficulties that arise in measuring thermal conductivity is connected with the heat losses from the heater or the thermometers. In order to take into account these effects the relative method of measuring $\varkappa$ is employed. In this case, a preliminary experiment is carried out with a material whose thermal conductivity is known (and is sufficiently low).

Difficulties also arise during temperature measurements. In earlier works, gas thermometers were most often used. More recently, at temperatures down to the temperature of liquid helium the measurements have been made with the aid of thermocouples, and from the temperature of liquid hydrogen down to very low temperatures use has been made of carbon resistance thermometers. At temperatures below 4.2 K, apart from the static methods, thermal conductivity is also measured by means of dynamic methods (103, 104).

In spite of the fact that in recent years a number of experimental works (67, 105, 106) have been published in which the thermal conductivity of polymers was measured at very low temperatures (for example, Scott and his coworkers (105) measured thermal conductivity down to 0.15 K), the technique of such measurements is still rather complicated.

2.3. THERMAL CONDUCTIVITY OF POLYMERS AT LOW TEMPERATURES

The main emphasis in numerous investigations of thermal conductivity has been placed on the temperature range close to room temperature. Let us consider to what extent the regularities found for this region are applicable at $T \to 0$ K.

The thermal conductivity of polymers has been studied primarily over the temperature range —190 to +90°C. The purpose of the majority of investigations was to establish the dependence of thermal conductivity on structure, chemical constitution, and temperature. The most important point here is a substantial difference in thermal conductivity between amorphous and crystalline polymers.

A typical feature of amorphous polymers is that up to the glass-transition temperature (T_g) thermal conductivity increases with rise of temperature and above T_g it begins to decrease (Fig. 2.2). An analogous fall in thermal conductivity above T_g has been observed for a number of amorphous polymers: natural rubber (101, 108), polyisobutylene (101), atactic polypropylene (109), polyvinyl chloride (101), polymethyl methacrylate (110). This behaviour of thermal conductivity near T_g is evidently typical for all amorphous polymers. Eierman (111, 112) made an attempt to explain this phenomenon, using conceptual models which, in his opinion, could be applied to all amorphous materials.

Eierman assumed that in an amorphous substance each bond between neighbouring atoms is equivalent to thermal resistance and calculated such an elementary thermal resistance r_e. The thermal resistance of a macroscopic amorphous sample is, according to Eierman, a network of elementary thermal resistances with atoms situated at the entanglement points. The elementary thermal resistance depends on the bonding forces operating between atoms. It decreases with increases in the elastic constant k_b which characterizes the bond. Therefore, the principal-valency chain of the polymer has a considerably lower thermal resistance than the van der Waals bond. The magnitude of the elementary thermal resistance is given, according to Eierman, by the expression

$$r_e = \frac{1}{\text{const}\cdot C_A}\sqrt{\frac{m_A}{k_b}} \qquad (2.24)$$

where const ≈ 1; C_A is the heat capacity per atom; m_A is the mean arithmetic mass of two adjacent atoms.

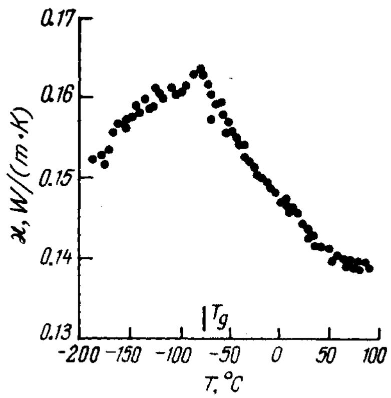

FIG. 2.2. Temperature dependence of the thermal conductivity ϰ of natural rubber.

Eierman's reasoning is based on the well-known Debye formula for the determination of thermal conductivity:

$$\varkappa = \Lambda\rho C\bar{c}l \qquad (2.25)$$

where Λ is a constant close to unity; ρ is the density; C is the heat capacity; $\bar{c}$ is the average velocity of sound; l is the mean free path of phonons.

Further it is assumed that

$$\varkappa = \Lambda\rho\sum_i C_i c_i l_i \qquad (2.26)$$

The subscript i refers to an individual wave from the vibrational spectrum. Assuming that the mean free path in amorphous substances coincides, at a first approximation, with the mean distance between two neighbouring atoms ($l \approx d$), Eierman writes the elementary thermal resistance in the form

$$r_e = \frac{1}{\varkappa_e} \cdot \frac{d}{ab} \tag{2.27}$$

where $\varkappa_e$ is the elementary thermal conductivity calculated from formula (2.25); the quantities a and b characterize the cross-sectional area of the volume element.

The velocity of sound in calculations of thermal resistance in the principal-valency chain is determined by the formula

$$\sqrt{\frac{k_b}{m}} \tag{2.28}$$

where k_b is the elastic constant which characterizes the bonding force between two neighbouring atoms with masses m_1 and m_2; $m = (m_1 + m_2)/2$.

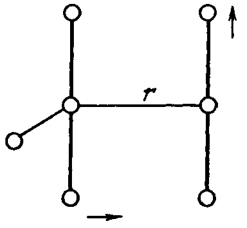

FIG. 2.3. The Eierman diagram of intermolecular interaction (111). The vertical arrow shows the direction of polymeric chains.

Formula (2.28) describes the propagation of a longitudinal wave in a chain of atoms. An analogous expression is written for a transverse wave. For the density of the volume element in Eq. (2.26) use is made of the formula $\rho_e = m/abd$. Such a consideration leads to the expression for the elementary thermal resistance (2.24). For the elementary thermal conductivity the following formula obtains:

$$\varkappa_e = \Lambda \frac{C_A d}{ab} \sqrt{\frac{k_b}{m}} \tag{2.29}$$

The thermal resistance due to the van der Waals interaction between adjacent chains is much greater than r_e in the chain of principal valency. To calculate the elementary thermal resistance due to the van der Waals forces, it is necessary to determine the corresponding elastic constants. They are found by using the intermolecular interaction potential in the form

$$\Phi_W = -2E\left(\frac{r_{\min}}{r}\right)^6 + E\left(\frac{r_{\min}}{r}\right)^{12} \tag{2.30}$$

where r is the distance between the interacting atoms situated in neighbouring polymeric chains (Fig. 2.3); $r_{\min}$ is the distance between the same atoms, corresponding to the minimum of the potential energy E.

The Eierman theory makes it possible to account for the fall of thermal conductivity in amorphous polymers above T_g. We know that in amorphous polymers above T_g the thermal expansion is substantially increased, as a result of which the free volume increases. This leads to an increase in the mean distance between neighbouring chains and, hence, to a decrease in the elastic constants caused by the intermolecular interaction. As a result, thermal resistance is increased and, hence, thermal conductivity decreases. Since the thermal conductivity of amorphous polymers depends first of all on the van der Waals bonds, the change in the temperature coefficient of thermal conductivity is intimately connected with the change in the thermal cubic expansion coefficient at T_g (111):

$$\Delta\left(\frac{1}{\varkappa}\cdot\frac{d\varkappa}{dT}\right)=-5.8\Delta\beta \qquad (2.31)$$

where $[(1/\varkappa)\cdot(d\varkappa/dT)]$ is the temperature coefficient of thermal conductivity; β is the cubic expansion coefficient.

Relation (2.31) holds true for various amorphous polymers and is independent of temperature (108).

In oriented amorphous polymers, the heat conduction in the direction of the orientation axis is greater than in the perpendicular direction. The Eierman theory (108, 111, 112) provides an explanation for this phenomenon. When polymeric chains are being oriented, the principal-valency bonds, which have a low thermal resistance, are arranged along the direction of orientation, and the van der Waals bonds, which have a high thermal resistance, are arranged at right angles to it. The model proposed by Eierman (111, 112) yields the following relation:

$$\frac{1}{\varkappa_{\parallel}}+\frac{2}{\varkappa_{\perp}}=\frac{3}{\varkappa_0} \qquad (2.32)$$

where $\varkappa_{\parallel}$ is the thermal conductivity of the polymer along the orientation axis; $\varkappa_{\perp}$ is the thermal conductivity of the same polymer, measured at right angles to the direction of orientation; $\varkappa_0$ is the thermal conductivity of an isotropic sample of the same polymer.

This equation works well for polymethyl methacrylate and some other polymers near room temperature.

Amorphous-crystalline polymers can be divided into two groups according to the temperature dependence of thermal conductivity. In the first group we find polyethylene and polyformaldehyde, whose thermal conductivities decrease with increasing temperature. The second group includes all other crystalline polymers (polyethylene terephthalate, isotactic polypropylene, polytrifluorochloroethylene, polytetrafluoroethylene, etc.), whose thermal conductivities increase with rise of temperature. The temperature dependence of the thermal conductivity of crystalline polymers belonging to the second group is analogous to that for amorphous polymers. The magnitude of thermal conductivity is appreciably affected by the degree of crystallinity of the polymer. This influence is especially pronounced at low temperatures.

The thermal conductivities of amorphous and crystalline polymers at low temperatures are fundamentally different. The temperature dependence of the $\varkappa$ of crystalline polymers is similar to the analogous dependence of imperfect crystals. On the curve of $\varkappa$ versus T we observe a maximum near 100 K, which shifts to low temperatures with increasing degree of crystallinity. The height of the maximum increases in this case (Fig. 2.4).

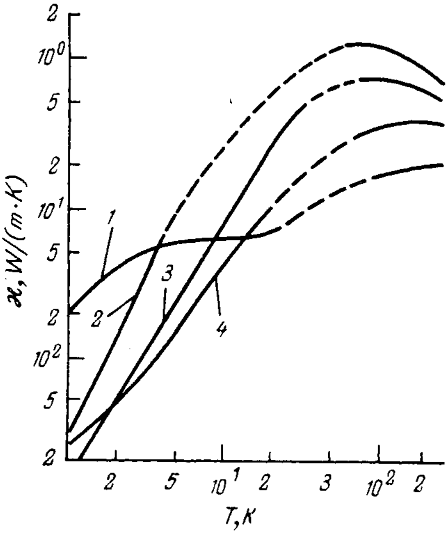

FIG. 2.4. Thermal conductivity of amorphous and crystalline polymers at low temperatures:

1—polymethyl methacrylate; 2, 3, 4—polyethylene samples with densities 0.98, 0,96, and 0.92 Mg/m³, respectively.

The temperature dependence of the thermal conductivity of amorphous polymers is similar to that of glass; it has no low-temperature maximum, but in the range 5-15 K a plateau appears. Above and below this region the thermal conductivity increases with rise of temperature. We have said above that the thermal conductivity of polymers depends significantly on the orientation. In the region of helium temperatures, however, the orientation either has no or a very slight effect on the thermal conductivity of amorphous polymers. Thus, it has been found that the thermal conductivities of isotropic, stretched (99) and extruded (97) samples of polymethyl methacrylate near the temperature of liquid helium are practically the same.

Theories that explain the thermal conductivity of polymers can be grouped into two classes: (1) theories which rely on the theory of the liquid state (111-114) and treat the transfer of energy between the repeat units via chemical bonds (primary or secondary) as an individual uncorrelated phenomenon; (2) theories which make use of the concepts of solid-state theory and deal with the cooperative motion of repeat units and the phenomena of phonon scattering which limit the region of energy transfer (115). At low temperatures, when vibrations are excited with a wavelength much greater than the distances between the repeat units, theories of the second type are resorted to.

In the case of amorphous polymers at high temperatures, when the mean free path is of the same order as the distance between the repeat units, the theories of the second type in application hardly differ from the theory of the liquid state. The criterion for the applicability of theories of the second type to the problems of heat conduction in polymers is as follows: the mean free path must be much greater than the distance between particles. Obviously, only in such a case can one speak of cooperative vibrations. In describing the thermal conductivity of polymers in the low-temperature region, mostly theories of the second type are used. Energy transfer in polymers is ordinarily described with the aid of the Debye formula, which, according to Klemens (91), can be written in the form:

$$\varkappa = \alpha C\bar{c}l \tag{2.33}$$

where $\alpha = \cos^2 \theta$ (θ is the angle between the direction of the path of phonons and the direction of energy transfer); C is the thermal conductivity per unit volume.

With the exception of oriented polymers, $\alpha = 1/3$.

The main task here, as in other cases, is to calculate the mean free path. There exist two types of phenomena which determine the magnitude of the mean free path: the interaction between phonons and the interaction of phonons with defects. For a number of amorphous-crystalline polymers the phonon-phonon interaction is probably the prevailing mechanism at relatively high temperatures. As a consequence, $\varkappa$ is proportional to $1/T$. If the thermal resistance of polymers were caused only by "Umklapp" processes, which can occur at $T < \theta_D$, then in this case at low temperatures the thermal conductivity would be proportional to exp (θ_D/T).

In the presence of defects the mean free path l decreases. Thermal conductivity is simultaneously reduced. Different types of defects necessarily give rise to different types of temperature dependence of $\varkappa$. Strictly speaking, these arguments apply to crystalline solids, whose thermal conductivity increases with fall of temperature, passes through a maximum and then decreases again.

The temperature of the maximum usually decreases as the number of defects is reduced.

One of the first attempts to extend the conceptions that are valid for crystalline solids to amorphous substances was undertaken by Klemens (91). He assumed that the "elastic" disorder in the structure of glassy substances can be responsible for the scattering of phonons at any temperature. Klemens coined the term "structural scattering" for processes of this kind. The origin of structural scattering is shown in Fig. 2.5. From this figure it is seen how the advancing front of a plane wave that passes through a medium in which there are regions with different sound velocities is distorted. The most important criterion for structural scattering is the ratio of the wavelength of the phonon to the length of elastic correlation. When the wavelength of the phonon and the elastic correlation length are of the same order of magnitude, the scattering is most intensive and the mean free path will be of the same order as the length of elastic correlation. If the wavelength is much larger than the length of elastic correlation, the resulting distortion of the wavefront is not great and the difference between the successive wavefronts is smaller than the difference between the sites of elastic disorder.

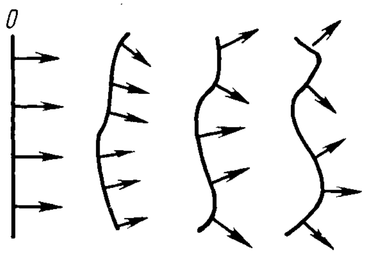

FIG. 2.5. Diagram showing structural scattering. The arrows indicate the direction of the velocity of an elastic wave; as a result of structural scattering, the wavefront changes by a distance equal to one wavelength.

Klemens assumed that in the case of long waves the mean free path of the phonon, l, is connected with its wave vector k by the following relation:

$$l = A/(ak^2) \tag{2.34}$$

where A is a constant characterizing the elastic correlation length; a is the distance between oscillating units.

From the Klemens theory it follows that at low temperatures thermal conductivity must be proportional to the absolute temperature.

The structural scattering of phonons was studied by Klemens (116, 117) and later critically analysed by Ziman (92) (see page 55). Klemens found (116) that if the correlations have a non-spherical symmetry (l is not proportional to $1/k^2$), then at $T \rightarrow 0$ there are possible temperature dependences of thermal conductivity which are different from the dependence $\varkappa \propto T$. The theory of structural scattering predicts that for short waves l is proportional to Aa and for long waves l is proportional to $1/k^2$. While examining the question of the nature of the plateau in the temperature dependence of thermal conductivity for silicate glasses, Klemens had to assume (117) that the parameter A for longitudinal waves is much larger than for transverse waves. In fact, this hypothesis is based on the assumption that in a glassy material the change of the velocity, δc_T, of transverse waves is considerably greater than that of the velocity, δc_L, of longitudinal waves. From this hypothesis it follows that the main contribution to low-temperature thermal conductivity comes from longitudinal waves. A more detailed analysis led Klemens to a conclusion on the manner in which the predominant effect of longitudinal phonons on thermal conductivity is realized. As a result of the interaction, longitudinal phonons are converted into transverse phonons, which are intensively scattered. The transformation of longitudinal into transverse waves limits the mean free path and leads to the appearance of a low-temperature plateau in the temperature dependence of thermal conductivity. In order to account for this process, Klemens formulated thermal conductivity as follows:

$$\varkappa = \varkappa_L + \varkappa_T \tag{2.35}$$

where $\varkappa_L$ is the contribution of longitudinal waves to thermal conductivity and $\varkappa_T$ is the contribution made by transverse waves.

The expression for $\varkappa_L$ takes the form

$$\varkappa_L = \frac{k_0^2}{3\pi h} \cdot \frac{A}{a} T y^2 \int_0^\infty \frac{e^x}{(e^x - 1)^2 x^2} \cdot \frac{x^2}{x^2 + y^2} \, dx \tag{2.36}$$

where k_0 is the Boltzmann constant; h is Planck's constant; x and y are dimensionless parameters [$x = h\nu/(k_0 T)$; $y^2 = (T_0/T)^3$, where T_0 is the parameter which has the dimensions of temperature and characterizes the process of transformation of longitudinal into transverse phonons].

The expression for $\varkappa_T$ has the form

$$\varkappa_T = \frac{1}{3} v_T C l_T \tag{2.37}$$

where v_T is the group velocity of transverse phonons; l_T is the mean free path of transverse phonons ($l_T = A_T \cdot a$).

Rees (115) modified the Klemens theory, assuming that expression (2.37) can be formulated as the sum of two terms, just as in the Tarasov model of the heat capacity of polymers. Then, the part of the thermal conductivity due to three-dimensional lattice vibrations is given by

$$\varkappa_3 = \frac{1}{3} v_T C_3 l_T \tag{2.38}$$

where C_3 is the part of heat capacity due to three-dimensional vibrations.

The part of thermal conductivity that is associated with one-dimensional vibrations is defined as

$$\varkappa_1 = \alpha v_1 C_1 l_1 \tag{2.39}$$

where α is a whole number accounting for the orientation of chains; v_1 is the velocity of propagation of one-dimensional vibrations, which can be determined if the characteristic temperature θ_1 is known.

Taking cognizance of expressions (2.37) through (2.39), we can write formula (2.35) as follows:

$$\varkappa = \varkappa_L + \frac{1}{3} v_T C_3 l_T + \alpha v_1 C_1 l_1 \tag{2.40}$$

The use of formula (2.40) enabled Rees (115) to describe satisfactorily the thermal conductivity of some amorphous polymers at low temperatures.

An attempt has been made (118) to show that the low-temperature plateau on the curve of $\varkappa$ versus T, which is a specific feature of all amorphous substances, results from resonance scattering due to those vibrations which lead to excess heat capacity. The theory advanced by Dreyfus, Fernandes and Maynard (118) differs little from the Klemens theory, except for the terminology used.

2.3.1. THERMAL CONDUCTIVITY OF CRYSTALLINE POLYMERS

One of the parameters that have an appreciable effect on the magnitude and mode of variation of thermal conductivity at low temperatures is the degree of crystallinity λ. The thermal conductivity of a partly crystalline polymer is usually treated as a particular combination of the thermal conductivities of completely amorphous and crystalline samples of the same polymer. Hansen (114) assumed that the thermal conductivity of a partly crystalline polymer can be represented as follows:

$$\varkappa = \lambda \varkappa_{cr} + (1 - \lambda) \varkappa_{am} \tag{2.41}$$

where λ is the degree of crystallinity; $\varkappa_{cr}$ and $\varkappa_{am}$ are the thermal conductivities of a completely crystalline and a completely amorphous sample of the same polymer.

In order to take account of the effect of the degree of crystallinity on thermal conductivity, Eierman (111-113) made use of the formula derived by Maxwell for the determination of the electrical conductivity of a mixture consisting of spherical particles uniformly distributed in a homogeneous continuous medium:

$$\varkappa = \frac{2\varkappa_{am} + \varkappa_{cr} + 2\lambda(\varkappa_{cr} - \varkappa_{am})}{2\varkappa_{am} + \varkappa_{cr} - \lambda(\varkappa_{cr} - \varkappa_{am})]} \varkappa_{am} \tag{2.42}$$

Using formula (2.41) or (2.42), one can determine the thermal conductivity of amorphous and completely crystalline polymers. Calculations of this kind should be carried out very cautiously because the parameters $\varkappa_{cr}$ and $\varkappa_{am}$ vary strongly with a change of temperature over a wide range. In such a case, the densities of amorphous and crystalline samples are also greatly altered. Formulas (2.41) and (2.42) contain, as a rule, the values of crystallinity λ calculated by formula (1.68) from the results of calculations of ρ_{cr} and ρ_{am} at room temperature. The question of using formula (2.42) is highly problematic since it is valid only in those cases where the crystalline regions are uniformly distributed as inclusions in the amorphous matrix. In dealing with highly crystalline polymers, say, polyethylene and polytetrafluoroethylene, one finds instead disordered regions distributed in imperfect crystals, and formula (2.42) no longer holds true. Besides, formula (2.42) does not agree even qualitatively with experimental data at low temperatures. The use of formula (2.41) is more justifiable.

Polyethylene. Polyethylene is one of the most thoroughly studied polymers. But even for this polymer there are no experimental data on thermal conductivity in the temperature range from 4 to 300 K. The thermal conductivity of polyethylene has been experimentally studied in the range from 0.15 to 20 K and in the temperature region of 80-350 K (101, 119). There is still a gap in experimental values of the thermal conductivity of polyethylene (just as for other polymers) between 20 to 80 K.

The temperature dependence of the thermal conductivity of linear polyethylene at low temperatures is presented in Fig. 2.6 for three samples of differing density (33). A characteristic feature of the low-temperature dependence of the thermal conductivity of this polymer is the growth of $\varkappa$ with increasing degree of crystallinity accompanied by the shift of the low-temperature maximum to low temperatures. At very low temperatures (down to 5 K) the thermal conductivity of polyethylene increases almost linearly with rise of temperature. Above the temperature of the maximum, which is about 50 K, $\varkappa$ is proportional to $1/T$.

A detailed study of the thermal conductivity of polyethylene near the temperature of liquid helium (1-4.5 K) has been made by Rees and Tucker (40), who measured the $\varkappa$ value of three types of polyethylene samples with densities 0.964, 0.938, and 0.917 Mg/m^3 and crystallinities 85, 66, 51 per cent. The results of these measurements, which are given in Fig. 2.6, have been interpreted within the framework of the Klemens theory as modified by Chang and Jones (120). It was assumed that the low-temperature thermal conductivity of polyethylene is due to a combination of two processes: structural scattering and scattering on "internal" boundaries. The analysis was carried out with the aid of the following formula (120):

$$\varkappa = \frac{k_0^2 T}{6\pi^2 \hbar^2} \cdot \frac{A}{a} \int_0^\infty \frac{x^4 e^x}{(e^x - 1)^2} \times$$
$$\times \left(\frac{dx}{x^2 + \frac{A}{a} \cdot \frac{v^2}{l} \cdot \frac{\hbar^2}{k_0^2 T}} \right) \qquad (2.43)$$

where l is the mean free path (it is assumed that l is independent of temperature since it is determined by the boundaries of the crystalline regions); the remaining notation is the same as in formula (2.36).

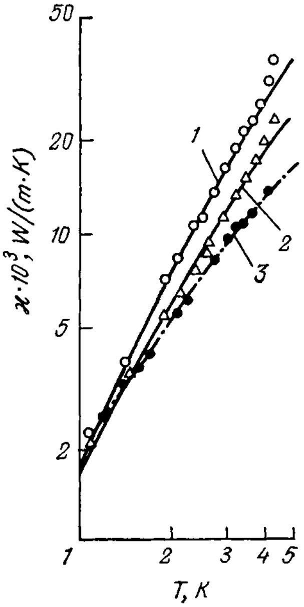

FIG. 2.6. Thermal conductivity of polyethylene at very low temperatures; the density of polyethylene is as follows, Mg/m^3:
1—0.964; 2—0.938; 3—0.917.

The values of the integral in formula (2.43) for different values of the integrand have been calculated by Callaway (121). In deriving formula (2.43) a number of fundamental assumptions were made: the processes indicated above proceed independently of each other; only longitudinal vibrations participate in heat transfer at low temperatures; the Debye formula can be used for the density of phonon states. Moreover, expression (2.43) is valid only at $T \ll \theta_D$. Using expression (2.43), Rees and Tucker (40) calculated the parameters A/a and l on the basis of their experimental data and compared them with the average diameters of spherulites, $\overline{D}$, in polyethylene, which they observed under an optical polarizing microscope. The results of this comparison are collected in Table 2.1.

The values of the average velocity of sound that were required for the calculation of A/a and l were calculated by Rees and Tucker from the formula

$$C/T^3 = 2\pi^2 k_0^4 / 5\hbar^3 \bar{v}^3 \qquad (2.44)$$

by using the values of heat capacity C measured by them. The good correlation obtained by Rees and Tucker between the mean free path due to scattering on the inner boundaries and the average diameter of spherulites seems to be accidental, given the crude assumptions made in the derivation of formula (2.43) and also because the values of the sound velocity used in the calculations were lower than those found experimentally at $T = 4.2$ K (122). The values of $\bar{v}$ listed in Table 2.1 are considerably lower than the velocities of longitudinal waves in polyethylene at helium temperatures (3690 m/s) and are closer to the speed of transverse waves (2015 m/s). Naturally, the value of $\bar{v}$ that appears in expression (2.44) must be greater than the speed of transverse waves [see formula (1.17)].

TABLE 2.1. *The Structural Parameters of Polyethylene*

Sample	ρ, Mg/m^3	$A/a \cdot 10^{-8}$, cm^{-1}	$l \cdot 10^4$, cm	$\bar{D} \cdot 10^4$, cm	$\bar{v} \cdot 10^{-5}$, cm/s
I	0.964	1.3	0.91	1.5	2.06
II	0.938	7.8	1.2	1.5	1.99
III	0.917	4.1	3.3	2.9	1.86

Kolouch and Brown (95) measured the thermal conductivity of several polyethylene samples with densities ranging from 0.914 to 0.971 Mg/m^3 in the temperature range 1.2-20 K and, having made calculations analogous to those carried out by Rees and Tucker (40), found no correlation between the mean free path and the sizes of spherulites. They modified expression (2.43), assuming that transverse phonons too make a contribution to thermal conductivity. The temperature-independent parameter l_1 found from these calculations increased with increasing thickness of polyethylene lamellae, the thickness being found by measuring the small-angle X-ray scattering. The results of this comparison are shown in Table 2.2 (L_1 and L_2 are the characteristic sizes associated with two diffraction maxima that were observed during the small-angle X-ray scattering; the parameter L_2 is, according to Kolouch and Brown, the thickness of the lamellae).

The mean free path l in polyethylene, calculated by means of formula (1.87) from experimental data (95), increases considerably with decreasing temperature and increasing of crystallinity

TABLE 2.2. *The Parameters of Polyethylene According to Thermal Conductivity Measurements (95) and Structural Investigations*

Sample	ρ, Mg/m³	CH_3/100°C	$\bar{v}\cdot 10^{-}$, cm/s	From formula (2.43)			From Ref. (95)			
				$A/a\cdot 10^{-8}$, cm^{-1}	$l\cdot 10^4$, cm	$\bar{D}\cdot 10^4$, cm	$B/a\cdot 10^{-8}$	l_T, Å	L_1, Å	L_2, Å
I	0.971	0.17	2.26	11.5	1.54	7.5	37.7	185	442	200
II	0.956	0.5	2.17	5.96	0.82	9.3	17	66	354	132
III	0.933	1.30	2.01	4.13	2.21	44.0	8.69	40	273	95

(Fig. 2.7). Theoretical calculations that have been carried out with account taken of the contribution of transverse waves to thermal conductivity (95) are in good agreement with experimental

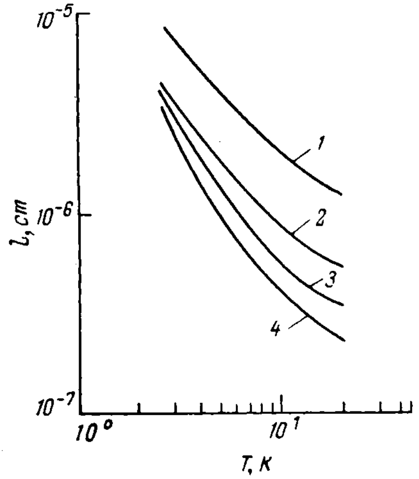

FIG. 2.7. The mean free path of phonons against temperature for polyethylene samples of various densities (Mg/m³):

1—0.971; 2—0.956; 3—0.933; 4—0.914.

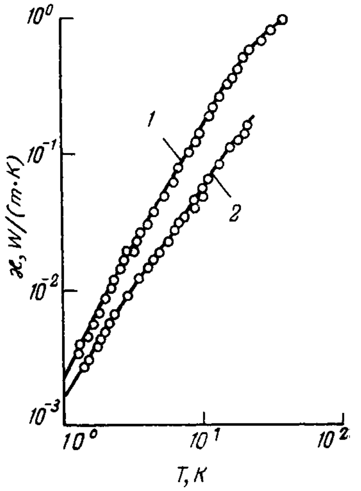

FIG. 2.8. Temperature dependence of the thermal conductivity of polyethylene of various densities, Mg/m³ (95):

1—0.971; 2—0.933.

values of ϰ for polyethylene (Fig. 2.8). Kolouch and Brown observed that for polyethylene near 8 K the thermal conductivity ϰ is proportional to T^3, while near 20 K the value of ϰ is proportional to T^2. The fact that in polyethylene there is a region in which ϰ is proportional to T^3 confirms the assumption that in this polymer there occurs phonon scattering on the boundaries of crystallites.

A substantial contribution to the low-temperature thermal conductivity of polyethylene is introduced by both the scattering on the boundaries of crystallites and the structural scattering of transverse waves.

Terry and his collaborators (105, 106) studied the thermal conductivity of polyethylene at very low temperatures (0.15 to 4 K). Their experimental results agree well with the data obtained by other investigators. Down to the temperature 1 K the values of $\varkappa$ obtained by Terry and his coworkers (105, 106) are described well by the Chang-Jones formula (2.43). Below 1 K a discrepancy is observed and the thermal conductivity depends on temperature more weakly than one would expect from formula (2.43) (Fig. 2.9). In order to describe theoretically experimental data, Terry (105) suggested that the Chang-Jones model be modified by replacing the three-dimensional (Debye) distribution function by a combination of two functions. It is supposed that the two-dimensional distribution function holds for frequencies less than a certain frequency ω_c (the cutoff frequency) and the three-dimensional distribution function is valid for frequencies $\omega > \omega_c$. The only physical argument in favour of this assumption is the lamellar shape of polyethylene crystallites. The use of the thus modified

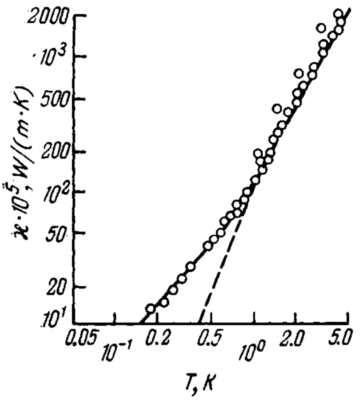

FIG. 2.9. Temperature dependence of the thermal conductivity of polyethylene (105). The dashed line represents the Chang-Jones model (128), and the solid line the Chang-Jones model as modified by Terry (105).

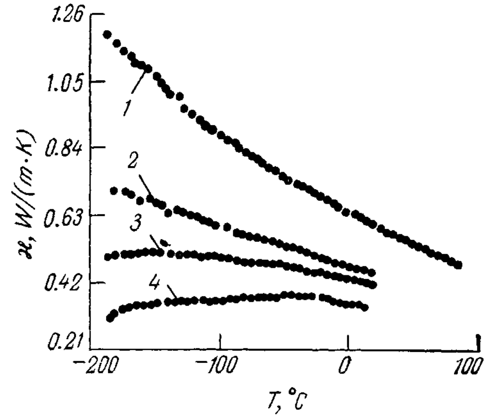

FIG. 2.10. Temperature dependence of the thermal conductivity of polyethylene of various densities, Mg/m³ (102):

1—0.982; 2—0.962; 3—0.951; 4—0.918.

Chang-Jones model has made it possible to describe well the experimental curve plotted by Terry and coworkers (105, 106). Other attempts have also been made to describe semi-empirically low-temperature heat conduction in polyethylene (123).

Detailed studies of the thermal conductivity of polyethylene at higher temperatures (80-350 K) have been conducted by Eierman (101, 102). Figure 2.10 shows the dependences $\varkappa = f(T)$ for polyethylene samples with different degrees of crystallinity.

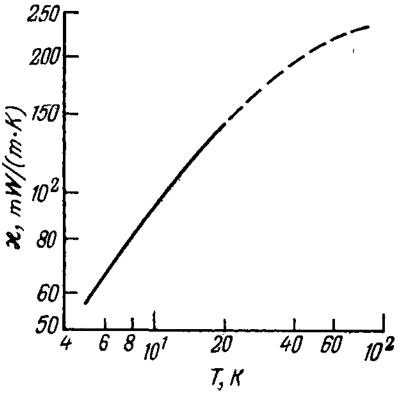

FIG. 2.11. Temperature dependence of the thermal conductivity of polytetrafluoroethylene. The dashed line shows the region of extrapolation.

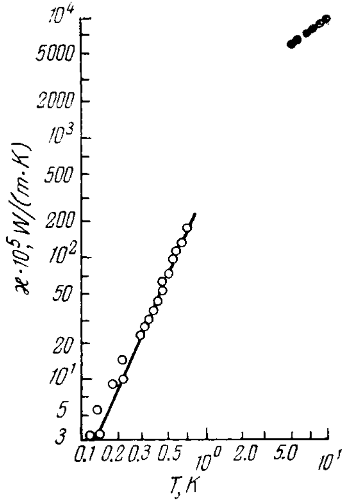

FIG. 2.12. Temperature dependence of the thermal conductivity of polytetrafluoroethylene at very low temperatures (96). Shown in the upper part are the experimental data obtained by Powell and coworkers (94).

Polytetrafluoroethylene. There are only a few works (40, 94, 96) devoted to the investigation of the thermal conductivity of polytetrafluoroethylene at low temperatures. Powell, Rogers and Coffin (94) measured the thermal conductivity of this polymer, with a density of 2.218 Mg/m^3, at temperatures from 5 to 20 K and also at 80 K (Fig. 2.11). The values of $\varkappa$ within the temperature range 20-80 K were obtained by interpolation. Anderson, Rees and Wheatley (96) measured the thermal conductivity of Teflon at lower temperatures (from 0.1 to 0.8 K) and found that, just as with some other amorphous polymers, the thermal conductivity of Teflon diminishes with decreasing T more rapidly than one would expect from the dependence $\varkappa \propto T$ (Fig. 2.12). In the range 0.3 to 0.7 K the thermal conductivity of polytetrafluoroethylene obeys the relation

$$\varkappa = \alpha T^n \tag{2.45}$$

where $\alpha = 3.8 \times 10^{-3}$ W/(m ·K^{n+1}); $n = 2.4$.

That n appears to be close to 3 indicates that the thermal conductivity of polytetrafluoroethylene at these temperatures is due to the scattering of phonons on "internal boundaries" (for example, on the boundaries of crystallites) with a temperature-independent mean free path. Anderson, Rees and Wheatley (96) have shown that the thermal conductivity of polytetrafluoroethylene at very low temperatures may be described by the following formula:

$$\varkappa = \frac{AT^3}{1+BT^2} \tag{2.46}$$

where $A = 0.83 \times 10^{-2}$ W/(m ·K^4); $B = 1.6$ K^{-2}.

To the same degree of approximation we can write for the mean free path:

$$l = \frac{15}{2\pi^2} \cdot \frac{\hbar^3 \bar{c}^2}{k^4} A \tag{2.47}$$

where A is the empirical constant found from formula (2.46).

The mean free path of phonons in polytetrafluoroethylene, as estimated from formula (2.47), is 0.460×10^{-4} cm. It is interesting that this value is 16 times less than the mean free path of phonons in an epoxide resin based on bisphenol A at the same temperatures. From this it follows that the departure of the thermal resistance (the inverse of $\varkappa$) from the dependence $1/\varkappa \propto 1/T^3$ must occur at a higher temperature for Teflon.

Later, Rees and Tucker (40) investigated the thermal conductivity of polytetrafluoroethylene ($\rho = 2.16$ Mg/m^3) in the temperature range 1 to 4.5 K. The results of these measurements are in good accord with the data obtained by Anderson, Rees and Wheatley (96) but they are 25 per cent lower than the $\varkappa$ values reported by Powell, Rogers and Coffin (94). This discrepancy is accounted for by the fact that Rogers *et al.* studied polytetrafluoroethylene with a higher degree of crystallinity ($\rho = 2.218$ Mg/m^3). An attempt to make use of expression (2.43) for describing the thermal conductivity of this polymer gives the following values: $A/a = 11 \times 10^8$ cm and $l = 0.78 \times 10^{-4}$ cm. In these calculations, however, Rees and Tucker (40) used the velocity of longitudinal waves ($\bar{v} = 1070$ m/s) computed by means of formula (2.44) from experimental data on heat capacity. The velocity of longitudinal ultrasonic waves in polytetrafluoroethylene, as measured experimentally, is 2330 m/s (122). Therefore, attempts to find a correlation between the mean free path of phonons in polytetrafluoroethylene and the sizes of its spherulites are not substantiated (40). In actual fact, no such correlation exists (just as in the case of polyethylene).

The results of investigations of the thermal conductivity of polytetrafluoroethylene (101, 119) at higher temperatures (80-350 K) show (Fig. 2.13) that the $\varkappa$ of this polymer increases monotonically with rise of temperature, just as in the case of amorphous polymers. The absolute values of $\varkappa$ for polytetrafluoroethylene are, however, twice as high as those for amorphous polyvinyl chloride. A salient feature of the temperature dependence of the thermal conductivity of polytetrafluoroethylene is the decrease of $\varkappa$ and the appearance of a step in the $\varkappa = f(T)$ curve at 20°C. This effect is caused by a first-order phase transition which occurs in polytetrafluoroethylene at 20° C and is associated with the transformation of its unit cell from the triclinic (below 20°C) to the hexagonal system (above 20°C).

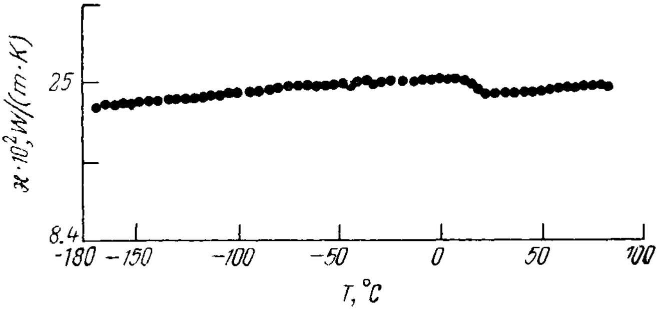

FIG. 2.13. Temperature dependence of the thermal conductivity of polytetrafluoroethylene.

Polyamides. The only representative of the polyamides whose thermal conductivity has been thoroughly studied is Nylon 6,6. Anderson, Rees, and Wheatley (96) measured the thermal conductivity of Nylon 6,6 at temperatures from 0.2 to 0.8 K (Fig. 2.14) and showed that the dependence $\varkappa = f(T)$ in this temperature range may be described with the aid of the empirical formula (2.45) if use is made of the following values: $\alpha = 2.6 \times 10^{-3}$ V/(m$\cdot$K^{n-1}) and $n = 1.75$. An alternative to this method of describing the experimental data is to use Eq. (2.46). It turns out that the parameters in Eq. (2.46) take on the following values: $A = 3.7 \times 10^{-2}$ V/(m$\cdot$K^4) and $B = 19.5$ K^{-2}. The mean free path calculated from experimental data (96) by formula (2.47) is equal to 2.1×10^{-4} cm. As in the case of polyethylene and polytetrafluoroethylene, an attempt has been made (40) to relate the values of the mean free path calculated from formula (2.43) to the average diameter of the spherulites. As a matter of fact, Rees and Tucker found that $l = 10.2 \times 10^{-4}$ cm and $\overline{D} = 11.8 \times 10^{-4}$ cm for one sample of Nylon 6,6 ($\rho = 1.144$ Mg/m^3) and $l = 1.8 \times 10^{-4}$ cm and $\overline{D} \leqslant 2.6 \times 10^{-4}$ cm for the other ($\rho = 1.140$ Mg/m^3).

But Kolouch and Brown (95) have shown that these values are incorrect and that, in fact, for Nylon 6,6 ($\rho = 1.41$ Mg/m^3) the value of l is equal to 2.32×10^{-4} cm [this being calculated from formula (2.43)] and $\overline{D} = 13.4 \times 10^{-4}$ cm. Thus, in the case of Nylon 6,6 there is no correlation between the mean free path and the size of spherulites. In contrast to polyethylene, in Nylon 6,6 there is no correlation between the mean free path calculated from expression (2.43) (as modified by Kolouch and Brown, that is with account taken of the contribution of transverse waves to thermal conductivity) and the characteristic size L_2, found from small-angle X-ray scattering. The latter quantity was termed the lamella thickness by Kolouch and Brown.

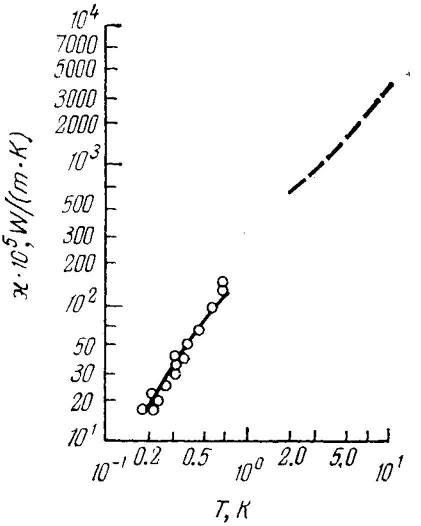

FIG. 2.14. Temperature dependence of the thermal conductivity of Nylon 6,6 at very low temperatures. The dashed curve represents the results of measurements made by Berman and coworkers (98).

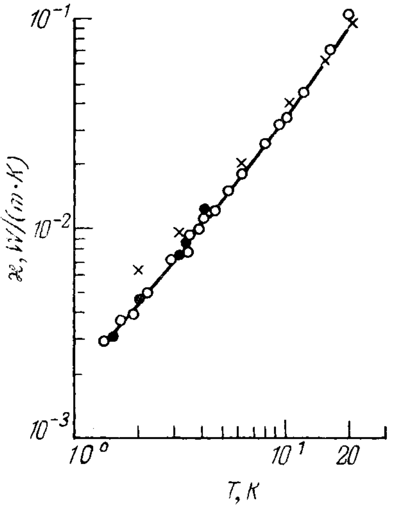

FIG. 2.15. Temperature dependence of the thermal conductivity o Nylon 6,6 (95).

At the same time, the experimental data obtained by Kolouch and Brown (95), which cover the temperature range from 1.2 to 20 K (Fig. 2.15), are in good agreement with the results of measurements carried out by Rees and Tucker (40) and also with

7he results of measurements in a monofilament fibre of Nylon 6,6 carried out by Berman and coworkers (98). Later measurements of thermal conductivity in Nylon 6,6 over the temperature range 0.15 to 4 K have also shown (105) that the main problem is to provide a theoretical interpretation rather than to establish a correlation between the experimental values of $\varkappa$ obtained by various authors (the experimental data obtained by different authors for Nylon 6,6 are virtually identical).

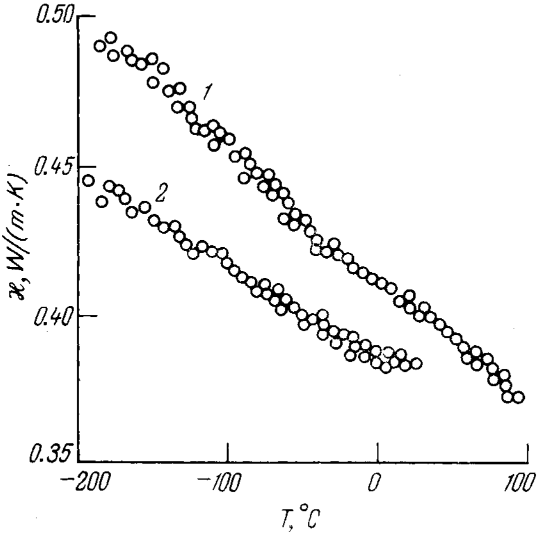

FIG. 2.16. Temperature dependence of the thermal conductivity of polyformaldehyde having the following densities (Mg/m^3):

1—1.441; 2—1.432.

Polyformaldehyde. This polymer (also known as polyoxymethylene) is a polymer whose thermal conductivity falls with increasing temperature (102). Eierman (102) measured the thermal conductivity of two well crystallized samples of polyformaldehyde ($\rho = 1.432$ Mg/m^3 and $\rho = 1.447$ Mg/m^3) at temperatures from 80 to 370 K (Fig. 2.16). If the thermal conductivity of fully crystalline polyformaldehyde is calculated with the aid of the Maxwell formula, it proves to be proportional to $1/T$.

The available experimental data on thermal conductivity are not sufficient to give a reasonable explanation for the fundamentally different dependences of the thermal conductivity of various crystalline polymers on temperature. The mechanism of heat conduction in crystalline polymers will be more clearly understood if one can obtain continuous dependences $\varkappa = f(T)$ for a number of different crystalline polymers at temperatures ranging from the liquid-helium temperature to the melting temperatures of these polymers.

2.3.2. THERMAL CONDUCTIVITY OF AMORPHOUS POLYMERS

A distinctive feature of the temperature dependence of the thermal conductivity of amorphous polymers is the absence of the low-temperature peak and also the existence of a plateau typical of crystalline polymers at temperatures 4-15 K. Below 2 K the temperature dependence of $\varkappa$ is usually close to linear, which agrees well with the predictions of the theory of structural scattering. Above the plateau region the thermal conductivity again begins to increase with rise of temperature. The thermal conductivity of amorphous polymers at low temperatures has been studied much less thoroughly than that of crystalline polymers. The most detailed and reliable experimental values available for $\varkappa$ at low temperatures are for polymethyl methacrylate.

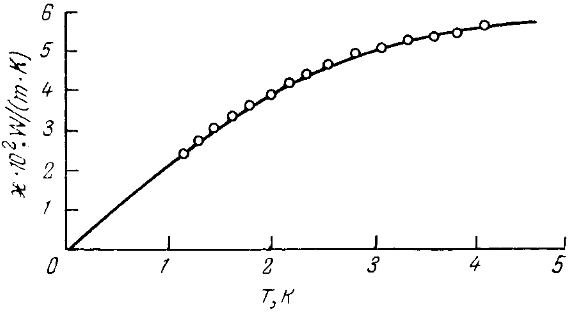

FIG. 2.17. Temperature dependence of the thermal conductivity of polymethyl methacrylate at low temperatures.

Polymethyl Methacrylate. Polymethyl methacrylate is a typical amorphous polymer: its low-temperature thermal conductivity has been thoroughly studied. As far back as 1951 Berman (97) studied the thermal conductivity of polymethyl methacrylate over a temperature range of 2.5-23 K. Later, Rees (99) investigated the thermal conductivity of polymethyl methacrylate at temperatures ranging from 1 to 4.5 K, using the same samples as had been used by Berman. Above 4 K the results of these investigations coincide, while below 4 K the values of $\varkappa$ obtained by Berman exceed the experimental data of Rees by 6.6 per cent (Fig. 2.17). Later, Stephens, Cieloszyk and Salinger (67) measured the thermal conductivity of polymethyl methacrylate below 1 K. At higher temperatures (from 90 to 400 K) the thermal conductivity of this polymer has been studied by Eierman (102, 119).

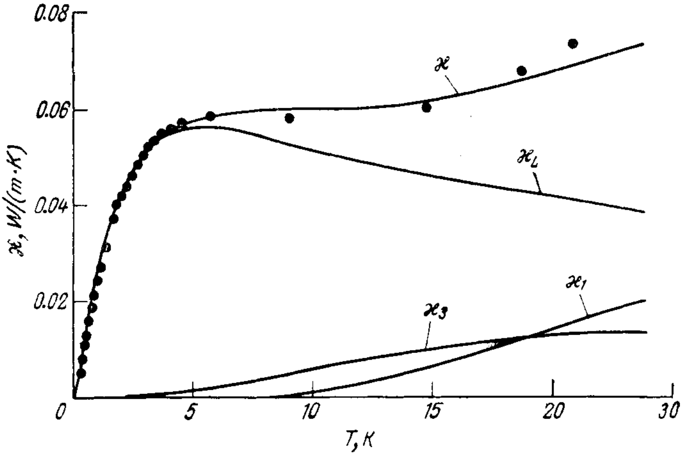

FIG. 2.18. Temperature dependence of the thermal conductivity of polymethyl methacrylate at low temperatures ($\varkappa_L$ is the part of thermal conductivity attributable to three-dimensional longitudinal vibrations; $\varkappa_3$ is the contribution of three-dimensional transverse vibrations; $\varkappa_1$ is the contribution of one-dimensional vibrations).

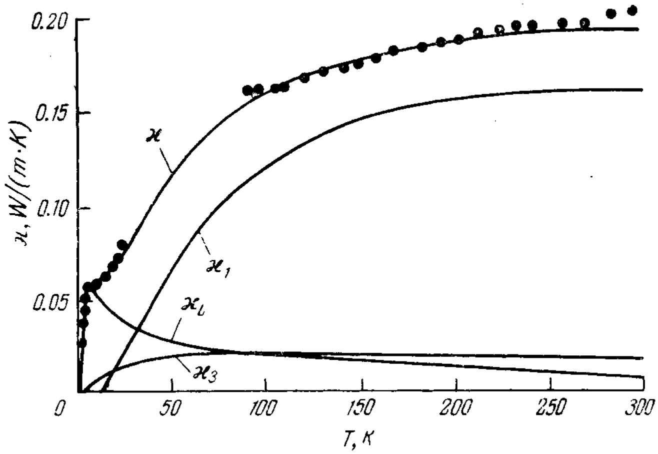

FIG. 2.19. Temperature dependence of the thermal conductivity of polymethyl methacrylate over a wide temperature range. The symbols are the same as in Fig. 2.18.

The temperature dependence of the thermal conductivity of polymethyl methacrylate is shown in Figs. 2.18 and 2.19 (67, 97, 99, 102, 119). To analyse the experimental data expression

(2.40) is used (33, 99), which is a modification of the results of the Klemens theory. A theoretical curve that describes the thermal conductivity of polymethyl methacrylate well has been plotted by using the following values of the parameters in formulas (2.36) through (2.40): $A/a = 22.4 \times 10^8$ cm^{-1}; $T_0 = 7$ K; the mean free path of transverse phonons $l_T = 7.1$ Å; $v_1 l_1 = 2.18 \times 10^{-2}$ cm^2/s. It has been demonstrated (115) that the mean free path resulting from longitudinal one-dimensional vibrations [see formula (2.39)], is $l_1 = 7.3$ Å. The characteristic temperatures are $\theta_3 = 39$ K and $\theta_1 = 171$ K. If it is assumed that the distance between the polymeric chains (estimated from the density) $a = 7.5$ Å, then $A = 168$ and $A_T = 0.63$.

Since these parameters are incorporated into the various terms ($\varkappa_L$ and $\varkappa_T$) on the right-hand side of Eq. (2.40), then it is obvious that the contribution of various types of phonons to thermal conductivity is not the same. The contribution of the transverse vibrations of a three-dimensional lattice to the total thermal conductivity of polymethyl methacrylate, $\varkappa$, is very small (Figs. 2.18 and 2.19). The fact that $A \gg A_T$ implies that the transverse three-dimensional vibrations are strongly damped and the major contribution to the low-temperature thermal conductivity of polymethyl methacrylate comes from the longitudinal waves. The fact that $A_T < 1$ creates certain difficulties in the application of the Klemens theory and for the explanation of the temperature dependence of $\varkappa$ for polymethyl methacrylate, since the mean free path of transverse phonons is $l_T = A_T a$.

According to the Klemens theory l must be of the same order as the distance a between the vibrating units. Nevertheless, it is believed (115) that the values of $A_T < 1$ can be accounted for on the basis of the Ziman theory (92); Ziman related the mean free path of phonons to the variation in sound velocity in an amorphous medium. In order for the values of $A_T < 1$ to be explained, one has to assume that large variations in the speed of transverse waves are possible and that the correlation length for such variations is very small, i.e., is commensurate with a.

From Figs. 2.18 and 2.19 it can be seen that the largest contribution to the low-temperature thermal conductivity of polymethyl methacrylate comes from longitudinal phonons. However, at higher temperatures (above 90 K) the contribution of $\varkappa_L$ to the total thermal conductivity becomes small, and the term $\varkappa_1$, depending on one-dimensional vibrations, begins to play a dominant role. This helps one understand why the orientation of amorphous polymers leads to a considerable increase in their thermal conductivity at high temperatures and does not substantially affect $\varkappa$ near the liquid-helium temperature. Indeed, it is known (99) that the thermal conductivity of polymethyl methacrylate stretched 3.75 times, measured in the direction of orientation in the temperature range 85-300 K, is 25-30 per cent higher than in an isotropic sample. At the same time, near the temperature of liquid helium this effect of orientation on $\varkappa$ becomes insignificant. Rees (99), while measuring the thermal conductivity of a sample stretched 2.15 times, found that it is only 6 per cent higher than in unoriented polymethyl methacrylate. The slight effect of orientation of the thermal conductivity of amorphous polymers at helium temperatures confirms the correctness of the conceptual model underlying formula (2.40).

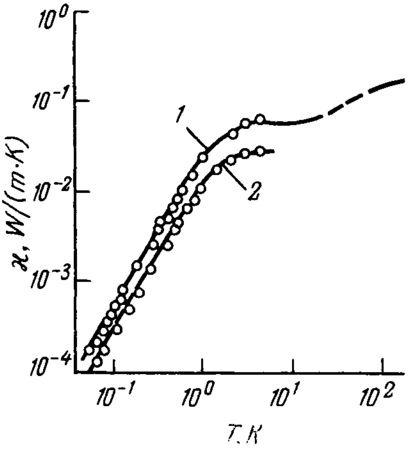

FIG. 2.20. Temperature dependence of the thermal conductivity of polymethyl methacrylate (1) and polystyrene (2) at very low temperatures.

The mean free path associated with three-dimensional vibrations and calculated for high temperatures on the basis of that model is found to be commensurate with a. This agrees well with the idea of elementary thermal resistance used by Eierman (111, 112) in his analysis of the thermal conductivity of polymers. A comparison of the theoretical concepts on which formula (2.40) is based leads one to the conclusion that the quantity $1/\varkappa_1$ plays a role analogous to that of thermal resistance due to covalent bonds in the Eierman model. The quantities $1/\varkappa_L$ and $1/\varkappa_3$ are to a certain degree analogous to the thermal resistances of the secondary bonds. It is interesting to note that the ratio of the thermal conductivity due to one-dimensional vibrations to the thermal conductivity associated with three-dimensional vibrations as calculated from Eqs. (2.38) through (2.40), is equal to 10 : 1 at 300 K, which fits the results following from the Eierman theory.

There is a considerable discrepancy between the theoretical values of $\varkappa$ and the experimental data at temperatures $T < 1$ K, at which the observed dependence of $\varkappa$ on temperature is stronger than the dependence of the type $\varkappa \propto T$ predicted by the theory. Indeed, Stephens and his coworkers (67) found that below 1 K for polymethyl methacrylate, as for some other amorphous materials (polystyrene, SiO_2, selenium), the thermal conductivity depends on temperatures as follows (Fig. 2.20):

$$\varkappa \propto T^n \qquad (2.48)$$

where $n = 1.8$.

It is assumed that the cause for this non-linear dependence of $\varkappa$ on temperature is an additional scattering mechanism analogous to boundary scattering in silicate glasses. Another factor that could lead to a dependence of the type (2.48) is a non-spherical symmetry of elastic correlations.

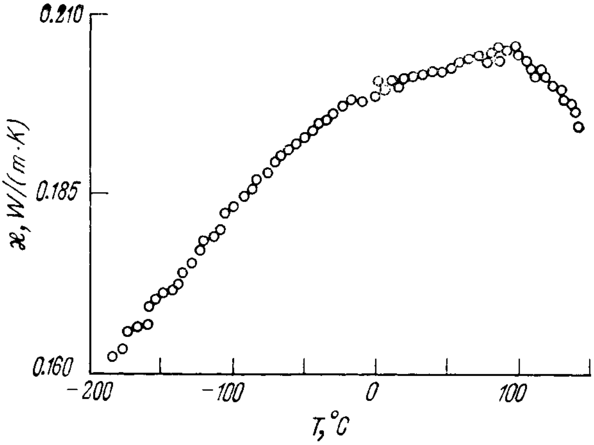

FIG. 2.21. Temperature dependence of the thermal conductivity of polymethyl methacrylate in the temperature range —196 to +140°C (102).

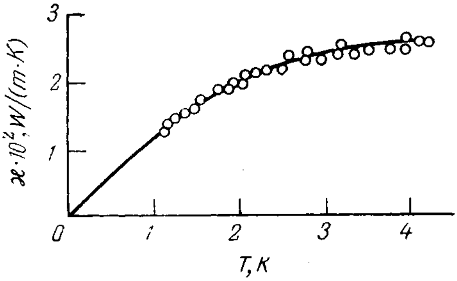

FIG. 2.22. Temperature dependence of the thermal conductivity of polystyrene at low temperatures.

For all amorphous materials for which the dependence (2.48) is valid one can observe a super-Debye excess heat capacity for the same temperature range (below 1 K). The low-temperature heat capacity of these substances is described by formula (1.85). The possibility cannot be excluded that a dependence of the type (2.48) and the presence of the super-Debye heat capacity at $T \ll 1$ K are features common to amorphous materials and do not depend on the chemical constitution (67).

The experimental values of $\varkappa$ for polymethyl methacrylate at $T > 80$ K have been obtained by Eierman (102, 119). A typical dependence of the thermal conductivity of this polymer on temperature is given in Fig. 2.21.

Polystyrene. There is a small amount of experimental data available on the thermal conductivity of polystyrene at low temperatures (67, 99). Rees (99) measured the thermal conductivity of two samples of polystyrene over the temperature range 1-4.5 K (Fig. 2.22). These results are in good agreement with the Klemens theory [see formulas (2.35) through (2.40)]. A comparison of the Klemens theory with experimental data (99) yields the following values for the parameters in formula (2.36): $A/a = 12.1 \times 10^8$ cm^{-1} and $T_0 = 6$ K. While the value of A/a for polystyrene appears to be lower by a factor of about 2 than for polymethyl methacrylate, the values of the parameter T_0, which characterizes the process of the transformation of longitudinal phonons to transverse ones, are practically the same for both polymers. As in the case of polymethyl methacrylate, $A \gg A_T$. This lends support to the Klemens hypothesis that transverse phonons are scattered more intensively than longitudinal phonons. In spite of the fact that the number of experimental values of $\varkappa$ obtained for polystyrene is very limited, it has nevertheless been possible to establish that the thermal conductivity of this polymer above 3 K is also independent of temperature (see Fig. 2.22). The upper limit of this low-temperature plateau cannot yet be determined because of the lack of relevant experimental data. It has been shown (67) that below 0.5 K the thermal conductivity of polystyrene depends on temperature in a non-linear fashion (see Fig. 2.20). At $T \to 0$, beginning at 0.5 K, the thermal conductivity of polystyrene varies in accordance with expression (2.48). It is believed (67) that this dependence of thermal conductivity on temperature at $T \to 0$ is typical for all amorphous materials.

In spite of some uncertainty in the interpretation of the non-linear temperature dependence of $\varkappa$ below 1 K, the mechanism of low-temperature heat conduction in amorphous polymers has been clarified in greater detail than in the case of crystalline polymers.

CHAPTER 3

THERMAL EXPANSION OF POLYMERS AT LOW TEMPERATURES

3.1. THERMAL EXPANSION OF SOLIDS

Thermal expansion is the change in the dimensions and shape of solids caused by a change of temperature. Any increase in temperature leads to an increase in the amplitude of the vibrations of atoms about their equilibrium positions. When considering thermal expansion the assumption that the vibrations of atoms are sinusoidal (harmonic) in character proves to be insufficient. The factor responsible for the thermal expansion of solids is the anharmonic nature of atomic vibrations.

The potential energy of two neighbouring vibrating atoms when they are displaced a distance x from the equilibrium position at a temperature of 0 K may be represented in the following form (3):

$$U(x) = \bar{f}x^2 - gx^3 - hx^4 \tag{3.1}$$

where $\bar{f}$ is the quasi-elastic force coefficient ($f = -\bar{f}x$); g is the anharmonicity factor.

The second term on the right-hand side of expression (3.1) takes account of mutual repulsion, while the third term allows for the "attenuation" of vibrations at high amplitudes. If the displacement of atoms from their equilibrium positions, x, is small, then the terms involving x^3 and x^4 may be neglected as compared with the term with x^2 and the vibrations will be harmonic. With relatively large displacements from equilibrium positions the vibrations become anharmonic, and these terms in the expansion can no longer be neglected. Let us find the average displacement $\bar{x}$ of atoms from their equilibrium positions, this being what determines the change in the size of solids with a change in temperature. To do this, use is made of the Boltzmann distribution function, which allows one to average out the values of any physical quantity with account being taken of the thermodynamic probability of the corresponding values. Then,

$$\bar{x}=\frac{\int\limits_{-\infty}^{\infty} x \exp\left[-U(x)/(kT)\right] dx}{\int\limits_{-\infty}^{\infty} \exp\left[-U(x)/(kT)\right] dx} \tag{3.2}$$

If the displacements of atoms are small enough (the anharmonicity of their vibrations is low), the integrand functions in expression (3.2) can be expanded into a series, and for the average displacement $\bar{x}$ we obtain the following expression (3):

$$\bar{x}=\frac{3kTg}{4f^2}=\varepsilon_T \tag{3.3}$$

where ε_T is the thermal expansion.

The coefficient of volume thermal expansion or volume expansivity is given by

$$\beta=3\alpha\frac{3gk}{4f^2} \tag{3.4}$$

where α is the coefficient of linear thermal expansion or linear expansivity.

If no anharmonicity is present (the anharmonicity factor $g = 0$) and the atoms vibrate harmonically, then the thermal expansion coefficient becomes zero.

In the equilibrium state the lattice vibrations occur in such a manner that the solid occupies a volume to which the minimum of Helmholtz free energy corresponds. With a rise in temperature the amplitudes of vibrations of atoms in the lattice and, hence, their mean average displacement $\bar{x}$ from their equilibrium positions increase. The anharmonic terms in expression (3.1) make such a contribution to the value of the free energy that it may be far from minimal. As a result, the solid will change its dimensions until its volume is such that it corresponds to the minimum of the potential energy.

The theory of the thermal expansion of solids is discussed in greater detail by Leibfried (82).

3.2. EQUATIONS OF STATE FOR SOLIDS

The thermal expansion coefficient is intimately connected with the main parameters of the equations of state of solids. To calculate the thermal volume expansion coefficient β of an isotropic solid we shall make use of the thermodynamic relations:

$$\beta=\frac{1}{V}\left(\frac{\partial V}{\partial T}\right)_p=3\alpha \tag{3.5}$$

Let us consider the product of the thermal expansion coefficient and the isothermal compressibility K_T:

$$\beta K_T = \frac{1}{V}\left(\frac{\partial V}{\partial T}\right)_p \left[-V\left(\frac{\partial p}{\partial V}\right)_T\right] = -\left(\frac{\partial p}{\partial T}\right)_V \qquad (3.6)$$

where p is the pressure.

It is known that

$$p = -\left(\frac{\partial F}{\partial V}\right)_T \qquad (3.7)$$

where F is the Helmholtz free energy; it is defined as

$$F = U - TS \qquad (3.8)$$

From relations (3.6) and (3.7) we find that

$$\beta K_T = \frac{\partial^2 F}{\partial V\, \partial T} \qquad (3.9)$$

The expression for the Helmholtz free energy can be represented as the sum of two terms, one of which depends on temperature and the other not. Assuming that the temperature-dependent part of the Helmholtz free energy of a solid is due to the lattice vibrations, we can write (124):

$$F = U_0 + \sum_j kT \ln\left[1 - \exp\left(-\frac{h\nu_j}{kT}\right)\right] \qquad (3.10)$$

where U_0 is the sum of the zero-point energy and the temperature-independent part of the internal energy.

The zero-point energy is defined as the energy of the lattice at $T = 0$ K. This energy corresponds to the lowest quantum-mechanical state and has a quantum nature. Even at absolute temperature the lattice of a solid has a zero-point energy composed of kinetic and potential energies. The classical concept of a lattice made up of atoms whose vibrations are stopped at absolute zero is incorrect. From quantum-mechanical considerations it follows that the vibrational motion of atoms is retained at absolute zero. The energy of the lowest quantum-mechanical state (the zero-point energy) is determined by the condition which states that the sum of the kinetic and potential energies must have a minimum. At low temperatures, when the kinetic energy of atoms is low, the positions of atoms in space appear to be "spread", which leads to an increase in the potential energy. The zero-point energy is, to a certain extent, a measure of such "spread". The "spread" of the positions of atoms in space will be especially great if the mass of the atoms is small. It should be pointed out that the zero-point energy can reach relatively high values. It can be compared with the thermal energy of atoms at room temperature.

Using relations (3.6) through (3.10), we get:

$$V\beta K_T = \sum_j \gamma_j \frac{dE_j}{dT} \tag{3.11}$$

The summation is carried out over all the normal lattice vibrations: E_j is the energy of the jth linear oscillator, and the parameter γ_j is equal to

$$\gamma_j = -\frac{V}{\nu_j}\left(\frac{\partial \nu_j}{\partial V}\right)_T = -\frac{d\ln \nu_j}{d\ln V} \tag{3.12}$$

The parameter γ_j is called the Grüneisen constant (or the Grüneisen gamma) and shows the relationship between the frequencies of normal vibrations and the volume of the solid. Grüneisen assumed (125) that all γ_j are equal.

This supposition is tantamount to assuming that the change in volume leads to a relative change in frequency which is the same for all vibrations. In such a case, expression (3.11) assumes the form:

$$V\beta K_T = \gamma \sum_j \frac{dE_j}{dT} \tag{3.13}$$

Hence,

$$V\beta K_T = \gamma C_v \tag{3.14}$$

The last expression is often written down in the form

$$\beta = \gamma \frac{C_v}{VK_T} \tag{3.15}$$

and is called the Grüneisen relation. From this equation it follows that the coefficient of volume thermal expansion is directly proportional to the heat capacity. Since at $T = 0$ K the heat capacity $C_v = 0$, it evidently follows that in this case the volume thermal expansion coefficient must vanish, which is in keeping with the third law of thermodynamics.

In the Grüneisen approximation γ is assumed to be a weakly varying function of volume. It is sometimes believed that the Grüneisen parameter is practically independent of temperature. Barron (126), however, has shown that the Grüneisen assumption that all γ_j are equal is not sufficiently accurate and he has introduced the concept of the mean value ν_m of the Grüneisen parameter. It has been demonstrated (126) that γ_m depends on temperature. In his calculations (126), Barron proceeded from the Born-von Kármán theory (6). A crystal consisting of N atoms is regarded by him (126) as an ensemble composed of $3N$ harmonic oscillators with frequencies of normal vibrations equal to ν_j. The equation of state is written in this case in the following way:

$$pV = -VE_0'(V) + \sum_{j=1}^{3N} \gamma_j \frac{h\nu_j}{\exp\left(\frac{h\nu_j}{kT}\right) - 1} \tag{3.16}$$

where p is the pressure; V is the volume; $E_0'(V)$ is the non-thermal contribution to the internal energy of the crystal.

Without resorting to the Grüneisen assumption of the equality of all parameters γ_j, we can calculate the mean value of the Grüneisen constant:

$$\gamma_m = \left[\sum_{j=1}^{3N} \gamma_j \frac{\frac{h\nu_j}{kT}}{\exp\left(\frac{h\nu_j}{kT}\right) - 1}\right] \div \left[\sum_{j=1}^{3N} \frac{\frac{h\nu_j}{kT}}{\exp\left(\frac{h\nu_j}{kT}\right) - 1}\right] \tag{3.17}$$

Employing this relation and the conceptual model of the interaction potential, Barron has shown (126) that $\gamma = f(T)$.

In the temperature region $T \ll 0.2\,\theta_D$ (here θ_D is the characteristic Debye temperature) when $kT \ll h\nu_j$, only long acoustic waves are excited in the lattice and the solid may be considered as a continuum. In this case the Grüneisen constant can be represented as a function of θ_D:

$$\gamma = -\frac{d \ln \theta_D}{d \ln V} = -\frac{V}{\theta_D} \cdot \frac{d\theta_D}{dV} \tag{3.18}$$

From the last equality it follows that the Grüneisen constant takes account of the effect of the change in volume on the Debye temperature. In fact, this concept is a very rough model of thermal expansion (127). Different lattice vibrations are influenced in different ways by thermal expansion. The Grüneisen constant for longitudinal elastic lattice waves is, as a rule, much larger than for transverse waves. Therefore, the contribution from different modes of lattice vibrations to thermal expansion is found to be different.

3.3. BASIC CONCEPTS OF THE THERMAL EXPANSION OF POLYMERS

3.3.1. THERMAL EXPANSION OF AMORPHOUS POLYMERS

There is as yet no sufficiently rigorous and consistent theory of the thermal expansion of polymers; this branch of polymer physics is now the object of intensive investigations. The major proportion of theoretical and experimental works are devoted to the study of the glass transition and the variation of the thermal expansion coefficient of polymers near T_g. It is sometimes presumed that polymers have two thermal expansion coefficients. One of them is taken to be independent of temperature at $T < T_g$, and the second to be weakly dependent on temperature at $T > T_g$ and greater than the first. At the same time, experimental data show that the thermal expansion coefficients of polymers vary with temperature below and above the glass-transition temperature. These data (128, 129) indicate that even at very low temperatures near the liquid-helium temperature the thermal expansion coefficients of all the polymers studied vary with temperature and tend to zero at $T \rightarrow 0$.

Let us now consider the thermal expansion of amorphous polymers in the glassy state, which occurs in polymers at low temperatures. The presence of an amorphous halo (the inner ring) on the X-ray diffraction patterns of amorphous polymers shows that they are not completely disordered systems; there are local regions in them in which a short-range order is retained. In this connection, there have been made attempts to apply the cell theory originally developed for simple liquids to amorphous polymers for the purpose of describing their thermal properties.

Prigogine and his coworkers (130-132) treated an n-dimensional molecule as a set of n point centres of mass of monomers. He conjectured that these centres form a quasi-crystalline lattice with a coordination number of 12 (the face-centred cubic lattice). In these computations, the intramolecular interaction was disregarded and attention was focused only on the forces of intermolecular interaction, which are characterized by the Lennard-Jones potential for the mass centres of repeating units. The distribution function was then sought on the basis of the cell model. The equation of state thus obtained satisfied the principle of corresponding states, which had been established (133) for liquids consisting of chain molecules without recourse to the cell model.

Simha, Havlik and Nanda (134, 135) examined the thermodynamic properties of polymeric and oligomeric liquids by proceeding from a cell theory which includes a parameter taking account of the external degrees of freedom of segments and serves as a measure of chain flexibility. The equation of state derived theoretically is in good agreement with the available experimental data on the dependence of volume on temperature.

Flory (136) differentiated between the segments situated at the ends of and within the chains, since they must have different numbers of external contacts. He also derived an equation of state for normal paraffins, assuming that the energy of intermolecular interaction is inversely proportional to the volume.

Di Benedetto (137) applied the cell model to amorphous polymers, assuming that each chain centre is surrounded at equal distances by four parallel chains. The equation of state obtained was based on the assumption that a potential of the Lennard-Jones type can be used to describe the interaction between the repeating units of the nearest chains forming a tetragonal lattice.

The relationship between pressure, temperature, volume and the glass-transition temperature has been examined. The molecular constants and cohesive energy density of some amorphous polymers have been calculated from experimental values of the thermal expansion coefficient and the isothermal compressibility. Nevertheless, this theory has not gained recognition since the free-volume concept is disregarded in the consideration of the rubbery (high-elastic) state; in particular, the formation of holes is ignored. Later, attempts were undertaken (138, 139) to describe amorphous polymers in terms of a cell theory in which holes were treated as necessary structural elements. Paul and di Benedetto (140) have shown that the thermodynamic properties of amorphous polymers can be described by introducing a structure parameter which takes account of the size of molecular units.

The problem of the thermal expansion of amorphous polymers has been examined in detail by Ishinabe and Ishikawa (141). They assumed that polymeric chains in the amorphous state form the hexagonal (coordination number 6) or tetragonal (coordination number 4) lattice. These authors discussed the asymmetry of the field of dispersion forces associated with the coupled interaction between the repeating units of the various chains. The total potential energy was determined through the summation of coupled interactions throughout the entire lattice, with the exception of the energy of each polymeric chain. This treatment is, in effect, analogous to that based on the use of the Einstein model for a solid and allows one to describe the thermodynamic properties of polymers in the glassy state with account taken of the part played by the van der Waals volume.

Let us consider in more detail the basic premises of the theory proposed by Ishinabe and Ishikawa (141), since they are typical of other theoretical investigations.

Since in amorphous polymers there exists a short-range order (and, possibly, ordered regions as well), it is assumed that at a certain distance the repeating units of polymeric chains arrange themselves parallel to one another, form *trans*-conformations and build the hexagonal lattice (Fig. 3.1). Furthermore, it is presumed that a polymer is a single-phase system consisting of N homogeneous n-dimensional chains, each of which can be regarded as a set of n centres of force. Each of these centres can move only in a plane perpendicular to the chain axes. The cross-sectional area of such a hexagonal lattice formed by polymeric chains is depicted in Fig. 3.2, with the size of the cells and the position of the shells rather strictly defined. The volume of one cell is

$$v = \lambda \gamma_c r^2$$

where λ is the distance between two neighbouring centres of force along the chain; γ_c is a geometric factor equaling 0.866

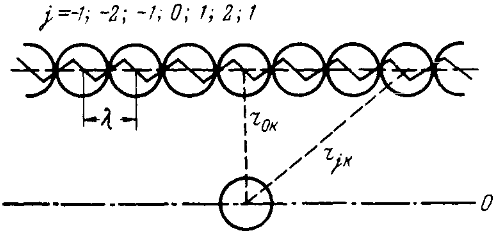

FIG. 3.1. The interacting-chain model (141) (λ is the distance between neighbouring centres along the chain; r_{0k} is the distance between the nearest force centres of neighbouring chains; r_{jk} is the distance between the centre of forces at the coordinate origin and the jth centre in the kth shell).

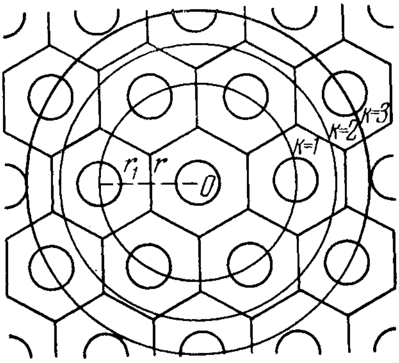

FIG. 3.2. The cross section of the hexagonal lattice formed by polymeric chains.

for the hexagonal lattice and 1 for the tetragonal lattice; r is the distance between the nearest centres of the neighbouring chains.

In both types of lattice the shells are situated at a distance $\sqrt{k} \cdot r$, where $k = 1, 2, 3, \ldots$.

The potential energy of the interaction of two centres, one of which is located at the coordinate origin and the other (the jth centre) in the kth shell, can be represented by a potential of the Lennard-Jones type:

$$\varphi_{jk} = \varepsilon^* f_{jk} \left[\left(\frac{r^*}{r_{jk}} \right)^{12} - 2 \left(\frac{r^*}{r_{jk}} \right)^{6} \right] \tag{3.19}$$

where ε^* and r^* are parameters characterizing the energy and distance; f_{jk} is a factor taking account of the asymmetry of the field of dispersion forces in coupled interactions.

The approximation for f_{jk} deduced from the London equation for the angular dependence of dispersion forces has the following form (142, 143):

$$f_{jk} = 1 - 2kp_{jk} + k^2 (5p_{jk} - 1) \tag{3.20}$$

where

$$p_{jk} = \frac{3}{2} \cdot \frac{r_k^2}{r_{jk}} - 1 \tag{3.21}$$

$$k = \frac{\alpha_{\parallel} - \alpha_{\perp}}{3\alpha} \tag{3.22}$$

Here $\alpha_{\parallel}$ and $\alpha_{\perp}$ are the polarizabilities of point centres in directions parallel and perpendicular to the chain axis, respectively; α is the average value of polarizability; $r_k = r_{0k}$ is the shortest distance between a given point centre and the kth chain.

Assuming the additivity of coupled interactions and disregarding intrachain interactions, we can define the lattice energy as

$$\Phi = \frac{Nn\varepsilon^*}{2} \sum_{k=1}^{\infty} \sum_{j=-\infty}^{\infty} n_k f_{jk} \left[\left(\frac{r^*}{r_{jk}} \right)^{12} - 2 \left(\frac{r^*}{r_{jk}} \right)^{6} \right] \tag{3.23}$$

where

$$r_{jk}^2 = r_k^2 + (j\lambda)^2 \tag{3.24}$$

Since the summation in Eq. (3.23) is carried out for the case $r_k > 2\lambda$, this equation may be written down as follows:

$$\Phi = \frac{Nnz\varepsilon^* r^*}{2\lambda} \left[A\xi \left(\frac{v^*}{v} \right)^{11/2} - B\eta \left(\frac{v^*}{v} \right)^{5/2} \right] \tag{3.25}$$

where the characteristic volume v^* is determined by the expression $v^* = \lambda\gamma_c (r^*)^2$; the constants A and B and the coordination number z have the following values: $A = 0.775$, $B = 2.654$, $z = 6$ for the hexagonal lattice and $A = 0.791$, $B = 3.063$, $z = 4$ for the tetragonal lattice; the parameters ξ and η are found from the relations:

$$\xi = 1 - 0.751k + 0.878k^2 \tag{3.26}$$

$$\eta = 1 - 0.502k + 0.255k^2 \tag{3.27}$$

Assuming that the polymeric chain consists of q units, each of which moves independently, we find that the average potential energy of such a kinetic unit is equal to $U_i = 2\Phi/Nq$. In calculating the potential energy account is taken only of the interactions between the closest chains. From the original premises given above we obtain (141) the following equation of state:

$$\frac{pV}{T}=s\left[1-0.831\left(\frac{\xi}{\eta}\right)^{1/6}\left(\frac{v^*}{v}\right)^{1/2}\right]^{-1}+ \\ +\frac{z\varepsilon^*r^*}{2\lambda kT}\left[A'\xi\left(\frac{v^*}{v}\right)^{11/2}-B'\eta\left(\frac{v^*}{v}\right)^{5/2}\right] \quad (3.28)$$

where $A' = 4.263$, $B' = 6.635$ for the hexagonal lattice and $A' = 4.351$ and $B' = 7.658$ for the tetragonal lattice; the parameter s characterizes the chain flexibility ($s = q/n$).

If the point centre has σ links, the parameter s_0 is introduced: $s_0 = s/\sigma = q/n\sigma$. This parameter ($s_0$) can have values ranging from 0 to 1. For rigid molecules $s_0 = 0$ and for very flexible molecules $s_0 = 1$. If we introduce the reduced temperature $\tilde{T}$, the reduced volume $\tilde{V}$ and the reduced pressure $\tilde{p}$, which are given by

$$\tilde{T}=\frac{2s\lambda kT}{z\varepsilon^*r^*};\quad \tilde{V}=\frac{v}{v^*};\quad \tilde{p}=\frac{2\lambda v^*p}{z\varepsilon^*r^*} \quad (3.29)$$

then the reduced equation of state can be written as follows:

$$\frac{\tilde{p}\tilde{V}}{\tilde{T}}=\left[1-0.831\left(\frac{\xi}{\eta}\right)^{1/6}\tilde{V}^{-1/2}\right]^{-1}+ \\ +(A'\xi\tilde{V}^{-11/2}-B'\eta\tilde{V}^{-5/2})\,\tilde{T}^{-1} \quad (3.30)$$

where the parameters ξ and η are close to unity (for example, $\xi = 1.035$ and $\eta = 1.023$ for polystyrene, and $\xi = 0.978$ and $\eta = 0.985$ for polyvinyl chloride).

At atmospheric pressure the left-hand side of Eq. (3.30) is very small and may be neglected as compared to the terms on the right-hand side of the equation. Then, assuming ξ and η to be equal to unity, we get an approximate expression:

$$\tilde{T}=-(1-0.831\tilde{V}^{-1/2})\,(A'V^{-11/2}-B'\tilde{V}^{-5/2}) \quad (3.31)$$

Equation (3.31) gives the relation between the van der Waals volume and the temperature at atmospheric pressure. The cubic expansion coefficient β can be found by differentiating this equation with respect to temperature:

$$\frac{1}{\tilde{\beta}}=(5.5A'\tilde{V}^{-11/2}-2.5B'\tilde{V}^{-5/2})-2.493\,(2A'\tilde{V}^{-6}-B'\tilde{V}^{-3}) \quad (3.32)$$

The reduced cubic expansion coefficient $\tilde{\beta}$ is given by

$$\tilde{\beta}=\frac{1}{\tilde{V}}\left(\frac{\partial\tilde{V}}{\partial\tilde{T}}\right)=\frac{z\,(1-f_0)\,\varepsilon^*r^*}{2s\lambda k}\,\beta \quad (3.33)$$

where f_0 is the relative free volume.

Thus, the thermodynamic properties of amorphous polymers in the glassy state can be described by Eqs. (3.31) and (3.32)

TABLE 3.1. *The Molecular Parameters of Selected Amorphous Polymers*

Polymer	ε^*, Å	s_0	T^* or ε^*/k, K	Type of lattice
Polystyrene	9.03	0.81	184.2	Hexagonal
Polymethyl methacrylate	7.89	0.66	229.2	Tetragonal
Polyvinyl chloride	6.11	0.34	134.9	Hexagonal

if the values of the molecular parameters r^*, ε^*, and z are known. The values of r^* and ε^* can be calculated theoretically (141, 144, 145) through the use of certain experimental data. The results of such calculations for some amorphous polymers are tabulated in Table 3.1.

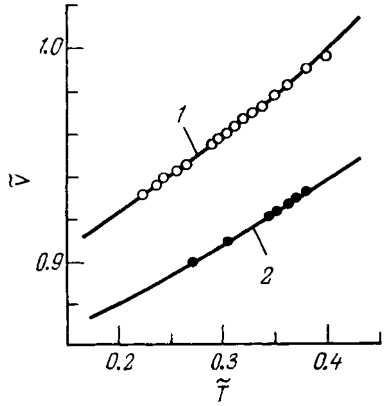

FIG. 3.3. Dependence of the reduced volume $\tilde{V}$ on the reduced temperature $\tilde{T}$ for the hexagonal (*1*) and tetragonal (*2*) lattices (○—polystyrene, ●—polymethyl methacrylate).

The results of a comparison of theoretical calculations with experimental data (146) for amorphous polymers, such as polymethyl methacrylate and polystyrene, are given in Fig. 3.3. From this figure it is seen that the results of theoretical calculations argee well with experimental data.

In spite of the fact that Eqs. (3.31) and (3.32) describe thermal expansion in the glassy state well, they do not fit even qualitatively the results of experimental investigations at low temperatures.

An attempt to describe theoretically the thermal expansion of amorphous polymers at low temperatures has been made by Simha and coworkers (147). They too proceeded from the cell model, supplementing it with quantum concepts based on the Einstein theory in one variant and on the Debye theory in the other. In deriving the equation of state they made use of the Lennard-Jones and Devonshire potentials (148). The Helmholtz free energy for a set of harmonic oscillators is written in this case in the form:

$$F = U_0 + U_{\mathrm{int}} + kT \sum_{i=1}^{3cN} \ln\left[1 - \exp\left(-\frac{h\nu}{kT}\right)\right] \qquad (3.34)$$

where U_0 is the zero-point energy; U_{int} is the energy of intermolecular interaction.

The summation is carried out over $3cN$ "external" modes of vibration, where $3c$ is the number of volume-dependent degrees of freedom per chain. Introducing the reduced variables and using the 6-12 potential, one obtains (147) the following reduced equation of state:

$$\tilde{p}\tilde{V} = \frac{2}{\tilde{V}^2}(A/\tilde{V}^2 - B) - \frac{h}{Nqz\varepsilon^*}\sum_i \nu_i \left(\frac{\partial \ln \nu_i}{\partial \ln V}\right)_T \times \left[\frac{1}{2} + \frac{\exp(-h\nu_i/kT)}{1-\exp(-h\nu/kT)}\right] \quad (3.35)$$

where $qz\varepsilon^*$ is the parameter characterizing the energy of intermolecular interaction referred to one chain.

Introducing the Grüneisen constant γ and the reduced characteristic Einstein temperature, we obtain:

$$\tilde{p}\tilde{V} = \frac{2}{\tilde{V}^2}\cdot\left(\frac{A}{\tilde{V}^2} - B\right) + 3\gamma\tilde{\theta}_E\left[\frac{1}{2} + \frac{1}{\exp\left(\frac{\tilde{\theta}_E}{\tilde{T}}\right) - 1}\right] \quad (3.36)$$

In an analogous way we can derive an equation of state in the Debye approximation. Two such equations in the limiting case of low temperatures (at $T \to 0$ K) lead to different temperature dependences of the thermal expansion coefficient:

$$\tilde{\alpha}_{0E} \propto (\tilde{\theta}_E/\tilde{T})^2 \cdot \exp(-\tilde{\theta}_E/\tilde{T})$$

$$\tilde{\alpha}_{0D} \propto (\tilde{T}/\tilde{\theta}_D)^3$$

where $\tilde{\alpha} = \alpha T^*$ and $\tilde{\theta} = \theta/T^*$.

Thus, in addition to reduced pressure, temperature and volume, the quantum-mechanical treatment also makes use of reduced characteristic temperature. The quantum theory imposes an additional condition for the fulfilment of the principle of corresponding states. This condition is that $\tilde{\theta} = \text{const}$. Only in this case will Eqs. (3.35) and (3.36) hold. Neglecting the left-hand side of Eq. (3.36), one can obtain an expression analogous to Eq. (3.31) which can be used to calculate the thermal expansion coefficient. In this way the thermal expansion coefficients of a number of amorphous polymers have been obtained (147). It has been found that the thermal expansion coefficients calculated according to the Einstein theory are in good agreement with experimental data at temperatures ranging from 10 to 50 K, with the reduced characteristic Einstein temperature being $\tilde{\theta}_E = 5 \times 10^{-3}$ ($\theta_E = 74$ K).

Above 50 K one observes a systematic departure of the theoretical curve from the experimental values of α. The results of such a comparison for polycyclopentyl methacrylate are presented in Fig. 3.4. The possibility can not be excluded that the temperature dependence of the linear thermal expansion coefficient at very low temperatures (below 4 K) is due to quantum tunnelling transitions (149).

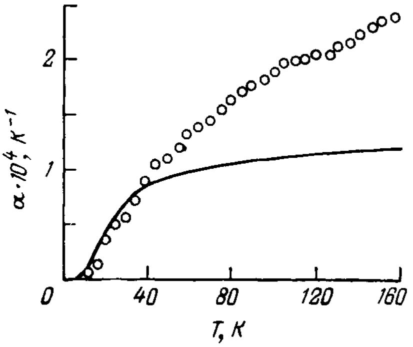

FIG. 3.4. Comparing experimental (unfilled circles) and theoretical (solid line) values of the thermal expansion coefficient of polycyclopentyl methacrylate at $\tilde{\theta}_E = 5\times10^{-3}$ (147).

3.3.2. THERMAL EXPANSION OF CRYSTALLINE POLYMERS

It is obvious that the thermal expansion coefficient of a crystalline polymer must be dependent not only on volume and temperature but also on the degree of crystallinity. If the polymer is neither completely crystalline nor completely amorphous, its specific volume V can be represented as a linear combination of the specific volumes of crystalline, V_1, and amorphous, V_2, regions. If these regions are in equilibrium at the same temperature and pressure, we can write:

$$V=\bar{\lambda}V_1+(1-\bar{\lambda})V_2 \qquad (3.37)$$

where $\bar{\lambda}$ is the so-called "weight" (or "mass") degree of crystallinity ($\bar{\lambda}=m_1/m$, where m_1 is the total mass of crystalline regions in the sample of a given polymer, and m is the mass of the entire sample).

Let us divide both sides of Eq. (3.37) by V_1^0 (the specific volume of a fully crystalline polymer at $T=0$ K and $P=0$) (150). Introducing the dimensionless parameters $x=V/V_1^0$, $x_1=V_1/V_1^0$ and $x_2=V_2/V_1^0$, we transform Eq. (3.37):

$$x=\bar{\lambda}x_1+(1-\bar{\lambda})x_2 \qquad (3.38)$$

The thermal expansion coefficient will in this case assume the form

$$\beta=\frac{1}{V}\left(\frac{\partial V}{\partial T}\right)_p=\frac{1}{x}\left(\frac{\partial x}{\partial T}\right)_p \qquad (3.39)$$

Equation (3.39) will then be written (150) in the following manner:

$$\beta=\frac{1}{x}\left[\bar{\lambda}x_1\beta_1+(1-\bar{\lambda})x_2\beta_2\right] \qquad (3.40)$$

The subscripts 1 and 2 refer, respectively, to the crystalline and amorphous regions of the polymer:

$$\beta_1 = \frac{1}{x_1}\left(\frac{\partial x_1}{\partial T}\right)_p; \quad \beta_2 = \frac{1}{x_2}\left(\frac{\partial x_2}{\partial T}\right)_p$$

Assuming that $\overline{\lambda}$ is a constant quantity, we can, via Eq. (3.40) calculate the thermal expansion coefficient β for a given degree of crystallinity if the parameters β_1, β_2, x_1, and x_2 are known. For polyethylene these parameters can be calculated theoretically (151) by means of the available equations of state for completely crystalline and completely amorphous polymers. An equation of the following type holds for both phases of polyethylene:

$$p\,(x,\ T) = p_0\,(x) + g\,(x)\,T \tag{3.41}$$

where $p_0\,(x)$ is the pressure at 0 K, and the product $g\,(x)\,T$ represents the thermal contribution to the pressure (p_T) at given volume and temperature.

The form of the two functions in Eq. (3.41) depends on the ratio of the crystalline to amorphous regions. Since $(\partial p/\partial T)_x = \beta B_T$, where $B_T = -x\,(\partial p/\partial x)_T$, then Eq. (3.41) yields the following expression for β:

$$\beta = p_T/(TB_T) \tag{3.42}$$

For crystalline polymers the principle of corresponding states holds in some cases (150), a circumstance that enables one to use Eq. (3.41) with the reduced variables.

There also exist other methods of describing the thermodynamic properties of crystalline polymers, in which such polymers are treated as three-dimensional crystals (152).

3.4. METHODS OF MEASURING THERMAL EXPANSION COEFFICIENTS OF POLYMERS

At low temperatures the experimentally determined characteristic of the thermal expansion of polymers is the linear thermal expansion coefficient α. There exist various methods, all giving substantially differing results for the determination of this coefficient. For example, the mean linear thermal expansion coefficient is defined as the unit elongation of a solid when its temperature is changed by one degree:

$$\alpha_m = \frac{1}{L_s}\,\frac{L_i - L_j}{t_i - t_j} \tag{3.43}$$

where L_i and L_j are the linear dimensions (length) of the solid at the temperatures t_i and t_j; L_s is the length of the solid at a certain reference temperature t_s (the reference temperature usually chosen is 0°K, 0°C or 20°C).

Besides, there are integral and differential thermal expansion coefficients. If $t_j = t_s$ and $L_j = L_s$ in formula (3.43), the quantity α_m calculated in this case is called the mean integral temperature coefficient of linear expansion. If the quantity L_s is replaced in formula (3.43) by L_j equal to the length of the test sample at the temperature t_j, we obtain the mean differential temperature coefficient of linear expansion.

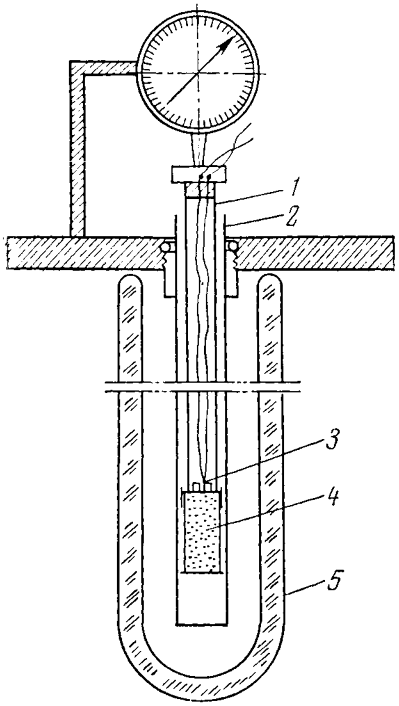

FIG. 3.5. Schematic representation of a low-temperature dilatometer (154):

1—inner quartz tube; 2—outer quartz tube; 3—thermocouple; 4—sample; 5—Dewar vessel.

Since the thermal expansion coefficient of polymers is, as a rule, substantially dependent on temperature, use is often made of the values of the so-called true linear expansion coefficient at a given temperature t, which is determined by the formula

$$\alpha_t = \frac{1}{L_t} \cdot \frac{\partial L}{\partial t} \qquad (3.44)$$

Thus all methods of determining α can be reduced to the measurement of the linear dimensions of a solid (or of its parts) at various temperatures and to the measurement of these temperatures. In spite of the basic simplicity of the method, the measurement of the thermal expansion coefficient of polymers over a wide temperature range presents considerable experimental difficulties. Such measurements are especially time-consuming and complicated at $T \to 0$ K.

Instruments used for the determination of thermal expansion coefficients (dilatometers) can be divided into two groups. Some dilatometers are designed for absolute measurement of thermal linear expansion coefficients, in which the linear dimensions of the sample (or changes in them) are directly measured at various temperatures, with the temperatures themselves being measured. Other dilatometers are designed for relative measurements, in which thermal expansion coefficients are determined through comparison with a reference standard with a known thermal expansion (determined by the absolute method).

A detailed description of various methods and instruments used for the determination of thermal expansion coefficients, including those at low temperatures, can be found in a monograph by Amatuni (153). It should be noted only that the use of modern laser techniques makes possible the design of dilatometers whose operation is based on a fundamentally different principle and which are free from the shortcomings mentioned by Amatuni (153).

Figure 3.5 is a schematic representation of a rather simple dilatometer, the one used by Laquer and Head (128, 154) to measure the thermal linear expansion coefficients of a number of polymers within the temperature range 20-300 K.

3.5. THERMAL EXPANSION COEFFICIENTS OF POLYMERS

The most detailed study of the thermal expansion of polymers at low temperatures has been made by Laquer and Head (128). In 1952 these authors published a work (128) containing the results of the measurement of the thermal expansion coefficients of 20 polymeric materials at temperatures ranging from 20 to 300 K. Subsequent review articles (129) have been based solely on the data obtained by Laquer and Head. A number of investigations devoted to the study of polymers at low temperatures have been carried out in recent years by Simha and coworkers (155-158). Other investigations (159-161) of the thermal expansion of polymers at low temperatures are not systematic. We shall concern here with ourselves the available experimental data on the thermal expansion of the most widely used polymers at low temperatures.

Polyethylene. The thermal expansion of polyethylene at low temperatures has been studied by a number of investigators (128, 157, 160). Simha and his coworkers (157) studied the temperature dependence of the α of three samples of polyethylene in the range 88-293 K with a view to investigating temperature transitions and comparing dilatometric data with the results of dynamic mechanical and dielectric measurements. A typical dilatometric curve obtained by Simha *et al.* (157) for polyethylene with a density of 0.929 Mg/m^3 and a crystallinity of 54 per cent is shown in Fig. 3.6. The dilatometric curve shows four temperature transitions characterized by the following feature: at temperatures exceeding the temperature of each transition there is observed an increase in the linear thermal expansion coefficient.

The temperatures of the transitions of polyethylene have the following values: —126, —62, —22, and —2°C. The positions of these transitions on the temperature scale correlate well with the results of dynamic mechanical and acoustical measurements

(70). The temperature transition observed on the $\alpha = f(T)$ curve at —126°C is due to the phenomenon of γ-relaxation, i.e., to the unfreezing (at this temperature) of the restricted rotation of a portion of the main chain of polyethylene, which contains four successively arranged methylene groups. According to the model proposed by Schatzki (162), the rotation takes place about two colinear bonds and resembles the motion of a crankshaft. This type of motion is possible only in amorphous regions and must lead to the appearance of low-temperature peaks of tan δ in acoustical (70) and dielectric (163) measurements.

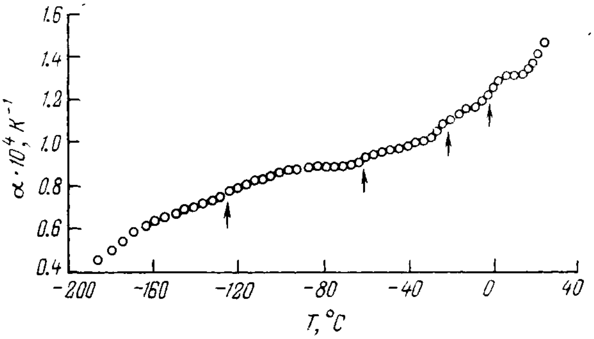

FIG. 3.6. Typical dilatometric curve for polyethylene with density 0.929 Mg/m³ and a degree of crystallinity of 54 per cent (157). The arrows indicate transitions.

The temperature transition observed at —22°C is due to the unfreezing (above this temperature) of the micro-Brownian segmental motion in the amorphous regions of polyethylene. Thus, for the polyethylene studied by Zakin, Simha and Hershey (157), the glass-transition temperature of the amorphous layer $T_g =$ $= -22$°C. If T_g is extrapolated to a sample with zero degree of crystallinity, it will be found to range from —80 to —90°C, which agrees well with the estimates obtained by Boyer (164), who maintains that the glass-transition temperature of completely amorphous polyethylene must be —80°C. The nature of the temperature transitions that occur at —62 and —2°C has not yet been fully clarified. We might expect that at least one of them is associated with the restricted motion of small elements of the main chain containing methyl groups, which play the role of branches in this polymer.

The results of dilatometric measurements (157) in the low-temperature region do not fit the earlier experimental data of Laquer and Head (128) (Fig. 3.7). For example, at —180°C, according to the data reported (157), $\alpha = 5 \times 10^{-5}$ K^{-1}, while, according to Laquer and Head (128), at this temperature $\alpha = 10.4 \times 10^{-5}$ K^{-1}. Recent measurements for polyethylene (160) have shown a good agreement with the results of Laquer and Head. The discrepancy between the available data (128, 160, 157) may be due to two factors. One of these is possibly that samples of differing degrees of crystallinity were investigated, which could lead to different values of α. It has been demonstrated (160) that in high-density polyethylene with a higher degree of crystallinity the thermal linear expansion coefficient $\alpha = 8.1 \times 10^{-5}$ K^{-1} at 77 K. At the same time, for low-density polyethylene, which has a lower degree of crystallinity, $\alpha = 13.4 \times 10^{-7}$ K^{-1} at the same temperature. The other possible factor is that Laquer and Head (128) and van de Voorde (160) measured the mean integral thermal coefficient of linear expansion, while Simha and coworkers (157) determined the true linear expansion coefficient calculated by formula (3.44).

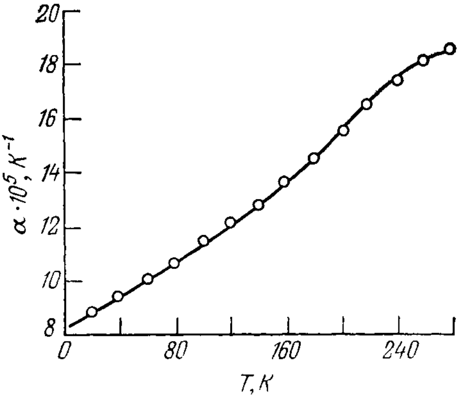

FIG. 3.7. Temperature dependence of the linear thermal expansion coefficient of polyethylene, after Laquer and Head (128).

Attempts have been made (151) to calculate the linear thermal expansion coefficient of polyethylene by using the equation of state of this polymer. For example, for polyethylene with a degree of crystallinity $\lambda = 40.5$ per cent it has been found (151) for the temperature range 0-109.5 K that

$$\alpha = 5.86 \times 10^{-7}\ T \tag{3.45}$$

and for the range 109.5-240.7 K

$$\alpha = 0.2761 \times 10^{-4} + 3.065 \times 10^{-7}\ \mathrm{T} \tag{3.46}$$

Near the liquid-helium temperature the results of calculations using formula (3.45) lead to α values which differ by an order of magnitude from experimental data (128, 160). Near the liquid-nitrogen temperature (77 K) the values of α calculated by formula (3.45) are in good accord with the experimental data of Simha and coworkers (157). Using the methods of X-ray structure analysis, Swan (43) measured the linear thermal expansion coefficients for the parameters of the unit cell of polyethylene for the temperature range —70 to +130°C and also at —196°C. It is interesting that along the "a" axis $\alpha = 1.1 \times 10^{-5}\ K^{-1}$ at —196°C,

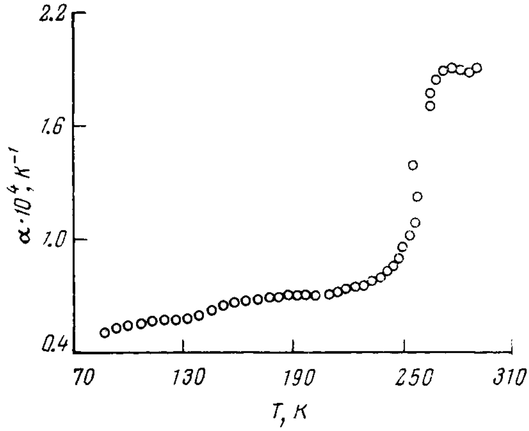

FIG. 3.8. Temperature dependence of the linear thermal expansion coefficient of polypropylene having a degree of crystallinity of 18 per cent.

which is less than the thermal linear expansion coefficient of isotropic partly crystalline polyethylene by a factor of 10 (128).

Polypropylene. The thermal linear expansion coefficient of polypropylene in the temperature range —185 to +20°C has been measured by Simha and coworkers (157). They have also studied the thermal expansion of polypropylene-polyethylene blends and propylene-ethylene copolymers. A typical dilatometric curve for polypropylene with a density of $\rho = 0.871\ Mg/m^3$ and a degree of crystallinity of $\lambda = 18$ per cent is given in Fig. 3.8. The biggest change in the thermal linear expansion coefficient is observed at —14°C, this being the glass-transition temperature of polypropylene. This result agrees well with the data (at —18°C) obtained by Reding (165) and Manaresi and Gianella (166) and also with the value of $T_g = -15°C$ which has been reported in the literature (167, 168). Wilkinson and Dole (169), while studying the temperature dependence of the specific heat capacity of polypropylene, obtained a value of $T_g = -12°C$, and Passaglia and Kevorkian (58) found that $T_g = -14°C$. For polypropylene with $\lambda = 18$ per cent the difference between the thermal linear expansion coefficients above and below T_g is 1×10^{-4} K^{-1} (157), which correlates well with the magnitude of the variation of the thermal cubic expansion coefficient at T_g (166) of completely amorphous polypropylene, equal to $\Delta\beta = 4 \times 10^{-4}$ K^{-1}. The temperature transition that appears on the $\alpha =$ (T) graph at —126°C (see Fig. 3.8) could possibly be connected with the unfreezing of the rotation of the methyl groups.

In polypropylene-polyethylene blends the glass-transition temperature lies between —9 and —14°C and the variation $\Delta\alpha$ of the linear expansion coefficient at T_g falls off with increasing polyethylene content.

Polytetrafluoroethylene. The most detailed study of thermal expansion in polytetrafluoroethylene (Teflon) in the temperature range —190 to +300°C has been conducted by Kirby (170) and also by Novikova and Leksina (171). To measure the thermal expansion of Teflon, Novikova and Leksina (171) employed two different dilatometers designed by Strelkov (172-174). The thermal linear expansion coefficient was calculated by formula (3.43), where $L_s = L_0$ (L_0 is the length of the sample at 0°C). The temperature ranges of measurement, $t_2 - t_1$, were 5°C, and within the range of a sharp variation of the linear thermal expansion coefficient, 0.5°C. The tests were carried out on samples of strongly crystallized, annealed polytetrafluoroethylene with a density of $\rho = 2.25$ Mg/m³.

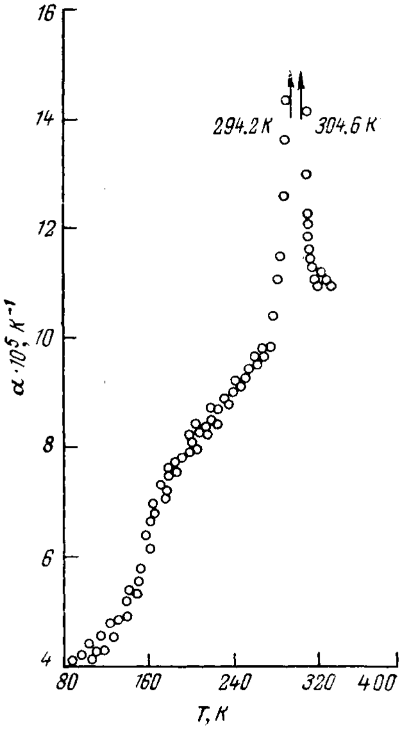

FIG. 3.9. Temperature dependence of the thermal expansion coefficient of polytetrafluoroethylene having a density of 2.25 Mg/m³.

The temperature dependence of the thermal linear expansion coefficient of this sample of Teflon is given in Fig. 3.9. The increase in the linear expansion coefficient at 150-160 K is associated with the unfreezing of the segmental motion in amorphous regions, i.e., with the transition of the amorphous layer from the glassy to the rubbery state. This temperature transition is relatively weakly pronounced on the graph (see Fig. 3.9) because a highly crystalline sample of polytetrafluoroethylene (degree of crystallinity $\lambda = 83$ per cent) was used, and also because a strongly prominent peak of the linear expansion coefficient at 20°C is superimposed on the high-temperature branch. Nevertheless, while carrying out calorimetric measurements, Furukawa, McCoskey and King (38) observed a slight spontaneous rise in temperature (0.001 K/min) between 160 and 170 K for highly crystalline polytetrafluoroethylene and in the region of 145-175 K for samples with a lesser degree of crystallinity. They noted that such a spontaneous increase in temperature is observed for amorphous solids near T_g.

A relatively weak variation of the linear thermal expansion coefficient of polytetrafluoroethylene in the region of the glass-transition temperature is, to a considerable extent, associated with the dominant effect of the phase transition observed at 20°C. On the $\alpha = f(T)$ plot this transition manifests itself as a sharply pronounced peak, at the maximum of which the thermal linear expansion coefficient increases 13 times. This peak does not appear in Fig. 3.9, but some idea of it can be gained from Fig. 3.10. The change in the specific volume involved in this transition is about 1 per cent, which corresponds to 85 per cent of the total change in volume in all the temperature transitions occurring in this polymer. The peak of thermal expansion in polytetrafluoroethylene at 20°C is due to phase transition of the first kind, that is, a change in the type of unit cell from the triclinic to the hexagonal system as a result of the change in the chain conformation and the vibrations about the chain axis, which lead to a slight coiling and uncoiling of the polymeric chain. Thus, this temperature transition consists of an orientational disordering of macromolecules above 20°C and is a transition of the "orientational melting" type predicted by Frenkel (175). The second temperature transition (see Fig. 3.10) occurs at about 30°C. Above this temperature the macromolecular conformations cease to be regular and therefore no rotations of the macromolecules about their axes occur (176).

In the low-temperature region, down to 20 K, the thermal expansion of Teflon (Fig. 3.11) has been measured by Laquer and Head (128). The results obtained by these authors at $T > 80$ K agree satisfactorily with the experimental data of Kirby (170), but they are 1.5 to 2 times higher than the values obtained by Novikova and Leksina. This discrepancy is probably due to the fact that Novikova and Leksina used strongly crystallized samples of Teflon ($\lambda = 83$ per cent), while the degree of crystallinity of this polymer usually ranges from 40 to 60 per cent. It is known (171) that in the low-temperature region the thermal linear expansion coefficient of Teflon decreases with increasing crystallinity.

In a recent article van de Voorde (160) gives the values of the thermal linear expansion coefficient at 4.2 K ($\alpha = 6.8 \times 10^{-5}\ K^{-1}$) and 77 K ($\alpha = 7.6 \times 10^{-5}\ K^{-1}$), which are in satisfactory agreement with the data of Laquer and Head.

Polyalkyl Methacrylates and Some Other Polymers. The thermal expansion of 14 polyalkyl methacrylates at temperatures ranging from —180 to +100°C has been thoroughly studied by Haldon and Simha (155). The aim of their work was to investigate temperature transitions in these polymers, to compare these transitions with the results of dynamic mechanical and dielectric studies, and also to test the Simha-Boyer relation.

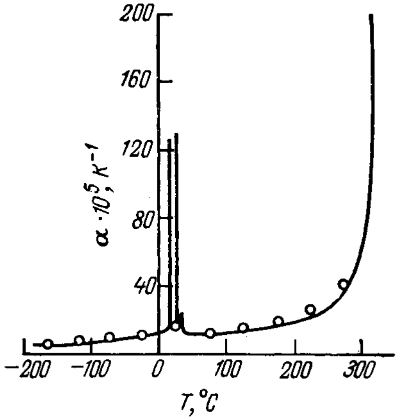

FIG. 3.10. Temperature dependence of the linear thermal expansion coefficient of polytetrafluoroethylene over a wide temperature range.

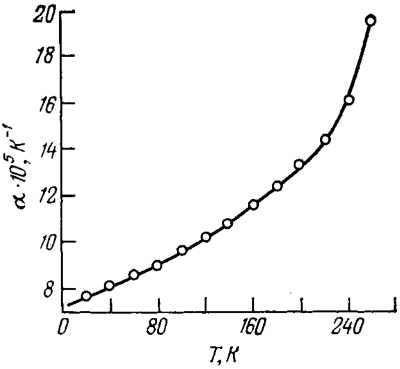

FIG. 3.11. Temperature dependence of the linear thermal expansion coefficient of polytetrafluoroethylene, after Laquer and Head (128).

Simha and Boyer (177) proposed a simple method for calculating the free volume of polymeric materials at their glass-transition temperatures, based on the use of the values of their thermal expansion coefficients. If we denote the thermal expansion coefficients above and below their glass-transition temperatures by β_l and β_g, then, according to Simha and Boyer (177),

$$(\beta_l - \beta_g)\,T_g = \Delta\beta T_g = k \tag{3.47}$$

where k may be regarded as the free-volume fraction. It has been found that the parameter k assumes values around 0.113 for polymers in which no sharply pronounced molecular motion takes place below T_g. The findings of Rogers and Mandelkern (178), however, do not confirm the validity of relation (3.47). It does not hold, for example, for the series of polyalkyl methacrylates, where k decreases with increasing length of the side chain. It is supposed (155, 177) that this departure from the Simha-Boyer rule is caused by the intensive motion of side groups below T_g. Simha and Boyer maintain that as a result of the motion of side chains in polyalkyl methacrylates there is retained in the glassy state an extra free volume which leads to much higher values of β_g than usual, which must in turn reduce the value of $\Delta\beta T_g$. It is therefore suggested (155) that formula (3.47) be written in the form $(\beta_l - \beta_{g1}) T_g = k$, where β_{g1} is the thermal expansion

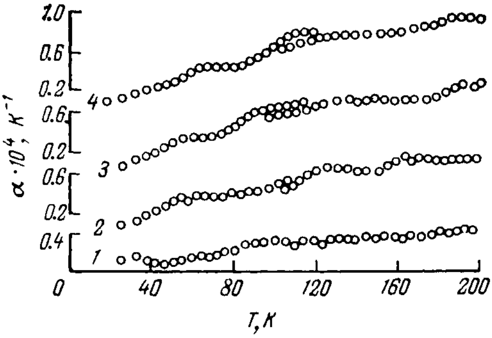

FIG. 3.12. Temperature dependence of the linear thermal expansion coefficients of polymethyl methacrylate (*1*), polyethyl methacrylate (*2*), poly-*n*-propyl methacrylate (*3*), and poly-*n*-butyl methacrylate (*4*).

coefficient at temperatures lower than the temperature at which the mobility of side groups is unfrozen. According to dilatometric measurements (155), in polymethyl methacrylate, apart from the glass-transition temperature ($T_g = 376$ K), there are observed temperature transitions at 288 K and 143 K. If the value $3\alpha_{g1}$ measured at $T < 143$ K is taken as β_{g1}, then $3(\alpha_l - \alpha_{g1}) T_g = 0.12$, which is in satisfactory agreement with the Simha-Boyer rule.

An interesting feature of this work is that the authors, using the dilatometric method, succeeded in observing multiplet temperature transitions in a number of polymers in the glassy state, whereas as the length of side chains increases these transitions will not be found in dynamic mechanical measurements at low frequencies. Furthermore, it has been found (155) that in polymers with very flexible side chains there occur temperature transitions near the lower end of the temperature range used. Such temperature transitions caused by relaxation phenomena have been studied by dynamic mechanical methods for polyalkyl methacrylates (179, 180) and also for systems with flexible side chains—polyalkyl acrylates (181), polyalkyl vinyl esters (181), and poly-α-olefins (182).

Later, Haldon and Simha (156) extended the temperature range of their investigations to low temperatures and measured the thermal expansion coefficients of 10 polyalkyl methacrylates, poly-4-methyl 1-pentene and ethylene-propylene copolymer (the

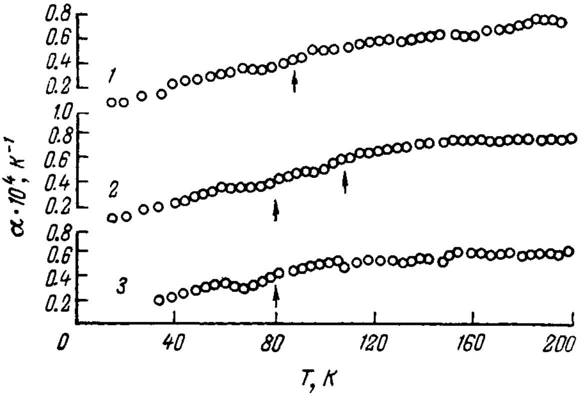

FIG. 3.13. Temperature dependence of the linear thermal expansion coefficients of poly-*sec*-butyl methacrylate (*1*), polyisobutyl methacrylate (*2*), and poly-*tert*-butyl methacrylate (*3*).

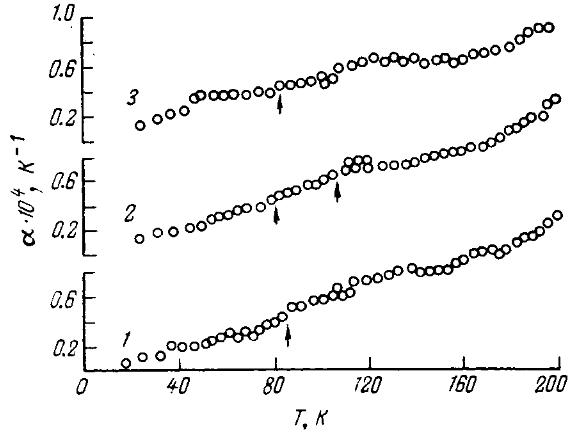

FIG. 3.14. Temperature dependence of the linear thermal expansion coefficients of poly-*n*-hexyl methacrylate (*1*), poly-*n*-octyl methacrylate (*2*), and poly-*n*-decyl methacrylate (*3*).

ethylene-propylene ratio being 49 : 51) in the temperature range 20-120 K. The temperature dependence of the thermal expansion coefficients of polyalkyl methacrylates is shown in Figs. 3.12, 3.13, and 3.14. The curves obtained by Haldon and Simha (155,

156) fit in well with these graphs. There is a small discrepancy in the case of some polymers, due to the different thermal histories of the samples. For all the polymers, except for polymethyl methacrylate, there is clearly observed between 20 and 40 K an increase in the thermal expansion coefficient. At higher temperatures, for most of the polymers there is a plateau region on the $\alpha = f(T)$ graph, the position and extent of which depend on the specific features of the polymer. The low-temperature plateau ends with a sufficiently clear-cut temperature transition.

In the temperature range 20 to 60 K the linear expansion coefficient of polymethyl methacrylate is approximately equal to 1×10^{-5} K^{-1}. The value of α then increases over a rather wide temperature range (about 35 K). The middle point of this range lies at about 83 K. At higher temperatures, up to 200 K, no temperature transitions are observed in this polymer. Polyethyl methacrylate, poly-*p*-propyl methacrylate, and all butyl isomers (see Fig. 3.13) show an increase in their linear expansion coefficients between 20 and 50 K, an increase which ends with a plateau. Beyond the plateau region, there is observed for each of the polymers a temperature transition, the middle point of which lies between 80 and 110 K, depending on the type of the polymer. The corresponding transition temperatures are given in Table 3.2.

With polyisobutyl methacrylate there are observed two low-temperature transitions which can be readily reproduced. There is no plateau region for poly-*n*-hexyl methacrylate and poly-*n*-octyl methacrylate, but the latter probably has two not very pronounced transitions.

It is interesting to compare the temperature dependence of α for polymethyl methacrylate and polyethyl methacrylate with the results of measurements of the loss tangent tan δ in the same temperature range.

Woodward has shown (318) that for polymethyl methacrylate (at 5 K) and polyethyl methacrylate (at 50 K) the loss tangents have peaks measured at a frequency of about 10^4 Hz. Sinnott (184) observed the peaks of the loss tangent in these polymers at $T_m < < 4.2$ and $T_m = 41$ K respectively, at frequencies of a few Hz. The results of dynamic mechanical investigations of polyethyl methacrylate can be compared with the initial increase of α in Fig. 3.12. Such a comparison cannot be made for polymethyl methacrylate because of the lack of reliable dilatometric data near the liquid-helium temperature.

The peaks of the loss tangents correspond to the transitions detected in poly-*n*-propyl methacrylate, poly-*n*-butyl methacrylate and poly-*sec*-butyl methacrylate (179, 180). The mechanical loss maxima for the first two polymers measured at a frequency of 1 Hz are respectively situated at 86 and 93 K. In polyisobutyl methacrylate there are observed two transitions, one of which lies 20° higher than the transition in poly-*sec*-butyl methacrylate. The same difference was observed by Shen and coworkers (180) in dynamic mechanical investigations of the same polymers.

The molecular motion associated with these relaxation phenomena is usually ascribed to the re-orientation of the side alkyl groups (179). In certain cases the mechanism of this motion is perhaps analogous to the movement of a crankshaft (162). We resort to a molecular mechanism of this kind in order to describe the process of γ-relaxation in polyethylene. It quite possibly operates in polyalkyl methacrylates containing four or more methylene groups in the side chain. The investigation of polymethyl methacrylate carried out by the nuclear magnetic resonance method (185) shows that the low-temperature relaxation in this polymer is associated with the movement of the ester methyl groups.

Such an interpretation of low-molecular transitions is in good agreement with the results of dilatometric measurements. From Table 3.2 it can be seen that the variation in the thermal expansion coefficient, $\Delta\alpha$, which characterizes to a certain degree the intensity of the unfreezing motion, increases with increasing length of the side chain. This is valid for at least the first members of the series, including poly-*n*-butyl methacrylate. In this case, the value of α approximately doubles during a temperature transition, this being an indication that the molecular motion of the side chains, which becomes unfrozen upon transition, is independent and evidently non-cooperative. When the side chains become sufficiently long, the molecular motion becomes more complicated and its mechanism less clear (as, for example, in the case of poly-*n*-octyl methacrylate). The slight change in the linear expansion coefficient near T_{tr} in poly-*n*-decyl methacrylate is probably due to the ordering in the arrangement of the side chains. In the series of butyl isomers the value of $\Delta\alpha$ has a tendency to decrease with increases in size of side groups, since for the very bulky alkyl groups a smaller volume is needed for the re-orientational motion to be unfrozen.

Polyvinylalkyl Esters. A number of polyvinylalkyl esters with side ester chains of varying length have been investigated using the dilatometric method (158) at temperatures ranging from 60 K to the relevant glass-transition temperatures. The results of measurements of the linear expansion coefficient were compared with the results of dynamic mechanical measurements carried out on a torsion pendulum and with the temperature dependence of dielectric losses. Apart from the glass-transition temperature, in each of the polymers studied there were also detected two low-temperature transitions at $T < T_g$. The first

TABLE 3.2. *Transition Temperatures T_{tr} and Values of α Below and Above T_{tr}*

Polymer	Alkyl side group	T_{tr}, K	$\alpha\cdot10^5$ ($T<T_{tr}$)	$\alpha\cdot10^5$ ($T>T_{tr}$)	$\Delta\alpha\cdot10^5$
Polymethyl methacrylate	$-CH_3$	83	1.6	3.3	1.7
Polyethyl methacrylate	$-CH_2-CH_3$	110	3.5	6.0	2.5
Poly-*n*-propyl methacrylate	$-CH_2-CH_2-CH_3$	84	3.3	6.2	2.9
Poly-*n*-butyl methacrylate	$-CH_2-CH_2-CH_2-CH_3$	97	4.1	7.3	3.2
Poly-*n*-hexyl methacrylate	$-(CH_2)_5-CH_3$	85	3.5	6.5	3.0
Poly-*n*-octyl methacrylate*	$-(CH_2)_7-CH_3$	81 107	4.1 5.8	5.8 7.8	1.7 2.0
Poly-*n*-decyl methacrylate	$-(CH_2)_9-CH_3$	83	3.6	4.7	1.1
Poly-*sec*-butyl methacrylate	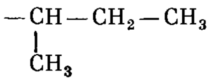 $-\underset{\underset{CH_3}{\vert}}{CH}-CH_2-CH_3$	88	3.2	5.1	1.9
Polyisobutyl methacrylate*	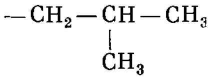 $-CH_2-\underset{\underset{CH_3}{\vert}}{CH}-CH_3$	81 109	3.3 4.7	4.7 6.3	1.4 1.6
Poly-*tert*-butyl methacrylate	$-C(-CH_3)_3$	82	3.0	4.6	1.6

* Two temperature transitions.

temperature transition $T_{gg}(1)$, which is situated below T_g, obeys the same regularity as was observed for the glass-transition temperature: the temperature $T_{gg}(1)$ falls off with increasing length of the side chain (Table 3.3).

TABLE 3.3. *Temperature Transitions in Polyvinylalkyl Esters*

Polymer	T_g, K	T_{gg} (1), K	T_{gg} (2), K
Polyvinylethyl ester	240	183	95
Polyvinyl-*n*-butyl ester	217	168	97
Polyvinylisobutyl ester	251	—	105
Polyvinyl-*n*-hexylethyl ester	199	151	96
Polyvinyl-*n*-octyl ester	193	163	103
Polyvinyl-*n*-decyl ester	211	183	—

This regularity is not obeyed by the last two polyesters presented in Table 3.3, since in these cases crystallization may occur with a greater length of the aliphatic side chain.

The second temperature transition T_{gg} (2) takes place at about 100 K and is independent of the length of the side chain. Any similarity in behaviour at temperatures T_g and T_{gg} (1) possibly indicates that the temperature T_{gg} (1) is associated with the unfreezing of the motion of the main chains. It is interesting that the change in the linear expansion coefficient, $\Delta\alpha$, at T_{gg} (2) is larger than $\Delta\alpha$ at T_{gg} (1). Perhaps this is an indication that the transition at T_{gg} (2) is associated with the re-orientation of the side chains (158).

The value of the product $(\beta_l - \beta_g)\, T_g$ calculated by Schell, Simha and Aklonis (158) decreases with increasing length of the side chain; this confirms the assumption that flexible side chains retain an extra free volume in the glassy state.

CHAPTER 4

ELECTRICAL PROPERTIES OF POLYMERS AT LOW TEMPERATURES

4.1. BASIC CONCEPTS OF THE ELECTRICAL PROPERTIES OF POLYMERS

The majority of polymers are typical dielectric materials. When they are placed in an electric field, an electric moment arises in them, i.e., electrical polarization takes place. The polarization of the unit volume of a dielectric, P, can be represented by the following sum:

$$P = P_{\text{or}} + P_{\text{def}} \tag{4.1}$$

where P_{or} is the polarization due to the orientation of permanent dipoles; P_{def} is the polarization due to the deformation of the electron shells or to the displacement of atomic nuclei.

The permanent dipoles are characterized by the magnitude of the dipole moment p_0:

$$p_0 = ql \tag{4.2}$$

where q is the magnitude of the charge: l is the distance between the charges.

In the absence of an electric field the permanent dipoles may be randomly distributed; the total dipole moment of such a system is zero. When an electric field is applied, there occurs a specific orientation of the dipoles and the orientation electric moment arises, characterized by the polarization vector $\vec{P}_{\text{or}}$. The role of permanent dipoles in polymers is played by polar groups. For instance, in the case of polyvinyl chloride the C—Cl group is such a dipole.

In non-polar dielectrics the electric moment is generated when an electric field is applied. Under the influence of an electric field the electric charges in molecules (or in parts of molecules) of the dielectric are displaced and induced electric dipoles appear. The moment of an induced dipole, p_0, is directly proportional to the strength E_i of the applied electric field:

$$p_0 = \alpha E_i \tag{4.3}$$

where α is the polarizability of the molecule (or its part).

If the unit volume contains N induced dipoles, then the polarization vector for the unit volume is given by

$$\vec{P}_{\text{def}} = N\vec{p}_0 = N\alpha\vec{E}_i \tag{4.4}$$

Here $\vec{P}_{\text{def}}$ is the deformation part of the polarization vector, due to the deformation of electron shells or to the displacement of atomic nuclei.

The electrical properties of dielectrics are characterized by the electric moment arising when an electric field is applied. The deformation part of this moment appears very rapidly, in 10^{-13} to 10^{-14} s. The time during which the orientation moment is set up depends to a considerable extent on the temperature, the shape of the molecules (or parts of molecules which have permanent dipole moments) and the forces of intermolecular interaction.

The properties of dielectrics are usually characterized by the permittivity or dielectric constant ε. If the dielectric is placed in a static electric field, its behaviour is described by the static dielectric constant ε_0. In the case of gases, according to Debye*,

$$\frac{\varepsilon_0-1}{\varepsilon_0+2} = \frac{4}{3}\pi N\left(\alpha + \frac{p_0^2}{3kT}\right) \tag{4.5}$$

where N is the number of molecules in the unit volume; α is the molecular polarizability; p_0 is the dipole moment of the molecule.

The parameter α is defined by the Clausius-Mosotti equation:

$$\frac{\varepsilon_\infty-1}{\varepsilon_\infty+2} = \frac{4}{3}\pi N\alpha \tag{4.6}$$

where ε_∞ is the dielectric constant measured at such a high frequency ($\omega \to \infty$) that the contribution of the dipole orientation to the quantity ε can be ignored.

The most efficient theory of dielectric relaxation has been worked out by Debye for polar liquids. He has shown that the polarizability due to the orientation of molecules may be represented in the form

$$\alpha = \frac{\alpha_0}{1+i\omega\tau} \tag{4.7}$$

where α_0 is the static polarizability; τ is the relaxation time.

From the Debye theory it follows that the polarization of polar molecules in a liquid does not occur instantaneously and is determined by the relaxation time. For spherical molecules the dielectric relaxation time depends on the viscosity of the liquid η and its temperature T:

---

* Equations expressing the relationships between the quantities are given in a form corresponding to the CGSE system.

$$\tau = \frac{4\pi\eta a^3}{kT} \tag{4.8}$$

where a is the radius of the molecule; for the majority of polar liquids the relaxation time τ is of the order of 10^{-10} to 10^{-11} s. Whereas the orientation of dipoles in liquids takes place comparatively freely and rapidly, in solids the orientation of molecules (or parts of molecules) with permanent dipole moments occurs much more slowly and is accompanied by relaxation processes having various relaxation times.

4.2. DIELECTRIC CONSTANTS OF SOLIDS

Of great importance in a consideration of the electrical properties of dielectrics is the calculation of the strength of the electric field acting on an atom or molecule. The strength of such a local field is given by

$$E_i = E + \frac{4\pi}{3} P \tag{4.9}$$

where E is the strength of the macroscopic average field; the quantity P characterizes the field arising from the polarization of all other atoms or molecules of the sample.

A considerable role in a description of the electrical properties of solid dielectrics is played not only by the macroscopic electric field strength $\vec{E}$ inside the dielectric but also by the electrical induction (electric displacement) $\vec{D}$. In anisotropic solids the electric displacement is a tensor. The relationship between the quantities $\vec{D}$ and $\vec{E}$ allows one to determine the dielectric constant of the solid. For an isotropic medium

$$\vec{D} = \varepsilon\vec{E} = \vec{E} + 4\pi\vec{P} \tag{4.10}$$

Hence the dielectric constant is equal to

$$\varepsilon = 1 + 4\pi P/E = 1 + 4\pi\chi \tag{4.11}$$

where $\chi = P/E$. In accordance with expressions (4.4) and (4.9),

$$\chi = \frac{\sum\limits_{j=1} \alpha_j N_j}{1 - \frac{4\pi}{3} \sum\limits_{j=1} \alpha_j N_j} \tag{4.12}$$

where the subscript j specifies the type of atom or part of the molecule.

In the case of dielectrics which are subjected to the action of varying electric fields, the relationship between the electric displacement $\vec{D}$ and the electric field strength $\vec{E}$ can be represented in the following manner:

$$\vec{D} = \varepsilon^* \vec{E} \tag{4.13}$$

The complex dielectric constant or relative permittivity ε^* is given by

$$\varepsilon^* = \varepsilon' - i\varepsilon'' \tag{4.14}$$

The part ε' of the complex dielectric constant ε^* is called the real dielectric constant; it characterizes the most important electrical properties of dielectrics. The imaginary part ε'' characterizes the dissipation of the energy of electrical oscillations in a dielectric subjected to the action of an alternating electric field. In this case, there arises a phase lag between the electric displacement vector $\vec{D}$ and the electric field strength $\vec{E}$, described by the dielectric loss tangent or dissipation factor:

$$\tan \delta = \varepsilon''/\varepsilon' \tag{4.15}$$

The magnitude of the dielectric constant of polymers ε' is determined by their chemical constitution, structure and composition. The parameters that characterize the dielectric losses (ε'' and $\tan \delta$) depend on the specific features of molecular motion in polymers and, hence, on their chemical constitution and structure.

4.3. PHENOMENOLOGICAL RELAXATION THEORY OF THE DIELECTRIC PROPERTIES OF POLYMERS

4.3.1. BASIC EQUATIONS

Let us consider the relationship between the electric displacement $\vec{D}$ and the electric field strength in a polymeric dielectric. We shall make use of some concepts that have been developed for describing the processes of acoustic relaxation in polymers (70). Since the analogy between acoustic relaxation and dielectric relaxation is based on the detailed physical similarity of these processes, it is natural that these concepts be employed in the study of the dielectric properties of polymers.

The electric displacement in an isotropic medium may be represented as the following sum:

$$\vec{D} = \vec{D}_\infty + \vec{D}_1 \tag{4.16}$$

where $\vec{D}_\infty$ is the electric displacement in the dielectric material, corresponding to a case where the frequency of electrical oscillations $\omega \to \infty$.

The vector $\vec{D}_\infty$ is defined as follows:

$$\vec{D}_\infty = \varepsilon'_\infty \vec{E} \tag{4.17}$$

where ε'_∞ is the dielectric constant measured at frequency $\omega \to \infty$.

The vector $\vec{D}_1$ is the "dissipation" part of the electric displacement:

$$\vec{D}_1 = \varepsilon_1 \vec{E} \tag{4.18}$$

where ε_1 is the dielectric constant of the dielectric. It must be a particular operator in a general form.

Representing the electric displacement as the sum of two terms is probably justified since the electric moment of the dielectric, resulting from the application of an electric field, has two components, one of which (the deformation component) is established very rapidly (10^{-13} s).

It should be remarked that expressions for the electric displacement $\vec{D}$ such as (4.17) are, strictly speaking, valid only for steady (time-independent) electric fields. If the electric field $\vec{E}$ applied to a dielectric varies periodically with time, the electric displacement $\vec{D}$ at each point of the medium at a given moment of time will depend not only on the electric voltage and the rate of its variation but also on the previous history of the material. If the period of variation of the electric field becomes commensurate with the time required for establishing a statistical equilibrium, then relaxation processes will play an active part in the medium. It is obvious that the transition to equilibrium can occur in such a way that the relaxation processes are superimposed. Therefore, in a real polymeric dielectric placed in a sinusoidally varying electric field the electric displacement vector must take account of the past history of the material in some way.

Thus, in order to describe the dielectric properties of polymeric dielectrics, use must be made of certain non-equilibrium values of $\vec{D}_1$ different from the steady-state values of $\vec{D}_{01}$, which correspond to static (time-independent) electric fields.

Assuming that the difference between $\vec{D}_1$ and the steady-state value $\vec{D}_{01}$ is not great, we can write the following relaxation equation:

$$\frac{\partial \vec{D}_1}{\partial t} = -\frac{1}{\tau}(\vec{D}_1 - \vec{D}_{01}) \tag{4.19}$$

Equation (4.19) may be regarded as a corollary of the fundamental propositions of the thermodynamics of non-equilibrium (irreversible) processes. If the electric displacement $\vec{D}_1$ is steady-state, then $\partial\vec{D}_1/\partial t = 0$ and $\vec{D}_1 = \vec{D}_{01}$. The parameter τ is the dielectric relaxation time.

In the case of periodic harmonic processes Eq. (4.19) becomes

$$i\omega\tau\vec{D}_1 = -\vec{D}_1 + \vec{D}_{01} \tag{4.20}$$

From this equation it follows that

$$\vec{D}_1 = \frac{\vec{D}_{01}}{(1+i\omega\tau)} \tag{4.21}$$

From a comparison of Eq. (4.21) with Eq. (4.18) it becomes evident that the dielectric constant ε_1 can be given in a complex form:

$$\varepsilon_1 = \frac{\varepsilon_{01}}{1+i\omega\tau} \tag{4.22}$$

where ε_{01} is the quasi-static value of the dielectric constant (at $\omega \to 0$).

Real polymeric dielectrics are commonly described by a spectrum of relaxation times rather than by a single relaxation time. There are several reasons for the appearance of a relaxation-time spectrum. They include unequal rates of relaxation processes in various portions of the material and the occurrence of different relaxation mechanisms. In the case of polymers, relaxation-time spectra probably appear as a result of the presence of long polymeric chains and the specificity of intermolecular interaction.

With an arbitrary number of relaxation processes, expression (4.22) may be written in the form:

$$\varepsilon_1 = \sum_{j=1}^{n} \frac{\varepsilon_{0j}}{1+i\omega\tau_j} \tag{4.23}$$

Thus, taking cognizance of expressions (4.16), (4.17), (4.18), and (4.23), we get:

$$\vec{D} = \left(\varepsilon_\infty + \sum_{j=1}^{n} \frac{\varepsilon_{0j}}{1+i\omega\tau_j}\right)\vec{E} \tag{4.24}$$

The expression enclosed in parentheses may be looked upon as an operator of the dielectric constant:

$$\hat{\varepsilon} = \varepsilon_\infty + \sum_{j=1}^{n} \frac{\varepsilon_{0j}}{1+i\omega\tau_j} \tag{4.25}$$

This operator can be presented in a different form:

$$\hat{\varepsilon}=\varepsilon_\infty+\sum_{j=1}^{n}\frac{\varepsilon_{0j}}{1+\tau_j\frac{\partial}{\partial t}} \tag{4.26}$$

Comparing expressions (4.13), (4.14), (4.16), and (4.24) and separating the real and imaginary parts in expression (4.24), we arrive at the following formulas for ε' and ε'':

$$\varepsilon'=\varepsilon_\infty+\sum_{j=1}^{n}\frac{\varepsilon_{0j}}{1+\omega^2\tau_j^2} \tag{4.27}$$

$$\varepsilon''=\sum_{j=1}^{n}\frac{\varepsilon_{0j}\omega\tau_j}{1+\omega^2\tau_j^2} \tag{4.28}$$

These formulas indicate the presence of a discrete spectrum of dielectric relaxation times arising in a polymer under the influence of the applied varying field. In passing from the discrete to a continuous spectrum at $n\to\infty$, we obtain from expressions (4.27) and (4.28):

$$\varepsilon'=\varepsilon_\infty+\int_0^\infty\frac{H(\tau)\,d\tau}{1+\omega^2\tau^2} \tag{4.29}$$

$$\varepsilon''=\int_0^\infty\frac{H(\tau)\,\omega\tau\,d\tau}{1+\omega^2\tau^2} \tag{4.30}$$

where $H(\tau)$ is the density of the dielectric relaxation time spectrum.

Let us consider a case where $\omega\tau\to\infty$. Then $\varepsilon'=\varepsilon_\infty$ and $\varepsilon''\to 0$. For polymers this condition corresponds either to very high frequencies ($\omega\to\infty$, $\tau=\text{const}$) or to very low temperatures ($\omega=\text{const}$, $\tau\to\infty$). Thus, from phenomenological relaxation theory it follows that at low temperatures the dielectric constant ε' and the corresponding losses determined by the parameter ε'' can be expected to decrease.

In the other limiting case where $\omega\tau\to 0$, which corresponds to low frequencies or high temperatures, the quantity ε' increases, attaining the value

$$\varepsilon'=\varepsilon_\infty+\int_0^\infty H(\tau)\,d\tau \tag{4.31}$$

and ε'' tends to zero.

4.3.2. DIELECTRIC PROPERTIES OF A SYSTEM WITH A SINGLE RELAXATION TIME

The expressions for ε' and ε'' assume the simplest form in the case of a relaxation process characterized by a single relaxation time. If in Eqs. (4.27) and (4.28) one of the values of τ_j and one of the quantities ε_{0j} corresponding to this relaxation time are different from zero ($\tau_j \neq 0$; $\varepsilon_{0j} \neq 0$), then ε' and ε'' can be given by

$$\varepsilon' = \varepsilon_\infty + \frac{\varepsilon_1}{1+\omega^2\tau^2} \tag{4.32}$$

$$\varepsilon'' = \frac{\varepsilon_1 \omega\tau}{1+\omega^2\tau^2} \tag{4.33}$$

It should be noted that formulas (4.32) and (4.33) coincide exactly with the corresponding Debye formulas (163, 186), though this is not obvious at first glance.

Let us consider the dependence of ε' on the parameter $\omega\tau$, equal to

$$\omega\tau = 2\pi\tau/T = 2\pi D \tag{4.34}$$

where τ is the relaxation time; T is the time of variation of the electric field in the dielectric; D is the parameter first introduced by Reiner (187) and termed the Deborah number ($D = \tau/t$, where t is the time of observation).

An analysis of equations that describe relaxation processes in polymers is preferably carried out by using the Deborah number (or, what is the same thing, the parameter $\omega\tau$). Obviously, in dealing with periodic processes the vibration period is considered instead of the time of observation.

At $D = 0$ ($\omega\tau = 0$)

$$\varepsilon_0 = \varepsilon_\infty + \varepsilon_1 \tag{4.35}$$

At $D \rightarrow \infty$ ($\omega\tau \rightarrow \infty$)

$$\varepsilon' = \varepsilon_\infty$$

Thus, when the value of $\omega\tau$ changes from 0 to ∞, the dielectric constant varies from ε_0 to ε_∞, i. e., decreases. Substituting ε_1 found from expression (4.35) into formulas (4.32) and (4.33), we obtain expressions for ε' and ε'' in a more usual canonical form:

$$\varepsilon' = \varepsilon_\infty + \frac{\varepsilon_0 - \varepsilon_\infty}{1+\omega^2\tau^2} \tag{4.36}$$

$$\varepsilon'' = (\varepsilon_0 - \varepsilon_\infty)\frac{\omega\tau}{1+\omega^2\tau^2} \tag{4.37}$$

It is not difficult to show that within the framework of the model under discussion the expression for the loss tangent has the form

$$\tan\delta = 2\tan\delta_m \frac{\omega\tau_1}{1+\omega^2\tau_1^2} \qquad (4.38)$$

where

$$2\tan\delta_m = \frac{\varepsilon_0 - \varepsilon_\infty}{\sqrt{\varepsilon_0\varepsilon_\infty}} \qquad (4.39)$$

The relaxation time τ_1 differs from the relaxation time τ in formulas (4.36) and (4.37):

$$\tau_1 = \tau\sqrt{\frac{\varepsilon_\infty}{\varepsilon_0}} \qquad (4.40)$$

It is easy to see that $\tan\delta$ has a maximum ($\tan\delta_m$) at $\omega\tau_1 = 1$, while ε'' passes through a maximum at $\omega\tau = 1$. Typical frequency dependences of ε', ε'', and $\tan\delta$ calculated from formulas (4.36) through (4.38) on the assumption that $\varepsilon_0 = 10$, $\varepsilon_0/\varepsilon_\infty = 5$ and $\tau = 10^{-4}$ s are presented in Fig. 4.1.

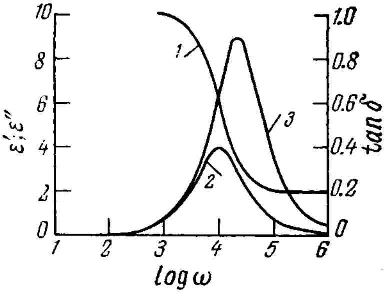

FIG. 4.1. Frequency dependences of ε'(1), ε''(2) and $\tan\delta$ (3) calculated from formulas (4.36) through (4.38) on the assumption that $\varepsilon_0 = 10$, $\varepsilon_\infty = 2$and $\tau = 10^{-4}$ sec.

The Debye equations (4.36), (4.37), and (4.38) for ε', ε'', and $\tan\delta$ very closely resemble the corresponding expressions for the components of the complex elastic modulus (70, 163), the electric field strength $\vec{E}$ being analogous to the mechanical stress σ and the electric displacement $\vec{D}$ to the strain ε. In its turn, the complex dielectric constant is analogous to the complex compliance J^*.

As a rule, dielectric relaxations in polymers are associated with the presence of a relaxation-time spectrum. Apart from formulas (4.29) and (4.30), other methods of describing the dielectric properties of polymers are also used (163, 188-193).

4.3.3. TEMPERATURE DEPENDENCE OF DIELECTRIC PROPERTIES

From the above expressions for ε', ε'', and $\tan\delta$ it can be seen that these parameters depend on the frequency and the relaxation time τ. The temperature dependence of dielectric properties is determined by the character of the dependence of the relaxation time on temperature. If we assume that τ depends on temperature T in accordance with an expression of the type

$$\tau=\tau_0 e^{U/RT} \tag{4.41}$$

(where τ_0 is a constant quantity; U is the energy of activation; R is the universal gas constant), then Eqs. (4.36) and (4.37) may be written in the form:

$$\varepsilon'=\varepsilon_\infty^T+\frac{\varepsilon_0^T-\varepsilon_\infty^T}{1+\omega^2\tau_0^2 e^{2U/RT}} \tag{4.42}$$

$$\varepsilon''=(\varepsilon_0^T-\varepsilon_\infty^T)\frac{\omega\tau_0 e^{U/RT}}{1+\omega^2\tau_0^2 e^{2U/RT}} \tag{4.43}$$

where ε_0^T and ε_∞^T are the corresponding dielectric constants at temperature T.

The plot of ε'' against $1/T$ is often used for the analysis. It has been shown (163, 194) that if the difference $\varepsilon_0-\varepsilon_\infty$ does not depend on temperature, then the area under the curve of the function $\varepsilon''=f(1/T)$ depends only on the activation energy and the parameter $\varepsilon_0-\varepsilon_\infty$ and does not depend explicitly on frequency:

$$\int_0^\infty \varepsilon'' d\left(\frac{1}{T}\right)=(\varepsilon_0-\varepsilon_\infty)\frac{\pi R}{2U} \tag{4.44}$$

For polar molecules, from the Onsager, Fröhlich, and Debye theories it follows that

$$\varepsilon_0-\varepsilon_\infty=A/T \tag{4.45}$$

where A is a constant.

In this case, the dependence of ε'' on $1/T$ appears to be more complicated (163, 194). Apart from the area under the $\varepsilon''=f(1/T)$ curve, the magnitude of the activation energy of relaxation processes is also associated with the half-peak width of the curve. In fact, formula (4.37) can be rewritten in the form:

$$\varepsilon''=2\varepsilon_m''\frac{\omega\tau}{1+\omega^2\tau^2} \tag{4.46}$$

If we introduce the notation $\varepsilon_m''/\varepsilon''=r$, then $\omega\tau=r\pm\sqrt{r^2-1}$. It can be shown (70, 163) that

$$U=\frac{2.303R\log(r\pm\sqrt{r^2-1})}{\frac{1}{T_i}-\frac{1}{T_m}} \tag{4.47}$$

where T_i is the temperature corresponding to ε_i''; T_m is the temperature at which the maximum of ε'' occurs.

If we put $r = 2$, which corresponds to $\varepsilon'' = 0.5\ \varepsilon''_m$, then

$$U = \frac{2.63}{\frac{1}{T_{0.5}} - \frac{1}{T_m}} \qquad (4.48)$$

where $T_{0.5}$ is the temperature which corresponds to $\varepsilon'' = 0.5\ \varepsilon''_m$ on the $\varepsilon'' = f\,(1/T)$ graph.

If the relaxation process cannot be described by a model that presupposes the existence of a single relaxation time, then the relationship between the activation energy and the half-peak width on the $\varepsilon'' = f\,(1/T)$ plot becomes more complicated (163).

4.4. THE MECHANISM OF DIELECTRIC RELAXATION

One of the first scientists to study the mechanism of dielectric relaxation in solids was Debye, who assumed that molecular dipoles placed in a constant electric field may align themselves, at a first approximation, in two directions: parallel or antiparallel to the field. If no electric field is applied, both positions are equivalent and equal potential energies correspond to them. If the potential energy of the dipole is represented as a function of the angle of rotation, then it will be a curve with two equal minima separated by a maximum (the potential barrier), the height of which relative to the minimum will determine the probability of the transition of the dipole from one position to the other (rotation through 180°).

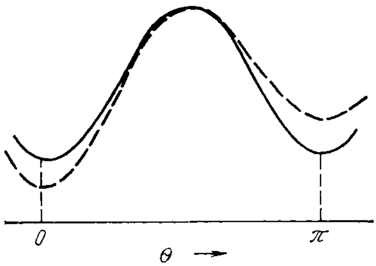

FIG. 4.2. The potential energy of a dipole as a function of the angle of rotation (the solid curve—in the absence of an electric field, the dashed line—with an applied electric field).

When an electric field is applied, the energies of the dipoles situated on each side of the potential barrier are changed. The dipoles parallel to the field have a lower potential energy (Fig. 4.2); and dipoles antiparallel to the field will have a potential energy minimum lying somewhat higher. In such a case, the probabilities of a switchover from position 1 to position 2 and vice versa will not coincide. The dipoles will perform oscillations at frequency ν_0 about their equilibrium positions and their transition from one position to another will be associated with the possibility of rotation. A detailed examination of the process of jumping over the potential barrier leads one to the conclusion that the dielectric relaxation time depends on temperature in accordance with an equation of the type (4.41). These problems have been examined in detail by Fröhlich (189) and Hoffman (195) and treated by other authors (163, 188-195). We shall note only that in order to calculate the activation energies of the processes of dielectric relaxation, resort is occasionally made to the theory of absolute reaction rates (196, 197). In this case, instead of τ_0, use is made of the pre-exponential factor h/kT in Eq. (4.41), where h is Planck's constant.

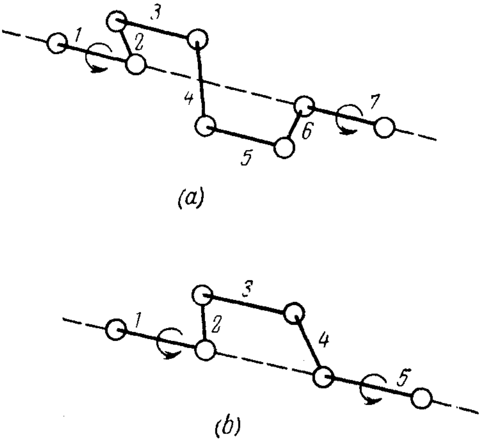

FIG. 4.3. The molecular mechanism of γ-relaxation. The movement of aliphatic carbon atoms (the crankshaft rotation):
a—the Schatzki model; *b*—the Boyer model.

Models that describe the rotation of dipoles associated with the jump over the potential barrier hindering rotation are widely used to depict dielectric relaxations occurring in polymers at low temperatures. The relaxation processes caused by the restricted rotation of side groups are explained on the basis of concepts of this kind.

Another possible mechanism of both dielectric and mechanical relaxation (γ-relaxation) is the crankshaft rotation observed below the glass-transition temperature (Fig. 4.3). Schatzki (162) assumed that this mechanism leads to a relaxation process observed near —120°C in measurements at a frequency of 1 Hz in polymers containing a linear sequence of methylene groups $(-CH_2-)_n$, where $n \geqslant 4$. This relaxation process, which has come to be known as the γ-relaxation, is observed in polyethylene, aliphatic polyamides and polyesters, and some polymethacrylates containing linear methylene chains in side branches. The mechanism of molecular motion proposed by Schatzki is shown in

Fig. 4.3. It consists of the simultaneous rotation of a segment of the polymeric chain about the bonds 1 and 7 in such a way that the carbon atoms contained in this chain unit move like a crankshaft. It is essential here that bonds 1 and 7 are collinear. The other parts of the chains or side groups may remain frozen, the motion taking place in only a relatively small volume. If all the valence angles and bond lengths are equal, then, according to Schatzki, four carbon atoms must be present between the collinear bonds.

Boyer (198) conjectured that the chain unit that effects the hindered rotation associated with the transition from one conformation to another contains only two carbon atoms (see Fig. 4.3). This structure of the kinetic unit responsible for the γ-relaxation contains, however, an energetically less favourable *cis*-conformation about bond 3, and so seems less probable than the Schatzki model. The possibility of this kind of movement (crankshaft rotation) in polymers containing aliphatic linkages is also pointed out by Wunderlich (13), who maintains that collinear bonds may in this case be separated by three carbon atoms. There is a large body of experimental data confirming the molecular mechanism of γ-relaxation based on crankshaft rotation. The presence in the polymeric chain of runs of three or more CH_2 units, each of which is linked to immobile groups, leads to the appearance of γ-relaxation (70).

The available experimental data indicate that this mechanism is possible only in amorphous polymers or in amorphous regions of crystalline polymers. This is because the crankshaft rotation can only occur about two collinear bonds. This condition is not fulfilled in crystalline regions, where the sequences of methylene groups form mainly *trans*-conformations. The activation energy of the γ-relaxation process observed in amorphous regions ranges from 50 to 63 kJ/mole, which is in good agreement with the values predicted by Schatzki (54 kJ/mole). His value for activation energy was obtained on the basis of the assumption that for the crankshaft rotation to be realized it is necessary that the potential barrier that exists in butane ($U = 31$ kJ/mole) and the potential barrier of the van der Waals type ($U = 21$-25 kJ/mole) calculated from the cohesive energy density be overcome. It is interesting that the predicted free volume required for this to occur is four times greater than the molar volume of the methylene group. This agrees well with estimates made on the basis of experimental investigations.

Despite the fact that, according to Boyer (198), the crankshaft rotation may prove to be the principal mechanism of a secondary (below T_g) relaxation in various polymers, no theory has been developed that could predict on the basis of this mechanism the intensity or the peak width of the dielectric or mechanical relaxation.

Most theories of relaxation phenomena in polymers, including the one considered above, rest on the fundamental assumption of the possibility of the internal rotation of the individual elements of macromolecules about certain chemical bonds. Processes of this type are thermal-activation processes and involve the jump of atoms (or groups of atoms) over a potential-energy barrier from one equilibrium position to another. There are other quite different mechanisms which might enable one to explain dielectric relaxation processes in polymers. Such mechanisms have been examined by Yamafuji and Ishida (199), Gotlib and Salikhov (200) and others (201). One of these mechanisms involves repressing the oscillations of segments of the polymeric chain which occur near the equilibrium position. This relaxation mechanism is called the local mode. A mechanism of this kind was used by Hill (202) for calculating the dispersion of the dielectric constant in polar liquids.

Saito *et al.* (201) considered the oscillations of a molecule surrounded by other molecules about the position corresponding to the local equilibrium conformation. The analysis rests on the assumption that the superposition of oscillations is a set of normal vibrations. The characteristic frequency of the nth normal vibration is given by

$$\omega_n = \sqrt{c_n/m} \tag{4.49}$$

where c_n is the relevant force constant; m is the mass of the vibrating unit.

The expression for $\bar{x}_n$ (the mean square of the amplitude) of the nth vibration has the form

$$\sqrt{(\bar{x}_n)^2} = \frac{2kT}{m\omega_n^2} \cdot \frac{\frac{\hbar\omega_n}{kT}}{e^{\frac{\hbar\omega_n}{kT}} - 1} \tag{4.50}$$

The characteristic frequencies and mean amplitudes have a rather wide distribution. Though the force constants for torsional vibrations are very small as compared with the force constants for other modes of vibration, torsional vibrations may be regarded as vibrational modes with the lowest frequency and the largest amplitude. It is evident that torsional vibrations of large amplitude will be strongly damped in the glassy state, which is characterized by a very high viscosity. All this may lead to the occurrence of a relaxation process. Saito and his coworkers (201) carried out a detailed investigation of this relaxation process, introducing the friction ξ_l into the Kramers-Chandrasekhar, diffusion equation. The relaxation time for local oscillations is defined as

$$\tau_\lambda = \xi_l / c_\lambda \gg 1/\omega_\lambda \tag{4.51}$$

where c_λ is the force constant for torsional vibration λ; ω_λ is the corresponding intrinsic frequency.

From expression (4.51) it follows that at large ξ the relaxation frequency τ_λ^{-1} will be much lower than the characteristic frequency of the original normal vibrations. The order of magnitude of the activation energy associated with the viscosity was estimated on the assumption that the moving group is surrounded by vacancies, the volume of which is larger than a certain critical value. The critical volume is calculated on the basis of the potential of intermolecular interaction in the form of the Lennard-Jones potential. The calculated value of the activation energy for the local mode is about 42 kJ/mole. It has been shown (201) that for this relaxation process

$$\varepsilon_0 - \varepsilon_\infty = \frac{4\pi n N g p_0^2}{3c_\lambda} \cdot \frac{3\varepsilon_0}{2\varepsilon_0 + \varepsilon_\infty} \left(\frac{\varepsilon_\infty + 2}{3} \right)^2 \tag{4.52}$$

where n is the number of dipole units in the chain; g is the correlation factor; p_0 is the dipole moment of the repeat unit.

Expressions for the difference $\varepsilon_0 - \varepsilon_\infty$ which are more exact and, hence, more complicated than formula (4.52) have been used to describe the processes of low-temperature relaxation caused by local vibrational modes in such polymers as polyvinyl chloride, polyethylene terephthalate and polyformaldehyde.

The theory of local vibrations is employed in a number of cases to account for some subsidiary relaxation processes and predicts correctly the level of dispersion in dielectric relaxation. Nonetheless, this theory, like other theories, relates the relaxation time to a certain viscosity coefficient which is very difficult to determine.

The problem of the effect, on dielectric properties, of such parameters as the degree of crystallinity (in crystalline polymers), the degree of cross-linking (in network polymers), the plasticizer concentration (in plasticized polymers) has been tackled by a number of investigators (70, 190, 191).

4.5. METHODS OF STUDYING THE DIELECTRIC PROPERTIES OF POLYMERS

Dielectric measurements in polymers usually cover a very wide range of frequencies, from 10^{-4} to 3×10^{10} Hz. The need for measurements over such a wide frequency range arises from the very wide spectrum of dielectric relaxation processes taking place in polymers. It is natural that this wide frequency range cannot be covered by any one method. A salient feature of dielectric measurements in polymers is that in measurements of tan δ at relatively high frequencies over a wide temperature range the relaxation maxima shift towards higher temperatures with increasing frequency and, being superimposed, reduce the resolving power of the method. In measurements at high temperatures the interpretation of the results of dielectric measurements in polymers becomes very complicated because of the losses associated with electrical conduction. Various methods of measurement have been considered in detail in a number of monographs and review articles (163, 203, 204). The overwhelming majority of measurements of parameters that characterize the dielectric properties of polymers (ε' and tan δ) are usually carried out over the frequency range 3 to 3×10^6 Hz. Bridge circuits are commonly employed for measurements at these frequencies. At higher frequencies use is made of resonance methods.

The main difficulties arising in dielectric measurements in polymers at low temperatures are due to the fact that at $T \to 0$ the dielectric losses (tan δ) are sharply reduced in most polymers and attain a value of about 10^{-5} near the liquid-helium temperature in such polymers as polyethylene. Other difficulties that arise in low-temperature dielectric measurements in polymers are associated with the need to take account of the change in the thickness of the test sample, with the specific problems of designing special cryostats, and with the need for accurate thermostatting and temperature measurements.

Most dielectric measurements in polymers in the cryogenic region are made with the aid of precision bridges which allow one to measure absolute values of tan δ of the order of 10^{-5} to 10^{-6}. Chant, who used a Schering precision bridge, points out (205) that since the sensitivity of the bridge is usually proportional to the frequency, at frequencies lower than 75 Hz errors in the measurements sharply increase. The most accurate measurements of dielectric losses in polymers at very low temperatures have probably been made by the calorimetric method (206-208), using the instrument designed in the Cavendish Laboratory (of Cambridge University) by Vincett (206). At a voltage of 1 kV with a capacitance of 200 pF Vincett succeeded in obtaining, at a frequency of 1 kHz, a resolution for the value of tan δ equal to 2×10^{-8}. Detailed information concerning the instrument and the specificity of dielectric measurements at low temperatures is available in the literature (159, 205-210).

4.6. DIELECTRIC PROPERTIES OF POLYMERS

The rapid development of modern engineering in recent years has stimulated interest in the investigation of the dielectric properties of polymers at low temperatures. The need to investigate these properties arose from work on the use of superconduction phenomena, the development of low-temperature power-transmission lines, superconducting magnets, low-temperature switching devices, and cryogenic gyroscopes (205, 206, 211). A powerful impetus was given to such investigations by the problems associated with the exploration of outer space (212) and the development of cryogenic engineering. The purpose of these investigations was to uncover the possibilities of exploiting polymeric materials at low temperatures, the choice of the most suitable materials, and also to establish the fundamental regularities in behaviour that would enable one to determine the factors governing the properties of polymers at low temperatures.

In spite of the fact that the dielectric properties of polymeric materials at high temperatures have been studied fairly well, no investigations have as yet been carried out in the low-temperature region at temperatures around —150° C. With the exception of some studies by Mathes (204, 211, 212), the dielectric properties of polymeric materials at low temperatures, down to the liquid-helium temperature, have hardly been studied at all until recently.

Mathes measured the dielectric properties of a number of polymers at audio frequencies at temperatures down to 4.2 K. He has shown that typical polar polymers have a relaxation region near —50°C; at lower temperatures the loss tangent decreases, as a rule, with fall of temperature and the dielectric constant remains unchanged. While studying polyvinyl fluoride, Mathes found that the loss tangent ($\tan \delta$) of this polymer at 4.2 K is strongly dependent on frequency, and decreasing with increasing frequency. He came to the conclusion that this phenomenon is associated with residual ionic conduction. It can be shown theoretically (189) that the dielectric constant of polar solids must decrease at temperatures down to a certain critical temperature, and below that temperature the material must behave as a nonpolar dielectric. The experimental results obtained by Mathes indicate that this theory requires thorough experimental verification.

Chant (205), Allan and Kuffel (209) have carried out a thorough study of the dielectric properties of a number of thermoplasts at temperatures down to 4.2 K. A detailed investigation of the dielectric properties of polyethylene at very low temperatures has been undertaken by Vincett (206), Phillips (207), and Carson

(208) in the Cavendish Laboratory, and also Heybey and Müller (210). We shall undertake a more detailed consideration of the dielectric properties of some polymers at low temperatures.

Polyethylene. The dielectric properties of polyethylene at low temperatures have been thoroughly investigated. Mathes (211) has shown that two maxima appear in the temperature dependence of tan δ for this polymer, as measured at a frequency of 1 kHz. One of the peaks of tan δ lies at 70° C and the other near —100°C (Fig. 4.4). The measurements were made only down to —130°C, since below this temperature values of tan δ below 1×10^{-4} were obtained, at which level large errors become evident. To avoid these difficulties, Hara (213) studied low-density polyethylene that had been subjected to the ultraviolet radiation in the air for 48 hours at 50°C. The dielectric loss in the polyethylene resulting from the irradiation increases by almost two orders of magnitude, which makes it possible (213) to study this polymer at temperatures ranging from 130°C to the liquid-helium temperature (4.2 K). The low-temperature loss peak (213) measured at a frequency of 300 Hz was found to be situated at —130°C. This γ-relaxation maximum was distinctly relaxational in nature and shifted towards higher temperatures with increasing frequency.

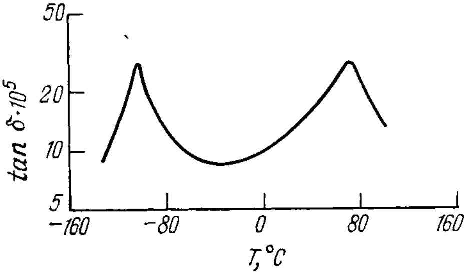

FIG. 4.4. Temperature dependence of the loss tangent for linear high-density polyethylene at $\nu = 1$ kHz.

Using the theory of absolute reaction rates, Hara (213) calculated the activation energy of this relaxation process, finding it to be equal to 42 kJ/mole. It is supposed that this low-temperature peak is due to local vibrations (214, 215). Chant (205) measured the loss tangent in commercial samples of polyethylene at a frequency of 75 Hz and observed a single sharply pronounced maximum at 150 K. The value of tan δ measured in polyethylene at 4.2 K was found to be equal to 2.5×10^{-5}. Chant has shown that the dielectric constant of polyethylene measured at the same frequency depends very little on temperature between 4.2 and 300 K, decreasing only slightly with increasing temperature.

A detailed study of the dielectric properties of polyethylene at low temperatures has been carried out by Allan and Kuffel (209). They have demonstrated that the dielectric loss tangent of polyethylene is dependent to a considerable degree on temperature and frequency (Fig. 4.5). Attempts have been made to account for such clear-cut dielectric relaxation processes in a nonpolar polymer such as polyethylene in terms of the heterogeneity of the material, the presence of carbonyl groups formed through the oxidation of polyethylene in the preparation of the samples, and also by the slight difference in polarity of the C—H bonds at the primary, secondary and tertiary carbon atoms. The most intriguing result obtained by Allan and Kuffel (209) is that below 90 K the loss tangent of polyethylene is independent of temperature, though slightly dependent on frequency. Since the loss value at these temperatures was very low (2×10^{-5}), the authors did not exclude the possibility that the frequency dependence of tan δ observed by them near the temperature of liquid helium could have been due to the frequency dependence of the measuring circuit.

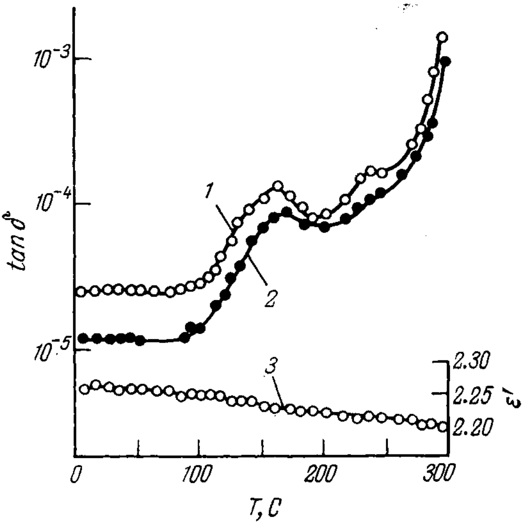

FIG. 4.5. Temperature dependence of the dielectric loss tangent tan δ (*1*, *2*) and the dielectric constant(*3*) of polyethylene at the following frequencies: *1*—1 kHz; *2*—5 kHz; *3*—2.34 kHz.

The decrease in the dielectric constant ε′ of polyethylene with a rise in temperature (see Fig. 4.5) could possibly be associated with the fact that the value of ε' was calculated over the entire temperature range using the thickness of the sample measured at room temperature and that changes in the thickness with changes in temperature were disregarded. Another factor responsible for the dependence of ε' on temperature may be the change of the density of polyethylene with the change of the temperature from 300 to 4.2 K.

A further study of the dielectric properties below 4.2 K was completed by Vincett (206), who succeeded in improving the accuracy of measurements two or three times using the calorimetric method. While investigating high-density polyethylene, he detected a maximum on the frequency curve of tan δ at some fixed temperatures (Fig. 4.6). The frequency ω_m corresponding to the peak of tan δ shifted to higher frequencies with increasing temperature. For example, whereas at $T = 1.35$ K the value of ν_m was equal to 1.3 kHz, at $T = 2$ K the frequency ν_m was 1.9 kHz, and at $T = 4.2$ K its value was 4 kHz.

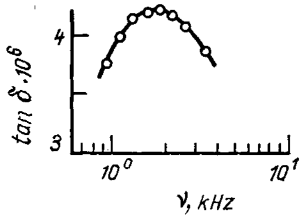

FIG. 4.6. Frequency dependence of the loss tangent for polyethylene at a temperature of 2 K(206).

At 4.2 K the frequency dependence of tan δ is well described by the Debye equation for a single relaxation time (4.38).

If the relaxation time were dependent on temperature in accordance with Eq. (4.41) (i.e., according to the Arrhenius equation), one could expect log ω_m to be proportional to $1/T$. From the examples cited above, however, it follows that the experimentally determined values of ω_m are proportional to temperature T. It has been found (206) that at low temperatures and certain frequencies the loss tangent of polyethylene increases as the voltage applied to the measuring cell is increased. For instance, in measurements made at 2 kHz with the voltage being changed from 230 to 340 V the value of tan δ increases by 6 per cent at 2 K and by 10 per cent at 9.35 K, while at 4.2 K the effect is 1.5 per cent. In measurements at a higher frequency (10 kHz) the effect manifests itself when use is made of a higher measuring voltage (500 V). Vincett attempted to find an analogous phenomenon in other polymers, but reported that, considering the possible experimental error, all the polymers studied, with the exception of polyethylene, could not be said to exhibit this phenomenon. Since instrumental error in such a case is hardly probable, it is possible that Vincett was dealing with the phenomenon of dielectric saturation. If this is so, the induced dipoles must have an energy of the order of kT, which can vary substantially depending on the field strength.

The low-temperature dielectric loss peak detected by Vincett can hardly be interpreted from the viewpoint of thermal activation leading to the transition through the potential barrier. In this case, the height of the potential barrier would have been too low and the value of the pre-exponential factor in Eq. (4.41) would have been equal to $\tau_0 = 1/\nu_0 = 1/5 \approx 2 \times 10^{-4}$ (kHz)$^{-1}$. Besides, the height of all the barriers must have been the same. Thus, the low-temperature relaxation process in polyethylene can hardly be described within the framework of classical relaxation concepts. The tunnelling mechanism associated with phonon effects seems to be more probable, just as is the case with quartz (216, 217). For such processes the frequency ω_m may be proportional to T.

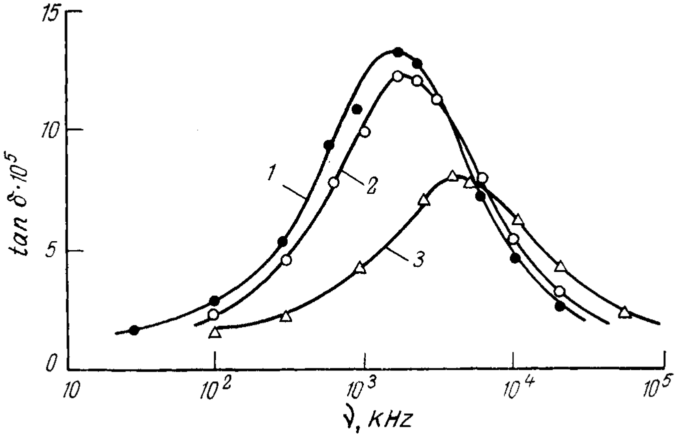

FIG. 4.7. Frequency dependence of the loss tangent for polyethylene (207) at temperatures:

1—1.73 K; 2—2,06 K; 3—4.2 K.

The interpretation of this low-frequency dielectric loss peak in terms of quantum-mechanical concepts has been confirmed in the work by Phillips (207), who measured tan δ in polyethylene over a frequency range of 10-10^6 Hz at temperatures from 1 to 4.2 K. Phillips also observed a peak in the frequency dependence of tan δ, whose maximum at $T = 4.2$ K corresponds to the frequency 4.3 kHz. It was found, however, that the form of the tan $\delta = f(\omega)$ curve differs from that predicted by the Debye theory based on the concept of a single relaxation time. The typical frequency dependences obtained by Phillips (207) are given in Fig. 4.7. At first sight it might seem that this relaxation process is a thermal activation, since with rise of temperature the loss peak shifts towards higher frequencies. But in practice this is not so. The most distinctive feature of thermal-activation processes is the linear dependence of log ω_m on the inverse temperature, $1/T$. It has been established (207) that this dependence does not hold true for the low-frequency relaxation process observed in polyethylene near the liquid-helium temperature (Fig. 4.8). Below 3 K the frequency ω_m is directly proportional to temperature (Fig. 4.9). Between 4 and 10 K the temperature dependence of τ is given by the expression

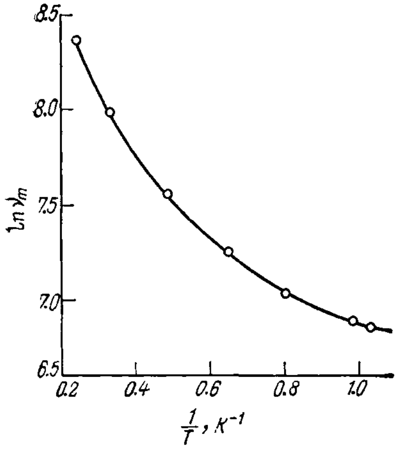

FIG. 4.8. The logarithm of the frequency γ_m corresponding to the loss tangent maximum for polyethylene against inverse temperature.

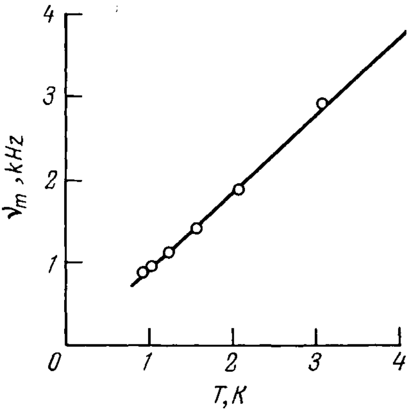

FIG. 4.9. Temperature dependence of ν_m for polyethylene.

$$\tau = \frac{\alpha}{1+(T/T_0)^{\beta}} \tag{4.53}$$

where α, β, and T_0 are constants.

A relation of the type (4.53) is an intermediate one, between a linear and an exponential relationship. It turns out that when the voltage of the constant electric field applied perpendicular to the thickness of the sample is increased to 1 kV and the measuring voltage is relatively low, the loss maximum is reduced.

Thus, the experimental data obtained by Phillips (207) cannot be accounted for within the framework of a relaxation theory of the thermal-activation type either. They can, however, be explained in terms of quantum-mechanical concepts. It has been suggested (207) that a relatively simple model can be used for the purpose. It has been proposed that a charged particle be treated as being in a potential well which has two potential energy minima separated by a barrier V_0; the energy difference between two such minima is 2Δ. This model can be used to describe the rotation of an asymmetric group between two equilibrium positions. Using the corresponding wave functions, Phillips derived expressions for the area under the peak of the $\varepsilon'' = f(\omega)$ curve and the relaxation time. In this model it is assumed that the transition of the particle from one potential energy minimum to another is accompanied by the emission or absorption of a phonon of energy 2ε.

At very low temperatures, according to this model, relaxation is due to spontaneous transitions and the relaxation time is independent of temperature. At somewhat higher temperatures, when $\varepsilon/kT < 1$, the relaxation time τ is found to be inversely proportional to temperature ($\omega_m \propto T$). It is the latter case that corresponds to the conditions of the experiment conducted by Phillips (207). He shows that the charged particle is a proton and that the low-temperature loss peak is probably associated with the rotation of the hydroxyl groups in the crystalline regions of the polymer. A small number of such groups linked to the carbon atoms in the main chain may exist in polyethylene (207).

The dielectric properties of polyethylene at low temperatures were further studied by Carson (208). Using the same experimental technique as employed by Vincett and Phillips (206, 207), he extended the frequency range to 100 MHz. While attempting to verify the assumption made by Phillips that quantum tunnelling is the mechanism of low-temperature dielectric relaxations in polyethylene, Carson investigated deuterated as well as ordinary polyethylene. If tunnelling does really take place in polyethylene, then the parameters of this process must depend on the mass of the tunnelling particle. One would therefore expect the replacement of the hydrogen atoms by deuterium atoms to shift the low-temperature relaxation peak observed on the $\tan\delta = f(\omega)$ plot at 4 kHz in the direction of lower frequencies.

Apart from ordinary polyethylene, Carson investigated samples subjected to swelling in the vapours of H_2O and D_2O. For the polyethylene samples oxidized at 150°C for 8 hours, there was detected on the $\tan\delta = f(\omega)$ plot another relaxation peak at 4 HMz, which was more intense and broader than that observed at 4 kHz. In deuterated and hydrated samples the low-frequency loss peak (at 4 kHz) completely disappears. After deuteration the peak at 4 MHz is sharply reduced but a new loss maximum appears at 30 kHz (Fig. 4.10). Subsequent treatment of polyethylene in vapours of H_2O completely eliminates the loss peak at 30 kHz and restores the intense maximum at 4 MHz. By subjecting the hydrated and deuterated samples to prolonged drying in a vacuum, Carson tried to move to its previous position the loss peak that was observed at 4 kHz in the original sample. However, even drying in a vacuum at 80°C for 1.5 months failed to return the loss peak to the previous place.

The experimental data obtained by Carson (208) support the validity of the quantum model proposed by Phillips (207).

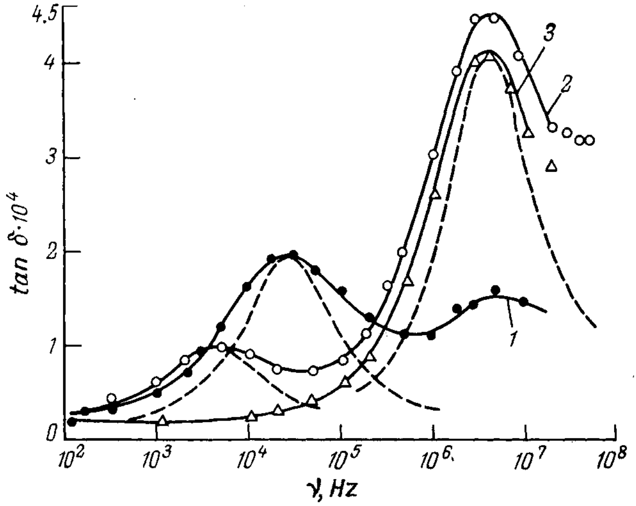

FIG. 4.10. Frequency dependence of the loss tangent for high-density polyethylene subjected to oxidation for 8 hours:

1—after deuteration for 48 hours; 2—immediately after oxidation; 3—after hydration for 48 hours. The dashed lines are theoretical curves drawn on the basis of a model with a single relaxation time.

Within the scope of this model the expression for the relaxation time can be given in the following form (208):

$$\tau \propto \frac{1}{\Delta_0^2 \varepsilon} \tanh\left(\frac{\varepsilon}{kT}\right) \tag{4.54}$$

where $\varepsilon^2 = \Delta^2 + \Delta_0^2$; the parameter $2\Delta_0$ characterizes the splitting of the principal energy level into a potential well with two symmetric minima (Fig. 4.11); 2Δ is the additional asymmetry of two potential wells.

Since the tunnelling process is strongly dependent on the mass of the tunnelling particle, the deuteration must affect the mass-dependent parameter Δ_0. Since for most experiments $\varepsilon < kT$, expression (4.54) simplifies to

$$\tau \propto (\Delta_0^2 T)^{-1} \tag{4.55}$$

with the proportionality factor being independent of the mass.

In order to calculate Δ_0 let us consider the movement of the particle described by a potential of the following type (218):

$$V = \frac{1}{2} V_0 \left[1 - \cos\left(\frac{\pi x}{l}\right)\right] \tag{4.56}$$

which takes account of the translational as well as the rotational motion of the particle. Substituting expression (4.56) into the Schrödinger equation and transforming it to the Mathieu equation, which can be solved numerically, we obtain the following expression for Δ_0 (208):

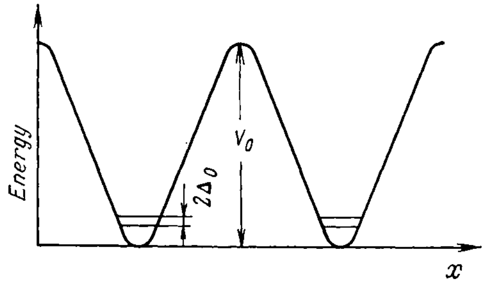

FIG. 4.11. Diagram of a potential well with two symmetric minima; $2\Delta_0$ is the splitting of the ground energy level (208).

$$\Delta_0 = A \left(\frac{V_0 \hbar^2}{m l^2}\right)^{1/2} \xi^{1/2} e^{-\gamma\xi} \tag{4.57}$$

where $\xi^2 = 2V_0 m l^2/\hbar^2$; γ and A are the fitting parameters.

Using expressions (4.55) and (4.57) in order to explain the low-frequency loss peak in polyethylene, one can show that the two-fold increase in mass, as is the case with deuteration, leads to a change in the relaxation frequency ν_m by four orders of magnitude (from 1.3×10^4 to 2 Hz). Thus, the quantum-mechanical model predicts that, as a result of the deuteration of polyethylene, the low-frequency loss peak observed by Phillips and Carson (207, 208) must shift to very low frequencies which lie beyond the capacity of the experimental technique used by these authors.

Crude estimates show (208) that as a result of deuteration the relaxation frequency of the loss peak, which lies in the megahertz region, must decrease by a factor of 150 ± 20. This shift is an indication that the appearance of the loss peak on the $\tan\delta = f(\omega)$ graph at 30 kHz is probably not accidental.

Calculations (208) based on the use of expression (4.57) and the parameters in it have shown that the dielectric relaxation in polyethylene may be caused by the rotations of the proton by 180° in a dipole 0.11 nm long.

This interpretation of the low-frequency loss peak in polyethylene at low temperatures is not the only one. Heybey and Müller (210), who measured dielectric losses in polyethylene at temperatures ranging from 1.15 K to room temperature at frequencies from 10 Hz to several kHz, maintain that the low-frequency tan δ peak in polyethylene is thermal-activational in nature. The activation enthalpy of this relaxation process, as calculated by these authors, is 0.02 kJ/mole, which is 10^3 times less than the corresponding values for relaxation processes of the thermal-activation type. This result probably disproves the authors' conclusion. Nevertheless, Heybey and Müller have discovered a number of important experimental facts associated with dielectric relaxation in polyethylene near 4.2 K. They observed that the low-temperature (low-frequency) loss peak is found only in deformed, extended samples. The magnitude of the peak increases with increasing degree of crystallinity and extension ratio. It has been found that some stretched samples exhibit a plateau on the $\tan \delta = f(T)$ curve at low temperatures. The value of tan δ at low temperatures greatly depends on the thermomechanical history of the samples under investigation and may vary from 10^{-6} to 10^{-4}. It is interesting that the dielectric losses for polyethylene samples that were melted and then cooled or quenched prove to be small.

Thus, even for the most thoroughly studied polymer, polyethylene, the nature of dielectric relaxation at $T \to 0$ K has not yet been fully clarified.

Polytetrafluoroethylene. Like polyethylene, polytetrafluoroethylene is a nonpolar polymer with a very low level of dielectric losses. Among the first scientists to measure the dielectric losses in this polymer near the liquid-helium temperature was Mathes (212). He obtained a rather low value of tan δ at 4.2 K (2×10^{-5}) ($\nu = 1$ kHz), while at 23°C, according to his data, $\tan \delta = 3 \times 10^{-4}$.

The most detailed investigation of the dielectric properties of polytetrafluoroethylene over the temperature range 4.2-300 K has been carried out by Chant (205). The results of these measurements at a frequency of 75 Hz are presented in Fig. 4.12. Polytetrafluoroethylene is the polymer with the lowest dielectric constant ($\varepsilon' \approx 2.1$), which decreases very slightly (by a factor of 0.05) as the temperature changes from 4.2 to 300 K. On the $\tan \delta = f(T)$ plot for polytetrafluoroethylene there is observed an intense dielectric loss maximum at 178 K ($\nu = 75$ Hz). The available experimental evidence is insufficient for the elucidation of the nature of this relaxation peak. It may be due to the unfreezing of the segmental motion in the amorphous regions or the γ-relaxation process or to the superposition of both these phenomena.

While studying the frequency dependence of tan δ in Teflon at $T = 4.2$ K, Chant detected a weak loss maximum at 180 Hz. This observation, however, was not confirmed by the subsequent and probably more accurate measurements carried out by Vincett (206). The value of tan δ for Teflon at 4.2 K over the frequency range 50 Hz to 10 kHz remains practically constant at 1.2×10^{-6} (Fig. 4.13). These values are less than the values of tan δ cited by Mathes and Chant by a factor of 10. Nonetheless, Hartwig and Grissom (219) found that at a frequency of 132 MHz the value of tan δ is 1.2×10^{-6}, the value of tan δ obtained by Siegel and coworkers (220) at 11 MHz being 9×10^{-6}. Such a range of values could be accounted for by the fact that the samples of polytetrafluoroethylene used by the different authors had different past histories, including different densities and degrees of crystallinity. No information on these characteristics was given by the authors.

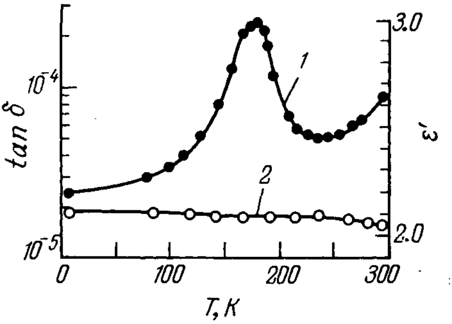

FIG. 4.12. Temperature dependence of tan δ (1) and ε′(2) for polytetrafluoroethylene at $\nu = 75$ Hz.

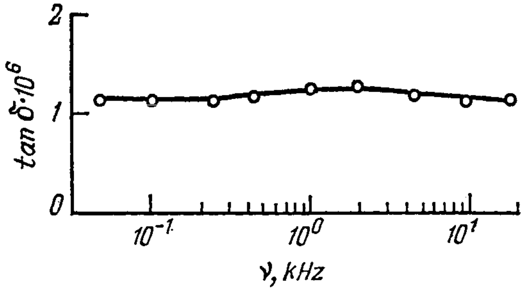

FIG. 4.13. Frequency dependence of the loss tangent for polytetrafluoroethylene at 4.2 K.

Polypropylene. This polymer, like the two polymers considered above, is nonpolar. The dielectric constant of polypropylene is somewhat higher than the dielectric constants of Teflon and polyethylene, but, as with these polymers, it depends very little on temperature (205), hardly changing within the temperature range 4.2-300 K (Fig. 4.14). At 116 K in polypropylene there appears an appreciable loss maximum ($\nu = 75$ Hz). From Chant's experimental data it follows that below this temperature there exists another loss maximum which is superposed by an intense and broad peak found at 116 K. At the liquid-helium temperature and a frequency of 75 Hz the value of tan δ for polypropylene is equal to 2×10^{-5} (205). The measurements made by Vincett (206) at the same temperature are not consistent with this result. The value of tan δ in polypropylene at 4.2 K over the frequency range 50 Hz to 20 kHz is practically independent of frequency at 3.5×10^{-6}. The same picture is observed at 2 K and 1.4 K. The value of tan δ obtained by Vincett agrees well with the results obtained by McCammon and his coworkers (221). The figure cited by these authors is 6×10^{-6} at 1 kHz and 4.2 K.

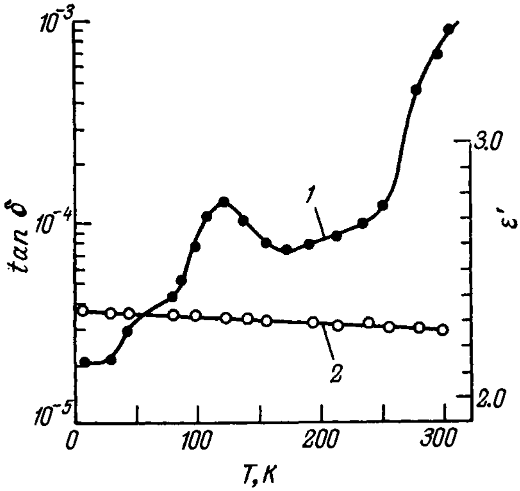

FIG. 4.14. Temperature dependence of tan δ (*1*) and ε' (*2*) for polypropylene at $\nu = 75$ Hz.

Dielectric measurements in polypropylene subjected to ultraviolet irradiation have shown (213) that no loss peaks are present in the case of annealed, well crystallized isotactic polypropylene over the temperature range 4.2-293 K. Nevertheless, in a quenched sample a weak maximum at 163 K ($\nu = 3$ kHz) is observed. It is believed that this maximum is due to the phenomenon of γ-relaxation. The intensity of this relaxation peak sharply increases with a decreasing degree of crystallinity, which points to its relationship to molecular mobility in the amorphous region. The activation energy of the relaxation process responsible for the appearance of this peak is 25 kJ/mole, which is considerably lower than the ordinary values characterizing γ-relaxation. At the same time, this activation energy corresponds to the process resulting from the unfreezing of the rotation of the methyl groups. The position of the low-temperature dielectric loss peak (116 K at a frequency of 75 Hz and 163 K at 3 kHz) agrees well with the temperatures at which, according to NMR data (235), the rotation of the methyl groups in polypropylene becomes free. The possibility cannot be excluded that it is precisely this rotation of the methyl groups that is responsible for the dielectric loss peak, though the dipolar orientation of the methyl groups does not manifest itself on the temperature dependence of the dielectric loss tangent.

Polyamides. Polyamides are polar crystalline polymers. The low-temperature properties of two representatives of the polyamide class have been thoroughly studied: Nylon 6,6 (205) and Nylon 11 (209).

Polyhexamethyleneadipamide (Nylon 6,6) has the following chemical structure:

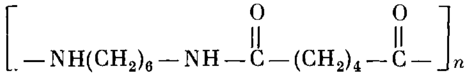

$$\left[-NH(CH_2)_6-NH-\overset{O}{\overset{\|}{C}}-(CH_2)_4-\overset{O}{\overset{\|}{C}}-\right]_n$$

The results of measurements of the dielectric constant ε' and the dielectric loss tangent, $\tan\delta$, in this polymer (205) are given in Fig. 4.15. The character of the temperature dependence of the dielectric constant of this polymer differs from the $\varepsilon' = f(T)$ graph for nonpolar crystalline polymers (polyethylene, polytetrafluoroethylene, polypropylene). Three regions can be distinguished on the $\varepsilon' = f(T)$ plot for Nylon 6,6. Between 4.2 K and 30-40 K the value of ε' is 2.9 and is independent of temperature. Between 40 K and 150 K the dielectric constant ε' increases only slightly with increase in temperature. Above 150 K the dielectric constant becomes more strongly dependent on temperature; the value of ε' at $T = 300$ K reaches 4.1. Thus, as the temperature changes from 4.2 to 300 K the dielectric constant of Nylon 6,6 increases by the amount $\Delta\varepsilon' = 1.2$. With the same temperature change the dielectric constant of polyethylene decreases from 2.27 to 2.20, i.e., by $\Delta\varepsilon' = -0.07$.

The temperature dependence of $\tan\delta$ ($\nu = 75$ Hz) for Nylon 6,6 has two maxima (at 160 K and 240 K) with the overall increase in the level of dielectric loss. The loss peak at 160 K is due to γ-relaxation and associated with the mobility of the chain units containing four or more CH_2 groups. The loss maximum observed at 240 K is due to the β-relaxation caused by the unfreezing of the motion of the chain units that, in addition to methylene groups, also contain amide groups which are not linked via hydrogen bonds to the amide groups of the neighbouring chains. The

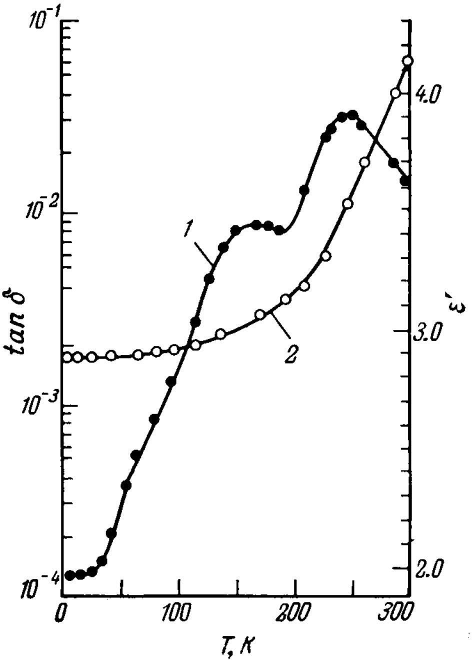

FIG. 4.15. Temperature dependence of tan δ (1) and ε' (2) for Nylon 6,6 at ν = 75 Hz.

β-relaxation in polyamides may be complicated and involve the mobility of complexes of the water-amide type, which are interlinked through hydrogen bridges. It is interesting that at low temperatures (from 30 to 4.2 K) the loss tangent of Nylon 6,6 is almost independent of temperature and assumes a value of about 1.2×10^{-4}, which is too low for a polar polymer. As the temperature changes from 4.2 to 300 K the loss tangent increases about 100 times. An essential point is that a low-temperature plateau appears on the $\varepsilon' = f(T)$ and $\tan \delta = f(T)$ graphs in about the same temperature range.

Nylon 11 has the following chemical structure:

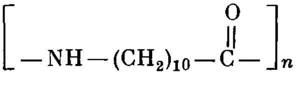

$$\left[-NH-(CH_2)_{10}-\overset{\overset{\displaystyle O}{\|}}{C}- \right]_n$$

Since the repeat unit of this polymer contains less polar groups than that of Nylon 6,6 and also because of the longer aliphatic linkages, Nylon 11 is a less polar polymer than Nylon 6,6. These factors affect its dielectric properties (209) at low temperatures (Fig. 4.16). The static dielectric constant of this polymer over a relatively wide temperature range (from 4.2 to 150 K) does not depend on temperature and is close in its value (2.4) to the ε′ value for polyethylene. Below 30 K the loss tangent is also independent of temperature and frequency.

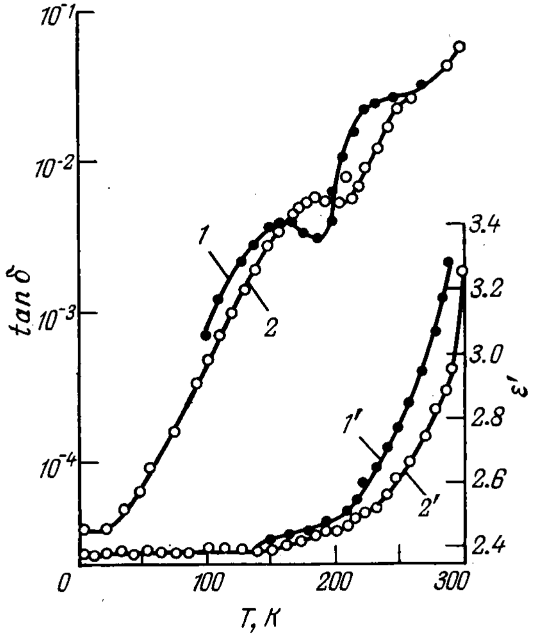

FIG. 4.16. Temperature dependence of tan δ (1—47 Hz; 2—2.34 Hz) and ε′ (1′—47 Hz; 2′—2.34 Hz) for Nylon 11.

Two relaxation regions are observed in the temperature dependence of tan δ in Nylon 11 (209). The low-temperature loss maximum, which lies at 160 K in measurements at 47 Hz, is due to γ-relaxation. The activation energy corresponding to this relaxation process is about 30.1 kJ/mole. The second relaxation region, with a centre at 225 K, is to a considerable extent masked by a strong increase in dielectric losses associated with the main relaxation region (the unfreezing of the segmental motion in the amorphous regions), the centre of which is located above 300 K. In measurements carried out at 47 Hz the value of tan δ_m for the low-temperature peak ($T_m = 160$ K) is 4×10^{-3}, while for the higher-temperature peak ($T_m = 225$ K) it is 3×10^{-2}. These values of tan δ are in good agreement with the corresponding increase in the static dielectric constant as the temperature rises. A characteristic feature of the temperature dependence of tan δ for Nylon 11 is that below 80 K the dependence on frequency becomes very weak, while below 30 K the value of tan $\delta \approx 3 \times 10^{-5}$ and is independent of either frequency or temperature. It is interesting that in the region of the low-temperature plateau the dielectric losses in Nylon 11 are very close to the corresponding values in polyethylene.

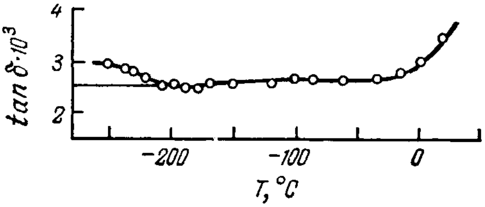

FIG. 4.17. Temperature dependence of the loss tangent for polymethyl methacrylate at $\nu = 60$ kHz.

Hence, both polyamides display a very important regularity: as the temperature falls (at $T \to 4.2$ K) the dielectric losses and the dielectric constant are sharply lowered. For both polyamides there is observed a low-temperature plateau near 4.2 K, where ε' and tan δ do not depend on temperature and frequency. The existence of this low-temperature plateau implies that with decrease in temperature the conditions are established (at the temperature corresponding to the high-temperature end of the plateau) in which all the dielectric relaxations in a polar linear crystalline polymer appear to be frozen, and in the region of the low-temperature plateau a polar polymer exhibits the properties of a non-polar polymer. This is especially distinctly pronounced in Nylon 11, whose dielectric properties in the low-temperature plateau region do not practically differ from those of polyethylene.

Polymethyl Methacrylate. Polymethyl methacrylate is a typical polar amorphous polymer. Investigations of dielectric losses in this polymer (Fig. 4.17) at a frequency of 60 kHz show that (213) below room temperature no loss maxima are present. From room temperature to — 50° C the dielectric losses decrease monotonically with fall in temperature. Further, down to — 200° C the loss tangent in polymethyl methacrylate is practically independent of temperature. Below — 200 °C the dielectric losses increase with further decrease in temperature. The cause of the increase of tan δ is not quite clear since the only possible explanation of this effect involves assuming the possibility of re-orientational motion of the methyl groups. Relaxation processes due to the mobility of the methyl groups cannot usually be recorded by dielectric spectroscopy methods.

Polystyrene. The dielectric properties of this weakly polar polymer have been studied particularly thoroughly (205, 223-226). The results of measurements of the real and imaginary parts, ε' and ε'', of the complex dielectric constant ε^* at a frequency of 1 kHz in amorphous atactic polystyrene (225) are given in Fig. 4.18. In the case of polystyrene there is observed a broad dielectric loss peak at 46 K with the value of ε''_m being 1.34×10^{-4}. The activation energy of this relaxation peak is $U = 13.8$ kJ/mole. Besides, between 130 and 170 K there is another, very weak maximum of ε''. The increase in ε'' above 300 K is attributed to the nearness of the main relaxation maximum, which corresponds to the transition from the glassy to the rubbery (high-elastic) state.

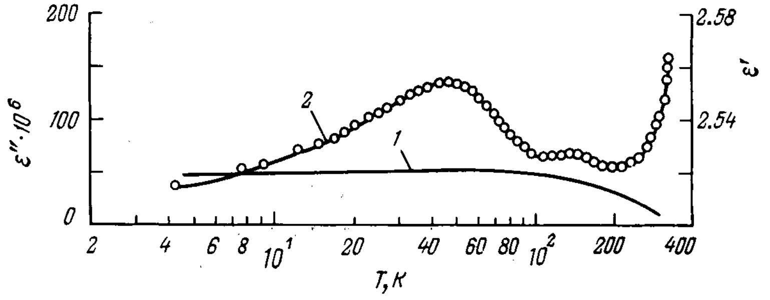

FIG. 4.18. Temperature dependence of ε' (1) and ε'' (2) for polystyrene at $\nu = 1$ kHz.

The dielectric constant of polystyrene over the temperature range 4.2-70 K is 2.52 and is independent of temperature. Between 70 and 300 K the value of ε' decreases slightly. On the whole the dielectric constant ε' of polystyrene varies in the same manner as the dielectric constant of nonpolar polymers such as polyethylene and polytetrafluoroethylene.

Of primary interest is the temperature dependence of the dielectric loss. The maxima observed on the curve are not artifacts and are not associated with the presence of impurities, since the polystyrene used by a number of workers was thoroughly purified and analysed. The low-temperature relaxations in polystyrene, which are observed by means of dynamic mechanical methods (70, 163) or the NMR method (185), are usually ascribed to the torsional vibrations or the rotation of the phenyl groups attached to the main chain as side groups.

McCammon, Saba and Work (225) maintain that this motion of the phenyl groups cannot lead to a dielectric relaxation if the dipole moment vector of the groups is situated along the axis of rotation. The authors propose another explanation of the low-temperature relaxation processes in polymers containing phenyl groups. Since the phenomena under consideration occur in the glassy state, it can be assumed that each individual molecule is largely in a single, fixed conformation and that only elastic distortions of the polymeric network are possible. The kinetic unit responsible for the low-temperature relaxation in polystyrene is believed to be the phenyl group. It is presumed that there corresponds to each phenyl group an internal hole which is connected both with the molecule to which the phenyl group is attached and with the other neighbouring molecules. Consideration of the molar volume of polystyrene confirms that the existence of such holes is possible and that their average size only slightly exceeds the dimensions of the kinetic units. Hence, a slight displacement of the phenyl groups is associated with the cooperative motion of only those carbon atoms in the main chain to which the side groups are attached. One can also suppose that the holes are distributed according to their size and shape, as a result of which the side groups can undergo various motions.

The motion of the phenyl group can be described with the aid of a local system of coordinates. If such a coordinate system is located so that its origin coincides with the position of the main-chain carbon atom to which a side group is attached, then the orientation of this group relative to the bond that links the side group to the main chain can be determined with the aid of the polar angle θ_i and the azimuthal angle Φ_i. Apart from the angles θ_i and Φ_i, we can also introduce the angle of rotation ω_i of the side group about the axis connecting it with the main chain. This axis is called here the ω axis.

The motion of each side group is governed by the potential energy, which is a function of the local coordinates. This energy depends on the presence or absence of atoms that form the walls of the hole and the structure of the molecule carrying a side group. The potential function of each side group has two or more minima separated by low potential barriers and makes a certain contribution to the relaxation spectrum. Since the holes in an amorphous polymer may have different sizes and shapes, one naturally expects the corresponding potential functions to differ widely.

The transition of the side groups of the polymer from one minimum to another is a thermal-activation process. In equilibrium and in the absence of an external field the distribution of side groups according to their orientations is determined by the statistical weight of the various potential energy minima. The application of an electric (or mechanical) field alters the statistical weights of these minima and there takes place a transition to a new equilibrium distribution which can be described by introducing a relaxation function. Such a relaxation function is a superposition of characteristic functions for holes of each type weighed proportionately to their number. Each transition to a new equilibrium position is governed by the form of the potential function, which takes account of the neighbouring molecules, and also by the distance between the minima of the potential energy. In general, such a transition is associated with the change in all the local coordinates. A relative change in the angular coordinates, when the side group jumps from one minimum to another, will be different for different holes. For example, the angle ω will be changed the most if the transition is associated with holes of a particular type and if an almost pure rotation of the side groups is realized in such a transition. The motion of side groups in holes of a different type may be associated with changes in the angles θ or Φ.

Since the motion relative to the axis ω does not involve the motion of even very small units of the main chain, it is natural to suppose that the rotation about this axis is limited by the lowest potential barrier. In accordance with this, at a constant temperature the largest contribution to the relaxation-time spectrum for an almost pure ω-motion is made by shorter relaxation times than those contributing to the motions associated with the predominant change in the angles θ or Φ. And, conversely, at fixed time intervals (constant frequencies) the ω-relaxation occurs at lower temperatures than does the θ- or Φ-relaxation. Intermediate cases are also possible, where several processes of the types indicated can be observed simultaneously.

Let us consider the effect of the orientation of the dipole moment vector of a side group on the relaxation spectrum. If the dipoles are oriented parallel to the ω axis, then the contribution to the dielectric relaxation is made only by the motion associated with the change in the angles θ or Φ. In this case, the largest contribution to the spectrum comes from the predominating θ- and Φ-motions, to which there corresponds that part of the distribution function of relaxation times which is due to longer times. If the dipole moment vector is perpendicular to the axis ω, then the principal role in the relaxation-time distribution function is played by shorter times.

Although the model discussed above presupposes a complex motion in the main chain, it differs fundamentally from the "local mode". In the model presently under consideration, the angular displacements of the side groups are so small that the cooperative movement of the main chain involves only one or two carbon atoms. Such a model allows one to account for the difference in the position of low-temperature dielectric loss maxima in substituted polystyrenes observed by McCammon and his coworkers (225). Since the dielectric losses in polystyrene and poly-*p*-chlorostyrene must be largely determined by the motion associated with the change in the angles θ and Φ, then in a broad dielectric loss maximum at low temperatures the high-temperature part of the relaxation process must predominate. Indeed, in measurements at a frequency of 1 kHz the peak of the dielectric loss factor (ε″) is observed at 46 K in polystyrene and at 47.5 K in poly-*p*-chlorostyrene (225). If the chlorine atom is in the *ortho*-position (as in poly-*o*-chlorostyrene), then the dipole moment vector is found to be almost parallel to the ω axis, which leads to an increase in the contribution of the ω-motion to the relaxation spectrum. As a result, the ε″ peak is shifted in the direction of lower temperatures (T_m = 32.7 K), which agrees well with the assumption that the rotation about the ω axis is associated with the jump over a lower potential barrier than in the case of θ- or Φ-motions. In poly-*m*-chlorostyrene, the ε″ peak is observed at an even lower temperature (17.5 K), this reflecting the decrease in the steric hindrances that limit the rotation about the ω axis as compared with poly-*o*-chlorostyrene. It should be noted that we are simplifying the question of the rotation relative to the ω axis, since this

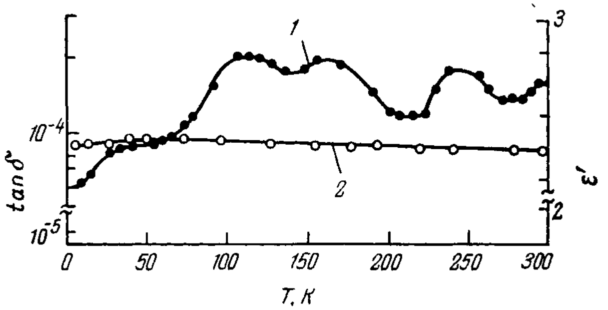

FIG. 4.19. Temperature dependence of tan δ (*1*) and ε′ (*2*) for polystyrene at ν = 75 Hz.

kind of motion depends greatly on the matrix surrounding the side group.

In principle, one might expect that under certain conditions in polymers containing phenyl side groups there will appear relaxation maxima due to the three modes of motion considered above.

It is possibly such multiplet relaxation peaks of tan δ that Chant (205), while carrying out dielectric measurements in polystyrene at a frequency of 75 Hz, observed at low temperatures (Fig. 4.19).

CHAPTER 5

NUCLEAR MAGNETIC RESONANCE IN POLYMERS AT LOW TEMPERATURES

5.1. BASIC CONCEPTS OF NUCLEAR MAGNETIC RESONANCE IN POLYMERS

Nuclear magnetic resonance (NMR) is a phenomenon caused by resonance transitions between the magnetic energy levels of atomic nuclei in an external field. Basic information on nuclear magnetic resonance can be found in a number of monographs (185, 227-230) and review articles (231-235). We shall recall only the most important principles. It is well known that the nuclei of isotopes have not only mass and charge but also a mechanical moment (momentum). The intrinsic angular momentum of nuclei is called the spin. The presence of a spin in a nucleus leads to the existence of an intrinsic magnetic moment. In this book we shall speak mainly of the nuclei, protons, of the hydrogen atom. The intrinsic magnetic moment of a proton is very small as compared with that of an electron and manifests itself only in special physical experiments.

In a number of cases, we can consider, as a first approximation, a system of isolated atomic nuclei placed in an external magnetic field (227). Obviously, the magnetic moment of an isolated proton in an external magnetic field can have two possible directions. One of them corresponds to the case when the magnetic moment of the proton is oriented parallel to the external field, and the second to the case when the magnetic moment of the proton is aligned antiparallel to the applied field. To each of these directions of the magnetic moment of the proton there correspond specific energy levels of the proton. The difference between the energies corresponding to these energy levels can be given in the form*

$$\Delta E = 2\mu H_0 \tag{5.1}$$

where μ is the magnetic moment; H_0 is the strength of the applied external field.

---

* Equations expressing relationships between quantities are given in a form corresponding to the CGSE system.

In accordance with the laws of quantum mechanics, the transition of the nucleus (proton) from one energy level to another is associated with the absorption or emission of a quantum of energy $\Delta E = h\nu$. It then follows that

$$h\nu = 2\mu H_0 \tag{5.2}$$

Thus, if an electromagnetic wave of frequency ν is propagating in a substance whose nuclei have a magnetic moment μ and which is placed in an external magnetic field H_0, then with condition (5.2) being fulfilled the absorption of energy is possible. As a result, the atomic nuclei can jump to another, higher energy level corresponding to another orientation of their intrinsic magnetic and mechanical moments. If the substance (a polymer) is placed between the poles of a magnet producing an external field of strength $H_0 = 10^4$ gauss, then the proton absorbs or emits an electromagnetic energy of frequency $\nu = 42.57$ MHz. The phenomenon of nuclear magnetic resonance is precisely that absorption or emission of the energy of electromagnetic high-frequency oscillations occurs when a substance is placed in a magnetic field.

In the very crude approximation given above, the absorption spectrum of the proton will constitute a single line. In fact, each proton of the polymer is also influenced by the magnetic fields of the surrounding protons. This leads to the appearance of a non-zero local magnetic field strength H_{loc}, due to the magnetic moments of the neighbouring protons. The local field can either reduce or enhance the magnetic field acting on the proton, depending on the orientation of the magnetic moments of the interacting protons. If we take account of the local field, the resonance condition (5.2) must be written in the form

$$h\nu = 2\mu (\overline{H}_0 + \overline{H}_{\text{loc}}) \tag{5.3}$$

The presence of a local field leads to the splitting of the energy levels and to the broadening of the absorption spectrum in resonance. The local field strength is not great: it is equal to 5-10 gauss with the external field strength H_0 being approximately equal to 10^4 gauss. Nevertheless, by virtue of the very large number of interacting protons (and also of isolated groups of protons) the local field leads to the appearance of an absorption spectrum with a complex shape and a finite half-width.

The experimental observation of nuclear magnetic resonance is usually conducted so that the frequency of the electromagnetic wave, ν, propagating in a polymer, remains constant and is equal to several tens of MHz, while the magnetic field strength H_0 varies smoothly within the relatively narrow limits sufficient for the resonance condition (5.3) to be fulfilled. In a general case, the resonance absorption curve can have a complex form. It is not the absorption curve that is most often recorded but its first derivative with respect to the magnetic field strength (Fig. 5.1)

The NMR Lineshape. The NMR signal lineshape in polymers depends on the chemical constitution, structure and the physical state of the polymer. In the case of amorphous polymers the presence of a local field and a strong intermolecular interaction gives a sufficiently broad absorption curve for such polymers in the glassy state. As the temperature rises the molecular mobility increases and the atoms (and, hence, their nuclei) begin to participate in this motion. This results in a certain time-averaging of the local field and, hence, to a decrease in it. The decrease in H_{loc} leads, in turn, to the narrowing of the resonance absorption curve. When the rubbery state is attained (this state being characterized by an intensive molecular motion), the absorption curve becomes very narrow as compared with the corresponding curve for the glassy state.

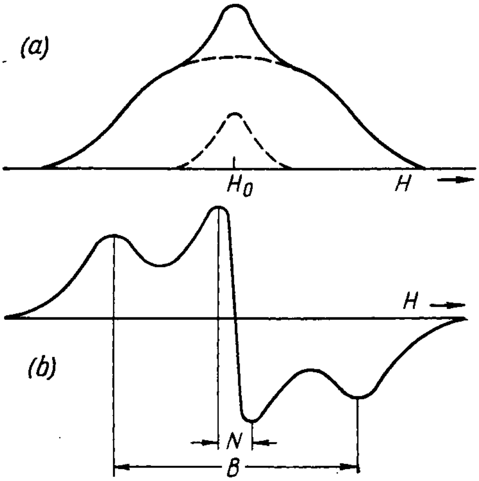

FIG. 5.1. Superposition of two NMR spectra:
a—resonance absorption curves (the solid line is an integral curve, the dashed lines representing the components); *b*—the first derivative with respect to the magnetic field intensity (N is the width of the narrow component; B is the width of the broad component).

In the case of crystalline polymers at temperatures above the glass-transition temperature of the amorphous layer the lineshape of the NMR signal is found to be more complicated. In this case the spectrum consists of two parts: a broad component corresponding to processes taking place in the crystalline regions, and a narrow component due to segmental mobility in the amorphous regions.

The main parameters characterizing the NMR lineshape are the linewidth δH and the second moment ΔH_2^2. These parameters in a number of cases can be calculated theoretically.

Linewidth. The linewidth δH of the NMR spectrum is the distance between the two points on the absorption curve at which the amplitude of the signal decreases by a factor of 2. Since it is usually the first derivative of the absorption curve with respect to the field which is written out, the linewidth is sometimes defined as the distance between the two points on the absorption curve at which the shape of the curve changes most. In the latter case, δH is defined as the distance between the corresponding extrema of the real NMR spectrum. In the case of crystalline polymers, one sometimes speaks of the width of the narrow and broad components of the spectrum. The linewidth is often measured as the distance between the outer maximum and minimum (see Fig. 5.1).

The Second Moment of the NMR Spectrum. A theoretical description of the shape of the NMR spectrum line is a very complicated task. However, it is possible in a number of cases to calculate sufficiently accurately the integral characteristic of the resonance absorption curve—the second moment of the resonance line contour. According to the van Vleck theory (236), the second moment ΔH_2^2 is defined by the expression

$$\Delta H_2^2 = \frac{\int\limits_{-\infty}^{\infty} f(H)\,(H - H_0)^2\,dH}{\int\limits_{-\infty}^{\infty} f(H)\,dH} \tag{5.4}$$

where $f(H)$ is the magnetic field strength function characterizing the lineshape; $(H - H_0)$ is the amount by which the field differs from the resonance value (the coordinate being taken from the centre of the spectral line).

In the denominator of expression (5.4) there is an integral introduced for normalization. Thus, the second moment of the NMR spectrum line may be regarded as a linewidth which is determined according to some special method and averaged; it is expressed in units of the magnetic field strength and is calculated from experimental curves. Since the first derivative of the resonance line $\varphi(H)$ is usually determined, the quantity ΔH_2^2 can be given in the following form (185):

$$\Delta H_2^2 = \frac{1}{3} \cdot \frac{\int\limits_{-\infty}^{\infty} (H - H_0)^3\,\varphi(H)\,dH}{\int\limits_{-\infty}^{\infty} (H - H_0)\,\varphi(H)\,dH} \tag{5.5}$$

The expression for ΔH_2^2 can be calculated theoretically (236) as a function of the magnitude and orientation of the internuclear vectors with respect to the applied external field. In this connection, it is possible, with the structural model being specified, to calculate ΔH_2^2 theoretically and, comparing it with experimental values, to come to some conclusions as to how reliably the model describes the actual structure.

Like the linewidth, the second moment will decrease with increasing temperature. The strong decrease in ΔH_2^2 with increasing temperature allows us to establish the temperature regions in which the various modes of molecular motion are unfrozen. The strongest decrease in ΔH_2^2 in amorphous polymers is observed on transition from the glassy to the rubbery state.

The Correlation Frequency and the Energy of Activation. It has already been mentioned above that δH and, hence, ΔH_2^2, depend on the strength of the local field H_{loc} that acts on each nucleus. If the atomic nuclei are involved in thermal motion, the local field strength is a function of time. Thus the parameters characterizing the time-averaged value of $\overline{H}^2_{\text{loc}}(t)$ and the rate of variation of this quantity are of greatest interest. In order to describe the average value of $\overline{H}^2_{\text{loc}}(t)$, use is made of the concept of the correlation function:

$$R\,(t) = \overline{H_{\text{loc}}\,(t) \cdot H_{\text{loc}}\,(t+\tau)} \qquad (5.6)$$

From expression (5.6) it follows that the correlation function in this particular case is the time-averaged value of the product of the strengths of the local fields separated by the time interval τ. In our case, the correlation function is a measure of the connection between two successive values of $H_{\text{loc}}(t)$. In this way we can introduce the concept of the correlation time τ_c, which is a parameter that characterizes the rate of variation of the local field with time and, hence, the rate of variation of the correlation function. If $\tau = \tau_c$, then the value of the correlation function $R\,(t)$ decreases by a factor of e (5.6). The correlation time is, to a certain extent, analogous to the dielectric relaxation time. This analogy becomes especially comprehensive when we are dealing with liquids. The correlation time τ_c in this case is connected by a simple relation with the dielectric relaxation time τ_D, found from formula (4.8) which follows from the Debye theory:

$$\tau_c \approx \tau_D/3 \qquad (5.7)$$

The difference between τ_c and τ_D is that τ_D characterizes the rotation of molecules due to thermal motion, which leads to the disorientation of electric dipoles after the electric field is removed; this motion is considered in terms of the fixed coordinate system. The correlation time τ_c determines the rate of variation of the local field with respect to a nucleus that is involved in thermal motion. Hence, τ_c characterizes the change in the local field relative to the coordinate system rigidly connected with the moving nucleus.

By analogy with relaxation-time spectra, one can also speak of correlation-time spectra. This is especially important when dealing with NMR in polymers. If the process associated with the unfreezing of some mode of molecular motion can be described with the aid of a single "effective", average correlation time, then the inverse of this time, $1/\tau_c = 2\pi\nu_c$, can be calculated from experimental data:

$$2\pi\nu_c = \frac{\alpha\gamma\delta H}{\tan\left(\frac{\pi}{2}\cdot\frac{\delta H^2 - B^2}{C^2}\right)} \tag{5.8}$$

where ν_c is the correlation frequency for a molecular motion leading to the narrowing of the resonance curve; α is a constant equal to 0.18; γ is the gyromagnetic ratio equal to the ratio of the magnetic moment to the momentum; δH is the linewidth over a temperature range in which a given mode of molecular motion is unfrozen [δH is the convected coordinate in Eq. (5.8)]; B is the linewidth at a temperature lying above the transition region; C is the linewidth at a temperature at which a given mode of motion is still "frozen".

Having determined the linewidth δH at several temperatures in the transition region, one can calculate, by means of Eq. (5.8), the average correlation frequency at several temperatures and then calculate the activation energy U of the process under study using the formula

$$\nu_c = \nu_\infty e^{-\frac{U}{RT}} \tag{5.9}$$

The Spin-Lattice Relaxation Time. Two methods are possible for investigating NMR in polymers. One method consists of treating a given volume of the polymer, which is in effect a set of macromolecules, as a specific "lattice". In this case, the lattice can be described not only as an ordered arrangement of chains in crystallites but also as a certain order ("short-range order") in amorphous polymers or in the amorphous regions of crystalline polymers. In the second method, one speaks of the ordering due to the orientation of magnetic dipoles, which is governed by the presence of nuclear spins.

Thus, a polymer can be looked on as a combination of two systems: a lattice and a system of spins. These systems interact weakly since the magnetic dipoles (the magnetic moments of the nuclei) usually interact much more strongly with the external magnetic field produced by the magnet in an NMR experiment than between one another ($H_0 \gg H_{loc}$). The polarization of the nuclear magnetic moments upon application of an external magnetic field exerts a decisive influence on the orientation of spins in a polymeric medium, with the thermal motion of atoms affecting the ordering in the arrangement of spins only slightly.

If a magnetic field is applied to a polymeric material which has nuclear magnetic moments and is then removed, the magnetic polarization of nuclei will begin to decay because of the thermal motion. The phenomenon of spin-lattice relaxation is a spontaneous decay of magnetic polarization in the absence of an external magnetic field, caused by the thermal motion of atoms. In spite of the fact that the characteristic times of thermal motion in polymers are sufficiently shorter, being equal to 10^{-5}-10^{-10} s, the spin-lattice relaxation time T_1 is usually long and equals several seconds or minutes. The cause of this is the weak interaction between the spin system and the lattice. It might seem that the thermal motion of atoms should alter the interaction between the nuclear magnetic moments sufficiently rapidly, but by virtue of the fact that the energy of such interaction is much lower than the total energy of the magnetic dipoles which have been polarized by the external magnetic field, the elements of the polymeric chains must undergo repeated re-orientations before the overall magnetic interaction is appreciably reduced. The decay of the magnetization vector (caused by the orientation of the nuclear magnetic moments) is a process of transition to equilibrium between the spin system and the lattice.

The spin-lattice relaxation associated with the molecular motion is most distinctly observed when the frequency of thermal vibrations is comparable with the NMR frequency. Therefore, the investigation of spin-lattice relaxation is carried out at frequencies of the order of 10^6 to 10^8 Hz. If measurements are made at a fixed frequency over a sufficiently wide temperature range, it turns out that the spin-lattice relaxation time passes through a minimum that appears at a quite definite temperature for each relaxation process. These minima are, to a certain extent, analogous to the maxima of the temperature dependence of dielectric losses.

The theory of the phenomenon of nuclear spin-lattice relaxation has been worked out by Bloembergen, Purcell and Pound (237), who derived a formula for the longitudinal spin-lattice relaxation time which takes account of a single correlation time

---

* This theory is known as the BPP theory.—*Tr.*

τ_c. Since polymers have a wide range of correlation times, the expression for the longitudinal spin-lattice relaxation time T_1 can be given in the following form (238-240):

$$\frac{1}{T_1}=\frac{2}{3}(\Delta H_2^2)\left\{\int\limits_0^\infty \frac{I(\tau_c)\,\tau_c\,d\tau_c}{1+\omega^2\tau_c^2}+4\int\limits_0^\infty \frac{I(\tau_c)\,\tau_c\,d\tau_c}{1+4\omega^2\tau_c^2}\right\} \tag{5.10}$$

where ΔH_2^2 is the second moment; $I(\tau_c)$ is the correlation-time spectrum density (the relaxation-time distribution function).

5.2. EFFECT OF THE STRUCTURE AND COMPOSITION OF POLYMERS ON NUCLEAR MAGNETIC RESONANCE

5.2.1. EFFECT OF THE DEGREE OF CRYSTALLINITY ON THE NMR LINEWIDTH

Maklakov and Grigoriev have shown (240-243) that the expression for the linewidth δH in the presence of a correlation-time spectrum may be given in the form (242):

$$(\delta H)^2=\frac{(\delta H_T)^2}{\pi}\int\limits_0^\infty \frac{I(\tau_c)\,\omega_0\tau_c\,d\tau_c}{1+\omega_0^2\tau_c^2} \tag{5.11}$$

where δH_T is the width of the NMR absorption line for the rigid lattice; $\omega_0 = a\gamma\delta H$ is the parameter with the dimensionality of cyclic frequency [a is a constant ($a \approx 1$); γ is the gyromagnetic ratio].

It might seem at first glance that it follows from Eq. (5.11) that at $\omega_0\tau_c \rightarrow \infty$ (the region of very low temperatures) $(\delta H)^2 \rightarrow 0$. In actual fact, this is not so since $I(\tau_c)$ is a function of $\omega_0\tau_c$. It can be shown that $I(\tau_c) = \omega_0\tau_c\bar{I}(\tau_c)$. Substituting this expression into Eq. (5.11), we get:

$$(\delta H)^2=\frac{(\delta H_T)^2}{\pi}\int\limits_0^\infty \frac{\bar{I}(\tau_c)\,\omega_0^2\tau_c^2\,d\tau_c}{1+\omega_0^2\tau_c^2} \tag{5.11a}$$

It can be seen that at $\omega_0\tau_c \rightarrow \infty$ the quantity $(\delta H)^2$ assumes a finite value, increasing with increasing $\omega_0\tau_c$. Maklakov and Grigoriev (240) calculated theoretically the value of $\delta H/\delta H_T$ and demonstrated that it increases with an increase in $\omega_0\tau_c$, approaching a constant value:

$$(\delta H)^2=\frac{(\delta H_T)^2}{\pi}\int\limits_0^\infty \bar{I}(\tau_c)\,d\tau_c \tag{5.11b}$$

Following Chujo (244), we assume that the correlation-time spectrum density of an amorphous-crystalline polymer, $I(\tau_c)$, can be presented in the form of a linear superposition of the correlation-time spectra of crystalline, $I_{cr}(\tau_c)$, and amorphous, $I_{am}(\tau_c)$, regions:

$$I(\tau_c) = \varkappa I_{cr}(\tau_c) + (1 - \varkappa) I_{am}(\tau_c) \qquad (5.12)$$

where $\varkappa$ is the "statistical" degree of crystallinity.

Chujo attempted to take account of the effect of crystallinity on the lineshape of the NMR signal in polymers by substituting expression (5.12) into the equation for the NMR absorption spectrum line contour derived by Mijake, and Kubo and Tomita (238, 239). He assumed, however, that all the correlation times corresponding to the crystalline regions are very long as compared with the τ_c of the amorphous regions. In view of this, Chujo disregarded the terms that contained the function $I_{cr}(\tau)$.

The Chujo assumption seems to be more or less justifiable only in those cases where the polymer is at a temperature exceeding the glass-transition temperature of the amorphous layer. At low temperatures, however, when the amorphous regions of a partly crystalline polymer are in the glassy state, the assumption could well prove to be invalid.

Substitution of expression (5.12) into Eq. (5.11) gives the dependence of the linewidth on the degree of crystallinity free from the assumptions made by Chujo:

$$(\delta H)^2 = \frac{(\delta H_T)^2}{\pi} \left[\varkappa \int_0^\infty \frac{I_{cr}(\tau_c)\,\omega_0 \tau_c d\tau_c}{1+\omega_0^2\tau_c^2} + \right.$$

$$\left. + (1-\varkappa) \int_0^\infty \frac{I_{am}(\tau_c)\,\omega_0 \tau_c d\tau_c}{1+\omega_0^2\tau_c^2} \right] \qquad (5.13)$$

Analysis of Eq. (5.13) shows that two different forms of the dependence of the NMR linewidth on the degree of crystallinity are possible. The nature of this dependence is determined by the relation between the integrals on the right-hand side of Eq. (5.13).

It is customarily believed that as the degree of crystallinity increases the total linewidth of a partly crystalline polymer also increases. Analysis of Eq. (5.13) indicates that this dependence is possible if the major contribution to δH comes from the first integral on the right-hand side of formula (5.13). This condition is valid when the polymer is at a temperature higher than the T_g of the amorphous layer. One would be right in expecting that in this case $I_{cr}(\tau_c)$ will also be greater than $I_{am}(\tau_c)$, since the local field is time-averaged as a result of the intensive segmental motion in the amorphous regions above T_g. It is this form of the dependence of δH on $\varkappa$ that is the most widespread (185, 233).

The main contribution to δH may, however, also come from the second integral on the right-hand side of Eq. (5.13). This is evidently possible only at a temperature lower than the glass-transition temperature of the amorphous layer, i.e., at low temperatures. One would expect $I_{\mathrm{am}}(\tau_c)$ to be greater than $I_{\mathrm{cr}}(\tau_c)$. If these conditions are fulfilled, the linewidth of the NMR signal will decrease with increasing degree of crystallinity. Inspection of Eq. (5.13) shows that in samples of the same polymer with different degrees of crystallinity, the linewidth can diminish with increasing $\varkappa$ at low temperatures (below T_g of the amorphous layer) and increase at relatively high temperatures (above T_g of the amorphous layer but below T_{melt} of the crystallites).

Thus, in certain polymers there is possible an inversion of the temperature dependence of the linewidth for samples of the same polymers which have different degrees of crystallinity. It is evident that the inversion region must lie near T_g of the amorphous layer measured at a corresponding frequency. When the temperature and the degree of crystallinity are changed, the correlation-time distribution function will also change. Maklakov and Grigoriev have shown (240-242) that when the distribution function of correlation times is changed on the graph of $\delta H/\delta H_T$ against $\omega_0\tau_c$ the curves calculated theoretically for different widths of the correlation-time distribution will undergo inversion. It is characteristic that the point of inversion is found to be located at values of $\omega_0\tau_c$ close to unity, which corresponds to the intensive manifestation of the relaxation process. Thus, the results of the analysis of Eq. (5.13) are in good agreement with the theoretical calculations of δH made by Maklakov and Grigoriev (240-242).

McCall and Slichter (245), while investigating low-density ($\varkappa \approx 50$ per cent) and high-density ($\varkappa \approx 70$ per cent) polyethylene, found that at low temperatures the width of the narrow component (which corresponds to the amorphous regions) in the less crystallized and more strongly branched polymer is much greater than the δH of the narrow component of the more crystallized linear polyethylene (Fig. 5.2). At high temperatures the situation is reversed and δH is greater for high-density polyethylene. It is interesting that the point of inversion on the $\delta H = f(T)$ graph for both polyethylenes is located at —20°C, which agrees well with the glass-transition temperature of the amorphous regions of polyethylene at frequencies of about 10^4 Hz.

It might seem at first sight incorrect to compare the values of δH for low-density and high-density polyethylenes for the purpose of estimating the effect of the degree of crystallinity, since not only their degrees of crystallinity are different but one of them is practically a linear polymer and the other has methyl groups as branchings. The presence of methyl groups in branched polyethylene, which, as will be shown at a later time, retains its mobility down to 0 K, must, however, reduce the δH of the narrow component, while at low temperatures

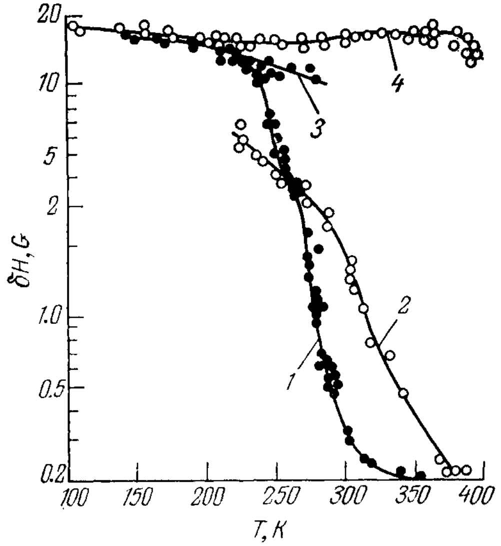

FIG. 5.2. The width of the lines of the narrow (*1*, *2*) and broad (*3*, *4*) components of the NMR signal for polyethylene of low (*1*, *3*) and high (*2*, *4*) density.

δH for branched polyethylene turns out to be greater than for linear polyethylene. It is interesting that the average correlation frequency ν_c for low-density polyethylene at low temperatures is substantially lower (τ_c is greater) than in the case of high-density polyethylene (Fig. 5.3), despite the commonly held belief to the contrary.

The results obtained by means of the NMR method agree well with the temperature dependence of Young's dynamic modulus for these polymers. It has been shown experimentally (70, 246) that at low temperatures Young's dynamic modulus and the velocity of sound in less crystallized low-density polyethylene exceed the corresponding values for the more strongly crystallized linear polyethylene. It has been shown (70) that the anomalous effect of the degree of crystallinity on the elastic modulus and the velocity of sound (at which these parameters decrease with increasing $\varkappa$) is associated with the change in the effectiveness of intermolecular interaction in the amorphous regions and is typical of crystalline polymers for which the Hosemann-Bonart structural model is valid. If this analogy between the effect of $\varkappa$ on acoustical properties and the NMR linewidth at low temperatures is correct, one may then expect the results similar to those given in Figs. 5.2 and 5.3 to be obtained at low temperatures for polyethylene terephthalate, polycapramide, polyamide 68.

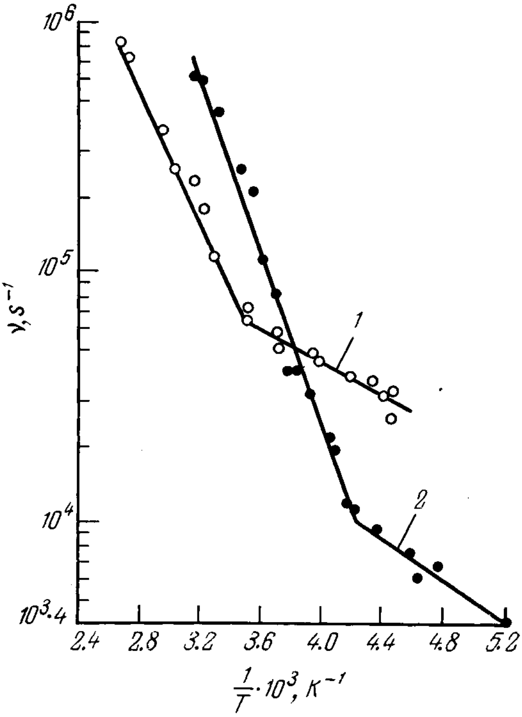

FIG. 5.3. Dependence of the mean correlation frequency on inverse temperature (245):
1—high-density polyethylene; 2—low-density polyethylene.

An analogous increase in the second moment below the glass-transition temperature T_g in amorphous samples of polyarylates as compared with crystalline samples has been observed (183).

5.2.2. EFFECT OF THE DEGREE OF CROSS-LINKING ON THE NMR LINEWIDTH

One of the most important characteristics of amorphous network polymers is the degree of cross-linking:

$$\nu = \rho/M_a = N_c/N_0 \qquad (5.14)$$

where ρ is the density; M_a is the molar mass of the portion of the chain between two neighbouring entanglement points of the spatial network; N_c is the number of network chains per unit volume; N_0 is Avogadro's number.

The network chain is usually defined as the portion of the polymeric chain that connects the neighbouring entanglement junctions. Thus, the degree of cross-linking (the network density) shows the number of moles of network chains per unit volume of the polymer.

For each network polymer there exists a maximum possible degree of cross-linking, ν_m, which depends on the chemical constitution and the content of reactive groups. One may therefore speak of the relative degree of cross-linking $\bar{\nu} = \nu/\nu_m$, where ν is the degree of cross-linking in the polymer. Obviously, $\bar{\nu}$ varies from 0 (an uncross-linked polymer) to 1 (a polymer with the densest spatial network).

Let us consider the effect of the network density on the NMR linewidth δH. To this end, we assume that the correlation-time spectrum density is given by

$$I(\tau_c) = \bar{\nu} I_1(\tau_c) + (1-\bar{\nu}) I_2(\tau_c) \qquad (5.15)$$

where $I_1(\tau_c)$ is the correlation-time spectrum density in a polymer having a maximum possible degree of cross-linking; $I_2(\tau_c)$ is the correlation-time spectrum density in a polymer which has the same chemical structure but has no chemical cross-links.

Substituting expression (5.15) into Eq. (5.11a), we have

$$(\delta H)^2 = \frac{(\delta H_T)^2}{\pi}\left[\bar{\nu}\int_0^\infty \frac{I_1(\tau_c)\,\omega_0^2\tau_c^2\,d\tau_c}{1+\omega_0^2\tau_c^2} + (1-\bar{\nu})\int_0^\infty \frac{I_2(\tau_c)\,\omega_0^2\tau_c^2\,d\tau_c}{1+\omega_0^2\tau_c^2}\right] \qquad (5.16)$$

Formula (5.16) allows one to account for, at least qualitatively, the dependence of δH on the network density at high temperatures and to predict it at low temperatures.

From formula (5.16) it follows that two kinds of dependence of the linewidth on $\bar{\nu}$ are possible. If the predominant contribution to δH is made by the first integral on the right-hand side, then the linewidth increases with increasing network density. This kind of dependence of δH on $\bar{\nu}$ must always be valid at $T > T_g$; it has been described in detail in the literature (185). It should be noted that this dependence can also be observed in the glassy state.

Another case is also possible: when $I_2(\tau_c) > I_1(\tau_c)$ and the linewidth is determined by the second term on the right-hand side of Eq. (5.16). In this case, the linewidth must decrease with increasing network density. This kind of dependence of δH on the degree of cross-linking can be expected to be valid in network polymers at low temperatures (at least, below T_g). Such an anomalous decrease in the linewidth at low temperatures must evidently be associated with the fact that the increase in the number of chemical cross-links will hinder the decrease in the distance between the kinetic unit of the neighbouring chains with decreasing temperature of the polymer, thereby reducing the effectiveness of intermolecular interaction. As a result, the localized molecular mobility in polymers with a larger $\bar{\nu}$ below T_g will be more intensive than in a slightly cross-linked polymer. Such a change in molecular mobility in network polymers below T_g has been repeatedly observed (70). In network polymers such as cured epoxide resins and copolymers of unsaturated polyesters with styrene, the mechanical loss peaks, which are due to molecular mobility and are situated below the glass-transition temperature, increase with increasing network density (70).

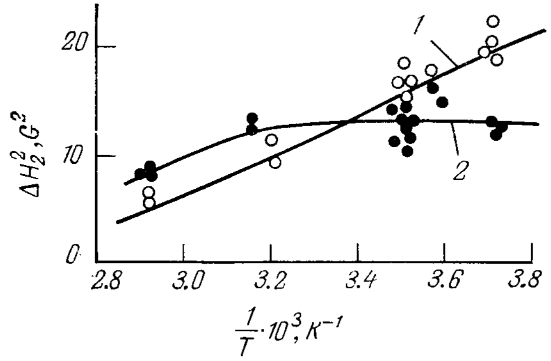

FIG. 5.4. Dependence of the second moment of the NMR signal on inverse temperature (247):
1—unirradiated polyethylene; 2—polyethylene irradiated with a beam of deutrons.

In investigating such polymers by the NMR method at low temperatures one may expect the increase in molecular mobility (of the non-segmental type) in the glassy state with increasing $\bar{\nu}$ to lead to a decrease in the local magnetic field and, hence, to a decrease in the linewidth δH of the NMR signal. It may be stated that for network polymers the δH values of which at low temperatures (below T_g) decrease with a rise in $\bar{\nu}$ the corresponding values will increase at high temperatures (above T_g) with increasing $\bar{\nu}$. It is natural that the second moment must vary, depending on $\bar{\nu}$ in a manner analogous to the change in δH. Such different dependences of ΔH_2^2 on the degree of cross-linking above and below T_g have, it seems, been observed by Fujiwara and his coworkers (247) for polyethylene irradiated with a beam of deuterons speeded up in an accelerator (Fig. 5.4). It is interesting that above 300 K (above T_g of the amorphous layer) the second moment for strongly irradiated polyethylene is higher than in the case of an unirradiated polymer. This is sufficiently convincing evidence that the irradiation of polyethylene has produced cross-linking. Below 300 K the ΔH_2^2 value for irradiated, radiation-cross-linked polyethylene is lower than for the unirradiated polymer. With a fall in temperature this difference increases (see Fig. 5.4).

5.2.3. EFFECT OF PLASTICIZER CONCENTRATION ON THE NMR SIGNAL LINEWIDTH IN PLASTICIZED POLYMERS

Let us examine the manner in which the concentration of a polar plasticizer added to a polar polymer influences the linewidth δH of nuclear magnetic resonance.

Suppose that the polar polymer and the polar plasticizer added to it are compatible over a certain range of concentrations (the possibility of unlimited compatibility is not excluded). Let the plasticizer concentration in the polymer be k and the maximum permissible plasticizer concentration at which the plasticizer is still compatible with the polymer be k_m. We introduce the dimensionless parameter $\xi = k/k_m$. It is evident that ξ may vary from 0 (an unplasticized polymer) to 1 (a polymer with a maximum possible plasticizer concentration). Hence, the parameter ξ indicates the degree of plasticization of the polymer.

Suppose that the correlation-time spectrum of a plasticized polymer, $\bar{I}(\tau_c)$, is represented as a linear superposition of the spectra of the infinitely plasticized polymer, $\bar{I}_1(\tau_c)$, and the unplasticized polymer, $\bar{I}_2(\tau_c)$, which have the same chemical structure. Then

$$\bar{I}(\tau_c) = \xi \bar{I}_1(\tau_c) + (1-\xi)\bar{I}_2(\tau_c) \tag{5.17}$$

Substitution of expression (5.17) into Eq. (5.11a) yields:

$$(\delta H)^2 = \frac{(\delta H_T)^2}{\pi}\left[\xi \int_0^\infty \frac{\bar{I}_1(\tau_c)\,\omega_0^2\tau_c^2 d\tau_c}{1+\omega_0^2\tau_c^2} + (1-\xi)\int_0^\infty \frac{\bar{I}_2(\tau_c)\,\omega_0^2\tau_c^2 d\tau_c}{1+\omega_0^2\tau_c^2}\right] \tag{5.18}$$

Inspection of this formula shows that in the region of the rubbery state, when for all τ_c that make a major contribution to the correlation-time spectrum the condition $\omega\tau_c \ll 1$ and $\overline{I}_2(\tau_c) > \overline{I}_1(\tau_c)$ is fulfilled, the dominant contribution to the linewidth will be introduced by the second term on the right-hand side of expression (5.18). This means that the linewidth δH will diminish with increasing plasticizer concentration. This form of the dependence of δH on ξ is well known (185) and is very frequently encountered.

It is possible that $\overline{I}_1(\tau_c) > \overline{I}_2(\tau_c)$ and the contribution to δH be made by the first term on the right-hand side of expression (5.18). In this case, the linewidth will increase with increasing plasticizer content in the polymer. This condition can be realized only for polymers in the glassy state and only in those cases where the addition of plasticizer to the polymer intensifies the intermolecular interaction in the polymer-plasticizer system below T_g, i.e., at low temperatures.

The intensification of intermolecular interaction in plasticized polymers leads to the suppression of molecular motion (70), which causes the broadening of the NMR line in plasticized polymers at low temperatures. Note that such an “anomalous” dependence of δH on ξ, when δH increases with increasing ξ if the polymer-plasticizer system is at a temperature below T_g, is a reflection of the effect of antiplasticization in nuclear magnetic resonance.

Antiplasticization has been thoroughly studied by acoustical methods (70). It means that upon addition of a polar plasticizer to a polar polymer the elastic modulus and the velocity of sound (and sometimes the strength also) in the polymer-plasticizer system at low temperatures (below T_g) increase with increasing plasticizer concentration. It has been found (70) that antiplasticization is caused by an increase in the intermolecular interaction in the polymer-plasticizer system in the glassy state. The macroscopic manifestation of this effect consists of an increase in the elastic modulus and the velocity of sound with increasing ξ (δH behaves in an analogous manner in NMR) and a sharp decrease in the mechanical loss peaks situated below T_g.

It has been shown experimentally that upon addition of some low-molecular-mass liquids (acetic acid, ethyl alcohol) to Nylon 6,6 the linewidth and the second moment increase at low temperatures (248). Slonim and Lyubimov (185) find this effect paradoxical. From the above it however becomes clear that this effect is a general one, being a reflection in NMR of quite a common phenomenon—antiplasticization.

Thus, even an approximate theoretical analysis of the effect of plasticizer content on the NMR linewidth δH allows one to come to certain conclusions concerning the manifestation of antiplasticization in nuclear magnetic resonance. These conclusions can be summarized as follows.

1. The increase in δH with increasing concentration ξ (antiplasticization) is possible only when the polymer is compatible with the plasticizer. This effect can be observed only in the glassy state (i.e., at low temperatures).
2. For the same polymer-plasticizer system δH increases with increasing ξ at low temperatures (at $T < T_g$) and diminish at high temperatures ($T > T_g$).
3. Both these dependences of δH on ξ lend themselves to a theoretical description.

5.2.4. EFFECT OF THE STRUCTURE AND COMPOSITION OF POLYMERS ON THE SECOND MOMENT AND THE SPIN-LATTICE RELAXATION TIME

In order to find out how the polymer structure affects the second moment and the spin-lattice relaxation time, we shall make use of Eq. (5.10). Introducing the notation $Q = T_1 \Delta H_2^2$, we can write Eq. (5.10) in the following form:

$$\frac{1}{Q} = \frac{2}{3}(f_1 + f_2) \qquad (5.19)$$

where f_1 and f_2 are the first and second integrals on the right-hand side of Eq. (5.10). It is obvious that f_1 and f_2 depend on the correlation time spectrum $I(\tau_c)$, τ_c, and ω.

Let us consider, for example, the effect of the plasticizer concentration on the ΔH_2^2 and T_1 of polymers. For this purpose, using the agruments given above and substituting the expression for $I(\tau_c)$ of the type (5.17) into f_1 and f_2, we reduce Eqs. (5.10) and (5.19) to the following form:

$$\frac{1}{Q} = \frac{1}{T_1 \Delta H_2^2} = \frac{2}{3}\left[\xi\left(\int_0^\infty \frac{I_1(\tau_c)\,\tau_c d\tau_c}{1+\omega^2\tau_c^2} + 4\int_0^\infty \frac{I_1(\tau_c)\,\tau_c d\tau_c}{1+4\omega^2\tau_c^2}\right) + \right.$$

$$\left. + (1-\xi)\left(\int_0^\infty \frac{I_2(\tau_c)\,\tau_c d\tau_c}{1+\omega^2\tau_c^2} + 4\int_0^\infty \frac{I_2(\tau_c)\,\tau_c d\tau_c}{1+4\omega^2\tau_c^2}\right)\right] \qquad (5.20)$$

It is obvious that if the predominant contribution to the right-hand side of Eq. (5.20) is made by the sum of integrals, having the factor $(1 - \xi)$, the parameter Q will increase with increasing plasticizer concentration. This case occurs at low temperatures (below T_g). Under these conditions the product of the spin-lattice relaxation time T_1 by ΔH_2^2 increases with increasing plasticizer concentration. Since the intensification of intermolecular interaction and the suppression of molecular motion are typical of this case, it is evident that the increase in Q is associated with the increase of the spin-lattice relaxation time as well as of the second moment.

At high temperatures (above T_g) the predominant contribution to the value of $1/Q$ is made by the integrals which have the factor ξ before them. As the plasticizer concentration increases the parameter $Q = T_1 \Delta H_2^2$ will diminish, which is ascribed to the decrease of both cofactors (T_1 and ΔH_2^2).

The effect of the degree of crystallinity and the network density on T_1 and ΔH_2^2 can be considered in an analogous way.

5.3. INVESTIGATION OF THE MOLECULAR MOTION IN POLYMERS AT LOW TEMPERATURES BY THE NMR METHOD

As the temperature falls the various modes of molecular motion in polymers become gradually frozen. This increases the second moment, which at very low temperatures tends to theoretical values calculated for the "rigid lattice". As a rule, the freezing of molecular motion in polymers at $T \to 0$ K may be regarded as a thermal-activation process resulting from the fact that the energy of the thermal motion of a particular kinetic unit diminishes, and when it becomes less than the height of the potential barrier that hinders its motion the given type of molecular motion becomes impossible. As a result the second moment ΔH_2^2 and the spin-lattice relaxation time T_1 increase.

The results of experimental investigations of molecular mobility in polymers (185, 231, 233-235) show that the lowest-temperature mode of molecular motion is due to the rotation of CH_3 groups. It is, however, not difficult to show that the height of the potential barrier that hinders the rotation of methyl groups is not less than 8.4 kJ and that at $T < 40$ K the classical rotation of CH_3 groups cannot lead to a change in ΔH_2^2 and T_1, since the energy of methyl groups under these conditions proves to be much lower than the height of the potential barrier.

In this connection, it has been assumed (249) that the re-orientational motion of methyl groups about the C_3 axis near 0 K is of a quantum nature and is caused by quantum-mechanical tunnelling transitions.

5.3.1. QUANTUM-MECHANICAL TUNNELLING TRANSITIONS IN POLYMERS CONTAINING METHYL GROUPS

From the standpoint of the concepts of classical physics, the potential barrier of height V is a "non-transparent partition" for all particles with energy $E < V$. A quantum-mechanical treatment of the motion of microparticles in microscopical fields shows that in a number of cases particles with energy $E < V$ can tunnel through the potential barrier.

Powles and Gutowsky (249) have shown that at low temperatures some of the methyl groups experience torsional vibrations (re-orientational motion) about the C_3 axis as a result of tunnelling through the barrier (at $E < V$) that hinders their classical rotation. Such tunnelling of CH_3 groups leads to a decrease in ΔH_2^2 for polymers containing methyl groups at $T \to 0$ K as compared with the value of the second moment calculated for the rigid lattice. The theory of quantum-mechanical tunnelling of CH_3 groups has been developed by a number of workers (249-251).

The theory of quantum-mechanical tunnelling has been expounded in the most systematic way by Stejskal and Gutowsky (251), who used it for calculation of the tunnelling frequency and the spin-lattice relaxation time T_1. This theory rests on the assumption that the methyl groups are separated from one another and are linked to the immobile chain matrix. It is presumed further that the potential of the restricted (frozen) rotation of the methyl group does not depend on time and can be given by

$$V = \frac{1}{2} V_0 (1 + \cos 3\Phi) \tag{5.21}$$

where V_0 is the height of the potential barrier; Φ is the angle of rotation of the CH_3 group.

Substituting the potential function V, defined by expression (5.21), into the Schrödinger equation, we obtain:

$$\frac{\hbar^2}{2I} \cdot \frac{\partial^2 \Psi(\Phi)}{\partial \Phi^2} + \left[E - \left(\frac{V_0}{2}\right)(1 + \cos 3\Phi)\right] \Psi(\Phi) = 0 \tag{5.22}$$

where $\Psi(\Phi)$ is the wave function defining the position of the methyl group; E is the energy of the methyl group; I is the moment of inertia of the methyl group relative to the axis of symmetry.

Solving Eq. (5.22) gives a set of the eigenvalues of energy E_i which correspond to the levels of torsional vibrations of the methyl group having a potential with a three-fold symmetry. It is essential that the eigenvalues of the energy are obtained for a pair of levels, one of which is degenerate. As a result of the overlap of the wave functions, each energy level is split into two sub-levels. The splitting $\Delta\nu$ of each level (being proportional to the difference in energy between two neighbouring sublevels) is very small for the lowest energy states and increases at large E_i (Fig. 5.5). The splitting, however, remains small as compared with the energy of the corresponding level of torsional vibrations.

As a result of the splitting of energy levels, the methyl group can be simultaneously in two neighbouring potential wells (252).

A consequence of this is that part of the methyl groups can move with a non-zero probability from one potential well to an identical energy level in another potential well. This makes possible the re-orientational motion of the methyl groups about the C_3 axis by tunnelling through the potential barrier. The tunnelling frequency depends on the height of the potential barrier V_0 and the energy E_i of the methyl group. The splitting $\Delta\nu$ is a measure of

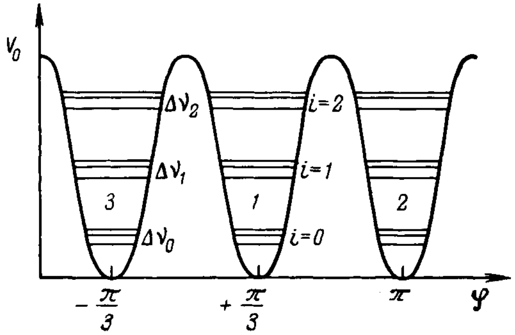

FIG. 5.5. Schematic representation of energy levels for a potential with a three-fold symmetry (253), corresponding to the methyl group.

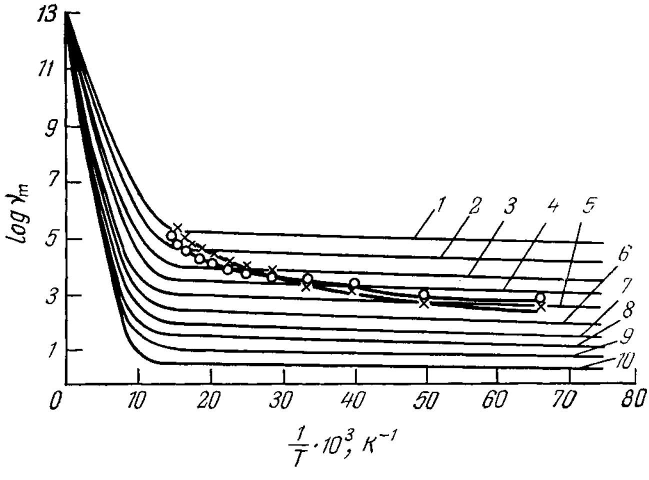

FIG. 5.6. The mean correlation frequency of the ester methyl group in polymethyl methacrylate (○) and polymethyl acrylate (×) against inverse temperature (253). For comparison, the tunnelling frequencies ν_t calculated by Stejskal and Gutowsky for various potential barrier heights are given: 1—14.1 kJ/mole; 2—16.2; 3—18.3; 4—21.0; 5—22.5; 6—24.6; 7—26.7; 8—28.9; 9—31.0; 10—33.0 kJ/mole.

the velocity with which the methyl group tunnels through the potential barrier. If the energy of the methyl group appears to be greater than the potential barrier V_0 with increasing temperature, the quantum-mechanical tunnelling changes to classical rotation.

The tunnelling frequency of the methyl group at temperature T can be given by (253):

$$\nu_T = \frac{1}{Q} \sum_i \Delta\nu_i \exp\left(-\frac{E_i}{RT}\right) = \sum_i a_i \Delta\nu_i \tag{5.23}$$

where Q is the partition function for torsional vibrations; a_i is the probability that the methyl group is in the ith vibrational state.

Obviously, ν_T is the average tunnelling frequency for the entire set of energy levels existing at a given temperature. Stejskal and Gutowsky (251) calculated the dependence of ν_T on temperature for potential barriers of various heights ranging from 9.89 and 33.35 kJ (Fig. 5.6). It is remarkable that below 70 K the average tunnelling frequency does not depend on temperature. This means that the re-orientation of methyl groups occurring through this mechanism is possible down to 0 K.

The theory of the quantum-mechanical tunnelling of methyl groups as applied to nuclear magnetic resonance has also been considered by Allen (254, 255) and Clough (256).

5.3.2. NUCLEAR MAGNETIC RESONANCE IN POLYMERS CONTAINING METHYL GROUPS

Nuclear magnetic resonance in polymers that contain methyl groups has been studied experimentally by a number of investigators (185, 231, 233-235), essentially only down as far as the liquid-nitrogen temperature (77 K), which is far from sufficient for the quantum nature of the re-orientation of methyl groups to be elucidated. There are only a few works (253, 257) dealing with investigations carried out at lower temperatures. Below we shall consider the results of experimental investigations of some amorphous polymers containing methyl groups.

Polymethyl Methacrylate. Nuclear magnetic resonance in this polymer has been studied (253) over the temperature range 5 to 293 K. The temperature dependence of the second moment in polymethyl methacrylate is given in Fig. 5.7. At room temperature the second moment of this polymer is $\Delta H_2^2 = 10\ \mathrm{G}^2$. As the temperature falls the second moment increases and at 120 K it reaches $\Delta H_2^2 = 19$ gauss², at which level it remains constant down to 75 K and then again increases. At 20 K a second, a very small low-temperature plateau appears with a value of $\Delta H_2^2 = 23\ \mathrm{G}^2$.

Using the van Vleck theory (236) and knowing the internuclear distances and valence angles, we can calculate the second moment of polymethyl methacrylate for the rigid lattice (253). For this case, $\Delta H_2^2 = 28\ G^2$. The theoretical value of the second moment, taking into account the rotation of one methyl group, is 20.2 G^2, and if the rotation of both CH_3 groups is taken into account, $\Delta H_2^2 = 12.5\ G^2$. A comparison of these values with experimentally measured values shows that above 120 K a decrease in the second moment due to the incipient rotation of the methyl group attached directly to the main chain is observed. Below 120 K (down to 77 K) rotation of the methyl group linked to the side ester group becomes possible.

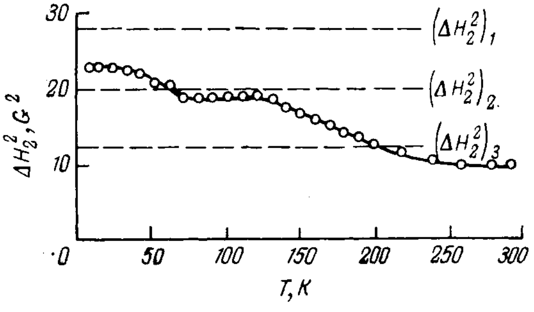

FIG. 5.7. Dependence of the second moment ΔH_2^2 of the NMR spectrum line on temperature for polymethyl methacrylate (257) [$(\Delta H_2^2)_1$ is the theoretical value for the rigid lattice; $(\Delta H_2^2)_2$ is the theoretical value corresponding to the rotation of one CH_3 group; $(\Delta H_2^2)_3$ is the theoretical value corresponding to the rotation of both CH_3 groups].

The value of $\Delta H_2^2 = 23\ G^2$, obtained experimentally at helium temperatures (5 K), differs greatly from the theoretical result obtained for the rigid lattice (28 G^2). This difference cannot be accounted for by the insignificant intermolecular contribution to the second moment. Nor can it be explained by the effect on the second moment of the intramolecular motion, which is partly frozen at helium temperatures.

Bergmann and Navotki (258) proposed a method which makes it possible to separate the contribution of mobile kinetic units from the experimentally measured values. This method makes use of the rotation parameter r_1 which is defined in this particular case as the ratio of the number of fixed methyl groups to the total number of methyl groups present in the polymer. Figure 5.8 is a plot of the parameter r_1 against temperature for polymethyl methacrylate. From this figure it can be seen that between 5 and 20 K the parameter r_1 has an average value of 0.76, i.e., 76 per cent of CH_3 groups are immobile at these temperatures. The discrepancy between the theoretically calculated and experimentally found values of the second moment becomes understandable if we take into account that 24 per cent of CH_3 groups are still mobile at 5 K. The mobility of CH_3 groups at such low temperatures cannot be explained within the framework of classical conceptions.

If the average correlation frequency is calculated from the experimentally found values of δH by means of formula (5.8), then

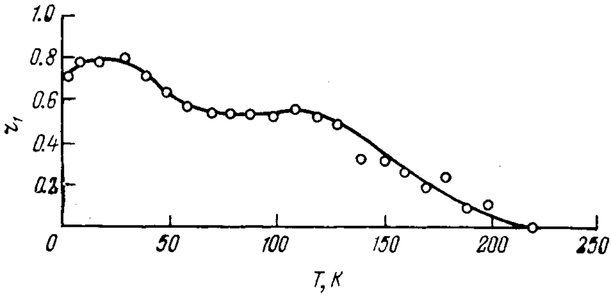

FIG. 5.8. The proportion of rigid methyl groups in polymethyl methacrylate against temperature (253).

in the case of a thermal-activation process log ν_a must, in accordance with the Arrhenius equation (5.9), depend linearly on the inverse temperature. The calculated activation energy U for the process resulting from the motion of α-methyl groups is 9.6 kJ/mole. The calculated correlation frequencies lie between 10^3 and 10^5 Hz and the limiting frequency $\nu_\infty \approx 10^7$ Hz. These values do not agree with the transition-state theory (197), according to which $\nu_\infty = 2.7 \times 10^{12}$ Hz. An even lower value of activation energy (0.75 kJ/mole) is obtained for the process caused by the motion of the ester methyl groups. This value of activation energy is too low for processes of the thermal-activation type.

When we compare the temperature dependence of correlation frequencies for the process resulting from the motion of α-methyl groups (253) (Fig. 5.9) with the temperature dependence of the tunnelling frequencies calculated by Stejskal and Gutowsky (251), it appears that the picture of the classical motion does not conform to reality. This is even more distinctly manifested in the case of the motion of the ester methyl groups (see Fig. 5.6). This is evidenced by the fact that the graph of log $\nu_a = f\,(1/T)$ is no longer a straight line and also by the fact that in the case of α-methyl groups the dependences of log ν_a and log ν_T exhibit a tendency towards agreement at low temperatures. At higher temperatures (above 120 K), at which the α-methyl groups begin to rotate, their thermal energy exceeds the height of the hindering barrier V_0. According to the quantum-mechanical model (249), tunnelling is transformed in this case into classical rotation.

The satisfactory fit between the correlation and tunnelling frequencies for the ester methyl groups is an indication that the quantum-mechanical model describes this mode of motion. It is interesting that in the low-temperature region the potential barrier height (see Fig. 5.6) was found to be equal to 22.6 kJ/mole, while the classical rotation model gives a value which differs from this value by more than one order of magnitude. From an analysis of the results presented in Fig. 5.6 it follows that the simple quantum-mechanical model describes well the motion of the ester methyl groups in polymethyl methacrylate at temperatures sufficiently low for classical rotation to be impossible.

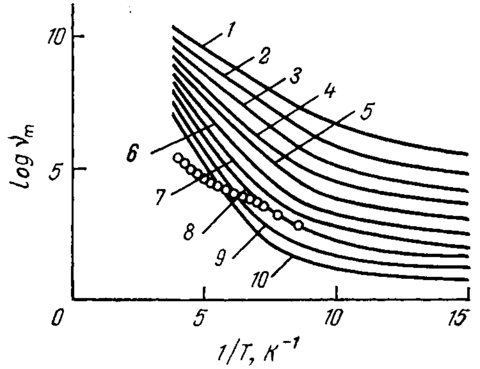

FIG. 5.9. The mean correlation frequency of the α-methyl group in polymethyl methacrylate against inverse temperature (253). For comparison, the tunnelling frequencies calculated by Stejskal and Gutowsky are given: 1—14.1 kJ/mole; 2—16.2; 3—18.3; 4—21.0; 5—22.5; 6—24.6; 7—26.7; 8—28.9; 9—31.0; 10—33.0 kJ/mole.

The question of which of the quantum-mechanical models is in better agreement with the experimental data is still not quite clear. Stejskal and Gutowsky have shown (251) that no value of the second moment that would agree satisfactorily with the available experimental data can be obtained by a simple quantum-mechanical model.

Allen (254) and Clough (259), basing themselves on their enery-level diagrams for the methyl group, calculated the value of H_2^2 at helium temperatures. From the calculations made by lough it follows that $\Delta H_2^2 = 20.2$ G^2 at 4.2 K for polymethyl ethacrylate, while according to the experimental data obtained by Kosfeld and Mylius (253), $\Delta H_2^2 = 23$ G^2 at 5 K. Such a substantial difference (2.8.G^2) between experimental and theoretical results is probably an indication that below the experimentally attained temperature $T = 5$ K one should expect the second moment (at $T \rightarrow 0$ K) (257) to decrease to the value predicted by theory (20.2.G^2). It will be shown below that such an extreme temperature dependence of ΔH_2^2 at $T \rightarrow 0$ K is in fact observed in some polymers containing methyl groups.

Polymethyl Acrylate. Kosfeld and Mylius (253) studied the temperature dependence of the second moment in this polymer between 5 and 293 K. The results of this investigation are presented in Fig. 5.10. The second moment in polymethyl acrylate at room temperature (20°C) is 8.7 G^2. A rapid fall in ΔH_2^2 above 293 K is due to the unfreezing of the segmental micro-Brownian motion, i.e., to the transition from the glassy to the rubbery state. Below 250 K one observes a slight linear increase in the second moment with decreasing temperature. This effect is evidently associated with a certain increase in density caused by the fall in temperature. At 75 K the second moment of polymethyl acrylate attains a value of 11.7.G^2. As the temperature drops further the second moment increases substantially and at 20 K it becomes equal to 17.1 G^2. The experimental results obtained by Kosfeld and Mylius in the temperature range 77 to 293 K are in good agreement with the data of other investigators (222, 260, 261).

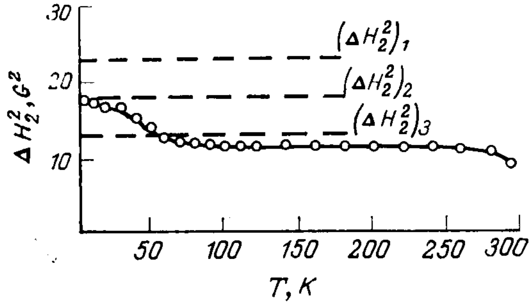

FIG. 5.10. Dependence of the second moment ΔH_2^2 of polymethyl acrylate on temperature (257) [$(\Delta H_2^2)_1$ is the theoretical value for the rigid lattice; $(\Delta H_2^2)_2$ is the theoretical value corresponding to the tunnelling of the CH$_3$ group; $(\Delta H_2^2)_3$ is the theoretical value corresponding to the rotation of the CH$_3$ group].

Calculations show (253, 261) that the ΔH_2^2 value corresponding to the rigid lattice is 22.9 G^2 for polymethyl acrylate. If the rotation of the methyl groups is taken into account, $\Delta H_2^2 = 12.9$ G^2.

The large difference between the experimental data at 5 K ($\Delta H_2^2 = 17.1$ G^2) and the theoretical value for the rigid lattice

(22.9 G^2) may arise from the fact that even at such low temperatures motion of the CH_3 groups is possible. The temperature dependence of the parameter r_1 for polymethyl acrylate is presented in Fig. 5.11.

At 5 K the parameter r_1 is equal to 0.36. In contrast to polymethyl methacrylate, polymethyl acrylate has only one methyl group in the repeat unit, and therefore the expected value of r_1 for the rigid lattice is 0.5. This means that 72 per cent of all the CH_3 groups in polymethyl acrylate are immobile at 5 K, the remaining 28 per cent retaining their mobility (253, 257). Beginning from 77 K, the value r_1 approaches zero, which corresponds to the rotation of all the ester methyl groups.

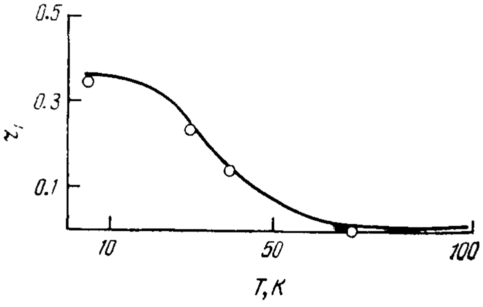

FIG. 5.11. The proportion of rigid methyl groups in polymethyl acrylate against temperature (253).

If we calculate the activation energy of the process associated with the motion of the methyl groups near the liquid-helium temperature on the basis of classical concepts, the resulting value (U = 0.84 kJ/mole) will be too low for the process under consideration to be thermal activation. The temperature dependence of the correlation frequency at low temperatures as calculated from experimental data is in good accord with the temperature dependence of the tunnelling frequency. At $T < 50$ K, both $\log \nu_c$ and $\log \nu_T$ are independent of temperature, and the value of the hindering potential V_0 is found to be equal to 22.6 kJ/mole. This coincides with the data for the re-orientational motion of the ester methyl groups in polymethyl methacrylate and points to the mobility of the methyl groups in polymethyl acrylate being due to quantum-mechanical tunnelling. This is also supported by the fact that the value of the second moment calculated by Clough (256, 259) at $T = 4.2$ K for polymethyl acrylate is 17.0 G^2, which is in excellent agreement with the experimental value of ΔH_2^2 near the liquid-helium temperature.

Polycarbonate. In the temperature range 293 to 77 K polycarbonate has been studied by several authors (185, 262). Figure

5.12 shows the temperature dependence of the second moment of polycarbonate at temperatures from 5 to 293 K (257). At room temperature the ΔH_2^2 of polycarbonate is 4 G². Between 170 and 77 K there is observed an appreciable increase in the second moment (by 13 G²), it being about 20 G² at 77 K. The second moment begins to decrease with a further fall in temperature and becomes equal to 15.5 G² at 5 K.

If we use the van Vleck theory (236) for the calculation of the second moment, the ΔH_2^2 value for polycarbonate in the case of

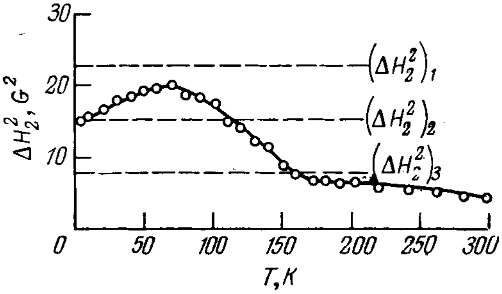

FIG. 5.12. Dependence of the second moment of ΔH_2^2 of polycarbonate on temperature (257) [$(\Delta H_2^2)_1$ is the theoretical value for the rigid lattice; $(\Delta H_2^2)_2$ is the theoretical value corresponding to the tunnelling of the methyl groups; $(\Delta H_2^2)_3$ is the theoretical value which takes account of the rotation of two CH_3 groups].

the rigid lattice will be equal to 22.7 G². If account is taken of the rotation of one CH_3 group in the repeat unit, the value of ΔH_2^2 will be 15.2 G². Upon rotation of both methyl groups $\Delta H_2^2 = 7.7$ G². It would seem that using these values allows one to explain the temperature dependence of the second moment presented in Fig. 5.12: the increase in the second moment between 170 and 77 K is accounted for by the freezing of the rotational motion of both CH_3 groups. The maximum value of the second moment at 77 K ($\Delta H_2^2 = 20$ G²) is, however, found to be lower than the value calculated for the rigid lattice (22.7 G²). The discrepancy between these values (about 3 G²) implies that not all the modes of intramolecular motion are frozen at 77 K.

The decrease in the second moment with fall of temperature below 77 K cannot be explained by a decrease in the thermal activation of the motion of the methyl groups, since in this case the value of ΔH_2^2 would have increased at T → 0 K. The calculation of activation energy based on the use of the temperature dependence of the correlation frequency corresponding to the Arrhenius equation leads to an activation energy of 5 kJ/mole, which is too low for the thermal-activation process. Thus, the decrease in the second moment at T → 0 K and the very low values of activation energy do not allow us to account for the motion of the methyl groups at very low temperatures within the scope of the classical model of rotation.

One would think that the dependence $\Delta H_2^2 = f(T)$ in polycarbonate at low temperatures can be explained quantum-mechanically. However, the simple quantum-mechanical tunnelling model (249-251) does not allow one to account for the decrease in the second moment at $T \to 0$ K. This effect cannot be explained either with the aid of the more complicated Allen model (254). Allen calculated ΔH_2^2 on the basis of a more accurate energy-level diagram for the methyl group. This is largely associated with the fact that these models deal with the motion of the methyl group in an isolated molecule.

Clough (256, 259) attempted to calculate the motion of the methyl group in a molecular crystal. He assumed that the motion of the methyl group alters the lattice state. Consideration of this phenomenon leads to the appearance, in expression (5.21) for the hindering potential, of an additional term due to the reverse action of the effect of a change in the lattice state on the methyl group. Using this potential, Clough calculated (256) the energy-level diagram for the methyl group. A distinctive feature of his theory is that the splitting of the energy level corresponding to the joint state of the methyl group and the lattice is small as compared with kT. From the calculations made by Clough it follows that ΔH_2^2 is equal to $8\mu^2 d^2/5$ for the classical rotation of the CH_3 group (the high temperature case), $\Delta H_2^2 = 32\ \mu^2 d^2/5$ for the rigid lattice, and $\Delta H_2^2 = 16\mu^2 d^2/5$ at low temperatures. Here $\mu = \gamma/2$ (where γ is the gyromagnetic ratio); $d = 3\mu R^{-3}/2$ (where R is the distance between the protons in the methyl group). The data given here mean that the value of ΔH_2^2 at low temperatures can be only half of the second moment for the rigid lattice.

The Clough theory allows one to account for the existence of a maximum in the temperature dependence of the second moment in polycarbonate. At the lowest temperatures the value of the second moment (15.5 G^2), which is low as compared with the ΔH_2^2 value for the rigid lattice, is due to the re-orientation of the methyl groups resulting from quantum-mechanical tunnelling. As the temperature rises (from 15 K) the intensity of lattice vibrations in polycarbonate increases. These lattice vibrations cause a sort of tunnelling frequency modulation, which leads to a decrease in the tunnelling motion of the methyl groups as the temperature rises. This effect is especially pronounced when the extent of tunnelling frequency modulation is great and the probability of classical rotation is still low.

Thus, one can expect that at sufficiently low temperatures the second moment will increase with increasing temperature, tending towards the level typical of the rigid lattice. Further rise of temperature leads to an increase in the energy of thermal motion (thermal activation) of the methyl groups and to the unfreezing of classical rotation and, hence, to a decrease in ΔH_2^2. Thus, by taking account of the lattice vibrations one is able to explain the increase in ΔH_2^2 with rise of temperature at low temperatures. According to the Clough theory, the onset of the broadening of the line with the increase in T, which is caused by the decrease in the tunnelling motion, must occur at 23 K.

From the conceptions expounded above one can expect that the increase in ΔH_2^2 with rise of temperature will depend on steric hindrances that impede the motion of methyl groups. If the steric hindrance that retards the motion of methyl groups is so small that classical rotation is possible even at low temperatures, then the increase in the second moment with increasing T must be very small. Conversely, if the classical rotation of methyl groups is hindered so strongly that it becomes possible only at higher temperatures, then at low temperatures one may expect the second moment to increase significantly with rise of temperature. Only at higher temperatures does the unfreezing of the classical rotation of the CH_3 groups lead to a decrease in ΔH_2^2.

It is the last case that agrees with the experimentally determined temperature dependence of the second moment for polycarbonate. On the other hand, the methyl groups in polycarbonate that are responsible for quantum-mechanical tunnelling are directly attached to the main chain, which leads to a higher hindering potential than in the case of the methyl groups present in the ester side groups. In this connection, it becomes understandable why in polycarbonate at low temperatures, in contrast to polymethyl methacrylate and polymethyl acrylate, the second moment increases with rise of temperature. It is interesting that the Clough theory (256, 259) yields a value of $\Delta H_2^2 = 15.5$ G^2 at 4.2 K, which fits the experimental data well. The subsequent fall in the second moment with rise of temperature above 77 K is due to the fact that at this temperature the classical rotation of the methyl groups in polycarbonate begins to be unfrozen.

Polyisobutylene. The temperature dependence of the second moment of NMR in this polymer (257) is shown in Fig. 5.13. The second moment at room temperature in polyisobutylene is 0.2 G^2. As the temperature falls the second moment increases and attains the value 33.6 G^2 at 77 K. Further decrease in temperature leads to a decrease in ΔH_2^2, while in the temperature range 5-30 K the second moment remains constant at 26 G^2. Calculations based on the van Vleck theory give a value of $\Delta H_2^2 = 40.3$ G^2 for the rigid lattice. The rotation of one methyl group lowers the second moment down to 25.9 G^2, and the rotation of both CH_3 groups reduces it to 12.5 G^2.

In polyisobutylene above 200 K one observes a sharp decrease in ΔH_2^2, which at room temperature assumes a very low value which probably corresponds to the rubbery state. This region of rapid change in the second moment evidently corresponds to the glass-transition region of this polymer. The second moment at 200 K

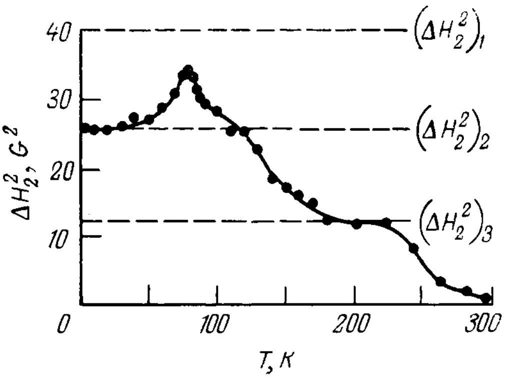

FIG. 5.13. Dependence of the second moment of ΔH_2^2 of polyisobutylene on temperature (257) [$(\Delta H_2^2)_1$ is the theoretical value for the rigid lattice; $(\Delta H_2^2)_2$ is the theoretical value corresponding to the tunnelling of the methyl groups; $(\Delta H_2^2)_3$ is the theoretical value corresponding to the rotation of two CH_3 groups].

is 12.6 G^2, which value can be attributed to the rotation of both methyl groups and is in good agreement with the theoretically calculated value (12.5 G^2). Further increase in the second moment is caused by the freezing of the rotational motion of the CH_3 groups. At 110 K a slight kink on the $\Delta H_2^2 = f\ (T)$ graph appears—the second moment at this temperature is equal to 26 G^2 and coincides with the theoretically predicted value (25.9 G^2), which corresponds to the rotation of only one CH_3 group in the repeat unit of the polymer. With a further drop in temperature the second moment reaches its maximum value, 33.6 G^2, at 77 K. This value differs greatly (by 6.7 G^2) from the second moment corresponding to the rigid lattice (40.3 G^2). Such a large difference between these values signifies that at 77 K the mobility of the CH_3 groups is still considerable.

The fall of the second moment as the temperature drops below 77 K is an indication that the observed effect is not thermal activation and, hence, cannot be accounted for on the basis of the classical conceptions of the rotation of methyl groups. Just as in the case of polycarbonate, the experimental data obtained for polyisobutylene are in good agreement with the Clough quantum-mechanical model. This theory is supported by the theoretical value of ΔH_2^2 (25.9 G^2) for $T = 4.2$ K, which for practical purposes coincides with that found by experiment, and also by the presence of a temperature region (5-30 K) where the second moment is independent of temperature.

Thus, in polymers such as polyisobutylene and polycarbonate the quantum-mechanical tunnelling of methyl groups at low temperatures is superimposed by an additional effect caused by thermal lattice vibrations, this effect leading to an unexpected decrease in the second moment with fall of temperature.

CHAPTER 6

DYNAMIC MECHANICAL PROPERTIES OF POLYMERS AT LOW TEMPERATURES

6.1. EFFECT OF CHEMICAL CONSTITUTION, STRUCTURE AND COMPOSITION ON THE DYNAMIC MECHANICAL PROPERTIES OF POLYMERS. BASIC CONCEPTS OF ACOUSTIC SPECTROSCOPY OF POLYMERS

The main parameters characterizing the dynamic mechanical properties of polymers are the components of the complex elastic modulus—the dynamic elastic modulus and the loss modulus (70, 263)—and also the loss tangent or loss factor:

$$\tan \delta = \frac{G''}{G'} \tag{6.1}$$

where G'' is the loss modulus and G' is the dynamic shear modulus.

The dynamic mechanical properties of polymers are usually studied by using low-frequency acoustic vibrations (not higher than 10^4 Hz) and may be regarded as low-frequency acoustical properties.

The parameters characterizing the dynamic mechanical properties of polymers are largely governed by two factors: the chemical constitution and the specific features of the supermolecular (supramolecular) structure.

When the frequency of acoustic vibrations and temperature vary over wide limits, the dynamic mechanical properties of polymers undergo considerable changes caused by relaxation processes which are associated with the various modes of molecular motion. The nature of molecular motion is governed by the chemical constitution and structure of the polymer. But additionally, the most important physical properties of polymers depend on the intensity and specific features of the relaxation processes and, hence, on the mode of molecular motion.

One of the main methods of investigating molecular motion in polymers is the study of the temperature dependences of the parameters characterizing the dynamic mechanical properties. The most important in this respect is the study of the dependence of the dynamic modulus, the loss factor (tan δ), and the loss modulus on temperature.

If the polymer is cooled down to a very low temperature at which no molecular motion is present (this cannot be attained in all cases since in some polymers the molecular mobility is still possible even at 0 K) and the parameters indicated above are measured with the temperature being raised gradually, the various modes of molecular motion in the polymer will begin to be successively unfrozen. In this process, each mode of molecular motion unfrozen will leave its imprint on the $\tan\delta = f(T)$, $G' = f(T)$, and $G'' = f(T)$ graphs. The temperature dependences of these parameters are, as it were, snapshots giving information on the various kinds of molecular motion which may occur in polymers and also on the structure of the polymer. Each type of molecular motion is usually associated with a specific relaxation process caused by a given mode of molecular motion.

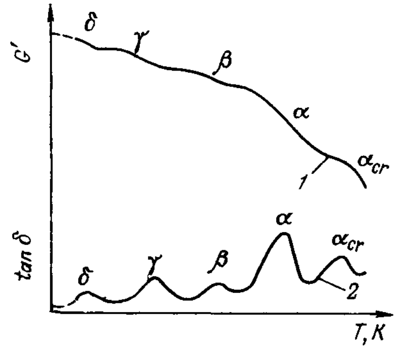

FIG. 6.1. Diagram showing temperature transitions in amorphous-crystalline polymers:
1—G'; 2—$\tan\delta$. Explanations are given in the text.

At very low temperatures (at $T \to 0$ K) the relaxation times of almost all relaxation processes are very great, and for them the condition $\omega\tau \gg 1$ is fulfilled. Since at a first approximation τ is proportional to $\exp(U/RT)$, it follows that all relaxation times decrease with increasing temperature and when the condition $\omega\tau = 1$ is fulfilled for a particular relaxation process, a maximum appears on the temperature dependence of $\tan\delta$ or G''. Under the same conditions the dynamic shear modulus is decreased.

If measurements are carried out at a constant frequency over a wide temperature range, it is possible to reveal all the relaxation processes characteristic of a given polymer, processes which are associated with the various types of molecular mobility that can be realized in the polymer. Manifestation of each mode of molecular motion, which leads to considerable changes in the temperature dependence of the dynamic mechanical properties, are usually treated as a temperature transition. The temperature transitions taking place in amorphous polymers are of a relaxational nature. In the case of crystalline polymers, thermodynamic phase transitions are also regarded as temperature transitions.

The general diagram of temperature transitions in amorphous-crystalline polymers is given in Fig. 6.1. Usually, temperature transitions, beginning from the highest-temperature transition (264, 265), are labelled by the Greek letters α, β, γ, and δ. Relaxation processes that occur with fall of temperature are denoted by the same letters.

The highest-temperature α_{cr}-transition shown in Fig. 6.1 may be a multiplet transition associated with the movement of polymeric chains in crystalline regions. According to the model proposed by Hoffman, Williams, and Passaglia (266), this temperature transition is associated with the motion of folds and the reorientation of polymeric chains. The apparent activation energy of a relaxation process of this type is 167-418 kJ/mole.

The dynamic mechanical properties of crystalline polymers are strongly influenced by the relaxation process caused by the glass transition of the amorphous layer (α_{am}-relaxation). In strongly crystallized polymers, this relaxation process degenerates and can be barely observed in this case on the temperature dependences of G', G'', and tan δ.

With amorphous polymers this relaxation process is dominant, being associated with the transition from the glassy to the rubbery state (or vice versa). This temperature transition is due to the unfreezing of segmental mobility of the micro-Brownian type and leads to the most marked change in the dynamic modulus of amorphous polymers (from 10^3 MPa in the glassy state to 1 MPa in the rubbery state) and to the appearance of the most intense loss maximum. The molecular mobility is in this case realized due to the large kinetic units in the main chain of the polymer. The temperature transition corresponding to α_{am}-relaxation can be singlet or multiplet (70, 267).

The next temperature transition which takes place at lower temperatures is known as the β-transition (β-relaxation). This temperature transition, which is located in the region of a secondary relaxation, usually involves relaxation processes caused by the motion of side groups or small units of the main chain. In view of this, by β-relaxation we mean the various temperature transitions. For example, while the β-relaxation occurring in polymethyl methacrylate is a process associated with the re-orientational motion of side chains (265), with polytrifluorochloroethylene the β-relaxation is caused by the glass-transition of amorphous regions (266), and in the case of crystalline polytetrafluoroethylene it is a phase transition (265) which leads to a change in the type of unit cell of the polymer. It has been suggested (264) that only the processes caused by the motion of side groups be included in the category of β-relaxations. The apparent activation energy for β-relaxations is 63-167 kJ/mole.

At lower temperatures, only those temperature transitions occur which are provoked by small kinetic units of the main or side chains of a polymer, these chains consisting of several successively linked carbon atoms. Such temperature transitions (γ-relaxations) are often connected with the movement of four or more CH_2 or CF_2 groups. In crystalline polymers one observes the phenomenon of γ-relaxation attributed to the re-orientation of chain ends in crystallites and to the presence of defects in them (γ_{cr}-relaxation) (266) and also to the mobility of several aliphatic carbon atoms in amorphous regions (γ_{am}-relaxation).

At very low temperatures, there are observed temperature transitions brought about by the mobility of terminal groups of atoms and some of those present in the branchings (δ-relaxations). An example of δ-relaxation is the motion of the phenyl groups in polystyrene or of the methyl groups in polypropylene at low temperatures. The δ-relaxation process may be of the complex multiplet nature.

The presence of the various temperature transitions in a polymer depends on its chemical constitution and structure.

It should be noted that the entire gamut of relaxation processes taking place in crystalline and amorphous polymers cannot be reduced to the relaxation mechanisms indicated above, these not even being self-evident themselves. It is, however, quite obvious that the molecular mechanism of relaxation processes in crystalline and amorphous polymers is largely governed by their supermolecular structure.

Thus, the dynamic mechanical properties of polymers are governed by their chemical constitution and structure. This is uniquely reflected in the temperature dependence of the loss modulus, the loss tangent (tan δ), and the dynamic modulus. It can be asserted that there are no two polymers of different chemical constitution whose temperature dependences of these parameters are identical.

This has recently led to the development of the acoustic spectroscopy of polymeric materials, the main task of which is to establish the relationship between chemical constitution, structure and composition, on the one hand, and the acoustic parameters (including the parameters which characterize the dynamic mechanical properties), on the other. Another objective of acoustic spectroscopy is to obtain information on the chemical constitution, structure and composition of polymeric materials on the basis of a study of the temperature or frequency dependences of the acoustic parameters.

The salient features of acoustic spectroscopy of polymers are each manifested in a specifically individual way during investigations of the dynamic mechanical properties of polymers in the low-temperature region.

Most of the works devoted to the study of the dynamic mechanical properties of polymers have been carried out with the temperature of the sample being changed from 77 K to the melting temperature, in the case of crystalline polymers, or to temperatures somewhat higher than T_g, in the case of amorphous polymers. The dynamic mechanical properties of polymers below 77 K have been studied in a comparatively limited number of works; an article with a review of these works has been written by Sauer and Saba (265). They stated that below the liquid-nitrogen temperature (77 K) mechanical relaxations are observed only in polymers containing side (pendant) groups. Such polymers include, for example, polymethyl methacrylate, polypropylene, and polyvinyl acetate, in all of which the δ-relaxation process results from the re-orientational motion of methyl groups. The phenomenon of δ-relaxation caused by the movement of ethyl groups in the side chains has been observed in polyethyl acrylate and polyvinyl propionate. The δ-relaxation process due to the motion of side phenyl groups or substituted phenyl groups have been repeatedly observed in polystyrene and its derivatives. At the same time, Sauer and Saba arrived at the conclusion that below 77 K no relaxation processes occur in such linear polymers as linear polyethylene, polytetrafluoroethylene or polyoxymethylene, which have no side groups.

A number of works have been published recently, which show that relaxation loss maxima also appear in linear crystalline polymers below the liquid-nitrogen temperature.

Armeniades and Baer (268) reported two new low-temperature loss maxima in polyethylene terephthalate, located at 46 and 27 K. It turns out that these mechanical loss peaks depend on the orientation and degree of crystallinity respectively. Later, analogous loss peaks were detected in polyethylene and polyoxymethylene (269, 270). It was established that these loss peaks depend on the supermolecular structure of polymeric chains in crystalline regions. In order to account for the mechanism of the low-temperature loss peaks in polyoxymethylene and polyethylene terephthalate, use was made of the hypothesis of the thermally activated motion of dislocation jogs and their interaction with conformational kink defects.

Hiltner and Baer (270) have found that no δ_{cr}-relaxation (the loss tangent maximum at 46 K) takes place in amorphous or rapidly quenched samples, and that this process is observed in rolled or stretched samples. The height of the δ_{cr} peak increases in oriented samples annealed in the stressed state (i.e., when the ends of the samples are rigidly clamped) but diminishes when the samples are annealed in the free state. It is assumed that the δ_{cr}-relaxation is of the same nature as the Bordoni peaks in metals.

6.2. METHODS OF INVESTIGATING THE DYNAMIC MECHANICAL PROPERTIES OF POLYMERS

Two methods are usually used to measure the parameters that characterize the dynamic mechanical properties of polymers at low temperatures. The most widely employed is the method of free torsional vibrations (70, 163). The apparatus based on this method—various types of torsion pendulum—are the most frequently used and have been described in detail (271, 272). In earlier works, the direct torsion pendulum was used; in recent years the measurements have been carried out on the inverted torsion pendulum. This type of apparatus enables one to study the dynamic mechanical properties of polymers over the temperature range 4.2 K to the melting temperature. As a rule, measurements are made at a frequency of around 1 Hz. The parameters measured are the dynamic shear modulus G' and the loss tangent $\tan \delta$ (or G'').

The second method used in studying the dynamic mechanical properties of polymers down to 4.2 K is the resonance method (the Bordoni method) (273, 274). This method allows one to measure Young's dynamic modulus E' and $\tan \delta$ in the 10^3 to 10^4 Hz frequency range. One instrument of this type, designed by Crissman and McCammon (275), makes it possible to measure E' and $\tan \delta$ over the temperature range 4.2 to 300 K.

The results obtained by means of these two methods are difficult to compare, since different elastic moduli are measured (the shear modulus and Young's modulus) at frequencies differing by 2-3 orders of magnitude.

It is commonly believed that dynamic mechanical properties should preferably be studied at the lowest frequencies. The supporters of this point of view assert that in high-frequency measurements the relaxation maxima shift with increasing frequency to higher temperatures and are superimposed upon one another, which sharply reduces the resolving power of the method. But here they are ignoring a curious feature of dynamic-mechanical measurements in polymers: in low-frequency measurements the relaxation maxima are found to be shifted towards low temperatures and they also may be superimposed on each other, which naturally also lowers the resolution of the method.

Thus, it can be said that the study of dynamic mechanical properties at low temperatures should best be carried out at high frequencies. In this case, the resolving power of the methods used will increase in the low-temperature region and decrease in the high-temperature region. The use of low-frequency methods, on the contrary, reduces the resolution at low temperatures and enhances it at high temperatures. Nonetheless, by virtue of the known simplicity of free torsional vibration methods, the majority of experimental studies of the dynamic mechanical properties of polymers have been carried out on the torsion pendulum at a frequency of about 1 Hz.

6.3. RELAXATION PROCESSES IN POLYMERS AT LOW TEMPERATURES

According to the results of the study of dynamic mechanical properties at low temperatures the polymers investigated can be divided into three groups: (1) linear crystalline polymers, such as polyethylene, polytetrafluoroethylene, polyoxymethylene, polycapramide, polyethylene terephthalate; (2) polymers containing methyl groups: polypropylene, poly-4-methyl 1-pentene, polymethyl methacrylate, polycarbonate; (3) polyvinyl chloride, polystyrene and its derivatives.

In the following we shall consider the molecular mobility and the associated relaxation processes observed at low temperatures in the polymers listed above.

Polyethylene. The dynamic mechanical properties of polyethylene have been studied by many investigators and discussed in a number of monographs (70, 163) and review articles (276-278). Measurements carried out on the torsion pendulum at a frequency of 1 Hz show that in branched polyethylene (low-density polyethylene) three loss maxima at temperatures 340, 250, and 150 K are found. These loss peaks are usually linked with α-, β-, and γ-relaxations. Most often only the α- and γ-relaxations are observed in linear polyethylene.

Usually, the tan δ peak observed in polyethylene near 340 K (α-relaxation) is attributed to mobility in the crystalline regions (279-282). Sinnott (281) attributed the α-peak to the re-orientation of the folds on the lamellar surfaces. Illers (283) ascribed the α-relaxation in polyethylene to the frozen (retarded) rotation of the long folds about the longitudinal axis of the polymer. Here it is presumed that this rotation takes place inside the crystal lattice. A dispute arises in the interpretation of the β- and γ-relaxation processes. Kline, Sauer and Woodward (284) point to a direct relationship between the β-relaxation process and the number of side chains (branches) in polyethylene. On the other hand, it is usually believed (70, 266) that the β-peak in polyethylene is associated with the unfreezing of the segmental motion of the main chains in the amorphous regions, i.e., with the glass-transition of the amorphous layer.

Even more controversial is the question of the mechanism of γ-relaxation in polyethylene. Boyer (164) and Schatzki (162) proposed for the γ-relaxation process the crankshaft rotation mechanism which involves several methylene groups. Both these investigators presume that the γ-relaxation is not associated with the glass-transition of the amorphous regions in polyethylene. There exist various mechanisms which allow us to attribute the γ-peak of tan δ in polyethylene to the motion of the kinetic units of polymeric chains on the surface of crystallites. Hypotheses of this type have been put forward by Fisher and Peterlin (285), Wada and coworkers (286), Crist and Peterlin (287). Stehling and Mandelkern (278) maintain that the γ-peak results from the superposition of two relaxation processes caused by mobility in the uncrystallized phase. Sinnott (281) believes that the γ-peak is a single (singlet) relaxation process connected with the motion of defects in crystallites. On the other hand, Illers (283), Pechhold (288), and Gray and McCrum (289) assume that the γ-relaxation is a multiplet process associated with mobility in both the crystallites and amorphous regions.

It has long been believed (265, 290) that in linear polymers such as polyethylene, polytetrafluoroethylene, and polyoxymethylene, which have no side groups pendant to the main chain, there are no mechanical loss maxima below 100 K. However, Papir and Baer (269), using the torsion pendulum ($\nu = 1$ Hz), demonstrated convincingly that in linear polyethylene one can observe two new mechanical loss peaks at low temperatures. In the temperature dependence of the logarithmic decrement these maxima show up at 48 K (the δ_{cr}-peak) and 20 K (the ε-peak). A remarkable feature is that both these maxima were detected while investigating samples of linear polyethylene subjected to preliminary rolling, extrusion or annealing in the fixed state (with the length of the sample rigidly clamped). It was found that the increase in the degree of orientation on extrusion or rolling leads to an increase in the height of these low-temperature loss maxima (Fig. 6.2).

An increase in the intensity of the δ_{cr}- and ε-peaks has also been observed on annealing polyethylene samples with rigidly clamped ends (Fig. 6.3). However, if the samples were in the unclamped free state during annealing, then no loss δ_{cr}- and ε-peaks were observed for the annealed samples. The activation energy for the δ_{cr}-relaxation process is 12.5 to 16.7 kJ/mole, which agrees well with the corresponding values obtained for the low-temperature relaxation processes in polyethylene terephthalate and polyoxymethylene (270, 308).

The mechanism of δ_{cr}- and ε-relaxations clearly cannot be connected with the presence in polyethylene of various impurities or various types of end groups. It is more likely that these low-temperature loss peaks can be explained on the basis of a model that takes into account the interaction of conformational kink-defects and dislocation jogs (270). Such a model is largely based on the ideas put forward by Pechhold (288) concerning the structure of a bulk crystallized polymer, according to which the segments of parallel-packed chains (crystallites) coexist with cooperatively folded regions. According to this model, the relaxation processes in polymers may be associated with the motion of specific rotation isomers (kink-isomers), which are defects in an almost parallel packing of chains. The model (291) proposed for describing the low-temperature loss peaks assumes that edge dislocations can interact with conformational kink-defects in the ordered regions of the polymer. From this model it follows that the intensity of the relaxation process must increase with increasing dislocation density and concentration of kink-defects. The existence of edge dislocations in single crystals of linear polyethylene has been proved experimentally (292, 293).

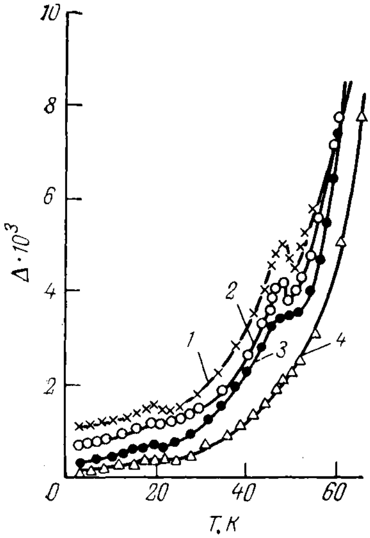

FIG. 6.2. Increase in the value of the logarithmic decrement Δ due to the cold uniaxial drawing of linear polyethylene (269); the draw ratio is as follows:

1—9; 2—8; 3—5; 4—original sample.

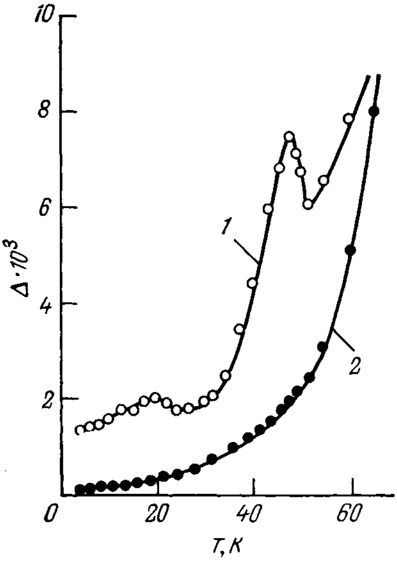

FIG. 6.3. Increase in the logarithmic decrement during the δ- and ε-relaxation processes in unoriented samples of linear polyethylene as a result of annealing in the clamped state (269):

1—sample subjected to annealing with its ends rigidly clamped; 2—sample annealed in the free, unclamped state.

The hypothesis of the presence in the lattice of defects in the form of kink-isomers was advanced by Reneker (294) and later modified by Clark (295) and Pechhold (288). The existence of these types of defects in the ordered regions of various linear polymers has been confirmed theoretically by de Santis *et al.* (296) and experimentally by Brown (297) and Koenig and Boerio (298).

The effect of the thermal history on relaxation processes in linear polyethylene at low temperatures is illustrated in Fig. 6.4. This figure shows schematically the units of polymeric chains which form the lattice, in which there are "bound" as well as "free" defects and also edge dislocations. We know that the annealing of oriented polymers in the free state (with unclamped ends) at temperatures T lower than the melting temperatures leads to an increase in the folding period and makes the crystal lattice more perfect. With such annealing the intensity of the δ_{cr}- and ε-maxima is reduced, which confirms the validity of the model under consideration. Indeed, the annealing of a crystalline polymer in the free state brings about a decrease in the number of dislocations and kink-defects per unit volume of the polymer. This reduces the height of the δ_{cr}- and ε-peaks of tan δ and leads to their complete degeneration for samples of linear polyethylene annealed in the free state (269).

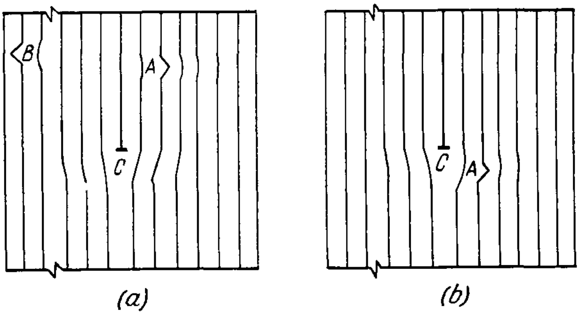

FIG. 6.4. Schematic representation of a model which takes account of the interaction of dislocations with conformational kink-defects and which has been proposed as an explanation of the low-temperature δ- and ε-relaxation in linear polyethylene, polyformaldehyde, and polyethylene terephthalate (269) before annealing (*a*) and after annealing (*b*). A, B, and C are, respectively, a bound kink-defect, a free kink-defect, and an edge dislocation.

The annealing of samples with clamped ends also leads to an increase in the ordering of the lattice. The improvement of the lattice is associated in this case with the motion of free kink-defects situated far from a dislocation (a defect of type B in Fig. 6.4). Besides, it is quite probable that with the annealing of stressed samples with clamped ends the dislocations are immobilized under the influence of stresses caused by the clamped ends. The energy of the distorted lattice, produced by the presence of defects, induces in this case the migration of the "bound" kink-defects (a defect of type A in Fig. 6.4) into the expansion regions located beneath the dislocations. Such thermoelastic aging processes in metals are well known.

Investigations carried out by means of X-ray structural analysis show (269) that kinks really can lead to a local expansion of the lattice. The migration of kinks to dislocations results in an increase in the total volume, which makes the dislocation jogs more mobile. As a result, the intensity of the relaxation peaks is increased at low temperatures. In this way one can explain the increase in the intensity of the δ_{cr}- and ε-peaks in polyethylene brought about by cold extrusion or rolling. Obviously, these two processes must lead to an increase in the dislocation density.

Polytetrafluoroethylene. The dynamic mechanical properties of this polymer have been studied by many investigators and described in detail in monographs (70, 163). The polymer has been investigated most thoroughly by McCrum (299), who measured the components of the complex shear modulus at a frequency of about 1 Hz in the temperature range 4.2 to 600 K and detected several peaks in the temperature dependence of the logarithmic decrement. The lowest-temperature loss maximum at —97°C is most prominent (Fig. 6.5). The intensity of this peak diminishes with increasing degree of crystallinity and, according to the data obtained by McCrum, is equal to 75.2 kJ/mole. No loss peaks have been detected in polytetrafluoroethylene at lower temperatures, but a slight increase in the dynamic shear modulus is observed with decreasing temperature.

Apart from the low-temperature peak, McCrum observed loss maxima at 18-29 and 127°C. He conjectured that the temperature transition observed in the form of the loss peak at 127°C is connected with the glass-transition of the amorphous regions of polytetrafluoroethylene.

It has been shown recently (70, 300) that the glass-transition temperature of polytetrafluoroethylene is in fact much lower (—110°C) (70) and that the transition observed near 130°C results from the unfreezing of the micro-Brownian motion in directions perpendicular to the chain axes (300-302). Thus, the temperature transition observed near 130°C is characterized by the appearance of molecular mobility in the paracrystalline phase. The thermophysical measurements carried out by Ohzawa and Wada (302) show that the content of the paracrystalline phase in polytetrafluoroethylene may exceed the content of amorphous regions.

It has also been found recently (70, 300) that in polytetrafluoroethylene at low temperatures (from —120 to —70°C) there exist two temperature transitions of the relaxation type, one associated with γ-relaxation (the motion of several CF_2 groups) and the other with the glass transition of the amorphous regions. It is interesting that in the lowest-frequency measurements ($\nu \approx 1$ Hz) only one intense loss peak is observed, resulting evidently from the superposition of two relaxation maxima, while in higher-frequency measurements (100-200 Hz) these two loss peaks can sometimes be resolved.

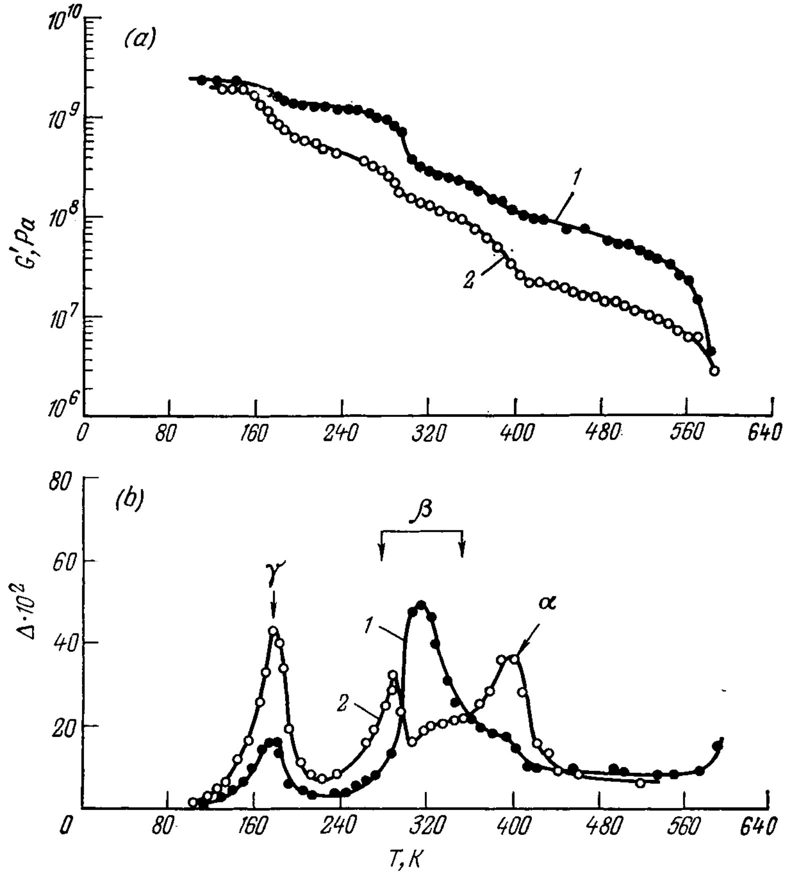

FIG. 6.5. Temperature dependence of the dynamic shear modulus (*a*) and the logarithmic decrement (*b*) for polytetrafluoroethylene at $\nu \approx 1$ Hz, the degree of crystallinity being 76 per cent (*1*) and 48 per cent (*2*) (163).

Polyformaldehyde. The dynamic mechanical properties of polyformaldehyde have been examined by many authors. A detailed review of these works is given in monographs by Perepechko (70) and by McCrum, Read and Williams (163). The temperature dependence of the logarithmic decrement at frequencies of about 1 Hz usually show three loss maxima located at 400 K (α), 260 K (β), and 205 K (γ). The highest-temperature α-peak, observed in polyformaldehyde at 400 K, is associated with the mobility in the crystalline regions and is probably due to the re-orientational rotation of folds in the crystals (α_{cr}-relaxation). It is commonly believed (70) that the most intense γ-peak (Fig. 6.6) is associated with the unfreezing of segmental motion in polyformaldehyde, which results from the transition of the amorphous regions from the glassy to the rubbery state. Read and Williams (303) also ascribe this peak to the transition from the glassy to the rubbery state.

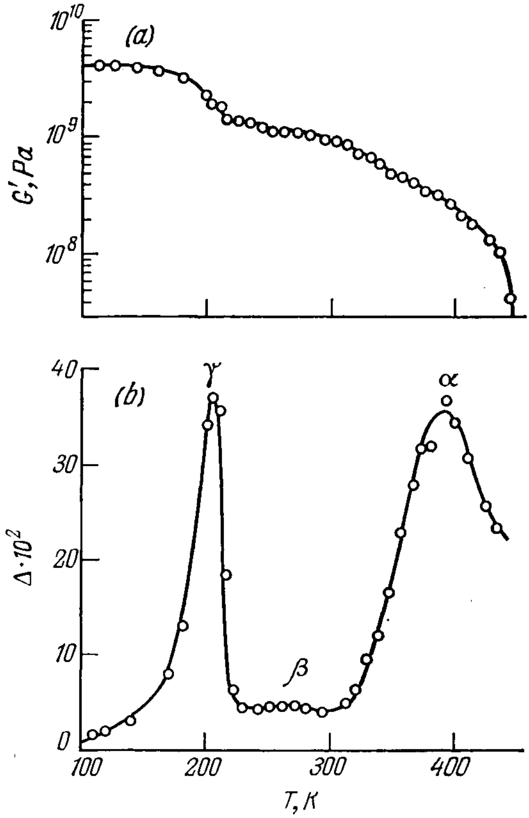

FIG. 6.6. Temperature dependence of the dynamic shear modulus (*a*) and the logarithmic decrement (*b*) for polyformaldehyde at $\nu \approx 1$ Hz (163).

The same conclusion can be drawn from investigations of polyformaldehyde by the NMR method (304) and dielectric spectroscopy (163, 305). Bohn (306) and Miki and his coworkers (307) believe, however, that the most intense low-temperature peak in polyformaldehyde is due to the local modes of molecular motion, say, the damping of the torsional vibrations of the main chains. Some authors believe (306) that the "rudimentary residue" of the glass-transition process is the weak β-peak sometimes detected in the temperature range —20 to +50°C (depending on the frequency). The available experimental data, however, allow one to conclude that the glass-transition temperature of the amorphous layer of polyformaldehyde is situated at a temperature not exceeding 195 K (70).

The dynamic mechanical properties of polyformaldehyde have mostly been studied at temperatures ranging from the liquid-nitrogen to the melting temperature. But in 1971 Papir and Baer (308) studied the dynamic mechanical properties of polyformaldehyde of the type Delrin-500 (molecular mass 40,000) down to the liquid-helium temperature. As a result of this investigation, which was carried out by means of a torsion pendulum at 1-3 Hz, two new loss peaks were detected, one located at 48 K (the δ_{cr}-peak) and the other below 4.2 K (the ε-peak). It was found that as the degree of crystallinity increases the intensity of the δ_{cr}-peak is substantially increased. For example, when the density of polyformaldehyde changes from 1.403 to 1.440 Mg/m^3, the height of the δ_{cr}-peak increases three-fold. The total loss level increases by the same amount at temperatures below 30 K (Fig. 6.7).

The orientation brought about by rolling polyformaldehyde gives rise to the same effect. For example, for a sample of polyformaldehyde extended by 70 per cent as a result of rolling the mechanical losses are three times greater than for the unrolled material (Fig. 6.8). The δ_{cr}-peak increases by the same amount if an unoriented sample of polyformaldehyde is annealed in the clamped state (with the ends being rigidly clamped). The magnitude of the δ_{cr}-peak in polyformaldehyde also increases when oriented samples with clamped ends are annealed. But if oriented samples of polyformaldehyde are annealed in a free, unclamped state, the height of the δ_{cr}-peak and the total level of mechanical losses are diminished. The viscoelastic behaviour of polyformaldehyde has been found to exhibit anisotropy (308). It has been established that while for samples cut from an oriented sheet plate of polyformaldehyde at angles 0 and 90° to the direction of the orientation axis the mechanical losses are the same, for those cut at an angle of 45° the intensity of the δ_{cr}-peak and the dynamic shear modulus is much higher.

It is supposed (308) that, as in the case of polyethylene, in polyformaldehyde the low-temperature loss maxima are of the same nature, being associated with the existence of kink-isomers and dislocations in these polymers. This is evidenced by the strong dependence of these peaks on the conditions of cold working (extrusion, rolling) and annealing and also by the anisotropy of the dynamic mechanical properties.

It seems natural to assume that the mechanism of low-temperature relaxation in polyformaldehyde has something in common with Bordoni peaks in metals. Indeed, the height of Bordoni peaks depends on the conditions of cold working and subsequent heat treatment. The activation energy for Bordoni peaks is comparable with that for the δ_{cr}-peak in polyformaldehyde (12.5-16.7 kJ/mole).

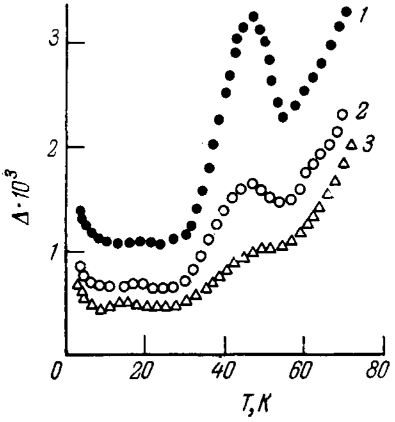

FIG. 6.7. Temperature dependence of the logarithmic decrement for the δ- and ε-relaxation processes in polyformaldehyde (308) with a high (*1*), an average (*2*), and a low (*3*) degree of crystallinity.

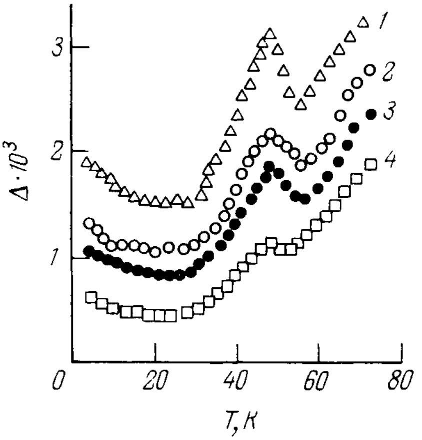

FIG. 6.8. Temperature dependence of the logarithmic decrement for the δ- and ε-relaxation processes in polyformaldehyde subjected to cold rolling in one direction (308); the draw ratio is as follows:

1—75 per cent; *2*—50 per cent; *3*—30 per cent; *4*—original sample. The rotation axis of the specimen on the torsion pendulum is parallel to the direction of rolling.

The main difference between these phenomena lies in the character of the dependence of the relaxation intensity on the concentration of point defects in the lattice. While the height of the δ_{cr}- and ε-peaks increases with increasing concentration of defects (308), the intensity of Bordoni peaks is decreased under the same conditions. Nonetheless, a mechanism analogous to that proposed for the explanation of Bordoni peaks (309, 310) can be used to account for the effect of orientation and crystallization on the intensity of δ_{cr}- and ε-relaxations in polyformaldehyde.

The supposed mechanism in these processes is connected with the interaction of dislocations and conformational kink-defects under the action of the externally applied stress. It is assumed that at low temperatures the dislocations are fixed, only some chain segments between the neighbouring pinning points being mobile. In constructing the model proposed by Papir and Baer (308) it was assumed that the intensity of the low-temperature relaxation process must increase with increasing dislocation density or concentration of kink-defects. The mechanism of this phenomenon is the same as in the case of polyethylene. It is likewise assumed that each point defect (kink-isomer) that arises under the action of the stress field in the lattice interacts with edge dislocations. If the defect is capable of migrating to a dislocation, the energy of the distorted lattice diminishes. The migrating defects move into the local-expansion region situated beneath the dislocation.

In the case of Bordoni peaks in metals the migration of point defects to dislocations leads to the fixing and damping of the latter. In polymers, conformational kinks lead to the expansion of the surrounding lattice regions, and the migration of kinks to dislocations increases the local volume, which is necessary for the motion of dislocation jogs. This in turn leads to an increase in the intensity or relaxation peaks. It is natural that the migration of kinks to dislocations is possible only under certain conditions. Such a model enables one to account for the effect of annealing and cold extrusion or rolling on the intensity of the δ_{cr}- and ε-peaks in crystalline polymers. The increase in the height of these peaks with increasing degree of crystallinity in polyformaldehyde can also be explained within the framework of this model. In this case, at relatively low rates of crystallization not only the concentration of kinks increases but these defects migrate to positions corresponding to the energy minimum, i.e., to the regions situated beneath the dislocation.

Attempts have been made to use the dislocation model (308) to account for the mechanism of γ-relaxation in polyformaldehyde. For instance, Papir and Baer resolved graphically the asymmetric γ-peak in polyformaldehyde into three maxima situated at 140 K (γ_1), 180 K (γ_2) and 205 K (γ_3). It is supposed that the cause of γ_1- and γ_2-relaxations is that with rise in temperature the breakaway motion of dislocations from minor pinning points becomes possible and the conditions are created for the motion of larger segments of dislocations. Another explanation also exists (70) for the mechanism of multiplet temperature transitions in the region of γ-relaxation.

The low-temperature loss peaks, which are probably due to the interaction between dislocations and kinks, have been detected in polyethylene terephthalate (268). In this polymer the δ_{cr}-peak at 46 K is observed only in uniaxially oriented samples and the ε-peak (at 26 K) in crystallized samples. The activation energy of these processes is almost the same, being equal to 16.7 kJ/mole.

It is possible to outline some of the features of δ_{cr}-relaxations common to a number of linear crystalline polymers (270). In completely amorphous samples (for example, in amorphous polyethylene terephthalate) and in polymers rapidly quenched from the melt (polyethylene, polyoxymethylene) no δ_{cr}-relaxation takes place. Relaxations of the δ_{cr} type are observed in rolled or stretched samples, and their intensity increases with increasing deformation of the polymer.

The intensity of the δ_{cr}-peak invariably depends on the thermal history of the polymer. The height of the δ_{cr}-peak increases in oriented samples annealed in the stressed state (with the size of the sample being fixed) but it diminishes in oriented samples annealed in the free state. In isotropic quenched samples the δ_{cr}-relaxation arises if the ends of the samples are rigidly clamped during heat treatment. If such samples are annealed in the unclamped free state, no δ_{cr}-peak is present.

For all polymers the temperature of the δ_{cr}-peak is independent of the deformation. The δ_{cr}-relaxation in linear crystalline polymers exhibits strong anisotropy. Samples in which the angle between the axis of torsion (on a torsion pendulum) and the direction of orientation is 45° display a stronger δ_{cr}-peak and a greater dynamic shear modulus than do samples with $\beta = 0°$ and $\beta = 90°$.

Apart from the principal δ_{cr}-peak at 45-50 K, another secondary transition is detected at lower temperatures in some polymers, this transition depending, like the δ_{cr}-peak, on the orientation and heat treatment.

The activation energy of the δ_{cr}-peak evidently does not exceed 16.7 kJ/mole.

This relaxation process cannot be characterized by a single relaxation time. The width of the δ_{cr}-peak is much larger than one would expect from the theory dealing with a single relaxation time.

The most probable mechanism for the δ_{cr}-relaxation is the thermally activated motion of dislocation jogs under the action of the applied stress. The dislocation mechanism of the low-temperature relaxation has been discussed in detail by Hiltner and Baer (270).

Polycapramide. The dynamic mechanical properties of this polymer have been the subject of many investigations. A review of these works can be found in monographs by Perepechko (70) and by McCrum, Read and Williams (163).

Usually, three loss maxima are observed in polycapramide at low frequencies: the α-peak near 60°C, attributed to the micro-Brownian segmental motion; the β-peak near 230 K, usually ascribed to the movement of kinetic units containing amide groups; the γ-peak near 120 K, which is linked with the motion of the aliphatic segments of the chains. The positions of these relaxation maxima depend largely on the degree of crystallinity, the moisture content (311, 312) and the content of low-molecular-mass fractions in the polymer, and also on the frequency at which measurements are carried out.

It has long been believed that no relaxation processes occur in polycapramide below the liquid-nitrogen temperature. It has been found, however, that as the temperature is lowered from 77 K to 4.2 K the elastic moduli of polyamides monotonically increase, changing by no more than 10 per cent, while at the liquid-helium temperature they attain levels ranging from 10^3 to 10^4 MPa. On the basis of such an increase in the elastic modulus one could suppose that in polyamides even in the helium-temperature region there may persist relaxation processes that make a noticeable contribution to the viscoelastic properties. A study of polycapramide carried out in recent years (313) in the temperature range 4.2 to 300 K by the free torsional vibration method has led to the discovery of three, hitherto unknown loss peaks near the liquid-helium temperature. Apart from the maxima in the temperature dependence of the logarithmic decrement situated at 350 K (the α-peak), 230 K (the β-peak) and 120 K (the γ-peak), new loss peaks at 53 K (the δ-peak) and at 20 K (the ξ-peak) have been detected; the existence of an ε-peak below 4.2 K is also suspected. The temperature and intensity of the new maxima depend very much on the degree of orientation, anisotropy and the content of absorbed moisture.

It is believed (313) that the δ-relaxation cannot be caused by the motion of defects in the crystalline regions, as is the case with polyethylene, polyformaldehyde, and polyethylene terephthalate, since the height of the δ-peak in polycapramide diminishes with increasing orientation. According to Papir, Kapur and Rogers (313), this effect is associated with the motion of defects in the amorphous regions of the polymer. An increase in the ordering of the amorphous layer due to orientation leads to a decrease in the intensity of the δ-peak. Since the ξ-peak is observed only in polycapramide samples with a considerable moisture content, it is assumed to be associated with mobility in ice aggregates in the amorphous regions.

Polypropylene. The relaxation processes in polypropylene have been studied by many investigators (163, 316). The temperature dependence of the logarithmic decrement usually shows (315) three loss peaks situated at —70°C (γ), near 0°C (β), and near 100°C (α). The nature of the α-relaxation peak is not yet clear. The most intense β-peak is attributed to the unfreezing of segmental motion in the amorphous regions of polypropylene. Its intensity decreases considerably with increasing degree of crystallinity.

The apparent activation energy of this relaxation process is 167 kJ/mole. The weak γ-peak is usually attributed to the torsional vibrations of a small number of CH_3, CH and CH_2 groups in the amorphous regions (314). The activation energy corresponding to this relaxation process is 54.3 kJ/mole.

The study of the dynamic mechanical properties of polypropylene at very low temperatures yields contradictory results (290, 317, 318). Sinnott (317), while studying the viscoelastic behaviour of polypropylene on a torsion pendulum at helium temperatures, came to the conclusion that there exist two loss maxima, one at 19 K (6 Hz) and the other at 53 K (7 Hz). The results of later investigations (290) carried out at a frequency of about 10^4 Hz are presented in Fig. 6.9. It was found that in polypropylene in the temperature range 10 to 30 K (10 kHz) a blurred maximum with a flat top is observed. Prolonged annealing of isotactic polypropylene leads to a decrease in this peak of 20 per cent and an increase in the elastic modulus of 10 per cent. The loss maximum detected by Sinnott at 53 K in a polypropylene sample with a degree of crystallinity of 75 per cent could not be found by Crissman *et al.* (290), either at this or other higher temperatures in either unannealed or annealed samples.

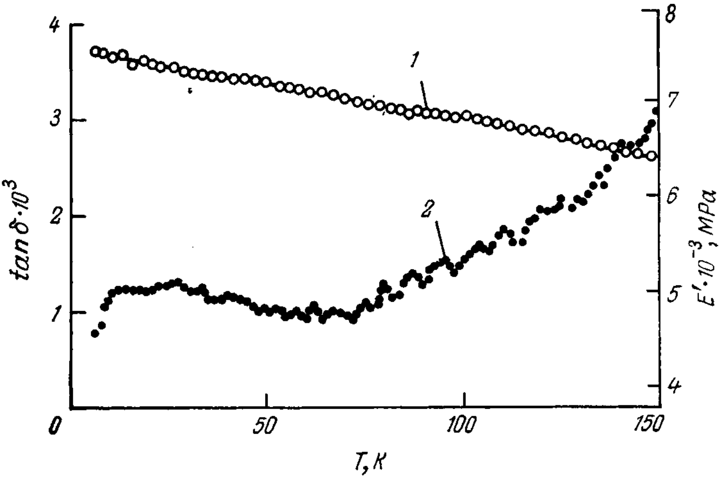

FIG. 6.9. Temperature dependence of Young's modulus (*1*) and of the loss tangent (*2*) for polypropylene at ν ≈ 10^4 Hz (290).

The low-temperature loss peaks in polypropylene were attributed by Sinnott (317) to the hindered rotation of the methyl groups. This interpretation, however, does not agree with the results of investigations carried out by the NMR method (319). Until recently the true cause of the appearance of low-temperature loss peaks in polypropylene was not clear.

Polymethyl Methacrylate. Many works have been devoted to the study of the dynamic mechanical properties of polymethyl methacrylate at temperatures close to the liquid-helium temperature (265, 290, 314). Crissman *et al.* (290) and Woodward (320) observed, at a frequency of about 10^4 Hz, a small loss maximum at a temperature of 5 K (Fig. 6.10). This had been predicted earlier by Sinnott (184, 317), who had carried out measurements at low frequencies. This loss maximum, according to Sinnott, is due to the motion of the ester methyl groups.

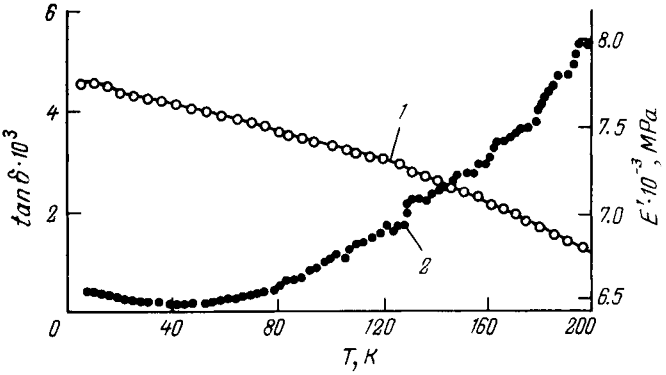

FIG. 6.10. Temperature dependence of E' (*1*) and $\tan\delta$ (*2*) for polymethyl methacrylate at $\nu \approx 10^4$ Hz (290).

One of the causes of the appearance of a loss peak at such low temperatures is probably the presence of impurities. This was pointed out by Woodward (320), who detected maxima at 40 and 150 K when studying commercial samples of polymethyl methacrylate. Gall and McCrum (321) have found that wetted samples of this polymer exhibit maxima at 190 K ($\nu = 1$ Hz). Purified samples of polymethyl methacrylate do not display such peaks; their presence in commercial samples mask relaxation processes that occur in a pure sample at very low temperatures.

Extensive studies of polymethyl methacrylate carried out by the NMR method allow one to conclude that the lowest-temperature loss peaks in this polymer are associated with the re-orientational motion of the methyl groups. Data on the activation energy corresponding to this motion of the methyl groups are not usually quoted, since the low-temperature maximum in dynamic mechanical measurements is not completely resolved and, besides, a difference of opinions exists concerning the exact position of the minimum of the spin-lattice relaxation time in investigations by the NMR method.

It is, however, known (265) that the activation energy of the rotation of the methyl groups in polymethyl methacrylate at the lowest temperatures is 1.7-14.6 kJ/mole. It is supposed that the motion of the α-methyl groups in polymethyl methacrylate is hindered more strongly than is the motion of the CH_3 groups in the ester grouping. Obviously, the mobility of the methyl groups responsible for relaxation processes in the region of super-low temperatures cannot be regarded as classical rotation about the C_3 axis, since calculations (327) show that this rotation is impossible even at temperatures $T < 40$ K. At such temperatures the height of the barrier to rotation of the methyl groups is greater than 8.36 kJ/mole, while the energy of CH_3 groups is much lower. Nonetheless, as has been shown by Stejskal and Gutowsky (251), in this temperature range a re-orientational quantum-mechanical tunnelling of the methyl groups through the potential barrier that hinders their rotation about the C_3 axis of symmetry is possible. The quantum-mechanical tunnelling of CH_3 groups may be responsible for the viscoelastic relaxation at temperatures close to 4.2 K in such polymers as polymethyl methacrylate and polypropylene.

The problem of the viscoelastic behaviour of polymethyl methacrylate at higher temperatures has been examined in detail (70, 163, 314).

Poly-4-Methyl Pentene-1. This polymer has a property unusual among polymers: the density (measured at room temperature) of an amorphous sample exceeds the density of a highly crystalline sample. X-ray (323, 324) and dilatometric (182) measurements show that the density of crystals of poly-4-methyl pentene-1 varies within the limits of 0.81-0.83 Mg/m^3, while the density of the amorphous layer is 0.838 Mg/m^3.

The study of the dynamic mechanical properties of poly-4-methyl pentene-1 at low temperatures (182, 265, 290, 325) has made it possible to detect the presence of loss maxima below the liquid-nitrogen temperature. The change in the dynamic elastic modulus of poly-4-methyl pentene-1 over the temperature range 4.2 to 77 K is about 20 per cent, which points to the existence in this polymer at helium temperatures of quite an intense relaxation process.

Indeed, Crissman *et al.* (290) and Woodward (318), while measuring the dynamic mechanical properties of poly-4-methyl pentene-1 at a frequency of 10 kHz, detected a small maximum of $\tan \delta$ at 25 K (Fig. 6.11). They ascribed the appearance of this maximum to the re-orientation of the methyl groups present in the side chains of the polymer. Later, Frosini and Woodward (325), while carrying out measurements on a torsion pendulum, observed the same peak at 10 K and likewise attributed it to the vibrations of the CH_3 groups. The shift of this loss peak observed by Frosini and Woodward (325) towards lower temperatures is valid as compared with the results obtained by Crissman and his colleagues (290) since Frosini and Woodward made measurements at a lower

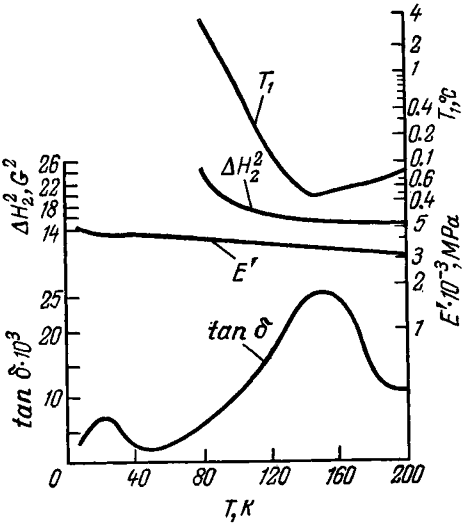

FIG. 6.11. Temperature dependence of E', tan δ, ΔH_2^2, and T_1 (the spin-lattice relaxation time) for poly-4-methyl pentene-1 (265).

frequency (2.9 Hz). In poly-4-methyl pentene-1 at higher temperatures there is another, more intense γ-peak observed at 120 K, in measurements conducted at 1 Hz and at 150 K (10^4 Hz). Such a shift of the loss maximum points to its relaxational nature.

The results of dynamic mechanical investigations are in good agreement with NMR data (265, 326), according to which the minimum of the spin-relaxation time is situated at temperatures near 150 K. There is no difference of opinions as to the nature of the relaxation process observed in poly-4-methyl pentene-1 at 150 K. It is believed that the factor responsible for its appearance is the rotation of both methyl groups in the side chains of this polymer.

The sharp increase in the second moment (see Fig. 6.11) observed at temperatures down to 77 K is noteworthy. The absence of experimental data at lower temperatures does not allow one to draw final conclusions; nevertheless, we may suppose that this increase of ΔH_2^2 at $T \rightarrow 0$ K must also occur at lower temperatures and that this effect is associated with the re-orientation of the methyl groups, which persists at temperatures much lower than 77 K.

6.3.1. THE MECHANISM OF VISCOELASTIC RELAXATION IN POLYMERS CONTAINING METHYL GROUPS

The mechanism of viscoelastic relaxation at low temperatures in polymers containing methyl groups has been examined in detail by Reich and Eisenberg (326, 327). They noted that on the basis of the concepts of classical physics it is impossible to account for the origin of the low-temperature loss maxima observed in the temperature range 5 to 60 K in polymers containing methyl groups. In fact, the appearance of these maxima is usually ascribed to the motion of methyl groups. Meanwhile, a simple calculation shows that the height of the barrier that hinders the rotation of methyl groups exceeds 8.36 kJ and that at temperatures below 40 K classical rotation cannot be the mechanism behind viscoelastic relaxation, since the relative fraction of methyl groups whose energy is enough for the potential barrier to be overcome is 10^{-11}.

Eisenberg and Reich (326, 327) presumed that the quantum-mechanical tunnelling of methyl groups relative to the C_3 axis is the principal relaxation mechanism at low temperatures for polymers containing methyl groups. The relationship between molecular processes and external excitation becomes most pronounced when the relaxation frequency is of the same order as the frequency of external excitation. The average tunnelling frequencies for CH_3 groups at low temperatures with barrier heights ranging from 9.89 to 33.35 kJ have been calculated by Stejskal and Gutowsky (251). An analysis of the results of their calculations (251) shows that at low temperatures there correspond to tunnelling frequencies of $5 \cdot 10^4$ Hz barrier heights of the order of 16.7-33.4 kJ. These values coincide in order of magnitude with the parameters of the uncorrelated motion of methyl groups in solids (250).

Proceeding from quantum-mechanical concepts, one can explain the main features of low-temperature loss peaks in polymers containing methyl groups. As has been shown by Stejskal and Gutowsky (251), at temperatures below 70 K the tunnelling frequency of CH_3 groups is practically independent of temperature. As a consequence, even at very low temperatures there are always some methyl groups capable of tunnelling. Since specific potential barrier heights correspond to tunnelling frequencies that coincide with the frequency of external excitation (the frequency of low-frequency acoustic vibrations at which measurements are made), then at the lowest temperatures tunnelling leads to a finite value of tan δ.

At first sight it seems unclear why tunnelling should lead to the appearance of loss maxima in the temperature dependence of tan δ. In order to account for this phenomenon, one should take into account the following factors. As pointed out above, methyl groups keep tunnelling down to very low temperatures. It is natural to presume that for real polymeric materials there is a distribution of potential barrier heights which can be attributed, apart from other factors, to the environment of each methyl group. Near 0 K only a small number of methyl groups are capable of tunnelling through the potential barrier at a frequency exactly coinciding with the frequency of external excitation. With a rise in temperature the structure of the polymer becomes more loose and an ever increasing number of methyl groups become capable of interacting with external excitation over a short time interval. Thus, the increase in tan δ with temperature increasing from 0 K becomes understandable.

With a further rise of temperature an ever increasing number of methyl groups assume an excited torsional state and the tunnelling frequencies begin to increase. As a result, the connection between tunnelling and external excitation is weakened and tan δ decreases. Thus, the appearance of low-temperature tan δ peaks in polymers containing methyl groups is the result of the competition of two processes: the increase in the number of tunnelling groups and the decrease in the connection between tunnelling and external excitation, which is caused by an increase in the tunnelling frequency.

An essential point here is that tunnelling is not an activation process and it is pointless to determine the apparent activation energy from a $\log \nu = f(1/T)$ plot.

The height of the potential barrier hindering the rotation of CH_3 groups depends on how these groups are attached to the main chain (326, 327). If the methyl groups are linked directly to the main chain (polypropylene, the α-methyl group in polymethyl methacrylate), the barrier height is 29-34 kJ. The presence of the C—O bond lowers the barrier height to 17 kJ (poly-4-methyl pentene-1, the ester methyl group in polymethyl methacrylate).

At sufficiently high temperatures, tunnelling motion and classical rotation may overlap. For example, if the height of the potential barrier is 13 kJ, both processes overlap at $T > 170$ K. In this case, the interpretation of experimental data becomes highly uncertain.

Polystyrene. The dynamic mechanical properties of polystyrene at low temperatures have been studied very thoroughly. While the first investigations (328, 329) did not reveal any transitions other than glass-transition in polystyrene, in later works (318, 330) mention was more and more frequently made of the occurrence in this polymer of relaxation processes at low temperatures. For example, in the case of amorphous atactic polystyrene a loss maximum at 45 K at a frequency of 10 kHz (318) was detected.

An analogous peak was observed (330) in an uncrystallized isotactic sample and in the same sample after annealing, as a result of which the polymer became partly crystalline. The annealing of isotactic polystyrene does not alter the position of this low-temperature maximum in the temperature dependence of the loss modulus, but it does increase the elastic modulus by 10 per cent in the temperature range 4.2 to 150 K. These findings are in good agreement with the investigations carried out by Sinnott (317), who detected this transition at 38 K at a frequency of 5.6 Hz in a thoroughly purified sample of polystyrene.

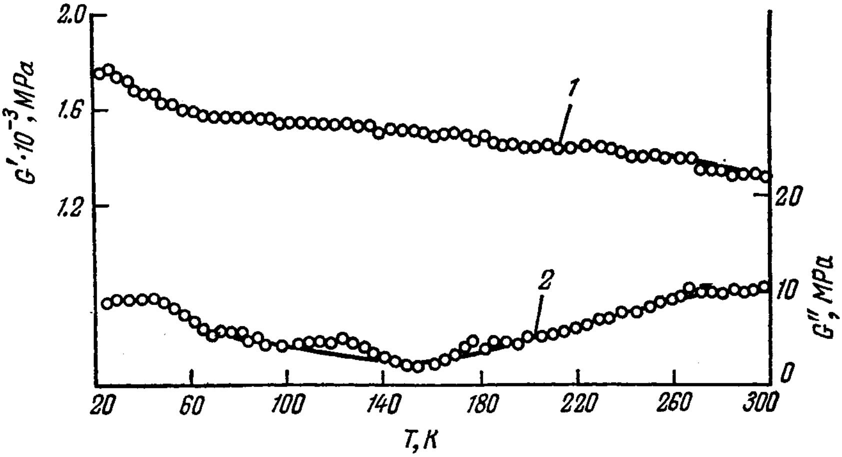

FIG. 6.12. Temperature dependence of G' (*1*) and G'' (*2*) for polystyrene at $\nu \approx 1$ Hz (331).

Chung and Sauer (331), while studying the secondary relaxation processes in polymers containing phenyl groups, detected this relaxation peak at 33 K at a frequency of 1.7 Hz (Fig. 6.12). The activation energy of the corresponding relaxation process is 9.6 kJ/mole. Similar results have been obtained by Frosini and Woodward (325), who, using a torsion pendulum, observed this peak with an activation energy of 8.4 kJ/mole at 35 K ($\nu =$ $= 2.9$ Hz). And, finally, Wada (332) observed the low-temperature δ-peak in polystyrene at 55 K ($\nu = 10$ kHz). The dielectric measurements for polystyrene carried out by McCammon and Saba (225) at 1 MHz revealed the presence of the δ-relaxation peak at

46 K as well. The activation energy calculated in this case was found to be equal to 13.8 kJ/mole.

The fact that this maximum has been detected in both dynamic mechanical and dielectric measurements is an indication of the common nature of mechanical and dielectric relaxations in polystyrene at low temperatures. Yano and Wada (332) ascribe this loss maximum to the defects in the chemical structure arising from the existence of syndiotactic fragments between the isotactic links. A theoretical approach to the solution of this problem shows that the δ-relaxation in polystyrene cannot be explained by rotation of the phenyl groups.

Frosini and Woodward pointed out (325) that the low-temperature loss maximum in polystyrene can be caused by the presence of impurities. They detected loss peaks in commercial samples of polystyrene at 23 K and 99 K ($\nu \approx 1$ Hz). It is most likely that impurities only shift the peaks typical of this polymer rather than cause the appearance of an additional loss maximum.

It should be pointed out that Rees (33), apart from the δ-peak at 55 K, detected a lower-temperature ε-peak at 25 K ($\nu = 10^4$ Hz), the nature of which is not yet clear.

Apart from the relaxation region which manifests itself in polystyrene at very low temperatures, several relaxation processes have been detected, which occur at temperatures below T_g. For example, Yano and Wada (332), using the results of measurements reduced to a frequency of 10 kHz, point out that below T_g in polystyrene one observes the β-peak (350 K), which they ascribe to the local vibrations of the main chains, and the γ-peak (180 K) which is assigned to the hindered rotation of the phenyl groups. The low-temperature relaxation maximum at 100 K (the γ′-peak) is observed only in dielectric measurements in block polystyrene and is caused, according to these authors, by the presence of polar (ester) groups which sometimes arise in the polystyrene chain as a result of this polymerization.

As the temperature is lowered and the molecular mobility is frozen the Young modulus and the shear modulus in polystyrene increase appreciably. When the temperature falls from 77 K to 4.2 K, the dynamic moduli of polystyrene increase by about 20 per cent (331). Such a large increase in the dynamic elastic moduli results from intense relaxation processes that occur in this polymer at low temperatures.

Polyvinyl Chloride. The dynamic mechanical properties of atactic polyvinyl chloride, which is practically an amorphous polymer, have been studied by many investigators (181,333-340). Schmieder and Wolf (181), using a torsion pendulum, found that there are two loss maxima for polyvinyl chloride: the principal maximum (α-relaxation) at 90°C and the secondary maximum (β-relaxation) at —30°C. The dynamic mechanical properties of polyvinyl chloride have been studied in detail by Perepechko (70), Pezzin and Pagliari (335) and Petersen and Ränby (337). Pezzin and Pagliari (335) have shown that the α-maximum in polyvinyl chloride lies near 90°C, but the authors could measure only the low-temperature branch of this peak. Using literature data and their experimental results, Pezzin and Pagliari constructed a $\log \nu_m = f(1/T)$ graph, from which they inferred that the apparent activation energy of the α-relaxation process in the temperature range 90 to 110°C remains nearly constant and equal to 334 kJ/mole, while at 75-80°C it is 840 kJ/mole. Thus, over the range 80-90°C there occurs a substantial change in the apparent activation energy. Since the glass-transition temperature of polyvinyl chloride is about 80°C, it is obvious that the α-relaxation is caused by the unfreezing of segmental mobility of the micro-Brownian type.

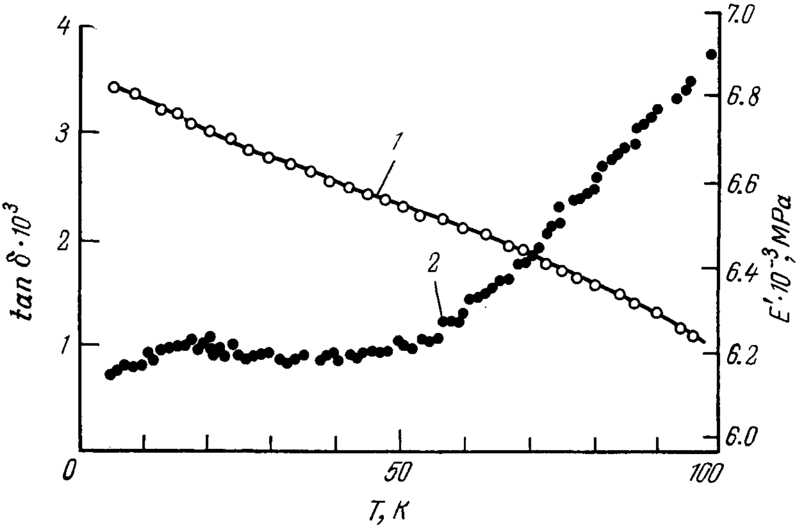

FIG. 6.13. Temperature dependence of tan δ and E' for polyvinyl chloride at $\nu \approx 10^4$ Hz (290).

The loss maximum corresponding to β-relaxation was observed (335) at —10°C at a frequency of 100 Hz and at +5°C (500 Hz). The activation energy determined from the $\log \nu_m = f(1/T_m)$ graph was found to be equal to 63 kJ/mole. The interpretation of this temperature transition remains controversial. Ishida (338) ascribes it to the vibration of dipolar C—Cl groups; Woodward and Sauer (341) attribute β-relaxation to the vibrations of small units of the main chain containing several carbon atoms.

The dynamic mechanical properties of polyvinyl chloride at lower temperatures have been investigated by Crissman, Sauer and Woodward (290) at frequencies of the order of 10^4 Hz. These authors observed a small loss maximum at 18 K ($\nu = 7225$ Hz) in the temperature dependence of tan δ (Fig. 6.13). The presence of a low-temperature plateau on the tan $\delta = f(T)$ graph in the temperature range 25-50 K was somewhat unexpected. The nature of this low-temperature loss peak in polyvinyl chloride is not yet clear.

The results of measurements of Young's modulus point to an almost linear dependence of this parameter on temperature, that is E' increases with decreasing temperature. At the lowest temperatures this increase in E' is not strong, which, according to Sauer and Saba (265), is an indication of the low intensity of relaxation processes in this temperature region.

CHAPTER 7

THE ACOUSTICAL PROPERTIES OF POLYMERS AT LOW TEMPERATURES

7.1. PROPAGATION OF ULTRASONIC WAVES IN DIELECTRICS

The propagation and absorption of ultrasonic waves in dielectrics at low temperatures depend, to a large extent, on the relationship between the ultrasonic wavelength and the mean free path of phonons. If the ultrasonic wavelength λ is small as compared with the mean free path of phonons, l, then the various phenomena attending the propagation of ultrasonic waves in a solid may be treated from the standpoint of the direct interaction between coherent (ultrasonic) and incoherent (thermal) phonons. Such an interaction has been discussed by Landau and Rumer (342). They have shown that the interaction between a coherent and a thermal phonon gives rise to a third phonon which acquires part of the energy of the sound wave. According to the Landau-Rumer theory, the damping of the ultrasonic wave caused by phonon processes becomes substantial only at $\lambda \ll l$, i.e., on the condition that $\omega\tau_N \gg 1$, where ω is the ultrasonic frequency and τ_N is the characteristic time of phonons, corresponding to "Normal" processes. In three-phonon processes of this kind the condition of conservation of pseudo-momentum must be fulfilled.

The Landau-Rumer theory, however, in fact describes phenomena that take place during the propagation of hypersonic waves at sufficiently low temperatures. In many cases, the mean free path of phonons, l, in dielectrics is so small that when use is made of the frequencies of the order of 10^6 to 10^8 Hz which are most frequently realized in experiments, the ultrasonic wavelength is found to be much larger than l. In this case, the condition $\lambda \gg l$ holds true and no direct interaction occurs between coherent and thermal phonons.

The absorption of ultrasound in a case where $\lambda \gg l$ has been examined in detail by Akheizer (343). He considered the most frequently encountered conditions in which the ultrasonic wavelength is much larger than the mean free path of phonons. According to Akheizer, in the absence of the sound field the number of Debye phonons in a particular state is determined by the Planck distribution function. Upon application of the sound field the distribution function is altered and is no longer Planckian. The sound field brings thermal phonons out of the state of equilibrium and then, through mutual interaction, they relax back to their equilibrium state. In this case, the absorption of sound is caused by the interaction of the sound field with the entire assembly of thermal phonons rather than by the interaction between separate coherent phonons and thermal phonons. Thus, in solids at both low and high temperatures there occurs a nonlinear interaction between the sound wave and thermal phonons, which may be accompanied by the dissipation of energy.

The idea put forward by Akheizer has been used to a certain extent by Woodruf and Ehrenreich (344), who treated the problem of the attenuation of sound at $\omega\tau < 1$. These authors also presume that an ultrasonic wave takes an assembly of thermal phonons out of the equilibrium state, after which, as a result of collisions, the energy is redistributed among the thermal phonons. The upset of the equilibrium state is considered to result from the modulation of the frequencies of all thermal phonons by the ultrasonic wave. The solution of the linearized Boltzmann equation gives the following expression for the ultrasound absorption coefficient:

$$\alpha = \frac{C_v T \overline{\gamma}^2 \omega^2 \tau}{3\rho c^3} \tag{7.1}$$

where C_v is the specific heat at constant volume; T is the temperature; $\overline{\gamma}$ is the averaged value of the Grüneisen constant; ρ is the density; c is the velocity of sound.

It should be remarked that the dispersion and absorption of sound in solid dielectrics are governed by heat conduction as well as by a change in the distribution of phonons. At high temperatures both factors play the same role. At low temperatures, however, the effect of heat conduction can be decisive.

Gurevich and Efros (345) attempted to take into account the effect of thermal conduction on the absorption and velocity of sound in dielectrics. They tried to take account of the effect not only of "Normal" processes, in which the phononic pseudo-momentum is retained, but also of "Umklapp" processes, which take place when the law of conservation of pseudo-momentum is violated. In this case, by "Umklapp" processes were meant not only flip-over processes proper but any processes involving the scattering of phonons by lattice defects. Gurevich and Efros quite correctly pointed out that in order to describe the process of distribution of sound waves in dielectrics it is not enough to use expression (1.86) for the heat flux density vector. Indeed, if the temperature gradient ∇T, which is a function of time, undergoes change in time $t \leqslant \tau_U$ (τ_U is the characteristic time of "Umklapp" processes), then it is obvious that the simple relation between q and ∇T of type (1.86) no longer holds. Under these conditions there occurs a time-dependent dispersion of the thermal conductivity tensor. Note that this effect was first theoretically discussed in the literature (346) in connection with the investigation of relaxation in gases and liquids.

The other problems associated with the propagation of ultrasound waves in dielectrics at low temperatures have been discussed in a number of works (347-354). Despite the fact that these works are concerned with phenomena which are important for an understanding of the propagation of ultrasound in all dielectrics (including polymers), they do not, strictly speaking, apply to polymeric materials, because they disregard viscoelastic properties of polymers.

7.2. THE PHENOMENOLOGICAL THEORY OF SOUND PROPAGATION IN POLYMERS

One possible way of describing the propagation of ultrasonic waves in a viscoelastic medium is based on the use of the theory of elasticity and of the basic concepts of the thermodynamics of irreversible processes (70).

Let us consider the propagation of a plane sound wave in a viscoelastic heat-conducting medium. Thermal conductivity is usually disregarded in the solution of problems of this kind. Thermal conductivity, however, is of vital importance when the propagation of ultrasonic waves in polymers at low temperatures is being discussed.

We choose, as the defining fundamental equations, the laws of conservation of mass, momentum, and energy, which can be given in the following form for a one-dimensional case:

$$\begin{gathered}
\frac{\partial \rho}{\partial t} + \rho\,\frac{\partial v_x}{\partial t} = 0 \\
\rho\,\frac{\partial^2 u_x}{\partial t^2} - \frac{\partial \sigma_{xx}}{\partial x} = 0 \qquad (7.2) \\
\rho C_v\,\frac{\partial T}{\partial t} - \frac{T\beta K_T}{\rho}\cdot\frac{\partial \rho}{\partial t} = -\frac{\partial q_x}{\partial x}
\end{gathered}$$

where $v_x = \dot{u}_x$ is the velocity of the particles of the medium; u is the displacement of points in the body on deformation; σ_{xx} is the diagonal term of the stress tensor; T is the temperature; C_v is the specific heat at constant volume; $\beta = (1/V)\,(\partial V/\partial T)_p$ is the thermal expansion coefficient (V is the specific volume); ρ is the density of the medium; $K_T = -V(dp/dV)_T$ is the isothermal bulk modulus; q_x is the component of the heat flux density vector $(\vec{q} = -\varkappa\nabla T)$.

In order to integrate the system of equations (7.2) one must find expressions for the stress tensor σ_{ik} and the heat flux density vector $\vec{q}$ which would take account of the propagation of ultrasonic waves in a viscoelastic medium.

The stress tensor in an isotropic viscoelastic medium can be written in the form:

$$\bar{\sigma}_{ik} = \sigma_{ik} + \sigma'_{ik} \tag{7.3}$$

where σ_{ik} is the stress tensor of an elastic solid; σ'_{ik} is the "dissipative" stress tensor.

It is known (353) that in an elastically deformed solid

$$\sigma_{ik} = \left(\frac{\partial F}{\partial u_{ik}}\right)_T \tag{7.4}$$

where F is the Helmholtz free energy of the deformed body; u_{ik} is the strain tensor.

Since the "dissipative" stress tensor has the same form as the viscous stress tensor for liquids, it follows that

$$\bar{\sigma}_{ik} = -K_T\,\beta(T - T_0)\,\delta_{ik} + 2G\left(u_{ik} - \frac{1}{3}\,\delta_{ik}u_{ll}\right) + \\ + K_T u_{ll}\delta_{ik} + 2\eta\left(\dot{u}_{ik} - \frac{1}{3}\,\delta_{ik}\dot{u}_{ll}\right) + \eta'\dot{u}_{ll}\delta_{ik} \tag{7.5}$$

where G is the shear modulus; $\eta = G\tau_1$ is the shear viscosity coefficient (τ_1 is the relaxation time); $\eta' = K_T\tau_2$ is the bulk viscosity coefficient (τ_2 is the relaxation time).

Expression (7.5) can be written in the following form:

$$\bar{\sigma} = -K_T\beta\,(T - T_0)\,\delta_{ik} + S + Z + S' + Z' \tag{7.6}$$

One might expect that, as a result of the rapidly changing gradients that arise during the propagation of a sound wave, the values of S', Z' and q would be different from the values of S'_0, Z'_0 and q_0, which correspond to the steady-state gradients. Assuming that the deviations of S', Z' and q from S'_0, Z'_0 and q_0 are not large, we can write the following response equations (70, 354):

$$\frac{\partial S'}{\partial t} = -\frac{1}{\tau_1}(S' - S'_0) \tag{7.7}$$

$$\frac{\partial Z'}{\partial t} = -\frac{1}{\tau_2}(Z' - Z'_0) \tag{7.8}$$

$$\frac{\partial q}{\partial t} = -\frac{1}{\tau_3}(q - q_0) \tag{7.9}$$

Having extended expressions (7.7), (7.8), and (7.9) to the case of an inhomogeneous material with an arbitrary number of relaxation processes, one can show (70) that

$$\bar{\sigma}_{xx} = -K_T\beta(T-T_0) + \hat{L}\frac{\partial u_x}{\partial x} \tag{7.10}$$

Here the operator $\hat{L}$ is given by

$$\hat{L} = \hat{K}_T + \frac{4}{3}\hat{G} \tag{7.11}$$

where

$$\hat{K}_T = K_T + \sum_{j=1}^{n} \frac{K_{Tj}\tau_{2j}\frac{\partial}{\partial t}}{1+\tau_{2j}\frac{\partial}{\partial t}} \tag{7.12}$$

$$\hat{G} = G_0 + \sum_{j=1}^{n} \frac{G_{0j}\tau_{1j}\frac{\partial}{\partial t}}{1+\tau_{2j}\frac{\partial}{\partial t}} \tag{7.13}$$

In an analogous way, for the case of periodic harmonic processes we obtain:

$$\vec{q} = -\Big(\sum_{j=1}^{n} \varkappa_{0j}/1 + i\omega\tau_{3j}\Big)\nabla T \tag{7.14}$$

Substituting expressions (7.10) and (7.14) into Eq. (7.2) and solving this system of equations, we can obtain (70) the following expression for the absorption coefficient and the velocity of propagation of a longitudinal sound wave in a viscoelastic medium:

$$c^2 = c_0^2\Big[1 + \frac{1}{\rho c_0^2}\Big\{\frac{4}{3}\sum_{j=1}^{n}\frac{G_{0j}\omega^2\tau_{1j}^2}{1+\omega^2\tau_1^2} + \sum_{j=1}^{n}\frac{K_{Tj}\omega^2\tau_{2j}^2}{1+\omega^2\tau_{2j}^2} + \sum_{j=1}^{n}\frac{\omega^2\tau_{3j}\chi_0\rho D}{1+\omega^2\tau_{3j}^2}\Big)\Big] \tag{7.15}$$

$$\frac{\alpha\lambda}{2\pi} = \frac{1}{2\rho c^2}\Big\{\frac{4}{3}\sum_{j=1}^{n}\frac{G_{0j}\omega\tau_{1j}}{1+\omega^2\tau_{1j}^2} + \sum_{j=1}^{n}\frac{K_{Tj}\omega\tau_{2j}}{1+\omega^2\tau_{2j}^2} + \rho D\sum_{j=1}^{n}\frac{\omega\chi_0}{1+\omega^2\tau_{3j}^3}\Big\} \tag{7.16}$$

Here χ_0 is the temperature conductivity coefficient given by

$$\chi_0 = \frac{\varkappa_0}{\rho c_v} \tag{7.17}$$

$$D = (c_0^2 - b_0^2)/c_0^2$$

where

$$b_0^2 = \frac{K_T + 4G_0/3}{\rho} \tag{7.18}$$

$$c_0^2 = \frac{K_s + 4G_0/3}{\rho} \tag{7.19}$$

(K_s is the adiabatic bulk modulus).

Passing to the continuous spectrum, we have:

$$\rho c^2 = \rho c_0^2 + \int_0^\infty \frac{H(\tau)\,\omega^2\tau^2}{1+\omega^2\tau^2}\,d\tau \tag{7.20}$$

$$\frac{\alpha\lambda}{2\pi} = \frac{1}{2\rho c^2} \int_0^\infty \frac{H(\tau)\,\omega\tau\,d\tau}{1+\omega^2\tau^2} \tag{7.21}$$

where $H(\tau) = \frac{4}{3}H_1(\tau) + H_2(\tau) + \rho D H_3(\tau)$, and each of the functions $H_1(\tau)$, $H_2(\tau)$, and $H_3(\tau)$ represents the relaxation-time spectrum density.

Thus, the use of the equations corresponding to the basic laws of conservation allows one to derive expressions for the absorption coefficient and the velocity of sound waves in viscoelastic heat-conducting media to which the majority of solid polymers belong.

It can be shown (70) that the application of the response equations to the components of the strain tensor yields the following expression for the velocity of sound:

$$\frac{1}{c^2} = \frac{1}{c_q^2} + \rho \int_0^\infty \frac{L(\tau)\,d\tau}{1+\omega^2\tau^2} \tag{7.22}$$

where c_q is the limiting (at $\omega\tau \to \infty$) frequency-independent value of the velocity of sound; $L(\tau)$ is the retardation-time spectrum density.

7.3. EXPERIMENTAL METHODS OF ACOUSTICAL MEASUREMENTS IN POLYMERS

The velocity of ultrasound in polymers at low temperatures is usually measured by the pulse method (70, 122, 356-358). Perepechko, Sorokin and Golub (122, 355, 356) used the buffer-rod method (70). These authors measured the velocity of ultrasound at helium temperatures using the pulse-phase method.

The block-diagram of the apparatus used for measuring ultrasound by the pulse-phase method (122, 356) is shown in Fig. 7.1. The videopulse is fed from the first channel of a two-channel generator *1* to the quartz transducer, which emits a packet of ultrasonic waves. The ultrasonic pulse passes through the first metal waveguide (a buffer rod), the test sample, and the second metal waveguide, and is then converted, in the second transducer, to an electric pulse. This electric pulse is fed, through an attenuator, to the input of a wide-band amplifier, is amplified and then travels to an electronic oscillograph with a triggered sweep. At the same time, a bell-shaped pulse, produced from the videopulse with the aid of a passive RLC circuit, is fed into the attenuator from the second channel of the generator; the amplitude and duration of such a comparison pulse are chosen so that they are equal to the amplitude and duration of the first half-wave of the sound pulse. This comparison pulse lags behind the probing pulse by a time interval equal to the transit time of the acoustic pulse and travels antiphase.

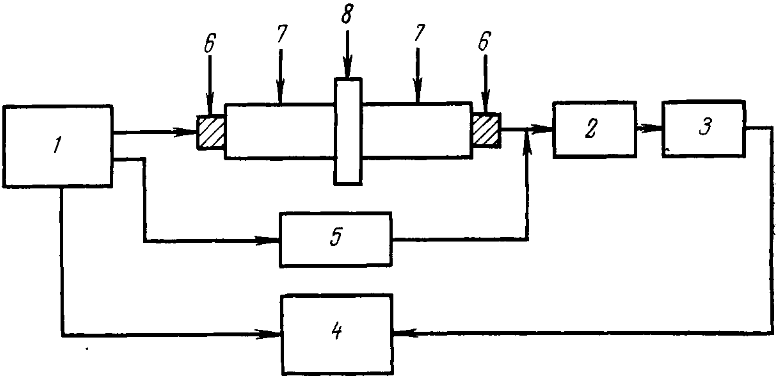

FIG. 7.1. Diagram of an apparatus for measuring ultrasonic velocity by the pulse-phase method (122):

1—two-channel pulse-generator; *2*—attenuator; *3*—wide-band amplifier; *4*—oscillograph; *5*—passive LC-circuit shunted by resistance *R*; *6*—piezoelectric transducers; *7*—buffer rods; *8*—sample.

When the comparison pulse and the first half-wave of the sound pulse are superimposed, a zero-line is clearly recorded on the screen of the oscillograph. Knowing the transit time of the sound pulse, $\Delta\tau$, which is read off on the scale of generator *1*, which has a calibrated time lag, and the length of the sample, *d*, one can easily find the velocity of the ultrasonic pulse in the test sample:

$$c = \frac{d}{\Delta\tau} \tag{7.23}$$

Since the sound pulse passes through the delay lines (buffer rods) and is delayed in them, it is necessary to take into account this delay. This is achieved by measuring the transit time of the pulse in the delay lines with the sample removed over the entire temperature range investigated. Then

$$\Delta\tau = \tau - \tau_0 \tag{7.24}$$

where τ is the total transit time of the sound pulse; τ_0 is the transit time of the same pulse in the delay lines without the sample.

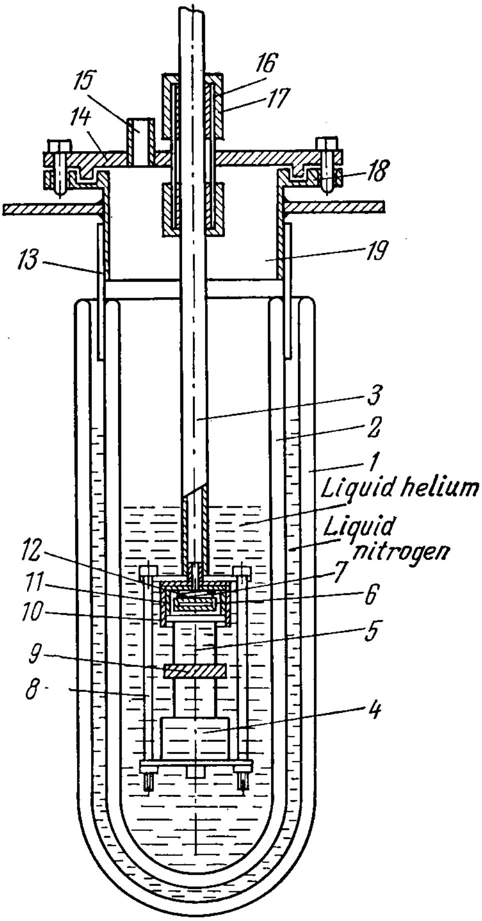

FIG. 7.2. Cryostat for measuring ultrasonic velocity in polymers at helium temperatures:

1—Dewar vessel filled with liquid nitrogen; *2*—Dewar vessel filled with liquid helium; *3*—thin-walled tube of stainless steel; *4*—quartz crystal holder; *5*—buffer rod; *6*—quartz crystal transducer; *7*—damper; *8*—pin; *9*—sample; *10*—quartz crystal holder casing; *11*—insulating bushing; *12*—spring; *13*—rubber sleeve; *14*—top flange; *15*—helium inlet; *16*—seal bushing; *17*—adapter nut; *18*—bottom flange; *19*—metal cylinder.

The sample to be tested is placed, together with the buffer rods, in a cryostat (355, 356) (Fig. 7.2), which consists of a Dewar vessel *1* filled with liquid nitrogen, inside which there is a Dewar vessel *2* filled with liquid helium. Inside Dewar vessel *2* there is a thin tube *3* of stainless steel. The lower end of this tube carries two quartz crystal holders *4* with buffer rods *5* made of stainless steel, the sample *9* being placed between the ends of the rods. In the tube are electrical cables and controlling and measuring thermocouples. The upper part of thin-walled tube *3* passes through a seal in a metallic cylinder which is hermetically connected with Dewar vessel *2* through a rubber coupling *13*.

The seal, which consists of an adapter nut *17* and a packing gland with a rubber bushing *16*, makes it possible to move the tube with the quartz crystal holders in the direction of the temperature gradient inside the Dewar vessel, thereby changing the temperature of the sample. The driving mechanism, placed in the upper part of the cryostat on a metallic cylinder *19*, consists of a reversible micromotor with a reduction gear, two guiding columns, a threaded rod rotated by the micromotor via the reduction gear, and a strip moving up and down along the thread of the rod. The strip in turn is rigidly connected with thin stainless-steel tube *3*, which makes it possible for the tube to move in the direction of the temperature gradient inside the liquid helium-filled Dewar vessel. This results in a change in the temperature of the sample.

The thermostatic control system (355, 356) is based on the principle suggested by Ponomarev (359), though used here for a wider temperature range. The thermostat system (Fig. 7.3) consists of a potentiometric circuit for measuring the temperature, a photocompensation amplifier, a power amplifier, and a mechanism used to move the measuring unit. A copper-constantan thermocouple is used as a temperature transducer for a temperature range of 4.2 to 240 K.

The temperature control is effected as follows (355, 356). A d.c. voltage corresponding to the e.m.f. of the thermocouple is set up in the d.c. potentiometer for the temperature at which the measurements are to be made. The photocompensation amplifier (see Fig. 7.3) amplifies the unbalance signal, which is then fed to the power amplifier, which has two relays at the output. These start the reversible motor and control the direction of rotation. Depending on the sign of the unbalance signal, one of the relays is closed and, accordingly, the motor moves the tube up or down, the upper part of the tube carrying a helium-filled Dewar vessel with two buffer rods with transducers and the test sample. When a copper-constantan thermocouple is used, the control system is able to maintain a constant temperature within the range 20-240 K with an accuracy of up to ±0.05 K and within the range 4.2-20 K with an accuracy of up to ±0.1 K.

The problem that arises in ultrasonic investigations of solids at low temperatures is to create a reliable acoustic contact between the piezoelectric transducer and the sample. This is especially important for substances with high linear expansion coefficients (polymeric materials are precisely such substances). As a result of the difference in the linear expansion coefficients of the piezoelectric transducer (10^{-7}) and the polymeric sample (10^{-5} to 10^{-6}),

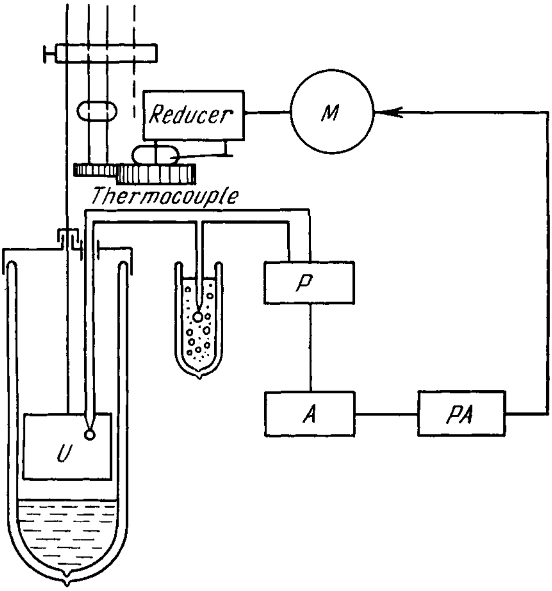

FIG. 7.3. Thermostat system for helium temperatures:

P—d.c. potentiometer; *A*—photocompensation amplifier; *PA*—power amplifier; *M*—reversible motor; *U*—unit for ultrasonic measurements.

large internal stresses appear in the contact layer as the temperature is lowered, which leads to the destruction of the transmitting layer and to the disappearance of the acoustic contact.

Stryukov and Shchegolev (360) proposed using an organosilicon oil of grade ГКЖ-94 as the contact layer for the investigation of metals. In ultrasonic investigations of solid plastics carried out at helium temperatures the use of this oil, however, does not produce the desired effect and the acoustic contact is broken at 130 K. Besides this organosilicon oil, other types of organosilicon liquids, organosilicon vaseline, epoxide resin, and Ramsay putty, were tested for this purpose. When these liquids and blends are used, the acoustic contact is broken at temperatures ranging from 120 to 170 K.

Finely ground raw talc with grade ГКЖ-94 oil as a binder in the ratio 2 : 1 by mass was found to be most suitable for the purpose (361, 362). The talc has a low coefficient of friction between its particles. Possibly, as the temperature is lowered and the polymeric sample is compressed, the talc particles slip over each other, the acoustic contact remaining intact.

An even better acoustic contact is produced if a finely ground boron nitride powder is used as the filler instead of talc (363, 364). It has been found that in the temperature range 2.1 to 260 K a reliable acoustic contact is produced and a steady transmission of ultrasound through the polymeric sample is provided, at least in the frequency range 1 to 10 MHz. Using various materials as the contact layer in ultrasonic investigations of polymers at very low temperatures has shown that the most suitable binder is organosilicon oil of grade ГКЖ-94, with many substances being suitable as additives. In general, many of the finely ground antifriction additives (363, 364) that are usually introduced into polymers to reduce friction can be employed with the ГКЖ-94 oil.

7.4. ULTRASONIC VELOCITY AND RELAXATION PROCESSES IN POLYMERS

The results of numerous experimental investigations carried out at low and very high (hypersonic) frequencies show (70, 365, 366) that the velocity of sound in polymers depends linearly on temperature and that only at those points where the mode of molecular motion is changed does the temperature coefficient of sound velocity change discontinuously. Thus, the unfreezing of this or that type of molecular motion can be judged from the kink in the temperature dependence of the velocity of sound.

Usually, temperature transitions of the relaxation type, detected from the kinks in the sound velocity vs. temperature curve are observed at lower temperatures than are the corresponding loss peaks. This is not surprising since the condition for the appearance of a maximum of $\tan \delta$ (or of the quantity $\alpha\lambda$, where α is the absorption coefficient and λ is the wavelength of the sound wave) is the equality $\omega\tau = 1$, this corresponding to the conditions under which the molecular motion is most intense. At the same time, the $c = f(T)$ graph (c is the velocity of ultrasound) shows a kink at a temperature above which the velocity of sound begins to decrease appreciably. This kink in the $c = f(T)$ graph corresponds to the conditions under which a given type of molecular motion begins to be unfrozen (the low-temperature start of the relaxation process). There must correspond to such a kink in the $c = f(T)$ curve the condition $\omega\tau = N$, where $N \gg 1$. It has been shown (70) that $N = 10^2$ to 10^3 for the glass-transition temperature of linear amorphous polymers, determined from a kink in the sound velocity vs. temperature curve.

If a temperature transition of the relaxation type is studied on the basis of a kink on the $c = f(T)$ graph at several frequencies, this transition shifts towards higher temperatures with increasing frequency. Assuming that $N = \text{const}$ for a given relaxation mechanism and the temperature dependence of the relaxation time is given by expression (4.41), one can calculate the activation energy from the formula

$$U = \frac{2.303\, RT_1T_2 \log(\omega_2/\omega_1)}{T_2 - T_1} \tag{7.25}$$

where U is the activation energy; R is the universal gas constant; T_1 and T_2 are the temperatures of transitions of the same type, measured from the kinks on the $c = f(T)$ graphs at frequencies corresponding to ω_1 and ω_2, respectively.

Numerous experimental data (70) show that the activation energies determined from the shift of temperature transitions observed on the $c = f(T)$ graph coincide, as the frequency is changed, with the U values found by ordinary methods (i.e., from the shift of tan δ peaks with changes in frequency).

Thus, when studying the temperature dependence of the velocity of ultrasound in polymers at several frequencies, one can obtain important information on the mechanism of relaxation processes.

The results of dynamic mechanical investigations, which were discussed in Chapter 6, show that loss maxima are observed for a number of polymers near the liquid-helium temperature and that for all polymers the dynamic elastic modulus increases as the temperature drops to 4.2 K. This is evidently an indication that relaxation processes can occur in polymers even at such low temperatures. This, however, refers to measurements carried out at frequencies not exceeding 10^4 Hz.

In this connection, it was interesting to try to "unfreeze" relaxation processes that can occur near 0 K by increasing the frequency of acoustic measurements by several orders of magnitude. A number of works which have recently been published are devoted to the study of the temperature dependence of the velocity of ultrasound in polymers at low temperatures and at frequencies of the order of 10^6 to 10^7 Hz.

It has been found that according to the results of ultrasonic investigations conducted at helium temperatures all the polymers studied can be divided into three groups.

(1) Linear crystalline polymers, such as polyethylene, polytetrafluoroethylene, a number of polyamides, polyvinylidene fluoride. The temperature dependence of the velocity of ultrasound for all these polymers shows a region (a low-temperature plateau) near 4.2 K (122, 355, 367) where the velocity of sound is

independent of temperature until the liquid-helium temperature is reached.

(2) Polymers containing methyl groups (polycarbonate, polypropylene, polymethyl methacrylate, poly-4-methyl pentene-1). The velocity of ultrasound in these polymers continuously increases up to 2.1-4.2 K. Besides, these polymers exhibit, even near 4.2 K, a noticeable dispersion of sound velocity. It will be shown below that there are sufficient grounds for believing that for all these polymers down to temperatures approaching 0 K the process of viscoelastic relaxation caused by quantum-mechanical tunnelling transitions associated with the re-orientation of methyl groups is still taking place.

(3) Polymers of the vinyl series, whose general chemical formula is $[-CR_2-CRR'-]_n$, where R = hydrogen or fluorine atom, R′ = chlorine or fluorine atom, or an aromatic ring. This group includes polymers such as polyvinyl fluoride, polyvinyl chloride, polytrifluorochloroethylene, polystyrene. Perhaps, the most common feature of polymers in this group is the presence of an asymmetric potential barrier which hinders the rotation of individual units. As with polymers of the second group, the velocity of ultrasound in these polymers increases as the temperature drops to 4.2 K.

7.5. ULTRASONIC VELOCITY AND RELAXATION PROCESSES IN LINEAR CRYSTALLINE POLYMERS AT HELIUM TEMPERATURES. THE LOW-TEMPERATURE PLATEAU

The results of the first ultrasonic investigations of polymers carried out near 4.2 K have revealed (355, 367) that for a number of linear polymers there exists a certain temperature T_{tr} below which the velocity of ultrasound is independent of temperature down to the lowest temperatures. Typical in this respect is the temperature dependence of the velocity of ultrasonic waves in polyethylene (Fig. 7.4). Apart from polyethylene, a low-temperature plateau near 4.2 K has been detected for polytetrafluoroethylene (122), polyformaldehyde (122), polyvinylidene fluoride, a number of polyamides (368), such as Nylon 6 (356), Nylon 7, Nylon 6,10 (polyamide 68), Nylon 11 and Nylon 12 (polyamide 12).

All polymers that show a low-temperature plateau are crystalline. The degree of crystallinity has a quite definite effect on the extent of the plateau and the temperature T_{tr}: as the crystallinity increases, so do the temperature T_{tr} and the extent of the plateau. For example, with polyethylene, as the crystallinity increases from 46 to 74 per cent the temperature T_{tr} measured at a frequency of 5 MHz for longitudinal waves increases from 100 to 120 K; in the case of polycapramide (Nylon 6), as the crystallinity changes from 34 to 46 per cent the temperature T_{tr} increases from 52 to 60 K.

An analogous low-temperature plateau near 4.2 K is observed in the temperature dependence of the velocity of shear waves.

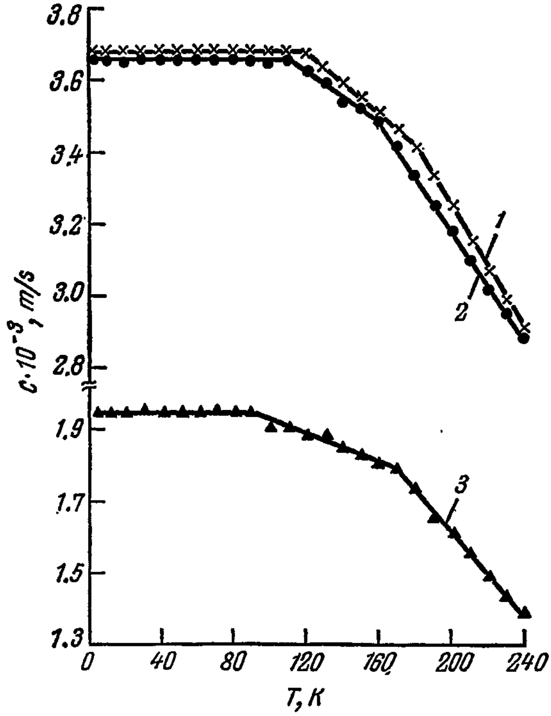

FIG. 7.4. Temperature dependence of the velocity of longitudinal and shear waves in low-pressure polyethylene:

1—longitudinal waves at $\nu = 5$ MHz; 2—longitudinal waves at $\nu = 1$ MHz; 3—shear waves at $\nu = 5$ MHz.

However, in the latter case the temperature T_{tr} (and the extent of the plateau) is lower than in the temperature dependence of the velocity of longitudinal ultrasonic waves. In both cases, T_{tr} depends on the frequency of the ultrasonic waves for which measurements are made: T_{tr} increases with increasing ultrasonic frequency. For instance, with high-density polyethylene when measurements are carried out at a frequency of 1 MHz the temperature T_{tr} is 110 K; at a frequency of 5 MHz it is equal to 120 K; for polycapramide T_{tr} is 54 K at a frequency of 1 MHz and 58 K at 5 MHz.

Another interesting feature has been observed (122, 356, 367, 368): in the low-temperature plateau region there is practically no dispersion of the velocity of ultrasound. At the same time, at temperatures higher than T_{tr} there is observed, as a rule, a dispersion of the ultrasound velocity.

Thus, we can conclude that the temperature T_{tr} is a certain characteristic temperature of a polymer, below which the relaxation spectrum of the polymer is completely unfrozen.

Indeed, we know (70) that the sound velocity in a polymer can be given as follows:

$$\frac{1}{c^2}=\frac{1}{c_q^2}+\rho\int\limits_0^\infty \frac{L(\tau)\,d\tau}{1+\omega^2\tau^2} \tag{7.22}$$

In the low-temperature plateau region at $T \to 0$ K all the retardation times τ_j increase indefinitely, since at a first approximation $\tau_j = Ae^{U/RT}$. Thus, at $T \to 0$ K the condition $\omega\tau \to \infty$ (or, at least, $\omega\tau \gg 1$) is valid. With this condition the second term on the right-hand side of Eq. (7.22) is negligibly small compared with $1/c_q^2$ and $c = c_q$. It thus follows that if these conditions are satisfied (this occurring in the region of the low-temperature plateau) the velocity of sound cannot depend on either frequency or temperature, whereas the dependence on the degree of crystallinity and orientation may still hold (70).

Evidently, analogous conclusions can be arrived at if use is made of expressions (7.15) and (7.20) for the velocity of sound. Thus, the low-temperature plateau in polymers can be explained in terms of phenomenological relaxation theory as the limiting case of this theory.

In this connection there arises the question of the mechanism of the relaxation process, which becomes unfrozen at $T < T_{\mathrm{tr}}$. According to the concepts of phenomenological relaxation theory, the lowest-temperature (or the highest-frequency) relaxation process is the relaxation of heat conduction. Formally, the effect of the relaxation process caused by heat conduction on the velocity of ultrasound in polymers at low temperatures can be described by using expressions (7.15) and (7.16). Let us consider the simplest case

Suppose that at low temperatures all the relaxation times τ_{1j} and τ_{2j} in formula (7.15) are so large that $\omega\tau_{1j}$ and $\omega\tau_{2j}$ are much greater than unity; we also assume that all τ_{3j} vanish, except for the single value τ_3. Then formula (7.15) assumes the following form:

$$c^2=c_0^2+b_0^2+c_0^2\,\frac{D\omega^2\tau_3\tau_\varkappa}{1+\omega^2\tau_3^2} \tag{7.26}$$

where $\tau_\varkappa = \chi_0/c_0^2$ is a certain characteristic time, usually termed the relaxation time of heat conduction.

Obviously, $\tau_3 = b_3\tau_\varkappa$, where b_3 is a constant. To a first approximation, $b_3 = 1$ and $\tau_3 = \tau_\varkappa$. From formula (7.26) it follows that in polymers at low temperatures a dispersion of ultrasonic velocity caused by heat conduction relaxation is possible. As the temperature drops further τ_3 increases and at sufficiently low temperatures a situation where $\omega\tau_3 \gg 1$ is possible. In this case

$$c^2 = c_0^2 + b_0^2 + c_0^2 D b_3 \tag{7.27}$$

and the velocity of sound depends neither on the frequency ω nor on τ, i.e., it is independent of temperature. It is under these conditions that the low-temperature plateau will be observed in the temperature dependence of sound velocity.

The use of phenomenological relaxation theory, however, does not allow us to elucidate the mechanism of the process and to estimate the limits of applicability of this theory. The question of the mechanism of the effect of heat conduction on the propagation of sound in dielectrics has been examined by a number of investigators (345, 347, 369). An analysis of these works shows that relations such as (7.15), (7.26) and (7.27) still hold at low temperatures, even when the heat conduction in polymers is phononic in nature. The condition for their applicability (345) is the inequality $\tau_U^{-1} \ll \omega \ll \tau_N^{-1}$, where τ_U is the characteristic time of "Umklapp" processes; τ_N is the characteristic time of "Normal" processes; ω is the ultrasonic frequency. We know that the most important role in heat conduction in polymers at low temperatures is played by "Umklapp" processes, which govern the finite thermal conductivity near 0 K. At low temperatures the characteristic time of "Normal" processes τ_N is considerably shorter than that of "Umklapp" (or flip-over) processes τ_U. It would be natural to suppose that the relaxation time $\tau_\varkappa$ coincides with τ_U in order of magnitude.

Since the phononic mechanism of heat conduction is most probable in dielectric crystals, it becomes clear why T_{tr} increases with increasing degree of crystallinity. Naturally, as the size of crystallites and their share of the total volume of a polymer increase, so does the characteristic time of phononic processes, since the mean free path of phonons becomes larger. As a result of an increase in $\tau_\varkappa$, the condition $\omega\tau_\varkappa \gg 1$ begins to be satisfied at lower frequencies or at higher temperatures.

In view of this, the temperature T_{tr} might be expected to determine the temperature region located at $T < T_{\mathrm{tr}}$, where the lowest-temperature relaxation process caused by heat conduction is found to be frozen. The processes of δ-relaxation (268-270) governed by the dislocation mechanism have probably not been observed at ultrasonic frequencies since in the latter case use was made of unoriented isotropic samples which were annealed in the free, unclamped state.

The temperature T_{tr} depends greatly on the chemical structure. The highest values of T_{tr} are shown by polymers that contain a sequence of identical linkages (polyethylene, polytetrafluoroethylene). The results obtained by measuring T_{tr} on longitudinal and shear waves are shown in Table 7.1.

TABLE 7.1. *Temperature Transitions in Linear Crystalline Polymers near the Liquid-Helium Temperature* ($\nu = 5$ MHz)

Polymer	Longitudinal waves			Shear waves		
	T_{tr}, K	T_1, K	T_2, K	T_{tr}, K	T_1, K	T_2, K
Polyethylene, high-density	120	180	—	90	170	—
Polyethylene, low-density	100	170	—	88	160	—
Polytetrafluoroethylene	80	160	200	60	150	187
Polyvinylidene fluoride	25	150	—	15	135	—
Polyformaldehyde	20	160	220	20	140	210
Nylon 6	58	160	235	42	142	214
Nylon 7	53	153	214	30	130	192
Nylon 6,10	40	145	217	33	129	195
Nylon 11	30	133	190	25	124	178
Nylon 12	35	133	183	28	117	170

It is interesting that the change from hydrogen to fluorine atoms in moving from polyethylene to polytetrafluoroethylene diminishes the extent of the low-temperature plateau by 40 K. An even greater decrease in T_{tr} is brought about by the introduction into the main chain of the polymer of oxygen atoms which alternate with carbon atoms. For example, in passing from polyethylene to polyformaldehyde the temperature T_{tr} decreases by 100 K. For polyamides, T_{tr} decreases, as a rule, with increasing length of the aliphatic component in the repeat unit of the polymer. The only exception is the level of T_{tr} in the case of Nylon 12.

The activation energy of the relaxation process associated with T_{tr} is 8.4-16.7 kJ/mole. For example, for high-density polyethylene $U = 17.5$ kJ/mole, and for cured polycapramide $U = 7.5$ kJ/mole.

From Table 7.1 it can be seen that the values of T_{tr} measured for shearing waves are lower than those obtained by measurements made for longitudinal waves. This confirms that the relaxation process that is evident in the temperature dependence of sound velocity at T_{tr} is caused by flip-over ("Umklapp") processes, which govern the character of the temperature dependence of thermal conductivity (see Chapter 2). As the temperature drops (at $T \to 0$ K) the "Umklapp" processes become frozen, since the energy of non-equilibrium phonons is no longer sufficient for these processes to be realized. From the microscopic theory of heat conduction (82) it follows that for transverse acoustic modes the "Umklapp" processes must be frozen at lower temperatures than for longitudinal modes. Thus, the results of the ultrasonic investigations of linear crystalline polymers carried out at low temperatures agree well with those predicted by the modern theory of heat conduction.

In addition to T_{tr} in the temperature range 130 to 180 K there is another temperature transition (T_1) on the $c = f(T)$ graph for each polymer of the first group. Besides, for most polymers (except for polyethylene and polyvinylidene fluoride) there is still another temperature transition (T_2) in the temperature range 180-230 K.

Polyethylene. For high-density polyethylene (122) ($\rho = 0.964$ Mg/m^3, $\varkappa = 74$ per cent), apart from T_{tr} (see Table 7.2) there is a temperature transition at 180 K on the graph of c against T ($v = 5$ MHz) (see Fig. 7.4). Above $T_1 = 180$ K the absolute value of the temperature coefficient of longitudinal ultrasonic waves is $|\Delta c/\Delta T| = 8.8$ m/(s·K). The activation energy corresponding to this temperature transition of the relaxation type is 36.4 kJ/mole. For low-density polyethylene ($\rho = 0.92$ Mg/m^3, $\varkappa = 46$ per cent) this transition is observed for longitudinal waves ($\nu = 5$ MHz) at $T_1 = 170$ K. At $T > T_1$ the temperature coefficient of sound velocity is somewhat higher than that for a more amorphous sample of polyethylene. This is an indication that the given relaxation process is most likely to be caused by mobility in the amorphous regions. Evidently, the temperature transition observed in polyethylene at ultrasonic frequencies at 170-180 K indicates the start of the γ-relaxation process. In measurements on a torsion pendulum ($\nu = 1$ Hz) this transition leads to the appearance of a tan δ peak at 150 K (see Chapter 6). Naturally, in measurements carried out at ultrasonic frequencies this temperature transition will be observed at higher temperatures.

A typical feature of polyethylene is a considerable increase in the velocity of sound in passing from room temperature to the liquid-helium temperature. For example, the velocity of longitudinal ultrasonic waves ($\nu = 5$ MHz) in high-density polyethylene increases by 45 per cent (from 2540 to 3690 m/s) and the velocity of transverse waves by 66 per cent (from 1180 m/s at 293 K to 1960 m/s in the low-temperature plateau region). The velocity of longitudinal and transverse ultrasonic waves in high-pressure polyethylene undergoes an even stronger change (by 58 and 83 per cent, respectively). The velocities of longitudinal waves, c_l, in low- and high-density polyethylene are very high in the low-temperature plateau region (3740 and 3690 m/s, respectively). These values are close to the velocity of sound in some metals (say, copper) measured at room temperature.

Polytetrafluoroethylene. As well as $T_{tr} = 80$ K, for polytetrafluoroethylene ($\rho = 2.141$ Mg/m^3, $\varkappa = 39$ per cent) there are also temperature transitions (122, 370) at $T_1 = 160$ K and $T_2 = 200$ K (Fig. 7.5). The activation energies of the relaxation processes corresponding to these transitions are 7.5, 32.2, and 50.2 kJ/mole.

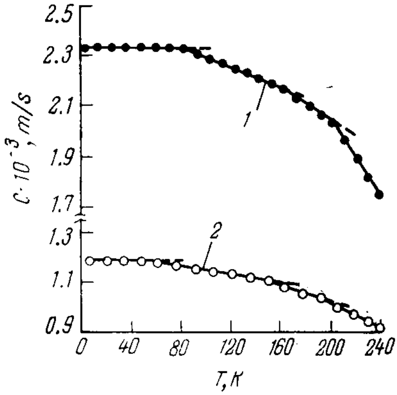

FIG. 7.5. Temperature dependence of ultrasonic velocity for polytetrafluoroethylene at $\nu = 5$ MHz:

1—longitudinal waves; 2—shear waves.

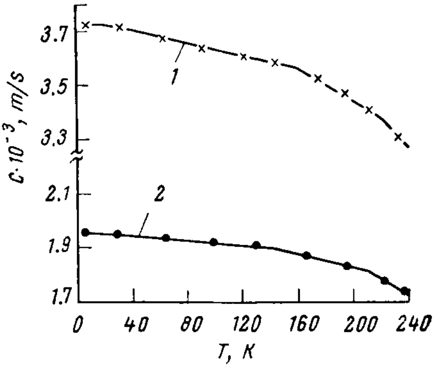

FIG. 7.6. Temperature dependence of ultrasonic velocity for polyformaldehyde at $\nu = 5$ MHz:

1—longitudinal waves; 2—shear waves.

The temperature transition at 160 K is brought about by the process of γ-relaxation. The transition at 200 K probably corresponds to the glass-transition temperature of the amorphous regions of the polymer measured at a frequency of 5 MHz and is associated with the unfreezing of the micro-Brownian motion in the amorphous layer. In low-frequency measurements ($\nu = 200$ Hz) this transition is observed (70) at 163 K. As with polyethylene, so with polytetrafluoroethylene the velocity of propagation of longitudinal and transverse waves increases considerably (by 65 per cent) in passing from room temperature to the liquid-helium temperature. In the low-temperature plateau region, (and, hence, at 4.2 K), however, the velocities of longitudinal and shear waves in polytetrafluoroethylene are relatively low (2330 and 1180 m/s, respectively) as compared with polyethylene.

Polyformaldehyde. As well as $T_{tr} = 20$ K, in polyformaldehyde ($\rho = 1.43$ Mg/m^3, $\varkappa = 74$ per cent) there are also temperature transitions (122) at 160 and 220 K, which have been detected in measurements on longitudinal ultrasonic waves at a frequency of 5 MHz (Fig. 7.6). These temperature transitions are in good agreement with two low-temperature tan δ peaks (at 193 and 221 K) detected (70) in measurements at a frequency of 200 Hz. The temperature transition at 160 K is probably due to the rotation of the terminal groups or the motion of several repeat units of the main chain in the amorphous regions. The activation energy of the relaxation process that begins to be unfrozen at 160 K is 15 kJ/mole.

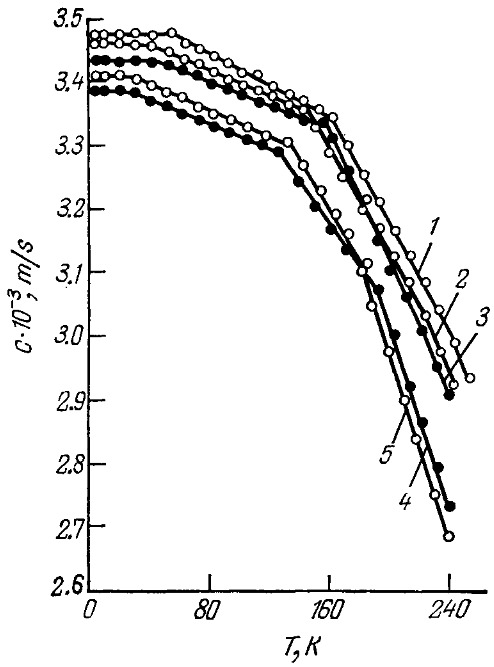

FIG. 7.7. Temperature dependence of the velocity of longitudinal ultrasonic waves for polyamides at $\nu = 5$ MHz:

1—Nylon 6; 2—Nylon 6, 10; 3—Nylon 7; 4—Nylon 12; 5—Nylon 11.

The transition at 220 K corresponds to the glass-transition temperature of polyformaldehyde measured at 5 MHz (the apparent activation energy being 62.7 kJ/mole). In low-frequency ($\nu \approx \approx 200$ Hz) measurements (70) the value of T_g, found from the $c = f(T)$ graph, is 193 K.

When the temperature moves from 293 to 4.2 K, the velocities of longitudinal and transverse ultrasonic waves in polyformaldehyde increase by about 40 per cent and reach quite high values (3730 and 1950 m/s) near 0 K.

Polyamides. The velocities of longitudinal and transverse ultrasonic waves in a number of crystalline polyamides (Nylon 6, Nylon 7, Nylon 6,10, Nylon 11, and Nylon 12) were measured (356, 368) at frequencies 1 and 5 MHz in the temperature range 2.1 to 240 K. The results of the measurements show (Fig. 7.7) that the velocities of longitudinal utrasonic waves in polyamides at 4.2 K range from 3400 to 3500 m/s, the velocity of sound in polymers with short aliphatic linkages (Nylon 6, Nylon 6,10, Nylon 7) being higher than that in polyamides with longer aliphatic fragments (Nylon 12 and Nylon 11).

The velocities of transverse ultrasonic waves, c_t, measured at 4.2 K do not obey this rule. The velocity of transverse waves has been found to be greater in Nylon 6,10 and Nylon 7. The velocities c_t in Nylon 6, Nylon 12 and Nylon 11 differ insignificantly from one another but they are much lower. This difference in the acoustical properties of the nylons points to the important role of the hydrogen bonds formed between the amide groups of neighbouring chains during the propagation of shear waves.

For all the polyamides mentioned above a temperature transition appears at temperatures between 130 and 160 K on the $c = f(T)$ graph, detected by a change in the temperature coefficient of sound velocity. Besides, in the range 180 to 235 K another temperature transition has been detected in polyamides. The temperatures corresponding to these transitions are given in Table 7.2 for each of the polyamides.

TABLE 7.2. *Transition Temperatures, Activation Energies, and Absolute Values of the Temperature Coefficients of Ultrasonic Velocity in Polyamides*

Polymer	T_{tr}, K	$\left\|\frac{\Delta c}{\Delta T}\right\|_{T > T_{tr}}$, m/(s·K)	U, kJ/mole	γ-Relaxation			β-Relaxation		
				T_γ, K	$\left\|\frac{\Delta c}{\Delta T}\right\|_{T > T_\gamma}$, m/(s·K)	U, kJ/mole	T_β, K	$\left\|\frac{\Delta c}{\Delta T}\right\|_{T > T_\beta}$, m/(s·K)	U, kJ/mole
Nylon 6	58	1.27	9.2	160	4.27	41.0	235	5.35	79.5
Nylon 7	53	1.25	8.8	153	4.29	43.5	214	5.77	84.0
Nylon 11	30	1.16	5.8	133	4.0	46.0	183	7.80	78.5
Nylon 12	35	1.02	5.0	133	3.60	46.0	190	6.84	72.5
Nylon 6,10	40	1.05	6.7	145	4.30	45.0	217	5.22	76.5

It should be noted that for polymers containing a larger number of methylene groups in the repeat unit the transitions are found in the lower temperature region, decreasing from 160 and 235 K (Nylon 6) to 133 and 190 K (Nylon 12) in measurements on longitudinal waves ($\nu = 5$ MHz).

The activation energies of the transitions and their positions on the temperature scale (see Table 7.2) allow one to state that the processes that occur in polyamides over the temperature range 130 to 160 K are γ-relaxations and those taking place at temperatures 180-235 K are β-relaxations.

It is commonly believed (70, 165, 265) that the temperature transition corresponding to the γ-relaxation process in polyamides results from the unfreezing of the mobility of a small number of methylene groups in the main chain of these polymers. Evidently, the β-relaxation process is induced by the motion of chain lengths containing amide groups which are not linked via hydrogen bonds to the equivalent groups of the adjacent macromolecules. We know that the β-relaxation process occurs in the amorphous regions of a polymer.

It is interesting to trace the change in the activation energy of the γ-relaxation process occurring in polyamides. Kawaguchi (371) noted that with an increase in the length of the aliphatic fragment in the repeat unit of the nylons the activation energy corresponding to the γ-transition increases. On the contrary, Perepechko has shown (70) that the value of U for this transition in Nylon 6 is higher than that in Nylon 12. The results of ultrasonic investigations (368) show that the activation energy of the γ-process in different polyamides remains practically unaltered, ranging from 42 to 46 kJ/mole (see Table 7.2).

If one proceeds from the interpretation of the γ-relaxation taking place in polyamides as being the result of the motion of three or more methylene groups in the main chain, then the constant value of activation energy for this process, in nylons with different lengths of methylene chains, can be regarded as resulting from the mobility of identical kinetic units of the polymeric chains. This is also evidenced by the value of the temperature coefficient of sound velocity, which is approximately the same for all polyamides in temperature regions lying above the temperature of the γ-transition.

The activation energy of the β-relaxation process in polyamides, as calculated from the results of ultrasonic investigations (368), is 71 to 83 kJ/mole. As the number of CH_2 groups in the repeat unit diminishes there is a tendency for the activation energy to increase. But the values of U for nylons with an even number of methylene groups in the repeat unit appear to be somewhat higher than in polyamides with an odd number of CH_2 groups.

This phenomenon is probably associated with the fact that in nylons with an odd number of CH_2 groups in the repeat unit only part of the hydrogen bonds are formed between the amide groups of neighbouring chains, while in nylons with an even number of methylene groups all the amide groups tend to form hydrogen bridges. Hence, it is clear that in the latter case the energy of intermolecular interaction in polyamides, being due to a larger number of hydrogen bonds, will be higher and a larger amount of activation energy will be needed to overcome the potential barrier hindering the motion responsible for β-relaxation.

7.6. ULTRASONIC VELOCITY AND RELAXATION PROCESSES IN POLYMERS CONTAINING METHYL GROUPS

It has recently been established experimentally (367, 372) that, in contrast to polymers of the first group (see page 217), in all the polymers studied which contain methyl goups, the velocity of ultrasound increases as the temperature falls to 4.2 K. Such

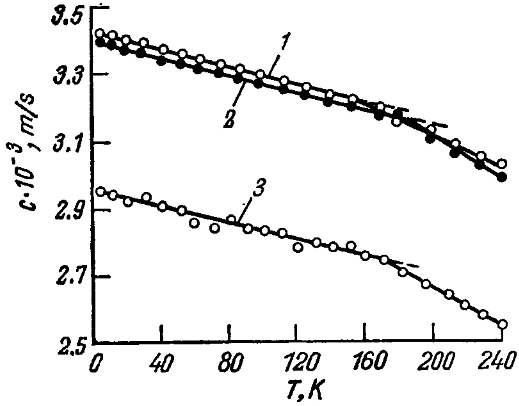

FIG. 7.8. Temperature dependence of the velocity of longitudinal ultrasonic waves at ν = 5 MHz for polypropylene (*1*), epoxide resin ЭД-5 (*2*), and polycarbonate (*3*).

a dependence of the velocity of ultrasound on temperature has been found for polycarbonate, polypropylene, epoxide resin ЭД-5 (based on bisphenol A) cured with metaphenylene diamine (Fig. 7.8), polymethyl methacrylate (Fig. 7.9) and poly-4-methyl pentene-1.

The noticeable increase in ultrasound velocity with decrease in temperature to 0 K is difficult to explain in terms of classical phenomenological relaxation theory. An increase in the velocity of ultrasound in polymers containing methyl groups is accompanied by dispersion as 0 K is approached. Characteristic in this respect are the results of measurements of ultrasound velocity in polymethyl methacrylate (see Fig. 7.9), from which it follows that the dispersion of the velocity of ultrasound is retained in this polymer even at 2.1 K, reaching 6 per cent with longitudinal waves and 4 per cent with shear waves. This exceeds several times the possible relative experimental error.

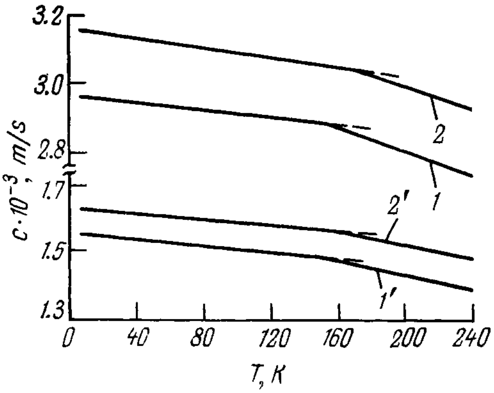

FIG. 7.9. Temperature dependence of the velocity of longitudinal (*1*, *2*) and shear (*1'*, *2'*) ultrasonic waves in polymethyl methacrylate at $\nu = 1$ MHz (*1*, *1'*) and $\nu = 5$ MHz (*2*, *2'*).

The presence of dispersion and the increase in ultrasound velocity at $T \to 0$ K indicate that polymers containing methyl groups can undergo viscoelastic relaxation even at the lowest temperatures.

It has already been noted (Chapter 6) that low-frequency measurements for polymers containing methyl groups reveal tan δ peaks near 4.2 K. These were ascribed to the classical rotation of methyl groups. Eisenberg and Reich (322, 326, 327) have shown, however, that this explanation is incorrect, because below 40 K CH_3 groups cannot undergo classical rotation since the height of the barrier to their rotation is 8.4 kJ/mole and the energy of methyl groups is much lower at these temperatures. These authors advanced a hypothesis that the low-temperature (low-frequency) loss maxima for polymers containing methyl groups are caused by the re-orientation of methyl groups as a result of quantum-mechanical tunnelling transitions. Eisenberg and Reich pointed to the most important feature of relaxation processes of this type, emphasizing that they are not thermal-activation processes, and applied successfully the Stejskal-Gutowsky theory (251) (see Chapter 5) to the description of these processes.

The mechanism of energy dissipation during viscoelastic relaxation due to the re-orientational motion of CH_3 groups resulting from their quantum-mechanical tunnelling remains obscure in their treatment. Indeed, if a methyl group jumps from one potential well to another in such a way that the energies of the torsional rotators in both states are identical, then such a process will not be associated with viscoelastic relaxation.

In this connection Eisenberg and Reich (373) resorted to the concept of the "inelastic" tunnelling of methyl groups. They assumed that when acoustical vibrations are propagating in a polymer under the influence of mechanical excitation there occurs a modulation of the height of the potential barrier hindering the rotation of CH_3 groups with the frequency of external (sound or ultrasound) excitation. The change in the barrier height is associated with the change in the energy of the torsional states of methyl rotators. If the tunnelling transition caused by the re-orientation of CH_3 groups occurs between two identical torsional states whose energies are only slightly different (the energy difference being due to the modulation of the barrier height under the action of the stress field), then this energy difference leads to the emission of a phonon upon tunnelling. The fate of this phonon will depend on whether it is coherent with the external ultrasound field applied to the sample. If thermal and ultrasound phonons are coherent, their interaction will be elastic and will not lead to the viscoelastic relaxation associated with energy dissipation. But since tunnelling is a random process, the phonons emitted will be incoherent with external excitation. The inelastic interactions of these phonons with other thermal phonons will result in the conversion of part of the energy of ultrasound excitation into heat. Reich and Eisenberg coined the term "inelastic" tunnelling for such a process.

It should be noted that if tunnelling occurs between energy levels of equal energy, no phonons will be emitted. Thus, the viscoelastic relaxation due to quantum-mechanical tunnelling is possible only upon application of an external field modulating the height of the potential barrier. On the other hand, if the potential barrier is modulated and no tunnelling occurs, the process will be completely elastic and will not lead to energy dissipation.

Using the concept of "inelastic" tunnelling, Reich and Eisenberg (373) showed that the relaxation process induced by the tunnelling of CH_3 groups is associated with phonon-phonon interaction. It is believed that upon propagation of sound (or ultrasonic) vibrations in a polymer the height of the potential barrier hindering the rotation of methyl groups is periodically modulated with the frequency of external excitation. As a result, the energy of the vibrational states of methyl rotators is somewhat changed. The tunnelling of CH_3 groups between two nearly identical vibrational states, whose energies are only slightly different due to the modulation of the potential barrier, involves the emission of phonons.

An estimate of the change in the vibrational energy of the methyl rotator resulting from acoustic excitation shows that the energy change is of the same order as the energy of the most probable phonon at low temperatures. Since the emission of a phonon is a random process, the phonon is incoherent for ultrasonic phonons. The phonons emitted upon tunnelling interact inelastically with the thermal phonons of the sample, this leading to the dissipation of the energy of ultrasonic vibrations.

The results of measurements of the velocity of ultrasonic waves (367, 372) show that the $c = f(T)$ graph plotted for polymers containing methyl groups shows a temperature transition in the temperature range 150 to 180 K (Table 7.3). The temperature of this transition T_1 shifts towards higher temperatures with increasing frequency, this being indicative of the relaxation nature of the process. The activation energy of the relaxation process corresponding to this temperature transition is about 12.5 kJ/mole.

TABLE 7.3. *Values of T_1 and U_1 and Velocities of Longitudinal and Shear Waves in Polymers Containing Methyl Groups*

Polymer	T_1, K	U_1, kJ/mole	c_l, m/s	c_t, m/s
Polypropylene	160	12.1	3420	1750
Polycarbonate	170	13.4	2960	1350
Epoxide resin ЭД-5	180	15.0	3360	1640
Poly-4-methyl pentene-1	150	14.2	2720	1240
Polymethyl methacrylate	165	17.6	3160	1630

With this in mind, one naturally assumes that the given transition is associated with the unfreezing of the classical rotation of CH_3 groups. This inference is consistent with the results of NMR investigations (see Chapter 5), which have shown that an abrupt change in the second moment in the temperature range 120 to 190 K is associated with the rotation of methyl groups.

Since in measurements using longitudinal waves ($\nu = 5$ MHz) the relaxation process due to the rotation of methyl groups below 160 K does not manifest itself, it is evident that further increases in sound velocity following a decrease in temperature and its dispersion are most likely to be associated with the relaxation process induced by quantum-mechanical tunnelling.

A typical feature of polymers containing methyl groups is that at liquid-helium temperatures they exhibit lower velocities of longitudinal ultrasonic waves than do linear crystalline polymers for which there is a low-temperature plateau.

7.7. ULTRASONIC VELOCITY AND RELAXATION PROCESSES IN POLYMERS WITH AN ASYMMETRIC POTENTIAL BARRIER

This group of polymers include vinyl polymers of the type $[-CR_2-CRR'-]_n$, where R = hydrogen or fluorine atom and R′ = chlorine or fluorine atom or an aromatic nucleus. The existence of an asymmetric centre in such macromolecules gives rise to a difference between the left- and right-hand rotations (374). The interactions caused by the rotations φ and $-\varphi$ about the main chain differ from each other, which makes it possible to distinguish an asymmetric chain from a symmetric one. The alternation of two different types of atoms (or groups of atoms) attached to the main chain of a polymer usually leads to the appearance of an asymmetric potential barrier which prevents the chain links from passing into a new equilibrium state. The asymmetry of the potential barrier is characterized by the existence of two potential energy minima, differing in magnitude. Typical representatives of such polymers are polyvinyl chloride, polyvinyl fluoride, polytrifluorochloroethylene and polystyrene, whose acoustical properties near 4.2 K are known (370, 375).

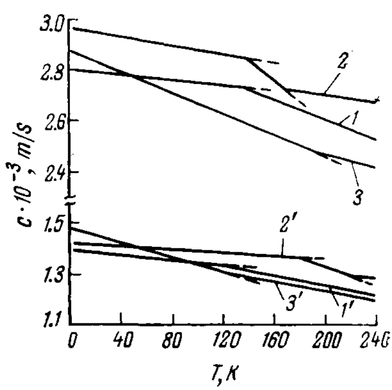

FIG. 7.10. Temperature dependence of the velocity of longitudinal (1, 2, 3) and shear (1′, 2′, 3′) ultrasonic waves at $\nu = 5$ MHz in polyvinyl chloride (1, 1′), polyvinyl fluoride (2, 2′) and polystyrene (3, 3′).

It has been found that for all these polymers the velocities of longitudinal and shear ultrasonic waves measured at 5 MHz (Fig. 7.10) and 1 MHz increase as the temperature falls to 4.2 K. For all the polymers listed above the dispersion of the velocities of longitudinal and shear waves persists at temperatures down to the liquid-helium temperature. The relative change in the velocity of ultrasound, $\Delta c/c$, with a five-fold change in frequency (from 1 to 5 MHz) in some polymers at 4.2 K is as follows for longitudinal and shear waves, respectively: 6 and 5 per cent for polyvinyl chloride; 4 and 6 per cent for polyvinyl fluoride; 3 and 3 per cent for polystyrene. An increase in the ultrasound velocity with decrease in temperature to 4.2 K and appreciable dispersion are indications of the occurrence in these polymers of a relaxation process which is retained at 4.2 K. At present, no unambiguous explanation can be given for this phenomenon on the basis of the available experimental data (370, 375). Nevertheless, some possible causes can be suggested.

The possibility cannot be excluded that viscoelastic relaxation near 4.2 K in polymers with an asymmetric potential barrier is provoked by the quantum-mechanical tunnelling of chlorine or fluorine atoms or an aromatic ring C_6H_5 (phenyl group) attached as pendant groups to the main chain. Tunnelling can probably produce the re-orientation of Cl, F and C_6H_5 (torsional vibrations or side rocking) even at very low temperatures. Indeed, Das (250) has shown theoretically that quantum-mechanical tunnelling transitions may occur as a result of the motion not only of methyl groups but also of bulkier (say, C_6H_5) groups or heavy halogen atoms.

The viscoelastic relaxation detected in polymers with an asymmetric potential barrier near 4.2 K (370, 375) can also be caused by heat conduction. If we assume that for the frequencies (1 and 5 MHz) used in experiments (370, 375) the value of $\tau_\varkappa = \tau_3$ is so small that the condition $\omega\tau_\varkappa \gg 1$ is not fulfilled, then the dispersion and increase in ultrasonic velocity can be expected to occur near 4.2 K with a decrease in temperature, as a result of the heat conduction relaxation.

A third possible mechanism is the hysteresis process of the viscoelastic behaviour of polymers with an asymmetric potential barrier. The molecular mechanism of hysteresis processes proposed by Golub and Perepechko (376) and by Hartman and Jarzynski (394) is based on the assumption that in polymers there exist a large number of local minima of the potential energy corresponding to metastable states. It is assumed that under the action of the applied mechanical stress induced by an ultrasonic wave the kinetic units of polymeric chains undergo some re-orientation. After the stress is removed not all the kinetic units revert to a state corresponding to their original orientation. Some of them appear to be captured by metastable states corresponding to certain particular minima of the potential energy. Hartman and Jarzynski (394) have shown that the absorption α per wavelength λ depends on the amount of free volume and increases with decreasing volume:

$$\alpha\lambda = a - bV \tag{7.28}$$

where V is the specific volume of the polymer; a and b are positive constants.

Hartman and Jarzynski (394) derived no formula taking account of the change in the velocity of ultrasound caused by hysteresis phenomena; nevertheless, the possibility cannot be excluded that the viscoelastic behaviour of polymers with an asymmetric potential barrier at $T \rightarrow 0$ K is connected with hysteresis phenomena.

A curious regularity attracts attention: while polymers of the first group (showing a low-temperature plateau) have very high velocities of longitudinal (3400-3700 m/s) and shear (1600-2000 m/s) waves at the liquid-helium temperature, polymers of the third group (with an asymmetric potential barrier) display the lowest values of c_l (2800-2900 m/s) and c_t (about 1400 m/s). The intermediate position in this series is occupied by polymers of the second group, which contain methyl groups: for these polymers c_l is 3100-3400 m/s and c_t is 1400-1850 m/s. Exceptions to this rule are polytetrafluoroethylene ($c_l = 2330$ m/s at 4.2 K), poly-4-methyl pentene-1 ($c_l = 2720$ m/s) and polytrifluorochloroethylene ($c_l = 2330$ m/s).

Dismissing these exceptions, it becomes obvious that there is a certain regularity. The highest values of ultrasonic velocity near 0 K are exhibited by polymers in which the molecular mobility is completely frozen under these conditions (polymers of the first group). Lower ultrasonic velocities near 0 K are shown by polymers in which the small groups, say CH_3 groups, are mobile at $T \rightarrow 0$ K (polymers of the second group). The lowest velocity of ultrasound at helium temperatures is displayed by polymers in which some mobility of heavy atoms (chlorine or fluorine atoms) or bulky atomic groups (C_6H_5) is retained at $T \rightarrow 0$ K.

The possibility cannot be excluded that molecular mobility is not the only cause of a decrease in ultrasonic velocity at $T \rightarrow 0$ K. Another possible cause is a large amount of free volume retained at $T \rightarrow 0$ K, because of the hindrances associated with the tight packing of macromolecules containing massive and bulky side groups. Perhaps, as a result of this polymers such as polytetrafluoroethylene, polytrifluorochloroethylene and poly-4-methyl pentene-1 depart from the general rule.

Let us consider relaxation processes in polymers of the third group.

In **polyvinyl chloride** (375) a single temperature transition has been detected (see Fig. 7.10) at 130 K for longitudinal waves ($\nu = 5$ MHz) and at 120 K for shear waves, with the same activation energy ($U = 30.6$ kJ/mole) in each case. The nature of this temperature transition is not yet clear but it can be expected that it is associated with the unfreezing of the restricted motion of chlorine atoms. If this is so, then at temperatures below the temperature of this transition only the re-orientational motion of chlorine atoms is retained, this leading to a further increase in the velocity of sound with decreasing temperature.

For **polyvinylidene fluoride** ($\rho = 1.39$ Mg/m^3) two kinks appear (see Fig. 7.10) on the $c_l = f(T)$ graph (375, 376). One of these at 140 K (at a frequency of 5 MHz) evidently corresponds to the low-temperature limit of the relaxation process, and the other at 168 K to the high-temperature limit. It is interesting that at $T >$ $>$ 168 K the temperature coefficient of sound velocity considerably decreases in absolute value. The activation energy corresponding to this temperature transition observed at 140 K is 11.3 kJ/mole. In measurements with shear waves this temperature transition occurs at 180 K and has a higher activation energy. It is possible that this temperature transition is one of the manifestations of γ-relaxation in the polymer.

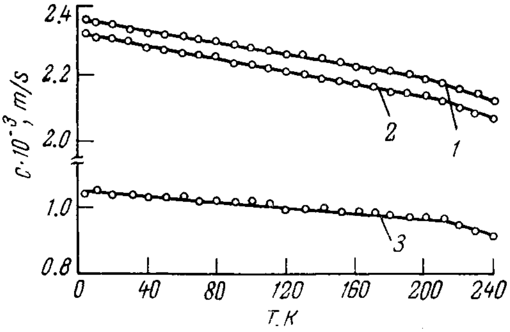

FIG. 7.11. Temperature dependence of the velocity of longitudinal (*1*, *2*) and shear (*3*) ultrasonic waves in polytrifluorochloroethylene at $\nu = 5$ MHz: the degree of crystallinity:
1—40 per cent; *2*, *3*—50 per cent.

With **polytrifluorochloroethylene** ($\rho = 2.135$ Mg/m^3) the $c = f(T)$ graph shows, at $\nu = 5$ MHz (Fig. 7.11), a single temperature transition at 210 K (370) (with longitudinal as well as shear waves) with an activation energy of 56.5 kJ/mole. It should be noted that in low-frequency measurements ($\nu = 200$ Hz) in this polymer the same transition, with an activation energy of 58.5-62.7 kJ/mole, was detected (70) at 190 K. It is thought to be caused by the mobility of chain linkages consisting of several carbon atoms (γ-relaxation).

For **polystyrene** a single kink appears in the temperature dependence of sound velocity (375, 376), situated at 190 K in the case of longitudinal waves ($\nu = 5$ MHz) and at 120 K in the case of shear waves (see Fig. 7.10). Since at temperatures exceeding the temperature of this transition the value of $|\Delta c/\Delta T|$ decreases, this transition can be expected to represent the high-temperature limit of the relaxation process. The low-temperature limit of this relaxation process, if there is such a limit, might be expected to lie at a temperature below 4.2 K and must evidently be observed at higher ultrasonic frequencies.

7.8. EFFECT OF STRUCTURE ON ACOUSTICAL PROPERTIES

One of the most important parameters of the crystal structure of polymers is the degree of crystallinity, $\varkappa$, this having a strong effect on the acoustical properties of partly crystalline polymers.

The concept of amorphous regions in crystalline polymers has recently been considerably revised. While in some cases, especially at a low degree of crystallinity, amorphous regions consist of uncrystallized (or non-crystallizable) links, in others, especially in highly crystalline polymers, the role of the amorphous phase is played by lattice defects in crystals. For example, according to the two-phase model of a crystalline polymer proposed by Pechhold (288), portions of parallel-packed chains (crystallites) coexist with cooperatively twisted regions, with the relaxation processes in the polymer being to a considerable extent associated with the motion of specific rotation isomers (kink-isomers), which are defects in the almost parallel packing of the chains.

It is commonly thought that with increasing crystallinity the velocity of sound in a polymer increases. This is associated with the enhancement of intermolecular interaction in the polymer resulting from an increase in the content of ordered crystalline regions. It is clear that this effect will be observed most distinctly if the amorphous regions of the polymer are in the high-elastic (rubbery) state, which is characterized by weaker intermolecular interaction. It is usually believed that in the glassy state (below T_g of the amorphous layer) the velocity of ultrasound is independent of the degree of crystallinity, since the densities of crystallites and amorphous regions below T_g do not differ. But, in a number of works [for example, (70)] it has been shown that the sound velocity does depend on the degree of crystallinity even below T_g.

Near room temperature a clear-cut dependence of sound velocity on the degree of crystallinity is observed for polymers such as polyethylene and polytetrafluoroethylene. Waterman, Davidse and Westerdijk (377), for example, have shown that for various types of polyethylene, regardless of the method of its synthesis, its degree of branching and its past history, there exists at room temperature a linear dependence of the velocity of ultrasound on the degree of crystallinity.

In order to describe analytically the dependence of the velocity of ultrasound on the degree of crystallinity we shall take advantage of the findings of Chapter 5.

Suppose that the retardation-time spectrum density for a partly crystalline polymer, $L(\tau)$, can be presented in the following form:

$$L(\tau) = \varkappa L_1(\tau) + (1 - \varkappa) L_2(\tau) \tag{7.29}$$

where the subscript 1 stands for a completely crystallized sample, and the subscript 2 for a completely amorphous sample of the same polymer.

Substituting expression (7.29) into Eq. (7.22) and assuming that $E_q = \rho c_q$ depends on $\varkappa$, the same as $L(\tau)$ does, we obtain:

$$\frac{1}{\rho c^2} = \varkappa \left(\frac{1}{E_{1q}} + \int_0^\infty \frac{L_1(\tau)\,d\tau}{1+\omega^2\tau^2} \right) + (1-\varkappa) \left(\frac{1}{E_{2q}} + \int_0^\infty \frac{L_2(\tau)\,d\tau}{1+\omega^2\tau^2} \right) \tag{7.30}$$

An analysis of this expression shows that two types of dependence of sound velocity on crystallinity are possible.

If the following inequality holds true:

$$\frac{1}{E_{1q}} + \int_0^\infty \frac{L_1(\tau)\,d\tau}{1+\omega^2\tau^2} \ll \frac{1}{E_{2q}} + \int_0^\infty \frac{L_2(\tau)\,d\tau}{1+\omega^2\tau^2} \tag{7.31}$$

then it is obvious that the main contribution to the velocity of ultrasound will be made by the second term on the right-hand side of formula (7.30) and that the ultrasonic velocity will increase with increasing degree of crystallinity. The inequality (7.31) is most frequently obeyed at $T > T_g$; it also holds at $T < T_g$ for some polymers. Such a dependence of the velocity of ultrasound on the degree of crystallinity is encountered very often and is considered to be normal.

In a case where a crystalline polymer is subjected to temperatures lower than the glass-transition temperature of the amorphous layer the most intensive relaxation processes, which make the major contribution to the relaxation spectrum of the amorphous sample, may appear to be "frozen" and the velocity of sound in the amorphous polymer may become rather high. This is often associated with the quite effective intermolecular interaction of the kinetic units of neighbouring macromolecules in the glassy state.

At the same time, we can imagine a polymer so completely crystalline that sufficiently intensive relaxation processes may occur at these same temperatures. This may result from the presence of a large number of defects in polymer crystals and the special packing of polymeric chains in crystallites. Thus, below the glass-transition temperature, T_g, of the amorphous layer a case is possible where

$$\frac{1}{E_{1q}}+\int_0^\infty \frac{L_1(\tau)\,d\tau}{1+\omega^2\tau^2} > \frac{1}{E_{2q}}+\int_0^\infty \frac{L_2(\tau)\,d\tau}{1+\omega^2\tau^2} \qquad (7.32)$$

Inequality (7.32) implies that the principal role in formula (7.30) can be played by the first term on the right-hand side of Eq. (7.30) and, hence, the velocity of ultrasound will diminish with increasing $\varkappa$. Such an "anomalous" dependence of c on $\varkappa$, where the sound velocity and dynamic elastic modulus decrease with increasing degree of crystallinity, have been observed in practice (70, 246, 378, 379) in polytrifluorochloroethylene, polyethylene and polyethylene terephthalate. At the same time, all these polymers are characterized by an ordinary dependence of sound velocity on $\varkappa$ at temperatures higher than the glass-transition temperature of the amorphous layer.

The "anomalous" dependence of sound velocity on crystallinity can be dealt with as follows. We can assume that such a dependence of c on $\varkappa$ results from the competition of two phenomena. On the one hand, as the degree of crystallinity increases the total proportion of crystalline regions in the polymer also increases and some ordering occurs in the arrangement of macromolecules inside the crystallites. As a result, the velocity of sound must increase. On the other hand, as the degree of crystallinity increases the density of the amorphous layer diminishes and so does the effectiveness of intermolecular interaction in it. This effect must result in a decrease in sound velocity. This is especially pronounced when the effectiveness of intermolecular interaction in the amorphous layer is sufficiently high, i.e., below T_g.

The "anomalous" dependence of sound velocity on crystallinity is observed only in those cases when the second process predominates. Note that the explanation given above is tantamount in some measure to asserting that the Hosemann-Bonart structural model is valid for crystalline polymers exhibiting an anomalous dependence of sound velocity on crystallinity.

At low temperatures both types of dependence of sound velocity on crystallinity are encountered for polymers. In polytetrafluoroethylene, for example, the sound velocity is almost independent of $\varkappa$, but at $T \to 0$ K the velocity of ultrasound in more crystallized samples is somewhat higher. The normal dependence of the velocity of ultrasound on crystallinity is also observed in Nylon 7, Nylon 11, Nylon 12 and some other polymers.

The "anomalous" dependence of the velocity of ultrasound on the degree of crystallinity, when c decreases with increasing $\varkappa$, is exhibited by polyethylene (Fig. 7.12), polycapramide (356), Nylon 6,10 and polytrifluorochloroethylene. It should be noted that the "anomalous" dependence of sound velocity on crystallinity in these polymers was also observed in low-frequency measurements (70). However, in low-frequency measurements the point of inversion at which the dependence of sound velocity on crystallinity for polycapramide undergoes a change lies at 305 K, while in ultrasonic experiments this point is located at 155 K. An analogous phenomenon is also observed in the case of polyethylene. While in low-frequency ($\nu \approx 200$ Hz) measurements the point of inversion at which the dependence of sound velocity on crystallinity undergoes a change is at 223 K, in ultrasonic measurements (see Fig. 7.12) it occurs much lower (167 K).

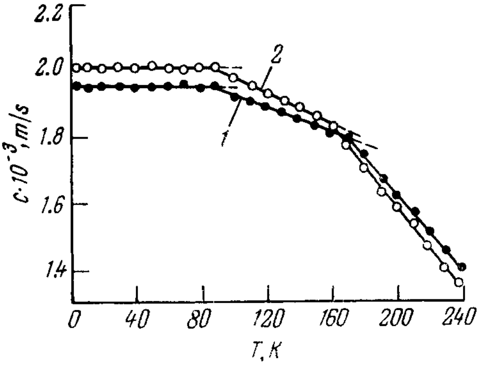

FIG. 7.12. Temperature dependence of the velocity of shear waves in low-pressure (1) and high-pressure (2) polyethylene at $\nu = 5$ MHz.

The velocity of ultrasound in samples with a higher degree of crystallinity decreases in polytrifluorochloroethylene (see Fig. 7.11) in the temperature range 4.2-240 K (370).

A change in the position of the point of inversion on the temperature scale in frequency measurements can be described in terms of phenomenological relaxation theory (70); it confirms the validity of the assumptions made in the derivation of formula (7.30). In this connection, let us consider two samples of the same polymer with different degrees of crystallinity ($\varkappa_1$ and $\varkappa_2$). Using relation (7.30), we can write expressions for the sound velocity in these samples in the following form:

$$\frac{1}{\rho_1 c_1^2} = \frac{\varkappa_1}{\rho_{01} c_{01}^2} + \frac{1-\varkappa_1}{\rho_{02} c_{02}^2}$$

$$\frac{1}{\rho_2 c_2^2} = \frac{\varkappa_2}{\rho_{01} c_{01}^2} + \frac{1-\varkappa_2}{\rho_{02} c_{02}^2}$$

At the point of inversion at which the sound velocity does not depend on the degree of crystallinity $1/\rho_1 c_1^2 = 1/\rho_2 c_2^2$. It thus follows that at the point of inversion $\rho_{01}c_{01}^2 = \rho_{02}c_{02}^2$. The latter equation can be written in the form:

$$\frac{1}{\rho_{01}c_{01}^2} - \frac{1}{\rho_{02}c_{02}^2} = \int_0^\infty \frac{L_{02}(\tau)\,d\tau}{1+\omega^2\tau^2} - \int_0^\infty \frac{L_{01}(\tau)\,d\tau}{1+\omega^2\tau^2} \qquad (7.33)$$

where the subscripts 01 and 02 refer, respectively, to a completely crystalline and a completely amorphous sample of the same polymer.

It is obvious that with a change in frequency, for expression (7.33) to be valid the quantities $L_{01}(\tau)$ and $L_{02}(\tau)$ and τ or their combinations must be changed. But τ can be changed only when the temperature is changed. This fact is consistent with the findings of the phenomenological theory of the acoustical properties of crystalline polymers (70).

The effect of other structural parameters on the acoustical properties of polymers at low temperatures has been little studied.

CHAPTER 8

VISCOELASTIC PARAMETERS OF POLYMERS AT LOW TEMPERATURES

8.1. DETERMINATION OF THE MAIN VISCOELASTIC PARAMETERS OF POLYMERS FROM ACOUSTIC MEASUREMENTS

The main parameters characterizing the viscoelastic behaviour of polymers are the dynamic elastic moduli and Poisson's ratio. The viscoelastic behaviour of an isotropic solid can be fully described if any two dynamic elastic moduli or one dynamic elastic modulus and Poisson's ratio are known. A knowledge of the elastic moduli of polymers at low temperatures becomes very important in connection with the vigorous development of a number of branches of modern engineering.

Until recently investigations of the viscoelastic properties of polymers carried out with a torsion pendulum at a frequency of 1 Hz or by the electrostatic method at frequencies 10^3 to 10^4 Hz enabled the determination of either the dynamic shear modulus G' ($\nu \approx 1$ Hz) or Young's dynamic modulus E' ($\nu \approx 10^4$ Hz). Such results, obtained at frequencies differing by four orders of magnitude for samples having different shapes and different past histories, do not allow one to calculate unambiguously the main viscoelastic parameters of polymeric materials at low temperatures. Such calculations become possible when use is made of ultrasonic methods of investigation, these enabling different types of ultrasonic waves to be excited in the same sample at the same frequency. The availability of data on the velocity of propagation of longitudinal and transverse (shear) waves in polymers at low temperatures (122, 356, 367, 368, 370, 372, 375) makes it possible to calculate (380, 381) their main viscoelastic parameters: Young's modulus E', the dynamic shear modulus G', the bulk (or volume) modulus of elasticity K'_s, and Poisson's ratio σ'.

We know that the velocities of longitudinal and transverse ultrasonic waves (c_l and c_t) are connected with the elastic characteristics of solids by the relations

$$c_l^2 = \frac{L'}{\rho} = \frac{1}{\rho}\left(K_s' + \frac{4}{3}G'\right) = \frac{E'}{\rho}\cdot\frac{(1-\sigma')}{(1+\sigma')(1-2\sigma')} \tag{8.1}$$

$$c_t^2 = \frac{G'}{\rho} = \frac{E'}{2\rho(1+\sigma')} \tag{8.2}$$

where $L' = K_s' + {}^4/_3 G'$ is the dynamic "longitudinal" modulus of elasticity; K_s' is the bulk modulus of elasticity; σ' is Poisson's ratio (the real part).

The dynamic shear modulus can be found immediately from expression (8.2):

$$G' = \rho c_t^2 \tag{8.3}$$

Having substituted the value of G' thus obtained into relation (8.1), we find the expression for the dynamic bulk modulus:

$$K_s' = \rho c_t^2\left[\left(\frac{c_l}{c_t}\right)^2 - \frac{4}{3}\right] \tag{8.4}$$

The complex Poisson ratio can be written in the following form:

$$\sigma^* = \sigma' - i\sigma'' = \frac{L^* - 2G^*}{2(L^* - G^*)} \tag{8.5}$$

where L^* and G^* are the corresponding complex elastic moduli.

Of greatest importance is the determination of the real part of σ^*, which can be found from the following approximate formula:

$$\sigma' = \frac{1}{2}\cdot\frac{L' - 2G'}{L' - G'} \tag{8.6}$$

Substituting the values of G' from Eq. (8.3) and $L' = \rho c_l^2$ into formula (8.6), we obtain an expression relating Poisson's ratio to the velocities of longitudinal and transverse ultrasonic waves:

$$\sigma' = \frac{1}{2}\cdot\frac{(c_l/c_t)^2 - 2}{(c_l/c_t)^2 - 1} \tag{8.7}$$

Using the well-known relation

$$E' = 2(1 + \sigma')G' \tag{8.8}$$

we obtain the following expression for Young's modulus:

$$E' = \rho c_t^2 \cdot \frac{3\left(\frac{c_l}{c_t}\right)^2 - 4}{\left(\frac{c_l}{c_t}\right)^2 - 1} \tag{8.9}$$

Thus, if the density of a polymer and the velocities of the longitudinal and transverse waves propagating in it are known, one can easily calculate the main elastic characteristics of the polymer, using formulas (8.3), (8.4), (8.7) and (8.9).

8.2. DYNAMIC ELASTIC MODULI OF POLYMERS

The dynamic elastic moduli of a number of polymers, which will be considered below, have been determined by ultrasonic measurements at a frequency of 5 MHz. The temperature dependences of Young's modulus E' for some polymers are given in Fig. 8.1 and in Table 5 (see Appendix). The rather high values of E' in the helium-temperature region should be noted.

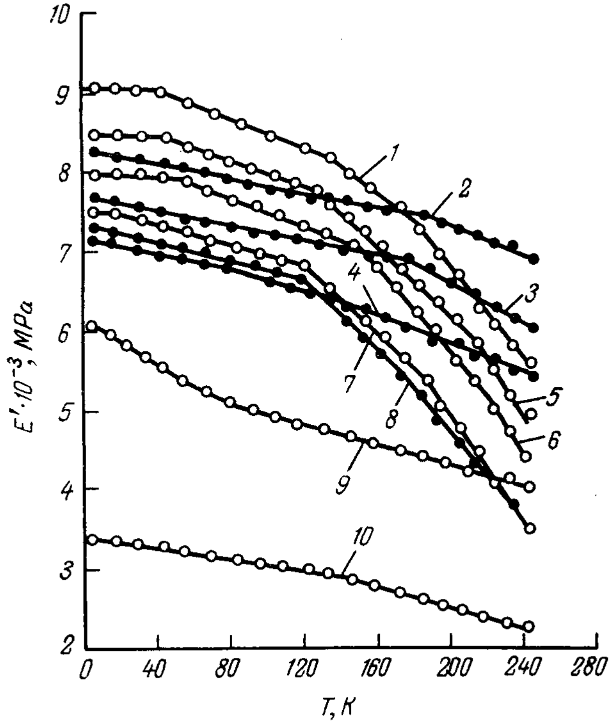

FIG. 8.1. Young's moduli E' of polymers at low temperatures: 1—Nylon 6,10; 2—polymethyl methacrylate; 3—polyvinyl fluoride; 4—polyvinyl chloride; 5—Nylon 7; 6—Nylon 6; 7—Nylon 12; 8—Nylon 11; 9—polystyrene; 10—poly-4-methyl pentene-1.

A comparison of Young's modulus E' measured at 4.2 K, with the theoretical values of the modulus calculated on the basis of data on the crystal structure and the potentials of intermolecular and intramolecular interactions, shows (381) that for linear polymers such as polyethylene and polytetrafluoroethylene the theoretical values of E' are 20-25 times higher than those measured at 4.2 K. This difference is much smaller for polymers whose chains have a more prominent helical shape (say, polyformaldehyde and polypropylene) but in this case too the experimentally observed values of E' are lower than the theoretical values by a factor of 5 to 10.

A comparison of the value of Young's modulus found from ultrasonic measurements at 4.2 K with the elastic modulus of crystallites measured by the X-ray method (382) at room temperature shows that the elastic modulus of crystallite measured along the axis of the polymeric chain exceeds by several times the values of E' found by ultrasonic measurements made at 4.2 K. For example, for Nylon 6 at 4.2 K Young's modulus $E' = 8 \times \times 10^3$ MPa and the elastic modulus of the crystallite measured by the X-ray method along the chain axis at 293 K is equal to 25×10^3 MPa. This difference arises mainly from the fact that the data obtained by Sakurada and Nakamae (382) are more likely to refer to a single crystal of Nylon 6, whereas the results of ultrasonic measurements refer to a polycrystalline polymer containing an amorphous layer. The elastic modulus of the crystallites of Nylon 6 measured by the X-ray technique at right angles to its chain axis at 293 K is 7.3×10^3 MPa, this result being somewhat lower even than the E' value found by means of ultrasonic measurements made at 4.2 K.

The high values of the dynamic elastic moduli at 4.2 K indicate that at this temperature the chain units present in the amorphous regions are involved in a very intensive intermolecular interaction.

The material with the highest values of E' (14.3×10^3 MPa), G' (5.4×10^9 MPa) and K_s' (12.6×10^3 MPa) at 4.2 K is polyformaldehyde. This polymer is characterized by the presence of an oxygen atom in the main chain, which is known to increase the chain flexibility, and also by the smallest proportion of main side groups (among the polymers studied at low temperatures), which is probably responsible for a decrease in the mean distance between the macromolecular skeletons. Considering that the main chain in polyformaldehyde has light hydrogen atoms attached to it, the C—H bond length being as small as 1.07 Å (383), it becomes clear that the mean distance r_m between the macromolecular skeletons in this polymer is the smallest among the polymers studied at low temperatures. We may therefore suppose that the energy of intermolecular interaction in polyformaldehyde is quite high, this being evidently responsible for the high values of the dynamic elastic moduli of the polymer.

As the number of hydrogen atoms in the side groups increases in moving from polyformaldehyde to polyethylene the distance r_m increases, i.e., the energy of intermolecular interaction between the skeletons of the main chains decreases and, as a consequence, the dynamic moduli are diminished. This explains why low-density polyethylene ($\rho = 0.92$ Mg/m^3, $\varkappa = 46$ per cent) has a value for Young's modulus $E' = 10.8 \times 10^3$ MPa at 4.2 K, which ranks second.

The presence of a fluorine atom instead of a hydrogen atom (in moving from polyethylene to polytetrafluoroethylene) probably leads to an even stronger increase in the mean distance r_m between the macromolecular skeletons, since the C—F bond length is 1.39 Å, and to an even stronger decrease in Young's modulus ($E' \doteq 7.9 \times 10^3$ MPa) and in the shear modulus ($G' = 3 \times \times 10^3$ MPa) at 4.2 K.

The intermediate position between polyethylene and polytetrafluoroethylene as far as the dynamic elastic moduli are concerned is occupied by polyamides. The highest values of E' and G' at 4.2 K have been observed for those crystalline polyamides which contain an even number of methylene groups: Nylon 6,10 ($E' = 9.2 \times 10^3$ MPa; $G' = 3.4 \times 10^3$ MPa) and Nylon 7 ($E' = 8.3 \times 10^3$ MPa; $G' = 3.1 \times 10^3$ MPa). It is known that in such polymers all the amide groups tend to form hydrogen bonds whose presence leads to a very strong interchain interaction. The values of E' and G' at 4.2 K for nylons containing very long aliphatic linkages (Nylon 11 and Nylon 12) are somewhat lower: the value of E' ranges from 7.3×10^3 to 7.5×10^3 MPa and $G' = 2.7 \times 10^3$ MPa.

The values of Young's modulus measured at 4.2 K for other polymers also depend primarily on the mean distance between macromolecular skeletons. This distance is usually governed by the type of pendant group in a polymer. For example, polyvinyl fluoride, with a fluorine atom attached to the main chain, the C—F bond length being 1.39 Å, has a rather high value of E' ($7.6 \times \times 10^3$ MPa) at the liquid-helium temperature. The side chain in polyvinyl chloride contains a more bulky chlorine atom (the C—Cl bond length being as large as 1.77 Å) and its Young's modulus is lower at 4.2 K ($E' = 7.2 \times 10^3$ MPa).

This point of view is supported by the lower values of the elastic moduli for polytrifluorochloroethylene at 4.2 K ($E' = = 6.5 \times 10^3$ MPa; $G' = 2.4 \times 10^3$ MPa). An even lower value of E' (6.1×10^3 MPa) is observed at the liquid-helium temperature for polystyrene, in which the side group is a very bulky phenyl group.

Of the polymers containing methyl groups epoxide resin ЭД-5 cured with *m*-phenylenediamine has the highest values of E' and G' ($E' = 8.6 \times 10^3$ MPa and $G' = 3.2 \times 10^3$ MPa). The intermolecular interaction in the epoxide polymer ЭД-5 is rather strong. The presence of a space network and relatively rigid chains between neighbouring chemical cross-links evidently leads to a more ordered and closer packing of the chain units below T_g and especially at $T \to 0$ K.

Low values of the dynamic elastic moduli ($E' = 6 \times 10^3$ MPa and $G' = 2.2 \times 10^3$ MPa) are exhibited by polycarbonate. Such values of the elastic parameters of polycarbonate at low temperatures are probably due to the presence in the main chain of very bulky phenylene groups and to the presence of CH_3 groups attached to the main chain. This may be responsible for the weaker intermolecular interaction between polymeric chains at helium temperatures, the relatively large free volume (which accounts for the high dynamic strength of this polymer) and for the low values of E' and G'. Polypropylene, which has no bulky aromatic groups in the main chain and has only one CH_3 group in its repeat unit, is intermediate between polycarbonate and the epoxide polymer ЭД-5 with respect to values of E' and G' ($E' = 7.3 \times 10^3$ MPa and $G' = 2.8 \times 10^3$ MPa).

The lowest values of Young's modulus ($E' = 3.4 \times 10^3$ MPa) and the shear modulus ($G' = 1.2 \times 10^3$ MPa) are shown by poly-4-methyl pentene-1. This is natural since the side chain of this polymer is a rather bulky branch consisting of C_4H_9 groups. The absence of polar bonds between the pendant groups is responsible for the weak interaction between neighbouring chains in poly-4-methyl pentene-1, which is why one would expect this polymer to have low values of the elastic moduli.

Different behaviour is exhibited by polymethyl methacrylate, which has a high value for Young's modulus at 4.2 K ($E' = 8.3 \times 10^3$ MPa), despite the fact that it is a branched polymer and has a bulky ester group in the side chain. In this case the high values for the elastic moduli are probably due to the strong intermolecular interaction provoked by the polar ester groups present.

It is interesting to trace the change in the value of E' as the temperature increases from 4.2 K (from 2.1 K for some polymers) to 240 K. In the case of nylons with short repeat units (Nylon 6 and Nylon 7) such a change in temperature leads to a decrease in E' by a factor of 1.7; for polymers containing a larger number of CH_2 groups in the repeat unit (Nylon 11 and Nylon 12) E' decreases in the same temperature range even more strongly (by a factor of 2.1). The elastic modulus of polyethylene changes in a similar manner in the same temperature range.

With other polymers the change in E' over the temperature range 2.1 to 240 K is substantially weaker. Some examples are: polymethyl methacrylate (16 per cent); polyvinyl fluoride (about 20 per cent); polyvinyl chloride (25 per cent); polystyrene and poly-4-methyl pentene-1 (about 33 per cent).

The intensity of molecular motion becoming unfrozen with increase in temperature can be assessed by a change in Young's modulus. In this connection, one can conclude that in the case of polyamides and polyethylene, as the temperature rises from 2.1 to 240 K, the large kinetic units of the chain become sufficiently mobile, while with some other polymers the rotation of small side groups can be retarded under the same conditions.

The $E' = f(T)$ graph for polymers of the first group (see Chapter 7), like the temperature dependence of sound velocity, shows a low-temperature plateau at temperatures close to the liquid-helium temperature, where E' depends neither on frequency nor on temperature. For polymers containing methyl groups, as for polymers with an asymmetric potential barrier, E' and G' increase monotonically with decreasing temperature and there is no low-temperature plateau.

Using the well-known expression of phenomenological relaxation theory (70) for the modulus of elasticity

$$\frac{1}{E'} = \frac{1}{E_q} + \int_0^\infty \frac{L(\tau)\,d\tau}{1+\omega^2\tau^2} \qquad (8.10)$$

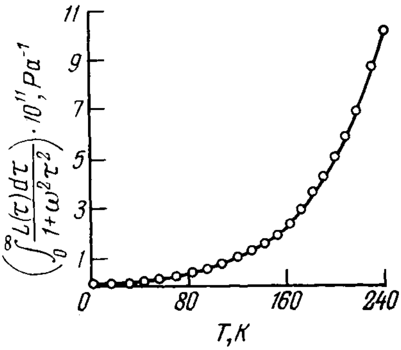

FIG. 8.2. Dependence of the quantity $\int_0^\infty \frac{L(\tau)\,d\tau}{1+\omega^2\tau^2}$ on temperature for Nylon 6.

and taking into account that $E' = E_q$ in the low-temperature plateau region, one can calculate the second term on the right-hand side of expression (8.10), which takes account of the relaxation contribution to the dynamic compliance.

Figure 8.2 is a plot of the quantity $\int_0^\infty \frac{L(\tau)\,d\tau}{1+\omega^2\tau^2}$ against temperature for Nylon 6. In the plateau region (near 4.2 K) this quantity is equal to zero, this being associated with the fact that under these conditions all the relaxation processes that make any contribution to the viscoelastic behaviour of a polymer are frozen. With a rise in temperature this quantity increases, i.e., the contribution of relaxation processes to the viscoelastic behaviour of the polymer becomes more and more substantial. Obviously, at sufficiently high temperatures $\omega\tau \to 0$ K (or, at least, $\omega\tau \ll 1$) and the value of $\omega^2\tau^2$ in the denominator of the integrand can be ignored. Then the second term on the right-hand side of Eq. (8.10) will be much greater than the first and will govern the subsequent behaviour of the modulus E'.

The values of the dynamic shear modulus G' calculated from ultrasonic measurements are lower than the values of Young's modulus by a factor of 2.6 to 2.8; at 4.2 K they range from 1.2×10^3 MPa (poly-4-methyl pentene-1) to 5.4×10^3 MPa (polyformaldehyde). Their temperature dependences repeat qualitatively the course of the $E' = f(T)$ curves of the corresponding polymers.

The temperature dependences of the bulk modulus of elasticity K'_s (Fig. 8.3), calculated from acoustic measurements at low temperatures, show that with a number of linear crystalline polymers the value of K'_s exceeds the value of E'. There are, however, some polymers (polyethylene, polyformaldehyde, Nylon 6,10 and some others) for which $E' > K'_s$ at 4.2 K.

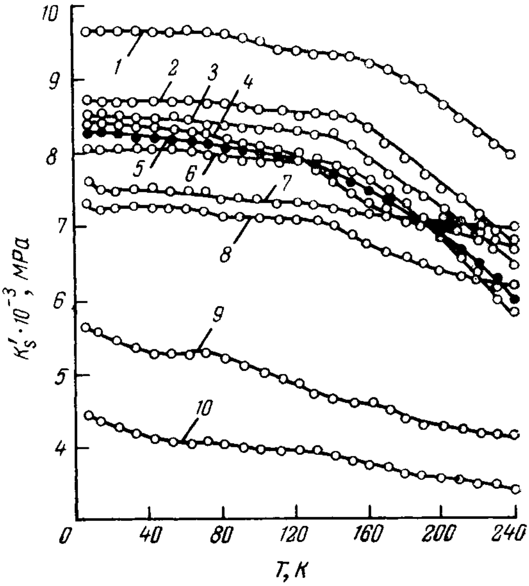

FIG. 8.3. Temperature dependence of the bulk modulus K'_s at low temperatures:

1—Nylon 6; 2—Nylon 7; 3—Nylon 6,10; 4—polyvinyl fluoride; 5—Nylon 11; 6—Nylon 12; 7—polymethyl methacrylate; 8—polyvinyl chloride; 9—polystyrene 10—poly-4-methyl pentene-1.

The value of K'_s for polyamides (see Table 8.1) is governed by the length of the aliphatic chain in the repeating unit. Here there is a clear-cut tendency for the quantity K'_s to decrease over the entire temperature range with an increasing number of CH_2 groups in the repeating unit.

The different relationships between the quantities K'_s and E' for polymers of differing structures become understandable if one makes use of the well-known relation:

$$K'_s = \frac{E'}{3} \cdot \frac{1}{1-2\sigma'} \qquad (8.11)$$

Analysis of this formula shows that the value of the bulk modulus of elasticity K'_s may exceed the value of Young's modulus only in those cases when Poisson's ratio is greater than one-third. At $\sigma' < 1/3$ the value of K'_s must be lower than that of E'.

TABLE 8.1. *The Elastic Parameters of Some Selected Polymers at* 2.1 K

Polymer	$E' \times 10^{-3}$, MPa	$K'_s \times 10^{-3}$, MPa	$G' \times 10^{-3}$, MPa	σ'
Nylon 6	8.0	9.7	2.9	0.36
Nylon 7	8.5	8.7	3.1	0.34
Nylon 6,10	9.2	8.6	3.4	0.32
Nylon 11	7.5	8.3	2.8	0.35
Nylon 12	7.4	8.1	2.7	0.35
Polymethyl methacrylate	8.3	7.7	3.2	0.32
Polyvinyl fluoride	7.6	8.5	2.8	0.35
Polyvinyl chloride	7.2	7.3	2.6	0.34
Polystyrene	6.1	5.7	2.3	0.32
Poly-4-methyl pentene-1	3.4	4.4	1.2	0.37

Indeed, from the results listed in Table 8.1 one can conclude that near the liquid-helium temperature the values of Poisson's ratio for such polymers as Nylon 6,10, polymethyl methacrylate and polystyrene are less than one-third. For these polymers K'_s is characteristically lower than E'. For the other polymers presented in Table 8.1, $\sigma' > 1/3$ and $K'_s > E'$ at 2.1 K.

8.3. POISSON'S RATIO FOR POLYMERS NEAR THE LIQUID-HELIUM TEMPERATURE

The values of Poisson's ratio for a number of polymers calculated from ultrasonic measurements are available in the literature (380, 381). By analyzing the dependence $\sigma = f(T)$ one arrives at the conclusion that the lowest value of Poisson's ratio (0.25) belongs to polyethylene, which has the simplest chemical structure.

Since the quantity σ characterizes the measure of lateral transverse compression on longitudinal extension, it has been assumed

(380, 381) that this parameter is to a certain extent determined by the amount of "free volume".

If one proceeds from this viewpoint, one should expect polymers with lighter and more compact atoms attached to the main chain to have lower Poisson's ratios at $T \to 0$ K. This must lead to a decrease in the free volume of such polymers at low temperatures. The replacement of light atoms by heavier ones must apparently lead to an increase in σ'. This tendency is observed in experiments (380, 381). It has already been mentioned that the minimum value of σ' occurs in polyethylene, in which the role of side groups is played by light hydrogen atoms. The change from hydrogen atoms to heavier fluorine atoms in passing from polyethylene to polytetrafluoroethylene results in a sharp increase in σ' (from 0.25 to 0.33) at 4.2 K. The replacement of one fluorine atom in the repeat unit of polytetrafluoroethylene by a chlorine atom in passing to polytrifluorochloroethylene leads to an even stronger increase in σ' (from 0.33 for polytetrafluoroethylene to 0.37 for polytrifluorochloroethylene).

This explains why the values of σ' measured at $T \to 0$ K depend on the chemical structure of polymers. For example, for polyamides containing an even number of CH_2 groups in the aliphatic linkage (Nylon 6,10 and Nylon 7) σ' is substantially lower than the corresponding values for Nylon 6 and Nylon 12 with an odd number of such groups in their repeating units. If Poisson's ratio is really associated with the amount of free volume, then it is evident that polymers with a closer packing of chains must have a lesser amount of free volume and, hence, they will have lower values of σ'. In the case of Nylon 6,10 and Nylon 7 the closer chain packing resulting from the presence of frequently spaced hydrogen bonds may be responsible for the relatively low values of Poisson's ratio (see Table 8.1).

The relatively high value of σ' (0.35) in the case of polyvinyl fluoride with a heavy fluorine atom attached to the main chain can probably be ascribed to the effect of the free volume. One might think that polyvinyl chloride should have a larger amount of free volume because the asymmetric side group in each of its repeating units is a chlorine atom which is heavier than the fluorine atom. But in polyvinyl chloride, which is a polar polymer, the polar groups can provide a sufficiently effective intermolecular interaction, which leads to a closer chain packing in the polymer. It is possibly for this reason that Poisson's ratio for polyvinyl chloride (0.34) at $T \to 0$ K is somewhat lower than that for polyvinyl fluoride.

The side groups in polystyrene are phenyl groups. At low temperatures these groups can strongly interact, this resulting in a sufficiently tight chain packing. Hence one can expect the values of σ' to be relatively low at low temperatures despite the presence of bulky side groups in the polymer. From Table 8.1 one can see that polystyrene has a value of $\sigma' = 0.32$ at 2.1 K.

Of the polymers containing methyl groups, polypropylene, with one CH_3 side group in each repeating unit, and polymethyl methacrylate have the lowest values of σ' (0.32) at 4.2 K. The latter polymer, despite the fact that it has bulky side chains with polar ester groups, apparently has very tight packing due to a strong intermolecular interaction between the polar groups of neighbouring chains. This explains why the value of σ' for polymethyl methacrylate is not very high at 2.1 K.

The presence of bulky phenylene groups and two CH_3 groups as side groups in each repeating unit in the main chain of polycarbonate leads to an increase in the free volume and, hence, to a relatively high value of σ' (0.37) at 4.2 K.

It can be assumed that the somewhat lower value of σ' in the case of epoxide resin ЭД-5 (0.35 at 4.2 K), which is similar in chemical constitution to a polycarbonate based on bisphenol A, results from an increase in intermolecular interaction due to the more ordered arrangement of the kinetic units of neighbouring chains forming the space network, this being evidently responsible for the closer packing together of the polymeric chains and for the decrease in the free volume.

A high value of σ' (0.37) at 2.1 K is shown by poly-4-methyl pentene-1, which has a C_4H_9 group as a side group. The asymmetric arrangement of this group produces a large free volume in the polymer, which is why its Poisson's ratio is high.

As the temperature increases one observes (Figs. 8.4 and 8.5) a rather monotonic increase in Poisson's ratio and only in the region of temperature transitions do maxima or points of inflection appear on the $\sigma' = f(T)$ graphs. The strongest change in Poisson's ratio with temperature is observed in low-density polyethylene (see Fig. 8.4). For example, while in the range 4.2 to 80 K the value of σ' for this polymer is 0.25, at 240 K it becomes equal to 0.33. Since at $T = 240$ K the amorphous layer of low-density polyethylene is in the rubbery state (at least, above T_g), the free volume at this temperature is large. But, high values of sound velocity at 4.2 K point to a high intensity of intermolecular interaction, this being probably associated with the rather close packing of the chains in the amorphous layer of the polyethylene. As a result, the free volume in polyethylene is small at $T \rightarrow 0$ K and, hence, the values of σ' are low. Thus, in the case of polyethylene the value of σ' changes with temperature in the same way as the free volume. Among other polymers, the strongest change in σ' with temperature is found in linear polyamides (see Fig. 8.5). As a rule, the value of σ' changes little with temperature.

This phenomenon is associated with the fact that rather long chain units in the amorphous layer of polyamides become mobile with increasing temperature, as a result of which the free volume of these polymers increases considerably. But with other polymers only side groups become capable of vibrating when the temperature rises from 4.2 to 240 K, their vibrations being responsible for a small increase in the free-volume fraction.

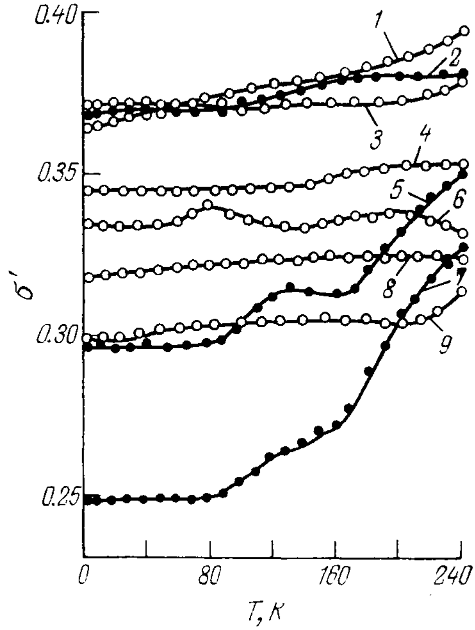

FIG. 8.4. Temperature dependence of Poisson's ratio at low temperatures: *1*—tetrafluoroethylene-vinylidene fluoride copolymer; *2*—polycarbonate; *3*—polytrifluorochloroethylene; *4*—epoxide resin ЭД-5; *5*—high-density polyethylene; *6*—polytetrafluoroethylene; *7*—low-density polyethylene; *8*—polypropylene; *9*—polyformaldehyde.

It should be noted that σ' undergoes the least change with temperature (within the range 4.2 to 240 K) in polymers having relatively high glass-transition temperatures (polycarbonates, polytrifluorochloroethylene, epoxide resin, polymethyl methacrylate, polystyrene).

Of importance is the dependence of the quantity σ' on the degree of crystallinity. An investigation of samples of the same polyamide with different degrees of crystallinity $\varkappa$ (380) leads to the conclusion that the values of σ' decrease with increasing $\varkappa$ over the entire temperature range investigated. This effect is most pronounced in Nylon 11 (Fig. 8.6). Obviously, as the degree of crystallinity increases, i.e., as the size of crystallites and theie

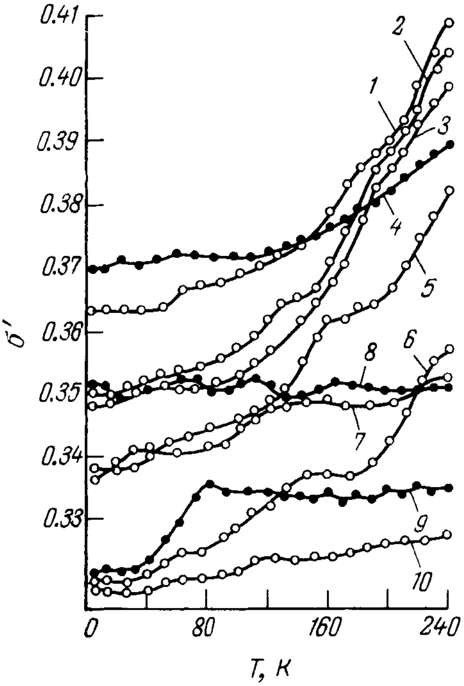

FIG. 8.5. Temperature dependence of Poisson s ratio in the region of helium temperatures:

1—Nylon 6; 2—Nylon 12; 3—Nylon 11; 4—poly-4-methyl pentene-1; 5—Nylon 7; 6—Nylon 6,10; 7—polyvinyl chloride; 8—polyvinyl fluoride; 9—polystyrene; 10—polymethyl methacrylate.

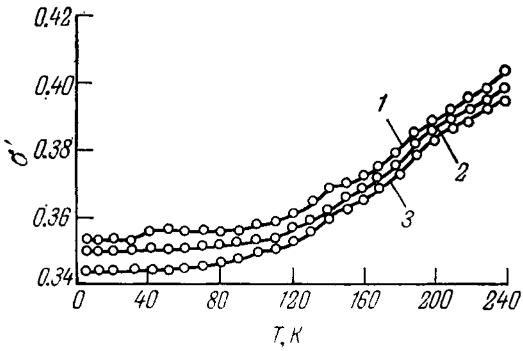

FIG. 8.6. Dependence of σ′ of Nylon 11 on density:

1—quenched sample ($\rho = 1.027$ Mg/m³); 2—original sample ($\rho = 1.036$ Mg/m³); 3—annealed sample ($\rho = 1.041$ Mg/m³).

share of the total volume of the sample increase, the macromolecular chains in the crystalline regions are packed more tightly. This in turn is associated with a decrease in the free volume of the polymer, which is accompanied by a decrease in Poisson's ratio.

Thus, from the facts considered above it follows that there exists a rather distinct correlation between Poisson's ratio and the free volume of polymers. In view of this, the value of σ' can be expected to change with a change in the free volume of the polymer. Moreover, the different values of σ' obtained at 4.2 K for the polymers considered are evidence that these polymers have different free volumes at $T \rightarrow 0$ K. Analogous conclusions have also been drawn by other investigators (384), who maintain that the relative free volume of different vitrified polymers may be different.

CHAPTER 9

DETERMINING THE THERMOPHYSICAL CHARACTERISTICS OF POLYMERS BY ACOUSTIC MEASUREMENTS AT HELIUM TEMPERATURES

9.1. DEBYE TEMPERATURES AND HEAT CAPACITIES DETERMINED BY ACOUSTIC MEASUREMENTS

Specific heat is one of the most important thermal characteristics of polymers. The existing theories of the heat capacity of chain-like structures (see Chapter 1) allow one to calculate the temperature dependence of specific heat if the characteristic Debye temperature θ_D is known. The Debye temperature $\theta_D = h\nu_m/k$, where k is Boltzmann's constant and h is Planck's constant, characterizes the maximum frequency of the Debye spectrum of a solid and is used in the treatment of a number of problems of the quantum thermodynamics of solids. The Debye temperatures of polymers are usually calculated from experimental data on specific heat near 0 K. As a rule, the specific heats of polymers at low temperatures are determined by direct measurements with the aid of adiabatic calorimeters. Since these measurements require complicated instruments and procedures, the amount of work done in this field is very limited and, hence, the information available on the Debye temperatures of polymers is scarce. The task is considerably simplified when use is made of acoustic methods of investigation (52, 385). These make it possible to calculate a number of thermophysical parameters, including the Debye temperature.

The Debye temperatures can be calculated from ultrasonic measurements. We know that the Debye temperature for an isotropic solid can be calculated (70) by using the formula

$$\theta_D = \frac{h}{k}\left(\frac{3P}{4\pi}\cdot\frac{N_0\rho}{M}\right)^{1/3}\bar{c} \qquad (9.1)$$

where P is the number of atoms in the molecule; N_0 is Avogadro's number; ρ is the density; M is the molecular mass; $\bar{c}$ is the average velocity of sound, which can be determined from formula (1.15).

For calculations using formula (9.1), apart from those for the velocities of longitudinal (c_l) and shear (c_t) waves in formula

(1.15), it is also necessary to know the number of atoms in the molecule and the molecular mass M, both of which are difficult to determine in the case of polymers. The task is simplified if one proceeds as follows (70). Let the average number of repeating units per macromolecule be n and the molecular mass of this unit M_0; then the molecular mass of the polymer, M, can be given by $M = nM_0$. In turn, the number of atoms in the macromolecule will be given by $P = nP_0$, where P_0 is the number of atoms in the repeating unit of the polymer chain. Obviously, $P/M = P_0/M_0$. This ratio can be easily calculated if the chemical structure of the polymer is known. For example, the structural formula of polyethylene is $[-CH_2-CH_2-]_n$ and, hence, $P_0 = 6$ and $M_0 = 28$. For polytetrafluoroethylene, which has the structure $[-CF_2-CF_2-]_n$, the corresponding figures are as follows: $P_0 = 6$ and $M_0 = 100$; for polyformaldehyde $[-CH_2O-]_n$, $P_0 = 4$ and $M_0 = 30$.

Ultrasonic measurements at helium temperatures (122, 367, 368, 370, 372, 375, 376) have been used (70, 385) to calculate Debye temperatures for some polymers with the aid of formula (9.1). The results of calculations of θ_D for a number of polymers are presented in Figs. 9.1 and 9.2. For low-molecular-mass substances the Debye temperature θ_D found from acoustic measurements depends little on temperature (386). The difference in the Debye temperatures found from measurements of sound velocity at 4.2 and 300 K is usually 10-12 per cent (386). In the case of polymers (see Figs. 9.1 and 9.2) θ_D depends strongly on temperature, changing sometimes by 1.5 times in the temperature range 4.2 to 240 K. This is associated to a considerable extent with the dispersion of the velocity of elastic waves at high temperatures Strictly speaking, θ_D can be determined only from acoustic or calorimetric measurements made near 0 K, when there is no dispersion of Debye waves.

It should be noted that with linear crystalline polymers for which there is a plateau near 4.2 K in the temperature dependence of sound velocity a plateau also appears near 0 K on the graph of θ_D against T. However, in this case also the Debye temperatures found from acoustic measurements always exceed the values of θ_D calculated from direct calorimetric measurements. For example, for polyethylene the Debye temperature determined on the basis of ultrasonic measurements from formula (9.1) is 320 K and for polytetrafluoroethylene it is 166 K, whereas the values of θ_D found from calorimetric measurements at 4.2 K are, respectively, 231 and 96 K.

The cause of this difference is not clear at present. It is possible that no explanation can be given on the basis of the harmonic approximation typical of the Debye theory, since it could be caused by anharmonicity (387). But evidently the presence of anharmonicity is not the only factor responsible for the discrepancy between the Debye temperatures found by acoustic and calorimetric measurements. The following regularity should be noted. As the degree of crystallinity increases the Debye temperature

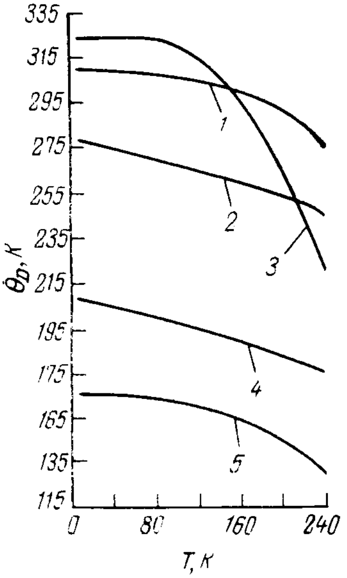

FIG. 9.1 Debye temperatures calculated from acoustic measurements:

1—polyformaldehyde; *2*—polypropylene; *3*—polyethylene; *4*—polycarbonate; *5*—polytetrafluoroethylene.

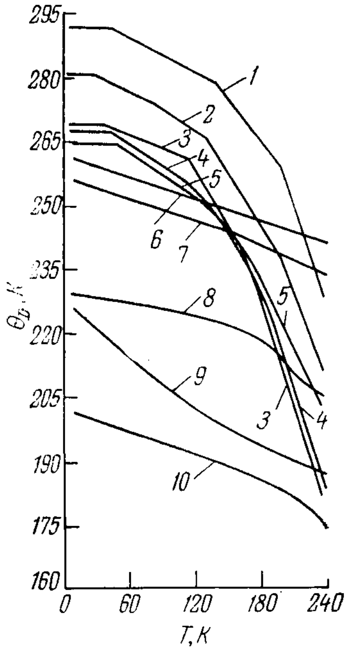

FIG. 9.2. Debye temperatures calculated from acoustic measurements for polymers (the values of M/P are given in parentheses):

1—Nylon 6,10 (5.6); *2*—Nylon 7 (5.8); *3*—Nylon 11 (5.4); *4*—Nylon 12 (5.3); *5*—Nylon 6 (5.95); *6*—polymethyl methacrylate (6.7); *7*—polyvinylidene fluoride (10.7); *8*—polyvinyl fluoride (7.7); *9*—polystyrene (6.5); *10*—polyvinyl chloride (10.4).

found by calorimetric measurements increases noticeably and the difference between $(\theta_D)_{ac}$ and $(\theta_D)_{cal}$ becomes smaller. However, in the case of amorphous polymers the difference is substantially greater. For example, the Debye temperatures calculated for polymethyl methacrylate and polystyrene from acoustic measurements at low temperatures are 262 and 227 K respectively, while the corresponding values of $(\theta_D)_{cal}$ are 115 and 95 K (66). For crystalline polymers the ratio $(\theta_D)_{ac}/(\theta_D)_{cal}$ is, as a rule, smaller than in the case of amorphous polymers. For instance, for crystalline polymers such as polyethylene and polytetrafluoroethylene the ratio is 1.39 and 1.73, respectively, and for polymethyl methacrylate and polystyrene (amorphous polymers) the ratios are 2.48 and 2.39. Since the Debye temperatures determined from acoustic measurements at low temperatures exceed $(\theta_D)_{\text{cal}}$, the heat capacities of polymers at $T \to 0$ K, calculated from the Debye formula (1.22) and using the values of $(\theta_D)_{\text{ac}}$, will appear to be considerably lower than those obtained from direct measurements.

Excessively high values of $(\theta_D)_{\text{ac}}$ might be expected to arise from the assumptions made in using the Debye formula (9.1). The heat capacity can, however, be calculated from acoustic measurements without resorting to the calculation of Debye temperatures. Indeed, substituting the value of θ_D from expression (1.17) into formula (1.22), we obtain the following expression for the specific heat:

$$\frac{C_v}{T^3} = \frac{2\pi^2 k^4}{5\hbar^3} \cdot \frac{1}{\rho \bar{c}^3} \tag{9.2}$$

where $\bar{c}$ is the average sound velocity determined from formula (1.15).

Except for the density and the velocities of longitudinal and transverse waves, no other parameters that have to be determined by experiment appear in formula (9.2). Nevertheless, calculations made by formula (9.2) also give values of specific heat for polymers (357) which are too low compared with those found from direct calorimetric measurements.

It has been shown (33, 66) that the Debye contribution to the low-temperature heat capacity of amorphous polymers (at $T < < 4.2$ K) is several times lower than values obtained experimentally. This means that at low temperatures the main contribution to heat capacity is made by non-acoustic vibrations, which can be described by the Einstein function. The mechanism of these vibrations and their relationship to the supermolecular structure of amorphous polymers were discussed in Chapter 1.

Note that for the temperature dependence of the heat capacity of polymers at $T \to 0$ K to be described fully by the Debye theory calorimetric measurements alone are not sufficient. Even if the heat capacity measured by direct methods displays a cubic dependence on temperature, we cannot yet be certain that the heat capacity can be fully described by the Debye theory. For such a statement to be made, it is necessary that the heat capacity calculated from acoustic measurements at high ultrasonic frequencies at $T \to 0$ K be consistent with the results obtained by calorimetric measurements.

The Debye temperatures found from acoustic measurements have been used (70, 385) to calculate the heat capacities of a number of polymers (Fig. 9.3) in the temperature range 10 to 240 K. The use of the Tarasov theory (8) allows us to calculate the temperature dependence of heat capacity from formula (1.37) for a number of polymers. The choice of a formula which gives a linear dependence of heat capacity on temperature is accounted for by the fact that most experimental results are described most successfully by a linear dependence. It has been found that for polytetrafluoroethylene in the temperature range 15 to 230 K and for polyethylene in the range 30 to 210 K the dependence of heat capacity on temperature is close to linear and that the heat capacities calculated from acoustic data agree quite satisfactorily with the results obtained by calorimetric measurements. The discrepancy between the calculated and experimentally found values of heat capacity does not exceed 10-11 per cent.

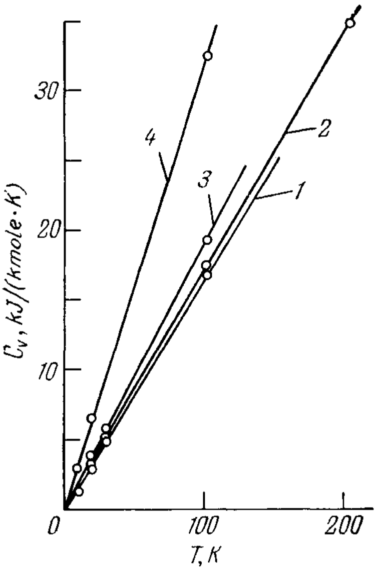

FIG. 9.3. Temperature dependence of the heat capacity calculated from acoustic measurements:

1—high-pressure polyethylene; 2—polyformaldehyde; 3—polypropylene; 4—polytetrafluoroethylene.

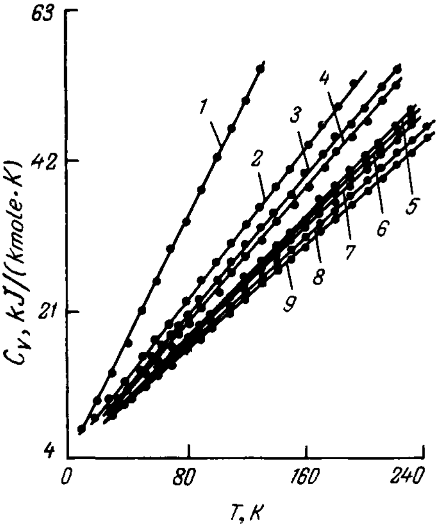

FIG. 9.4. Temperature dependence of the heat capacity calculated from acoustic measurements:

1—poly-4-methyl pentene-1; 2—polyvinyl chloride; 3—polystyrene; 4—polyvinyl fluoride; 5—polymethyl methacrylate; 6—Nylon 6; 7—Nylon 11; 8—Nylon 7; 9—Nylon 6,10.

The results of calculations of the heat capacity of other polymers are given in Figs. 9.3 and 9.4. These results were compared with the generalized heat capacity values used by Wunderlich (7), and also with the results of direct calorimetric measurements obtained by other authors. Comparison of these results with the data obtained by direct calorimetric measurements reveals an appreciable difference in the values of heat capacity. For example, the specific heats of polystyrene and polymethyl methacrylate (7, 65) exceed by 1.5-2 times the specific heat values calculated from acoustic measurements. A much better agreement is obtained between the calculated values of heat capacity and the results of direct measurements for polyvinyl chloride (388) and for poly-4-methyl pentene-1 (7). For polyvinyl chloride an especially good agreement is obtained in the low-temperature region (to 150 K). An increase in temperature up to 240 K produces a 25-percent difference between the values compared. In the case of poly-4-methyl pentene-1 a satisfactory agreement is obtained above 120 K (the difference not exceeding 20 per cent); below this temperature the agreement is poor.

A close agreement between the heat capacity values calculated from acoustic measurements by formula (1.37) and those found from calorimetric measurements is characteristic of linear polymers with a weak interchain interaction (polyethylene and polytetrafluoroethylene). This agreement is not surprising since formula (1.37) was derived by Tarasov for the case of non-interacting chains.

For polymers with a stronger intermolecular interaction (polystyrene, polymethyl methacrylate, polyamides) a considerable discrepancy arises when the heat capacity values found from acoustic measurements and formula (1.37) are compared with those obtained by calorimetric measurements; this discrepancy may be due to two factors. On the one hand, not only one-dimensional Debye vibrations but also other vibrational modes that can occur in the temperature range 20-240 K can make a contribution to heat capacity at these temperatures. On the other hand, the sufficiently strong intermolecular interaction observed in these polymers apparently does not allow one to use the version of the Tarasov theory based on the assumption that the interchain interaction can be ignored as compared with the interaction between the atoms that make up the skeleton of the polymeric chains.

The dependence of the specific heat of polymers, calculated on the basis of the results of acoustic measurements, on their chemical constitution (see Fig. 9.4) seems interesting. The results given in Fig. 9.4 show that the highest values of heat capacity are characteristically exhibited by polymers with a weak intermolecular interaction, in particular poly-4-methyl pentene-1. As the intensity of intermolecular interaction increases the value of specific heat decreases. The presence of the polar groups Cl, C_6H_5, or $COOCH_3$ in the side chain of polymers brings about an appreciable decrease in the specific heats of polyvinyl chloride, polystyrene, and polymethyl methacrylate as compared with poly-4-methyl pentene-1. The lowest values of heat capacity are shown by polymers with strong hydrogen atoms closely spaced between the chains: Nylon 7 and Nylon 6,10.

It is interesting that an analogous dependence is also typical of Poisson's ratios for these polymers (see Chapter 8), a fact which once again indicates that there is a close relationship between the viscoelastic behaviour of polymers and their thermophysical properties.

9.2. DETERMINING THE THERMAL EXPANSION COEFFICIENTS AND GRÜNEISEN CONSTANTS FROM ACOUSTIC MEASUREMENTS

An important parameter characterizing the thermal properties of polymers is the Grüneisen constant defined by

$$\gamma = -\frac{\partial \ln \theta_D}{\partial \ln V}$$

The Grüneisen constant characterizes the anharmonicity of the vibrations of atoms, which is responsible for thermal expansion; it is directly related to the potential of intermolecular interaction. For polymers with rigid chains, which are subject to a van der Waals interaction, such a relationship can be written in the form (392):

$$\gamma = (m + n + 2)/4 \tag{9.3}$$

where m and n are exponents in the interaction potential (for example, for the Leonard-Jones potential $m = 6$, $n = 12$ and $\gamma = 5$).

For an isotropic elastic body the Grüneisen constant is a scalar quantity and can be determined by two different methods. One is based on measurements of the velocities of longitudinal and transverse waves at different pressures (i.e., is based on the study of the dependence of θ_D on pressure). Indeed, by using expressions (1.17) and (3.18) it is not difficult to show that

$$\gamma = \frac{(1/c)\,(\partial \bar{c}/\partial p)}{\beta_T} + \frac{1}{3} \tag{9.4}$$

where $\bar{c}$ is the average velocity of sound [see formula (1.15)]; p is the pressure; β_T is the isothermal compressibility.

The second method of determining γ is based on the use of data on thermal expansion coefficients and adiabatic bulk moduli.

In this case, a modified Grüneisen equation is used (3.15):

$$\gamma = \frac{3\alpha K_s}{\rho C_p} \tag{9.5}$$

where α is the linear thermal expansion coefficient; K_s is the adiabatic bulk modulus; ρ is the density; C_p is the specific heat at constant pressure.

If the values of α, ρ and C_p are known, one can determine K_s by measuring the velocities of longitudinal and shear waves and find the Grüneisen constant (389-391) by using formula (9.5).

It is usually assumed that γ is independent of temperature. However, the values of γ calculated by formula (9.5) for polymers differing widely in chemical constitution and structure show (389-391) that $\gamma = f(T)$ for most polymers. Barker (392) has proposed a model according to which a polymer consists of a sequence of rigid, almost parallel chains with an interaction potential of the Mie or Morse type and has shown that the Grüneisen constant may depend on temperature.

Expression (9.5) has been used (385, 389-391) to determine the Grüneisen constant from acoustic measurements. The results of such calculations for the temperature range 4.2-240 K are given in Figs. 9.5 and 9.6. Over this temperature range quantity γ is strongly dependent on chemical constitution and increases with increasing intermolecular interaction in the polymer. The highest values of γ in the entire temperature range are shown by polyamides, in which the intermolecular interaction is quite intensive due to the presence of hydrogen bonds.

The lowest value of the Grüneisen constant is exhibited by polyethylene (see Fig. 9.5), which is characterized by a weak intermolecular interaction. Of interest is the fact that the values of Grüneisen constants depend on the molecular mass of the repeating unit of the polymer. The value of γ increases with increasing molecular mass of the repeating unit. The only exception is polystyrene ($M_0 = 104$), whose Grüneisen constant is lower than that of polymethyl methacrylate ($M_0 = 100$).

As the temperature falls (see Figs. 9.5 and 9.6) the value of the Grüneisen constant for all polymers increases. The sharpest increase in the Grüneisen constant occurs at the lowest temperatures, where the γ values are quite impressive. Since the Grüneisen constant is associated with the potential of intermolecular interaction, a relative increase in this potential with decreasing temperature serves as an indication of intensification of the intermolecular interaction in the polymer.

However, rather high values of γ at temperatures close to 4.2 K, which are indicative of strong anharmonicity in polymers under these conditions, contradict the usual concepts, according to which anharmonicity near 0 K must vanish. The possibility cannot be excluded that the equation of state (9.5), which is used to determine γ, does not hold at $T \rightarrow 0$ K. Nevertheless, the sharp increase in anharmonicity observed in polymers near 4.2 K deserves special consideration.

Such an increase in the Grüneisen constant with decreasing temperature was observed by Barker (390) for polystyrene and polyethylene. At room temperature the γ values of polystyrene and polymethyl methacrylate are close to unity (390). Analogous results at 20°C were obtained (389) for polymethyl methacrylate ($\gamma = 0.88$) and for Nylon 6 ($\gamma = 0.91$). The Grüneisen constant obtained for polymethyl methacrylate from data on the dependence of ultrasonic velocity on pressure at 25°C is 1.11 (391). It has been shown (385) that at room temperature the γ values of a

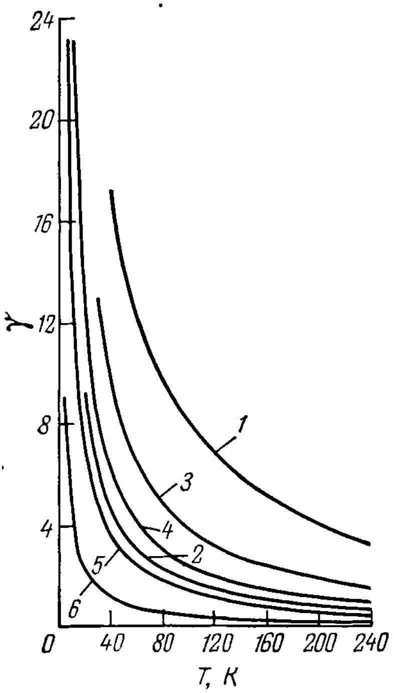

FIG. 9.5. Temperature dependence of the Grüneisen constant:

1—polycapramide; *2*—polyvinylidene fluoride; *3*—polymethyl methacrylate; *4*—polycarbonate; *5*—polytetrafluoroethylene; *6*—high-density polyethylene.

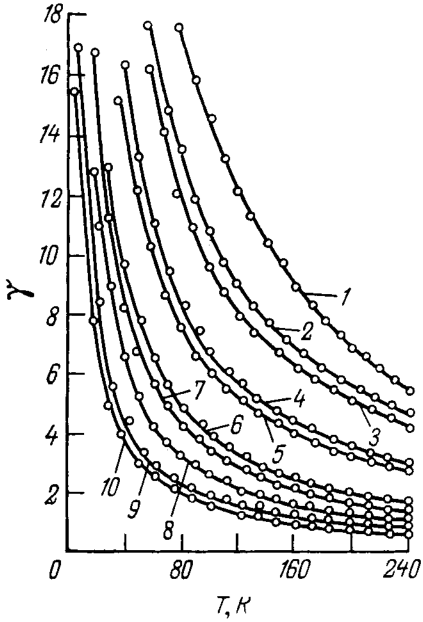

FIG. 9.6. Temperature dependence of the Grüneisen constant in the region of liquid-helium temperatures:

1—Nylon 6,10; *2*—Nylon 12; *3*—Nylon 11; *4*—Nylon 7; *5*—Nylon 6; *6*—polymethyl methacrylate; *7*—polystyrene; *8*—poly-4-methyl pentene-1; *9*—polyvinyl chloride; *10*—polyvinyl fluoride.

number of polymers are also close to unity. For example, the values of γ for Nylon 6, polymethyl methacrylate, polystyrene and polyvinyl chloride at 290 K are, respectively, 1.8, 1.4, 1.1, and 0.6.

Abnormally high values of γ (approximately equal to 4) have been obtained by Wada and his collaborators for polyethylene, polystyrene and polymethyl methacrylate (393). They used the dependence of sound velocity on pressure. Moreover, these authors conclude that the Grüneisen constant increases with increasing temperature, this being inconsistent with the results obtained by other workers (385, 389-391). This conclusion can be regarded as a very special case and may be valid only for a limited temperature range in the vicinity of T_g. It has been found (389) that the Grüneisen constant γ passes through a maximum as the glass-transition temperature of the polymer is being passed.

The very high values of the Grüneisen constant ($\gamma \approx 4$) for two polymers were obtained by Wada in an unusual way. Using expression (9.4), Wada first calculated the values of γ for polystyrene and polymethyl methacrylate and then the specific heats C_v of these polymers using Eq. (3.15). The values of C_v obtained in this way are equal to 0.26 kJ/(kg·K) for polystyrene and 0.22 kJ/(kg·K) for polymethyl methacrylate. These values of C_v are several times lower than those obtained by calorimetric measurements. In this connection, Wada (393) assumed that Eq. (3.15) must have the following form:

$$\gamma = \frac{\beta V K_T}{C_{\text{int}}} \tag{9.6}$$

where C_{int} is the heat capacity due to vibrations of the chain units, these being responsible for the intermolecular interaction in the polymer.

It is assumed (393) that Eq. (9.6) holds true for any molecular solids with two different bonding forces in the lattice. Thus, formula (9.6) is based on the assumption that the main contribution to the quantity γ is made by interchain vibrational modes. Wada used the Dulong-Petit law for calculating the molecular mass M_l of a vibrating unit and showed that the values of M_l obtained for polystyrene and polymethyl methacrylate ($M_l = 95$) are in satisfactory agreement with the molecular mass of the repeating units (104 and 100). However, analogous calculations (393) show that for polyethylene $M_l = 143$, which exceeds 10 times the molecular mass of the repeating unit.

The Wada hypothesis rests on two physical assumptions: (1) a polymer is regarded as a vibrating lattice; (2) low-frequency vibrational modes are assumed to be more sensitive to a change in density than high-frequency modes of vibration. Since the energy of intermolecular (interchain) interaction is much lower than the energy of interaction between the atoms present in the main chain of the polymer and linked to each other through covalent bonds, it is assumed that the anharmonicity of interchain vibrations is greater. In other words, low-frequency (interchain) vibrations are more sensitive to a change in volume and make a bigger contribution to the value of the Grüneisen constant and thermal expansion than do high-frequency (intrachain) vibrations.

This viewpoint is considered to be quite convincing, but the abnormally high values of γ which differ from the results obtained by other methods and also the tenfold overestimation of the value of M_l in the case of polyethylene do not allow reliable conclusions to be drawn as to how well the Wada hypothesis agrees with experiment.

There is a definite correlation between the viscoelastic parameters and thermal expansion of polymers. Barker (390, 392), for example, has shown that the following simple relation connecting Young's modulus E' with the linear thermal expansion coefficient α holds true for many polymers over a wide temperature range:

$$E'\alpha^2 \approx 15\ \mathrm{N/(m^2 \cdot K^2)} \tag{9.7}$$

This relation indicates that there must exist a correlation between the modulus of elasticity E', which is based on the harmonic nature of the bonding forces operating between atoms, and thermal expansion governed by the anharmonicity of atomic vibrations. This correlation implies the existence of a correlation between the harmonic and anharmonic moduli of elasticity. Barker attempted (390, 392) a theoretical substantiation of relation (9.7), but the only reasonable argument in its favour is the connection between the first and second compressibility coefficients (a_1 and a_2) in the Bridgman relation:

$$-\Delta V/V_0 = a_1p + a_2p^2 + a_3p^3 \tag{9.8}$$

where V is the volume and p is the pressure.

We know that for polymers (392)

$$c_2 = a_2/a = -4.0 \pm 0.1 \tag{9.9}$$

Formula (9.7) was tested by using the values of Young's modulus calculated from ultrasonic measurements in polyt trafluoroethylene over the temperature range 4.2 to 240 K (381) and the results of direct measurements of the linear thermal expansion coefficient of this polymer (171). It was found that the α values determined from dilatometric and acoustic measurements coincide only in order of magnitude (Fig. 9.7). Apart from the approximate nature of relation (9.7), this difference may also arise from the difference between the degrees of crystallinity of the polytetrafluoroethylene samples used for dilatometric ($\rho = 2.25$ Mg/m^3) and acoustic ($\rho = 2.18$ Mg/m^3) experiments. The best agreement is obtained for polycapramide.

The values of α obtained, by different methods, for polycapramide are rather close and differ by no more than 15 per cent for the temperature range 4.2-293 K. An especially good agreement is obtained at temperatures close to 4.2 K.

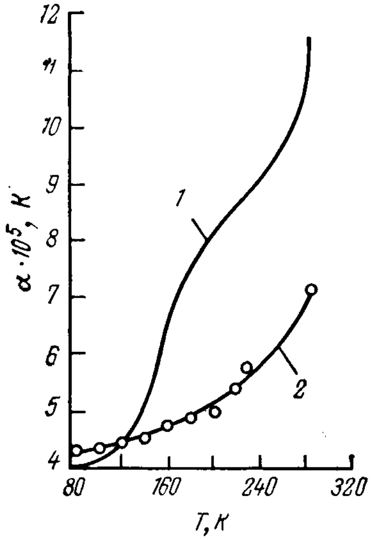

FIG. 9.7. Temperature dependence of the linear thermal expansion coefficient of polytetrafluoroethylene:

1—measured values (171); 2—values calculated from acoustic measurements.

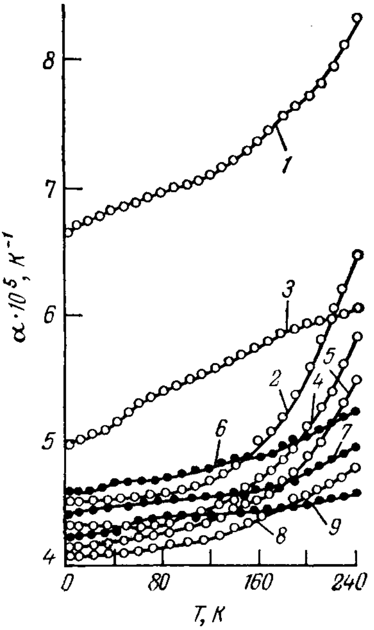

FIG. 9.8. Temperature dependence of the linear thermal expansion coefficient calculated by the Barker formula:

1—poly-4-methyl pentene-1; 2—Nylon 11; 3—polystyrene; 4—Nylon 6; 5—Nylon 7; 6—polyvinyl chloride; 7—polyvinyl fluoride; 8—Nylon 6,10; 9—polymethyl methacrylate.

The values of the linear thermal expansion coefficient obtained by dilatometric measurements (157) made at temperatures —180 to +20°C for polystyrene agree well with the results calculated from formula (9.7). The α values obtained for polystyrene by the two methods differ by no more than 12 per cent. The linear thermal expansion coefficients of polymethyl methacrylate and poly-4-

methyl pentene-1 determined at low temperatures (156) differ from the α values calculated from formula (9.7) (Fig. 9.8) by a factor of about two. It is, however, necessary to take into account that Barker, when deriving relation (9.7), implied that the right-hand side of this relation must include the coefficient S (for some materials of the type of organic glass $0.5 \leqslant S \leqslant 2$). If we apply this condition to polymethyl methacrylate and poly-4-methyl pentene-1, the values of α calculated in this way will agree satisfactorily with the results of direct dilatometric measurements.

Thus, the approximate Barker relation allows one to determine the thermal expansion coefficients of polymers quite accurately if the velocities of longitudinal and transverse waves in them are known.

APPENDIX

SOME THERMOPHYSICAL, DIELECTRIC, VISCOELASTIC AND ACOUSTICAL PARAMETERS OF POLYMERS AT LOW TEMPERATURES

TABLE 1. *The Heat Capacities C_p of Some Polymers at Low Temperatures*

Polymer	C_p, kJ/(kmol·K)			θ_D, K	θ_1, K (after Tarasov)	θ_3, K (after Tarasov)	ρ (Mg/m³) or ϰ (%)
	4 K	80 K	290 K				
Polyethylene, linear high-density (7):							
amorphous	28×10^{-3}	7.87	31.5	—	540	147	—
completely crystalline	7.1×10^{-3}	7.87	21.1	260	—	—	—
Polytetrafluoroethylene (7, 40)	0.284 (at 5 K)	16	51.7 (at 280 K)	96	—	—	2.16
Polypropylene (48):							
atactic	4.97	23.5	87.4	—	—	—	16%
isotactic	4.11 (at 20 K)	21.5	73.4	—	—	—	48%
Polytrifluorochloroethylene (40)	0.418	—	—	67	—	—	2.114
Polyformaldehyde (Delrin-1500) (48)	2.44 (at 20 K)	14.55	41.8	—	—	—	—
Nylon 6,6 (40)	0.232 (at 3.6 K)	—	—	73	—	—	—
Nylon 6 (59)	—	56.4	172 (at 300 K)	—	—	—	1.14
Nylon 7 (59)	—	66.5	236 (at 300 K)	—	—	—	—
Polymethyl methacrylate (7, 66)	0.206	46.0	134	115	—	—	—
Polystyrene, atactic (7, 66)	0.536	39.7	123	95	—	—	—
Polyvinyl chloride (7, 388)	—	23.3	57.5	—	350 (383)	175	—
Polycarbonate (48)	25.4 (at 20 K)	91.2	296	—	—	—	—

TABLE 2. *The Thermal Conductivities of Some Polymers at Low Temperatures*

Polymer	$\varkappa$, W/(m·K)			ρ, Mg/m^3
	4 K	80 K	290 K	
Polyethylene (105, 101)	2×10^{-2} (at 5 K)	0.47	0.397 (at 300 K)	0.95
Polytetrafluoroethylene (40, 94, 101)	4.4×10^{-2}	0.25	0.24	2.16 to 2.17
Nylon 6,6 (95, 98, 105)	1.2×10^{-2}	0.1 (at 20 K)	—	1.14
Polyformaldehyde (102)	—	0.493	0.42	1.441
Polystyrene (99)	2.5×10^{-2}	—	—	—
Polymethyl methacrylate (33, 99, 102)	5×10^{-2}	0.14	0.2 (at 300 K)	—

TABLE 3. *Linear Thermal Expansion Coefficients of Some Polymers at Low Temperatures*

Polymer	$\alpha\cdot10^5$ K^{-1}			
	4 K	20 K	80 K	280 K
Polyethylene (128)	—	8.9	10.7	18.4
Polyethylene, low-density (160)	7.1	—	13.4	—
Polytetrafluoroethylene (128, 160)	6.8	7.7	7.6-9.1	19.5 (at 260 K)
Polypropylene (157)	—	—	5.3	19.5
Polytrifluorochloroethylene (129)	—	4.1	4.5	6.9
Polystyrene (129, 157)	—	5.6	5.5-6.1	7.2-8.5
Polymethyl methacrylate (129)	—	4.4	4.9	7.6
Nylon 6,6 (129)	—	5.1	5.9	8.2

TABLE 4. *The Dielectric Properties of Some Polymers at Low Temperatures*

Polymer	ε'		$\tan\delta\cdot10^5$		ν, kHz
	4 K	290 K	4 K	290 K	
Polyethylene (209, 210):					
low-density*	—	—	2.7	39.6	1
high-density**	2.27	2.2	5.5	17.3	1
Polytetrafluoroethylene (205, 206, 212)	2.12	2-2.05	0.12-2.5	9-30	0.075-1
Polypropylene (205, 206, 221)	2.35	2.25	0.35-2	85	0.050-20
Nylon 6,6 (205)	2.9	4.1	12	1500	0.075
Nylon 11 (209)	2.4	3.22	3	4000	0.047
Polyethylene terephthalate (205, 212)	2.8	3.13-3.15	11.5-17	118-410	0.075-1
Polyvinyl fluoride (212)	3.45	9.2	56	1600	1
Polystyrene (205, 225)	2.52-2.63	2.5-2.6	1.49-6	11.5-40	0.075-1
Polycarbonate (212)	—	—	9.5	210	1

* $\varkappa = 48$ per cent.
** $\varkappa = 76$ per cent.

TABLE 5. *The Debye Temperatures Found for Some Polymers from Ultrasonic Measurements* ($\nu = 5$ MHz) *at* 4.2 K, 77 K *and* 240 K

Polymer	θ_D, K		
	4.2 K	77 K	240 K
Polyformaldehyde	310	306	274
Polyethylene, high-density	320	320	228
Polytetrafluoroethylene	166	164	130
Nylon 6	265	259	195
Nylon 7	282	273	212
Nylon 6,10	292	288	229
Nylon 11	269	264	183
Polypropylene	280	270	245
Polymethyl methacrylate	262	255	242
Polycarbonate	402	384	335
Poly-4-methyl pentene-1	195	187	158
Polystyrene	226	211	188
Polyvinyl fluoride	229	227	206
Polyvinyl chloride	202	195	176
Polytrifluorochloroethylene	141	136	122

TABLE 6. *The Velocities of Longitudinal and Transverse Ultrasonic Waves* ($\nu = 5$ MHz) *in Polymers at Low Temperatures*

Polymer	4.2 K		77 K		293 K	
	c_l, m/s	c_t, m/s	c_l, m/s	c_t, m/s	c_l, m/s	c_t, m/s
Polyformaldehyde ($\varkappa = 74$ per cent) (122)	3725	1950	3640	1920	2630	1390
Polyethylene, low-density ($\varkappa = 46$ per cent) (122)	3740	2015	3740	2015	2360	1100
Polyethylene, high-density ($\varkappa = 74$ per cent) (122)	3690	1960	3690	1960	2540	1180
Polytetrafluoroethylene ($\varkappa = 50$ per cent) (122)	2330	1180	2330	1170	1410	730
Nylon 6 ($\rho = 1.143$ Mg/m^3) (368)	3470	1610	3430	1570	2980*	1190*
Nylon 7 ($\rho = 1.06$ Mg/m^3) (368)	3430	1760	3410	1670	2930*	1270*
Nylon 6,10 ($\rho = 1.094$ Mg/m^3) (368)	3460	1780	3420	1750	2920*	1380*
Nylon 11 ($\rho = 1.037$ Mg/m^3) (368)	3410	1630	3350	1600	2690*	1090*
Nylon 12 ($\rho = 1.027$ Mg/m^3) (368)	3380	1630	3340	1590	2730*	1110*
Polypropylene ($\rho = 0.896$) (367)	3420	1750	3310	1690	2630	1340
Epoxide resin ЭД-5 (367)	3360	1630	3290	1600	2820	1340
Polymethyl methacrylate (372)	3160	1630	3110	1600	2940*	1490*
Polycarbonate (367)	2960	1360	2860	1290	2330	1030
Poly-4-methyl pentene-1 ($\rho = 0.811$)	2720	1230	2610	1180	2340*	1000*
Polystyrene (375)	2870	1480	2710	1350	2420*	1200*
Polyvinyl fluoride ($\rho = 1.402$) (375)	2960	1420	2900	1390	2670*	1280*
Polyvinyl chloride ($\rho = 1.389$) (375)	2800	1390	2760	1350	2530*	1220*
Polytrifluorochloroethylene ($\rho = 2.135$) (370)	2330	1060	2250	1020	1900	820

* These values were obtained at 240 K.

TABLE 7. *The Elastic Parameters of*

Polymer	4.2 K			
	$E' \cdot 10^{-3}$, MPa	$G' \cdot 10^{-3}$, MPa	$K'_s \cdot 10^{-3}$, MPa	σ'
Polyformaldehyde (265, 381)	14.3	5.2*-5.4	12.6	0.31
Polyethylene (265, 381)	10.3**-10.8	3.7	7.1	0.25
Polytetrafluoroethylene (265, 381)	7.9	2.2*-3.0	7.9	0.33
Polypropylene (265, 381)	7.3-7.5**	2.15*-2.8	6.8	0.32
Polytrifluorochloroethylene (381)	6.5	2.4	8.4	0.37
Nylon 6 (380)	8.0	2.9	9.7	0.36
Nylon 6,6 (265)	9.2**	—	—	—
Nylon 7 (380)	8.5	3.1	8.7	0.34
Nylon 6,10 (380)	9.2	3.5	8.5	0.32
Nylon 11 (380)	7.5	2.8	8.3	0.35
Nylon 12 (380)	7.3	2.7	8.1	0.35
Poly-4-methyl pentene-1 (265, 380)	3.4-5.0**	1.2-2.0*	4.4	0.37
Polymethyl methacrylate (265, 380)	7.8**-8.3	3.2*	7.7	0.32
Polycarbonate (381)	6.0	2.2	7.6	0.37
Epoxide resin ЭД-5 cured with *m*-phenylene diamine	8.6	3.2	9.3	0.35
Polyvinyl fluoride (380)	7.6	2.8	8.5	0.35
Polyvinyl chloride (265, 380)	6.8**-7.2	2.7	7.3	0.34
Polystyrene				
atactic (380)	6.1	2.3	5.6	0.32
isotactic (265)	6.1**	2.3*	—	—
isotactic, cured (265)	5.6**	—	—	—
Polyethylene terephthalate (265)	—	2.3*	—	—
Polypyromellite imide (265)	6.2**	—	—	—
Polyvinyl acetate (265)	—	2.0*	—	—

Note: 1. The elastic parameters were calculated (380, 381) from ultrasonic not at 293 K.

* Measured on a torsion pendulum at a frequency of about 1 Hz (265).

** Measured at a frequency of 10^4 Hz (265).

Polymers at Low Temperatures

77 K				293 K			
$E' \cdot 10^{-3}$, MPa	$G' \cdot 10^{-3}$, MPa	$K'_s \cdot 10^{-3}$, MPa	σ'	$E' \cdot 10^{-3}$, MPa	$G' \cdot 10^{-3}$, MPa	$K'_s \cdot 10^{-3}$, MPa	σ'
13.8	5.3	12	0.31	7.1	2.8	5.8	—
9.7**-10.8	3.7	7.1	0.25	2.9**-3.5	1.1	3.4	—
7.7	2.1*-3	7.9	0.33	3	0.35*-1.15	2.3	—
6.9-7.0**	1.9*-2.6	6.4	0.32	2.4**-4.2	1.6	3.8	—
6.0	2.2	7.8	0.37	4.1	1.4	5.7	—
7.7	2.8	9.7	0.37	4.4	1.56	8	0.41
8.6**	—	—	—	4.1**	—	—	—
8.15	2.9	8.7	0.34	4.9	1.7	6.8	0.38
8.8	3.3	8.4	0.325	5.6	2.1	6.5	0.36
7.2	2.7	8.1	0.35	3.5	1.25	5.75	0.4
7.0	2.6	8.0	0.36	3.5	1.2	6.0	0.4
3.10-4.1**	1.1-1.7*	4.0	0.37	2.25-2.3**	0.81-0.89*	3.3	0.39
7.5**-8.0	3.0-3.1*	7.4	0.32	7.0	2.6	6.75	0.33
5.5	2.0	7.1	0.37	3.7	1.26	4.7	—
8.3	3.1	8.9	0.35	6.0	2.2	6.6	—
7.3	2.7	8.1	0.35	6.2	2.3	7.00	0.35
6.4**-6.9	2.6	7.2	0.34	3**-5.5	2.1	6.1	0.35
5.1	1.9	5.2	0.34	4.1	1.5	4.1	0.34
5.0**	1.8*	—	—	4.4**	—	—	—
4.6**	—	—	—	3.3**	—	—	—
—	2.1*	—	—	—	1.1*	—	—
5.9**	—	—	—	3.4*	—	—	—
—	1.8*	—	—	—	—	—	—

measurements at 5 MHz. 2, The elastic parameters were obtained (380) at 240 K,

TABLE 8. *The Grüneisen Constants and Linear Thermal Expansion Coefficients of Some Polymers at* 4.2, 77 *and* 240 K *Found from Ultrasonic* ($\nu = 5$ MHz) *Measurements*

Polymer	4.2 K		77 K		240 K	
	$\alpha \cdot 10^5$, K^{-1}	γ	$\alpha \cdot 10^5$, K^{-1}	γ	$\alpha \cdot 10^5$, K^{-1}	γ
Nylon 6	4.3	10*	4.4	7.6	5.9	2.6
Nylon 7	4.2	11*	4.3	8.3	5.5	2.8
Nylon 6,10	4.1	28*	4.1	—	4.8	5.4
Nylon 11	4.5	16*	4.6	12	6.6	4.2
Nylon 12	4.5	17.9*	4.6	13.6	6.6	4.7
Polyvinyl chloride	4.6	8.4**	4.7	2.1	5.2	0.7
Polyvinyl fluoride	4.4	7.9**	4.5	1.9	4.9	0.6
Polystyrene	5.0	11.2***	5.4	4.3	6.1	1.3
Polymethyl methacrylate	4.2	13***	4.3	4.9	4.6	1.5
Poly-4-methyl pentene-1	6.7	13**	7	3.3	8.2	1.0

* At 60 K.
** At 20 K.
*** At 30 K.

REFERENCES

1. Einstein, A., *Ann. der Physik*, **22**, 1, 180 (1907).
2. Einstein, A., *Ann. der Physik*, **34**, 1, 170 (1911).
3. Kittel, C., *Introduction to Solid State Physics*, John Wiley, New York, 1976.
4. Debye, P., *Ann. der Physik*, 39, 4, 789 (1912).
5. Blackman, M., in: *Handbuch der Physik*, **7**, 1, 325 (1955).
6. Born, M. and Th. Kármán, *Phys. Z.*, **13**, 5, 297 (1912).
7. Wunderlich, B. and H. Baur, *Heat Capacities of Linear High Polymers*, Springer-Verlag, Berlin, Heidelberg, New York, 1970.
8. Tarasov, V. V., *Zhur. Fiz. Khim.*, **24**, 1, 111 (1950).
9. Tarasov, V. V., *Zhur. Fiz. Khim.*, **27**, 9, 1430 (1953).
10. Tarasov, V. V., *New Problems in the Physics of Glass*, Gosstroiizdat, Moscow, 1959 (in Russian).
11. Tarasov, V. V., *Doklady Akad. Nauk SSSR*, **46**, 1, 22 (1945).
12. Tarasov, V. V. *Doklady Akad. Nauk SSSR*, **54**, 9, 803 (1946).
13. Wunderlich, B., *J. Chem. Phys.*, **37**, 10, 2429 (1962).
14. Tucker, J. E. and W. Rees, *J. Chem. Phys.*, **46**, 4, 1388 (1967).
15. Lifshitz, I. M., *Zhur. Eksper. i Teoret. Fiz.*, **22**, 4, 475 (1952).
16. Lifshitz, I. M., *Zhur. Eksper. i Teoret. Fiz.*, **22**, 4, 471 (1952).
17. Landau, L. D. and E. M. Lifshitz, *Continuum Mechanics*, Gostekhizdat, Moscow and Leningrad, 1944 (in Russian).
18. Stockmayer, W. H. and C. E. Hecht, *J. Chem. Phys.*, **21**, 11, 1954 (1953).
19. Nernst, W. and F. A. Lindemann, *Z. Elektrochem.*, **17**, 18, 817 (1911).
20. Nernst, W., *Ann. der Physik*, 36, 12, 395 (1911).
21. Eucken, A., *Phys. Z.*, **10**, 17, 586 (1909).
22. Furukawa, G. T., *J. Res. Nat. Bur. Stand.*, 57, 2, 67 (1956).
23. Popov, M. M., *Thermometrics and Calorimetry*, 2nd ed., Izd. MGU, Moscow, 1954 (in Russian).
24. Mendelssohn, K., *Cryophysics*, Interscience, New York, 1960.
25. Keesom, P. and N. Pirlman, in: *Low Temperature Physics*, Berlin, 1956.
26. Scott, R., *Cryogenic Engineering*, Van Nostrand, New York, 1959.
27. White, G. K., *Experimental Techniques in Low-Temperature Physics*, 2nd ed., Clarendon Press, 1968.
28. Rose-Innes, A., *Low-Temperature Techniques*, London, 1964.
29. *Experimental Thermodynamics*, vol. 1, *Calorimetry of Non-Reacting Systems*, ed. by J. McCullough and D. Scott, New York, 1968.
30. Melia, T. P., *J. Appl. Chem.*, **14**, 11, 461 (1964).
31. Bartenev, G. M., Yu. A. Gorbatkina, and I. A. Lukyanov, *Plast. Massy*, 1, 56, (1963).
32. Wilhoit, R. C., *J. Chem. Educ.*, **44**, 10, A853, A855, A857, A862, A866, A870, A872, A874, A878, A882 (1967).
33. Rees, W., *J. Macromol. Sci.*, A, **3**, 7, 1257 (1969).
34. Worthington, A. E., P. C. Marx, and M. Dole, *Rev. Sci. Instr.*, **26**, 7, 698 (1955).
35. Karasz, F. E. and J. M. O'Reilly, *Rev. Sci. Instr.*, **37**, 3, 255 (1966).
36. Sorbo, W. de and G. E. Nichols, *J. Phys. Chem. Solids*, **6**, 4, 352 (1958).
37. Passaglia, E. and H. K. Kevorkian, *J. Appl. Polymer Sci.*, **7**, 1, 119 (1963).
38. Furukawa, G. T., E. McCoskey, and G. J. King, *J. Res. Nat. Bur. Stand.*, **42**, 4, 273 (1952).

39. Noer, R. J., C. W. Dempsey, and J. E. Gordon, *Bull. Am. Phys. Soc., Ser.* 2, **4**, 2, 108 (1959).
40. Rees, W. and J. E. Tucker, *J. Chem. Phys.*, **43**, 1, 105 (1965).
41. Genensky, S. M. and G. W. Newell, *J. Chem. Phys.*, **26**, 3, 486 (1957).
42. Sochava, I. V. and O. N. Trapeznikova, *Vestnik LGU*, 16, 65 (1958).
43. Swan, P. R., *J. Polymer Sci.*, 56, 164, 403 (1962).
44. Swan, P. R., *ibid.*, 409.
45. Nielsen, L. E., *J. Appl. Phys.*, 25, 10, 1209 (1954).
46. Sochava, I. V. and O. N. Trapeznikova, *Doklady Akad. Nauk SSSR*, **113**, 4, 784 (1957).
47. Sochava, I. V., *Doklady Akad. Nauk SSSR*, **130**, 1, 126 (1960).
48. Dainton, F. S. *et al.*, *Polymer*, 3, 3, 263 (1962).
49. Wunderlich, B., *J. Chem. Phys.*, 37, 6, 1203 (1962).
50. Wunderlich, B., *ibid.*, 1207.
51. Isaacs, L. L. and C. W. Garland, *J. Phys. Chem. Solids*, **23**, 3, 311 (1962).
52. Rees, W., *J. Appl. Phys.*, 37, 11, 3959 (1966).
53. Tasumi, M., T. Shimanouchi, and T. Miyazawa, *J. Mol. Spectr.*, **9**, 4, 261 (1962).
54. Gotlib, Yu. Ya. and I. V. Sochava, *Doklady Akad. Nauk SSSR*, **147**, 3, 580 (1962).
55. Gotlib, Yu. Ya., in: *The Glassy State*, *Trudy III Vsesoyuznogo Soveshchaniya* (Proceedings of the 3rd All-Union Conference), Izd. Akad. Nauk SSSR, Moscow and Leningrad, 104, 1960 (in Russian).
56. Heise, B., H. G. Kilian, and F. H. Müller, *Koll.-Z.*, **213**, 1-2, 12 (1966).
57. Gopal, E.S.R., *Specific Heat at Low Temperatures*, Plenum Press, New York, 1966.
58. Passaglia, E. and H. K. Kevorkian, *J. Appl. Phys.*, **34**, 1, 90 (1963).
59. Kolesov, V. P., I. E. Paukov, and S. M. Skuratov, *Zhur. Fiz. Khim.*, 36, 4, 770 (1962).
60. Roinishvili, E. Yu., N. N. Tavkhelidze, and V. B. Akopian, *Vysokomol. Soedin.*, B, 9, 4, 254 (1967).
61. Anderson, O. L., *J. Phys. Chem. Solids*, **12**, 1, 41 (1959).
62. Flubacher, P. *et al.*, *J. Phys. Chem. Solids*, **12**, 1, 53 (1959).
63. Zeller, R. C., *Phys. Rev.*, B, **4**, 6, 2029 (1971).
64. Rosenstock, H. B., *J. Phys. Chem. Solids*, **23**, 6, 659 (1962).
65. Sochava, I. V., *Vestnik LGU*, 10, 70 (1961).
66. Choy, C. L., R.G. Hunt, and G. L. Salinger, *J. Chem. Phys.*, 52, 7, 3629 (1970).
67. Stephens, R. B., G. S. Cieloszyk, and G. L. Salinger, *Phys. Letters*, A, **38**, 3, 215 (1972).
68. Zoller, P., D. L. Fehl, and J. R. Dillinger, *J. Polymer Sci.*, A-2, **11**, 7, 1441 (1973).
69. Zoller, P., D. L. Fehl, and J. R. Dillinger, *Phys. Letters*, A, 32, 4, 228 (1970).
70. Perepechko, I. I., *Acoustic Methods of Investigating Polymers*, Mir Publishers, Moscow, 1975.
71. Shozo, T. and G. Masaki, *Progr. Theor. Phys.*, **48**, 5, 1468 (1972).
72. Fulde, P. and H. Wagner, *Phys. Rev. Letters*, **27**, 19, 1280 (1971).
73. Madding, R. P., D. L. Fehl, and J. R. Dillinger, *J. Polymer Sci.*, A-2, **11**, 7, 1435 (1973).
74. Cieloszyk, G. S., M. T. Cruz, and G. L. Salinger, *Cryogenics*, **13**, 12, 718 (1973).
75. Baltes, H. P., *Solid State Comm.*, **13**, 2, 225 (1973).
76. Kargin, V. A., A. I. Kitaigorodsky, and G. L. Slonimsky, *Kolloid. Zhur.*, **19**, 2, 131 (1957).
77. Yeh, G.S.Y., *J. Macromol. Sci.*, B, **6**, 3, 451 (1972).
78. Arzhakov, S. A., N. F. Bakeev, and V. A. Kabanov, *Vysokomol. Soedin.* A, **15**, 5, 1154 (1973).

79. Debye, P., *Vorträge über Kinetische Theorie der Materie und Elektrizität*, Berlin, 1914.
80. Peierls, R., *Ann. der Physik*, **3**, 8, 1055 (1929).
81. Klemens, P., in: *Low Temperature Physics*, Berlin, 1956.
82. Leibfried, G., "Gittertheorie der mechanischen und thermischen Eigenschaften der Kristalle" ("*Microscopic Theory of Mechanical and Thermal Properties of Crystals*"), in: *Handbuch der Physik*, Bd. VII, Teil 1. Berlin, Springer-Verlag, 1955.
83. Mogilevsky, B. M. and A. F. Chudnovsky, *Thermal Conductivity of Semiconductors*, Nauka, Moscow, 1972 (in Russian).
84. Leibfried, G. and E. Schloemann, *Nachr. d. Akad. d. Wiss. Göttingen*, 2a, 4, 71 (1954).
85. Oskotsky, V. S. and I. A. Smirnov, *Defects in Crystals and Thermal Conductivity*, Nauka, Leningrad, 1972 (in Russian).
86. Callaway, J., *Phys. Rev.*, **113**, 4, 1046 (1959).
87. Walton, D., *Phys. Rev.*, 157, 3, 720 (1967).
88. Wagner, M., *Phys. Rev.*, **131**, 4, 1443 (1963).
89. White, G. K., S. B. Woods, and M. T. Elford, *Phys. Rev.*, **112**, 1, 111 (1958).
90. Kittel, C., *Phys. Rev.*, 75, 6, 972 (1949).
91. Klemens, P. G., *Proc. Roy. Soc.* (London), A, **208**, 1092, 108 (1951).
92. Ziman, J. M., *Electrons and Phonons*, Oxford University Press, 1960.
93. Godovsky, Yu. K., in: *Advances in Polymer Chemistry and Physics*, Khimiya, Moscow, 1970 (in Russian).
94. Powell, R. L., W. M. Rogers, and D. O. Coffin, *J. Res. Nat. Bur. Stand.*, 59, 5, 349 (1957).
95. Kolouch, R. J.. and R. G. Brown, *J. Appl. Phys.*, 39, 8, 3999 (1968).
96. Anderson, A. C., W. Rees, and J. C. Wheatley, *Rev. Sci. Instr.*, **34**, 12, 1386 (1963).
97. Berman, R., *Proc. Roy. Soc.* (London), A, **208**, 1092, 90 (1951).
98. Berman, R., E. L. Foster, and H. M. Rosenberg, *Brit. J. Appl. Phys.*, 6, 5, 181 (1955).
99. Rees, W., *J. Appl. Phys.*, **37**, 2, 864 (1966).
100. Roy, N. K., *Indian J. Phys.*, **27**, 4, 167 (1953).
101. Eierman, K., K. H. Hellwege, and W. Knappe, *Koll.-Z.*, **174**, 2, 134 (1961).
102. Eierman, K., *Kunststoffe*, 55, 5, 335 (1965).
103. Goodman, B. B., *Proc. Phys. Soc.*, 66, 399A, 217 (1953).
104. Nicol, J. and T. P. Tseng, *Phys. Rev.*, 92, 4, 1062 (1953).
105. Scott, T. A. *et al.*, *J. Appl. Phys.*, **44**, 3, 1212 (1973).
106. Giles, M. M. and C. Terry, *Phys. Rev. Letters*, **22**, 17, 882 (1969).
107. Chudnovsky, A. F., *Thermophysical Characteristics of Dispersed Materials*, Fizmatgiz, Moscow, 1962 (in Russian).
108. Eierman, K., *J. Polymer Sci.*, C, 6, 157 (1964).
109. Eierman, K., *Koll.-Z.*, **180**, 2, 163 (1962).
110. Shoulberg, R. H. and J. A. Shetter, *J. Appl. Polymer Sci.*, **6**, S32 (1962).
111. Eierman, K., *Koll.-Z.*, **198**, 1-2, 5 (1964).
112. Eierman, K., *Koll.-Z.*, 199, 2, 125 (1964).
113. Eierman, K., *Koll.-Z.*, **201**, 1, 3 (1965).
114. Hansen, D. and C. C. Ho, *J. Polymer Sci.*, A, **3**, 2, 659 (1965).
115. Rees, W., *J. Appl. Phys.*, **37**, 8, 3227 (1966).
116. Klemens, P. G., in: *Non-Crystalline Solids*, ed. by V. D. Frechette, New York, London, 1960.
117. Klemens, P. G., in: *Physics of Non-Crystalline Solids*, ed. by J. A. Prins, Amsterdam, North-Holland Publ. Co., 1965.
118. Dreyfus, B., N. C. Fernandes, and R. Maynard, *Phys. Letters*, A, **26**, 12, 647 (1968).
119. Eierman, K. and K. H. Hellwege, *J. Polymer Sci.*, 57, 165, 99 (1962).

120. Chang, G. K. and R. E. Jones, *Phys. Rev.*, **126**, 6, 2055 (1962).
121. Callaway, J., *Phys. Rev.*, **122**, 3, 787 (1961).
122. Perepechko, I. I. and V. E. Sorokin, *Akustich. Zhur.*, **18**, 4 95 (1972).
123. Phillips, W. A., *Phys. Rev.*, **3**, 12, 4338 (1971).
124. Blackman, M., *Proc. Phys. Soc.*, **70**, 9, 453B, 827 (1957)
125. Grüneisen, E., in: *Handbuch der Physik*, **10**, 1 (1926).
126. Barron, T. H., *Phil. Mag.*, **46**, 378, 720 (1955).
127. Ziman, J. M., *Principles of the Theory of Solids*, Cambridge, 1964.
128. Laquer, H. L. and E. L. Head, *Low-Temperature Thermal Expansion of Plastics*, Rept. A.E.C.D.—2161. US Atomic Energy Commission, Oak Ridge (Tenn.), 1952.
129. Corruccini, R. and J. J. Gniewek, *Thermal Expansion of Technical Solids at Low Temperatures*, NBS, Monograph 29, Washington, 1961.
130. Prigogine, I., N. Trappeniers, and V. Mathot, *Discussions Faraday Soc.*, 15, 93 (1953).
131. Prigogine, I., N. Trappeniers, and V. Mathot, *J. Chem. Phys.*, **21**, 3, 559 (1953).
132. Prigogine, I., A. Bellemans, and C. Naar-Colin, *J. Chem. Phys.*, **26**, 4, 751 (1957).
133. Hijmans, J., *Physica*, **27**, 5, 433 (1961).
134. Simha, R., and A. J. Havlik, *J. Am. Chem. Soc.*, **86**, 2, 197 (1964).
135. Nanda, V. S. and R. Simha, *J. Phys. Chem.*, **68**, 11, 3158 (1964).
136. Flory, R. J., R. A. Orwoll, and A. Vrij, *J. Am. Chem. Soc.*, **86**, 17, 3507 (1964).
137. Benedetto, A. T. di, *J. Polymer Sci.*, A, **1**, 12, 3459 (1963).
138. Nanda, V. S., R. Simha, and T. Somcynsky, *J. Polymer Sci.*, C, 12, 277 (1966).
139. Ishinabe, T. and K. Ishikawa, *Repts. Progr. Polym. Phys. Japan*, **11**, 225 (1968).
140. Paul, D. R. and A. T. di Benedetto, *J. Polymer Sci.*, C, 16, 1269 (1967).
141. Ishinabe, T. and K. Ishikawa, *Japan J. Appl. Phys.*, **7**, 5, 462 (1968).
142. London F., *J. Phys. Chem.*, **46**, 2, 305 (1942).
143. Brandt, W., *J. Chem. Phys.*, **26**, 2, 262 (1957).
144. Slater, J. C. and J. G. Kirkwood, *Phys. Rev.*, **37**, 6, 682 (1931).
145. Brandt, W., *J. Chem. Phys.*, **24**, 3, 501 (1956).
146. Hellwege, K. H., W. Knappe, and P. Lehman, *Koll.-Z.*, **183**, 2, 110 (1962).
147. Simha, R., J. M. Roe, and V. S. Nanda, *J. Appl. Phys.*, **43**, 11, 4312 (1972).
148. Barker, J. A., *Lattice Theories of the Liquid State*, Pergamon Press, London, 1963.
149. Papoular, M., *J. Phys., C. Solid. State Phys.*, 5, 15, 1943 (1972).
150. Pastine, D. J., *J. Appl. Phys.*, **41**, 13, 5085 (1970).
151. Pastine, D. J., *J. Chem. Phys.*, 49, 7, 3012 (1968).
152. Wu, C. K., G. Jura, and M. Shen, *J. Appl. Phys.*, **43**, 11, 4348 (1972).
153. Amatuni, A. M., *Methods and Instruments for Determination of Temperature Coefficients of Linear Expansion of Materials*, Izd. Standartov, Moscow, 1972 (in Russian).
154. Laquer, H. L., *Low-Temperature Thermal Expansion of Various Materials*, Rept. A.E.C.D.—3706. US Atomic Energy Commission, Oak Ridge (Tenn.), 1952.
155. Haldon, R. A. and R. Simha, *J. Appl. Phys.*, 39, 3, 1890 (1968).
156. Haldon, R. A. and R. Simha, *Macromolecules*, **1**, 4, 340 (1968).
157. Zakin, J. L., R. Simha, and H. C. Hershey, *J. Appl. Polymer Sci.*, **10**, 10, 1455 (1966).
158. Schell, W. J., R. Simha, and J. J. Aklonis, *J. Macromol. Sci. Chem.*, A, **3**, 7, 1297 (1969).
159. McCammon, R. D. and R. N. Work, *Rev. Sci., Instr.*, **36**, 8, 1169 (1965).

160. Van de Voorde, M., *IEEE Trans. Nucl. Sci.*, **20**, 3, 693 (1973).
161. McConnell, P. M., D.E. Daney, and J. B. Kirgis, *J. Appl. Phys.*, **41**, 13, 5066 (1970).
162. Schatzki, T. F., *Am. Chem. Soc. Polymer Preprints*, 6, 2, 646 (1965).
163. McCrum, N. G., B. E. Read, and G. Williams, *Anelastic and Dielectric Effects in Polymeric Solids*, London and New York, John Wiley, 1967.
164. Boyer, R. F., *Polymer Eng. Sci.*, 8, 3, 161 (1968).
165. Reding, F. P., *J. Polymer Sci.*, **21**, 99, 547 (1956).
166. Manaresi, P. and V. Gianella, *J. Appl. Polymer Sci.*, 4, 11, 251 (1960).
167. Kontos, E. G. and W. P. Slichter, *J. Polymer Sci.*, **61**, 171, 61 (1962).
168. Beck, D. L., A. A. Hiltz, and J. R. Knox, *SPE Trans.*; **3**, 4, 279 (1963).
169. Wilkinson, R. W. and M. Dole, *J. Polymer Sci.*, 58, 166, 1089 (1962).
170. Kirby, R. K., *J. Res. NBS*, 57, 2, 91 (1956).
171. Leksina, I. E. and S. I. Novikova, *Fizika Tverdogo Tela*, **1**, 3, 504 (1959).
172. Strelkov, P. G., G. I. Kosourov, and B. N. Samoilov, *Izv. Akad. Nauk SSSR, Ser. Fiz.*, **17**, 3, 383 (1953).
173. Strelkov, P. G., *Zhur. Neorg. Khim.*, **1**, 6, 1350 (1956).
174. Strelkov, P. G. and S. I. Novikova, *Pribory i Tekhnika Eksperimenta*, 5, 105 (1957).
175. Frenkel, Ya. I., *The Kinetic Theory of Liquids*, Izd. Akad. Nauk SSSR, Moscow, 1945 (in Russian).
176. Clark, E. S. and L. T. Muus, *Z. Kristallogr.*, **117**, 2-3, 119 (1962).
177. Simha, R. and R. F. Boyer, *J. Chem. Phys.*, 37, 5, 1003 (1962).
178. Rogers, S. S. and L. Mandelkern, *J. Phys. Chem.*, **61**, 7, 985 (1957).
179. Hoff, E.A.W., D. W. Robinson, and A. H. Willbown, *J. Polymer Sci.*, **18**, 88, 161 (1955).
180. Shen, M. C., J. D. Strong, and F. J. Matsik, *J. Macromol. Sci., Phys.*, **1**, 1, 15 (1967).
181. Schmieder, K. and K. Wolf, *Koll.-Z.*, **134**, 2-3, 149 (1953).
182. Woodward, A. E., J. A. Sauer, and R. A. Wall, *J. Polymer Sci.*, **50**, 153, 117 (1961).
183. Matochkin, V. S. *et al.*, *Doklady Akad. Nauk SSSR*, **204**, 6, 1359 (1972).
184. Sinnott, K. M., *J. Polymer Sci.*, 35, 128, 273 (1959).
185. Slonim, I. Ya. and A. N. Lyubimov, *Nuclear Magnetic Resonance in Polymers*, Khimiya, Moscow, 1966 (in Russian).
186. Debye, P. *Polar Molecules*, New York, Dover, 1945.
187. Reiner, M., *Phys. Today*, **17**, 1, 62 (1964).
188. Brown, W., Jr., *Dielectrics*, Berlin, 1956.
189. Fröhlich, H., *Theory of Dielectrics*, Oxford University Press, London, 1958.
190. *Electrical Properties of Polymers*, ed. by B. I. Sazhin, Khimiya, Leningrad, 1970 (in Russian).
191. *Dielectric Properties of Polymers*, ed. by F. E. Karasz, New York and London, Plenum Press, 1972.
192. Cole, R. H., in: *Progress in Dielectrics*, ed. by J. B. Birks, vol. 3, Heywood, London, 1961.
193. Meakins, R. J., in: *Progress in Dielectrics*, vol. 3, Heywood, London, 1961.
194. Read, B. E. and G. Williams, *Trans. Faraday Soc.*, 57, 11, 467, 1979 (1961).
195. Hoffman, J. D., *J. Chem. Phys.*, **22**, 1, 156 (1954).
196. Jackson, W., *Trans. Faraday Soc.*, **42A**, 91 (1946).
197. Glasstone, S., K. Laidler, and H. Eyring, *The Theory of Rate Processes*, McGraw-Hill, New York, 1941.
198. Boyer, R. F., *Rubb. Chem. Technol.*, **36**, 1303 (1963).
199. Yamafuji, K. and Y. Ishida, *Koll.-Z.*, **183**, 1, 15 (1962).
200. Gotlib, Yu. Ya. and K. M. Salikhov, *Vysokomol. Soedin.*, 4, 8, 1163 (1962).

201. Saito, N. *et. al.*, in: *Solid State Physics*, vol. 14, Academic Press, New York, 1963.
202. Hill. N. E., *Proc. Phys. Soc.*, **82**, 5, 529, 723 (1963).
203. Oehme, F., *Dielectrische Messmethoden*, Verlag Chemie GmbH, Weinheim/Berg, Str.
204. *Measurement of Dielectric Properties under Space Conditions*, ASTM Special Technical Publication No. 420, Philadelphia.
205. Chant, M. J., *Cryogenics*, **7**, 6, 351 (1967).
206. Vincett, P. S., *Brit. J. Appl. Phys.*, *Ser.* 2, **2**, 5, 699 (1969).
207. Phillips, W. A., *Proc. Roy. Soc.* (London), A, **319**, 1539, 565 (1970).
208. Carson, R.A.J., *Proc. Roy. Soc.* (London), A, **332**, 1589, 255 (1973).
209. Allan, R. N. and E. Kuffel, *Proc. IEE*, **115**, 3, 432 (1968).
210. Heybey, O. and F. H. Müller, *Koll.-Z. u Z. Polymere*, **251**, 6, 383 (1973).
211. Mathes, K. N., *Electro-Technology*, **72**, 3, 72 (1963).
212. Mathes, K. N., *SPE Journal*, **20**, 7, 634 (1964).
213. Hara, T., *Japan J. Appl. Phys.*, **6**, 2, 147 (1967).
214. Okamoto, S. and K. Takeuchi, *J. Phys. Soc. Japan*, **14**, 3, 378 (1959).
215. Mikhailov, G. P., S. P. Kabin, and B. I. Sazhin, *Zhur. Tekhn. Fiz.*, **25**, 590 (1955).
216. De Vos, W. J. and J. Volger, *Phisica*, **34**, 2, 272 (1967).
217. De Vos, W. J. and J. Volger, *Phys. Letters*, A, **24**, 10, 539 (1967).
218. Pauling, L., *Phys. Rev.*, **36**, 3, 430 (1930).
219. Hartwig, W. H. and D. Grissom, in: *Proc. 9th Int. Conf. on Low-Temperature Physics*, Pt. B. Columbus, Ohio, Plenum Press, 1965.
220. Siegel, K., R. Domchick, and F. Aroms, *Proc. IEEE*, 55, 3, 457 (1967).
221. McCammon, R. D., R. N. Work, and R. G. Saba, *Bull. Am. Phys. Soc.*, 9, 3, 221 (1964).
222. Odajima, A., A. E. Woodward, and J. A. Sauer, *J. Polymer Sci.*, **55**, 161, 181 (1961).
223. Hara, T., *Japan J. Appl. Phys.*, **6**, 9, 1138 (1967).
224. Nozaki, M., K. Shimada, and S. Okamoto, *Japan J. Appl. Phys.*, **10**, 2, 179 (1971).
225. McCammon, R. D., R. G. Saba, and R. N. Work, *J. Polymer Sci.*, A-2, **7**, 10, 1721 (1969).
226. Irvin, J. D. and R. N. Work, *J. Polymer Sci.*, A-2, **11**, 1, 175 (1973).
227. Skripov, F. I., *A Course of Lectures on Radio-Spectroscopy*, Izd. LGU, Leningrad, 1964 (in Russian).
228. Roberts, J. D., *Nuclear Magnetic Resonance*, McGraw-Hill Book Co., New Yorк, 1959.
229. Lösche, A., *Kerninduktion*, Deutsche Verlag der Wissenschaften, Berlin, 1957.
230. Slichter, Ch. P., *Principles of Magnetic Resonance with Examples from Solid State Physics*, Harper Row, New York, 1963.
231. Slichter, W. P., *Macromol. Chem.*, **34**, 67 (1959).
232. Aleksandrov, N. M. and F. I. Skripov, *Uspekhi Fiz. Nauk*, 75, 4, 585 (1961).
233. Slichter, W. P., *Erg. exact. Naturwiss* (1958).
234. Slonim, I. Ya., *Uspekhi Khim.*, 31, 5, 609 (1962).
235. Slichter, W. P.. in: *Transitions and Relaxations in Polymers*, Interscience Publishers, 1966.
236. Van Vleck, J. H., *Phys. Rev.*, 74, 9, 1168 (1948).
237. Bloembergen, N., E. M. Purcell, and R. V. Pound, *Phys. Rev.*, **73**, 7, 679 (1948).
238. Mijake, A., *J. Polymer Sci.*, **28**, 117, 476 (1958).
239. Kubo, R. and K. Tomita, *J. Phys. Soc. Japan*, 9, 6, 888 (1954).
240. Grigoriev, V. P. *et al.*, *Fizika Tverdogo Tela*, 9, 12, 3635 (1967).
241. Grigoriev, V. P. and A. I. Maklakov, *Vysokomol. Soedin.*, B, **13**, 9, 652 (1971).

242. Grigoriev, V. P. and A. I. Maklakov, *Vysokomol. Soedin.*, A, **15**, 11, 2576 (1973).
243. Grigoriev, V. P. and A. I. Maklakov, *Vysokomol. Soedin.*, B, **16**, 10, 737 (1974).
244. Chujo, R., *J. Phys. Soc. Japan*, **18**, 1, 124 (1963).
245. McCall, D. W. and W. P. Slichter, *J. Polymer Sci.*, **26**, 113, 171 (1957).
246. Perepechko, I. I. and L. A. Kvacheva, *Vysokomol. Soedin.*, B, **12**, 7, 484 (1970).
247. Fujiwara, S., A. Amamiia, and K. Shinohara, *J. Chem. Phys.*, **26**, 5, 1343 (1957).
248. Gupta, R. P., *J. Phys. Chem.*, 65, 7, 1128 (1961).
249. Powles, J. G. and H. S. Gutowsky, *J. Chem. Phys.*, **23**, 9, 1692 (1955).
250. Das, T. P., *J. Chem. Phys.*, **27**, 3, 763 (1957).
251. Stejskal, E. O. and H. S. Gutowsky, *J. Chem. Phys.*, **28**, 3, 388 (1958).
252. Landau, L. D. and E. M. Lifshitz, *Quantum Mechanics*, Fizmatgiz, Moscow, 1963.
253. Kosfeld, R. and U. Mylius, *Koll.-Z. u. Z. Polymere*, **250**, 11-12, 1081 (1972).
254. Allen, P. S., *J. Chem. Phys.*, **48**, 7, 3031 (1968).
255. Allen, P. S. and S. Clough, *Phys. Rev. Letters*, **22**, 25, 1351 (1969).
256. Clough, S., *J. Phys. C. Solid State Phys.*, **4**, 14, 2180 (1971).
257. Kosfeld, R. and U. Mylius, *Koll.-Z. u. Z. Polymere*, **250**, 11-12, 1088 (1972).
258. Bergmann, K. and K. Navotki, *Koll.-Z. u. Z. Polymere*, **219**, 2, 132 (1967).
259. Clough, S., *J. Phys. C. Solid State Phys.*, **4**, 9, 1075 (1971).
260. Slichter, W. P. and E. R. Mandell, *J. Appl. Phys.*, **30**, 10, 1473 (1959).
261. Sinnott, K. M., *J. Polymer Sci.*, **42**, 139, 3 (1960).
262. Vosskötter, G. and R. Kosfeld, *Koll.-Z. u. Z. Polymere*, **216-217**, 185 (1967).
263. Ferry, J. D., *Viscoelastic Properties of Polymers*, Wiley, New York, 1961.
264. Bartenev, G. M. and Yu. V. Zelenev, *Mekhanika Polimerov*, **1**, 30 (1969).
265. Sauer, J. A. and R. G. Saba, *J. Macromol. Sci.-Chem.*, A, **3**, 7, 1217 (1969).
266. Hoffman, J. D., G. Williams, and E. Passaglia, in: *Transitions and Relaxations in Polymers*, ed. by R. Boyer, Interscience Publishers, 1966.
267. Perepechko, I. I. and O. V. Startsev, *Vysokomol. Soedin.*, B, **15**, 5, 321 (1973).
268. Armeniades, C. D. and E. Baer, *J. Polymer Sci.*, A-2, **9**, 8, 1345 (1971).
269. Papir, Y. S. and E. Baer, *J. Appl. Phys.*, **42**, 12, 4667 (1971).
270. Hiltner, A. and E. Baer, *Polymer J.*, **3**, 3, 378 (1972).
271. Sinnott, K. M., *J. Appl. Phys.*, **29**, 10, 1433 (1958).
272. Armeniades, C. D. *et al.*, *J. Macromol. Sci.*, B, **1**, 4, 777 (1967).
273. Bordoni, P. G., *Nuovo Cimento*, **4**, 3-4, 177 (1947).
274. Baccaredda, M., *Polymer Letters*, **3**, 3, 189 (1965).
275. Crissman, J. M. and R. D. McCammon, *J. Acoust. Soc. Am.*, **34**, 11, 1703 (1962).
276. Boyer, R. F., *Macromolecules*, **6**, 2, 288 (1973).
277. McKenna, L., T. Kajiama, and N. J. MacKnight, *Macromolecules*, **2**, 1, 58 (1969).
278. Stehling, F. C. and L. Mandelkern, *Macromolecules*, **3**, 2, 242 (1970).
279. Perepechko, I. I. and L. A. Bodrova, *Plast. Massy*, 7, 56 (1967).
280. Hopkins, I. L. and K. Kerkjian, in: W. P. Mason, *Physical Acoustics. Principles and Methods*, vol. II, part B. *Properties of Polymers and Nonlinear Acoustics*, New York, Academic Press, 1965.
281. Sinnott, K. M., *J. Appl. Phys.*, **37**, 9, 3385 (1966).
282. Illers, K. H., *Rheol. Acta*, **3**, 4, 202 (1964).
283. Illers, K. H., *Koll.-Z. u. Z. Polymere*, **231**, 1-2, 622 (1969).

284. Kline, D. E., J. A. Sauer, and A. E. Woodward, *J. Polymer Sci.*, **22**, 102, 455 (1956).
285. Fisher, E. W. and A. Peterlin, *Makromol. Chem.*, **74**, 1 (1964).
286. Wada, Y., R. Hayakowa, and T. Nishi, *J. Polymer Sci.*, C, 15, 101 (1966).
287. Crist, B. and A. Peterlin, *J. Polymer Sci.*, A-2, **7**, 7, 1165 (1969).
288. Pechhold, W., *Koll.-Z.*, **228**, 1-2, 1 (1968).
289. Gray, R. W. and N.G. McCrum, *J. Polymer Sci.*, A-2, **7**, 8, 1329 (1969).
290. Crissman, J. M., J. A. Sauer, and A. E. Woodward, *J. Polymer Sci.*, A, **2**, 12, 5075 (1964).
291. Miki, K. *et al.*, *Japan J. Appl. Phys.*, 5, 9, 818 (1966).
292. Holland, V. F., *J. Appl. Phys.*, **35**, 11, 3235 (1964).
293. Holland, V. F. and P. H. Lindenmeyer, *J. Appl. Phys.*, 36, 10, 3049 (1965).
294. Reneker, D. H., *J. Polymer Sci.*, **59**, 168, 39 (1962).
295. Clark, E. S., in: *Cryogenic Properties of Polymers*, ed. by T. T. Serafini and J. L. Koenig, Marcel Dekker, New York, 1967.
296. Santis, P. de *et al.*, *J. Polymer Sci.*, A, **1**, 4, 1383 (1963).
297. Brown, R. G., *J. Chem. Phys.*, **40**, 10, 2900 (1964).
298. Koenig, J. L. and F. J. Boerio, *J. Chem. Phys.*, **52**, 8, 4170 (1970).
299. McCrum, N. G., *J. Polymer Sci.*, **34**, 127, 355 (1959).
300. Kvacheva, L. A. and I. I. Perepechko, *Akustich. Zhur.*, **18**, 3, 408 (1972).
301. Perepechko, I. I. and L. A. Bodrova, *Vysokomol. Soedin.*, B, 9, 2, 116 (1967).
302. Ohzawa, Y. and Y. Wada, *Japan J. Appl. Phys.*, **3**, 8, 436 (1964).
303. Read, B. and G. Williams, *Polymer*, **2**, 3, 239 (1961).
304. Urman, Ya. G., I. Ya. Slonim, and A. G. Konovalov, *Vysokomol. Soedin.*, **6**, 9, 1651 (1964).
305. Mikhailov, G. P. and M. P. Eidelnant, *Vysokomol. Soedin.*, **2**, 10, 1552 (1960).
306. Bohn, L., *Koll.-Z. u. Z. Polymere*, **201**, 1, 20, (1965).
307. Miki, K., J. Yasukawa, and M. Kaneko, *Japan J. Appl. Phys.*, **8**, 2, 159 (1969).
308. Papir, Y. S. and E. Baer, *Mater. Sci. and Eng.*, 8, 6, 310 (1971).
309. Seeger, A., *Phil. Mag.*, 1, 7, 651 (1956).
310. Seeger, A. and P. Schiller, *Acta Met.*, **10**, 4, 348 (1962).
311. Kolarik, H. and J. Janacek, *J. Polymer Sci.*, C, 16, 441 (1967).
312. Brown, W. B., G. A. Campbell, and J. B. Nowell, *Am. Chem. Soc. Polymer Preprints*, **10**, 2, 647 (1969).
313. Papir, Y. S., S. Kapur, and Ch. E. Rogers, *J. Polymer Sci.*, A-2. **10**, 7, 1305 (1972).
314. Woodward, A. E. and J. A. Sauer, in: D. Fox, M. M. Labes, and A. Weissberger (Eds.), *Physics and Chemistry of the Organic Solid State*, vol. II, New York, Interscience Publishers, 1965.
315. Passaglia, E. and G. M. Martin, *J. Res. Nat. Bur. Stand.*, A., 68, 5, 519 (1964).
316. Sauer, J. A. *et al.*, *J. Appl. Phys.*, 29, 10, 1385 (1958).
317. Sinnott, K. M., *SPE Trans.*, **2**, 1, 65 (1962).
318. Woodward, A. E., *J. Polymer Sci.*, C, 14, 89 (1966).
319. Powles, J. G. and P. Mansfield, *Polymer*, **3**, 3, 399 (1962).
320. Woodward, A. E., in: *Transitions and Relaxations in Polymers*, ed. by R. Boyer, Interscience Publishers, 1966.
321. Gall, W. G. and N. G. McCrum, *J. Polymer Sci.*, **50**, 154, 489 (1961).
322. Reich, S. and A. Eisenberg, *J. Polymer Sci.*, A-2, **10**, 7, 1397 (1972).
323. Litt, M., *J. Polymer Sci.*, A-1, 6, 2219 (1963).
324. Geil, P. H., *Polymer Single Crystals*, Wiley, New York, 1963.
325. Frosini, V. and A. E. Woodward, *J. Polymer Sci.*, A-2, **7**, 3, 525 (1969)

326. Reich, S. and A. Eisenberg, *Am. Chem. Soc. Polymer Preprints*, 10, 2, 655 (1969).
327. Eisenberg, A. and S. Reich, *J. Chem. Phys.*, **51**, 12, 5706 (1969).
328. Jenckel, E., *Koll.-Z.*, **136**, 2/3, 142 (1954).
329. Sauer, J. A. and D. E. Kline, *J. Polymer Sci.*, **18**, 18, 491 (1955).
330. Crissman, J. M., J. A. Sauer, and A. E. Woodward, *J. Polymer Sci.*, A, **3**, 7, 2693 (1965).
331. Chung, C. I. and J. A. Sauer, *J. Polymer Sci.*, A-2, 9, 6, 1097 (1971).
332. Yano, O. and Y. Wada, *J. Polymer Sci.*, A-2, 9, 4, 669 (1971).
333. Petersen, J. and B. Ränby, *Makromol. Chem.*, **133**, 251 (1970).
334. Becker, G. W., *Koll.-Z.*, **140**, 1, 1 (1955).
335. Pezzin, G. and A. Pagliari, *Chim. ind.*, **48**, 5, 458 (1966).
336. Pezzin, G., G. Airoldi, and C. Garbuglio, *J. Appl. Polymer Sci.*, **11**, 12, 2553 (1967).
337. Petersen, J. and B. Ränby, *Makromol. Chem.*, **133**, 263 (1970).
338. Ishida, Y., *Koll.-Z.*, **171**, 1, 71 (1960).
339. Perepechko, I. I., L. A. Ushakov, and R. S. Barshtein, *Plast. Massy*, 10, 35 (1971).
340. Perepechko, I. I., L. A. Ushakov, and R. S. Barshtein, *Vysokomol. Soedin.*, A, **14**, 12, 2553 (1972).
341. Sauer, J. A. and A. E. Woodward, *Rev. Mod. Phys.*, **32**, 1, 88 (1960).
342. Landau, L. D. and G. Rumer, *Phys. Z. Sowjetunion*, **11**, 18 (1937).
343. Akheizer, A., *Zhur. Eksper. i Teoret. Fiz.*, **8**, 12, 1318 (1938).
344. Woodruf, T. O. and H. Ehrenreich, *Phys. Rev.*, **123**, 1553 (1961).
345. Gurevich, V. L. and A. L. Efros, *Zhur. Eksper. i Teoret. Fiz.*, **51**, 6, 1693 (1966).
346. Perepechko, I. I., in: *The Application of Ultra-Acoustics to the Investigation of Substances*, MOPI, No. 9, 103 Moscow, 1959 (in Russian).
347. Ozvold, M., *Phys. Status Solidi*, **37**, 1, 79 (1970).
348. Zvryanov, P. S. and G. G. Talun, *Zhur. Eksper. i Teoret. Fiz.*, **54**, 3, 855 (1968).
349. Maris, H. J., *Phys. Rev.*, **188**, 3, 1303 (1969).
350. Klein, R., *Phys. Letters*, **23**, 11, 651 (1966).
351. Weyman, H. D., *Phys. Rev.*, **176**, 3, 838 (1968).
352. Jackle, J., *Z. Phys.*, **257**, 3, 212 (1972).
353. Landau, L. D. and E. M. Lifshitz, *Theory of Elasticity*, Pergamon Press, Oxford, 1959.
354. Perepechko, I. I., *Akustich. Zhur.*, **10**, 3, 335 (1964).
355. Perepechko, I. I. and V. E. Sorokin, *Vysokomol. Soedin.*, B, **13**, 3, 171 (1971).
356. Perepechko, I. I. and P. D. Golub, *Vysokomol. Soedin.*, A, **16**, 2, 275 (1974).
357. Athougies, A. D. *et al.*, *Cryogenics*, **12**, 2, 125 (1972).
358. Shimizu, K. *et al.*, *J. Polymer Sci.*, A-2, **11**, 8, 1641 (1973).
359. Ponomarev, Ya. G., *Pribory i Tekhn. Eksperim.*, 6, 218 (1966).
360. Stryukov, V. B. and I. F. Shchegolev, *Pribory i Tekhn. Eksperim.*, 5, 248 (1966).
361. Sorokin, V. E. and I. I. Perepechko, *Pribory i Tekhn. Eksperim.*, 5, 217 (1970).
362. Sorokin, V. E. and I. I. Perepechko, *Cryogenics*, **11**, 5, 406 (1971).
363. Perepechko, I. I. and P. D. Golub, *Pribory i Tekhn. Eksperim.*, 6, 216 (1972).
364. Perepechko, I. I. and P. D. Golub, *Cryogenics*, **13**, 8, 499 (1973).
365. Baccaredda, M., *Chim. ind.*, **44**, 12, 1383 (1962).
366. Friedman, E. A., A. J. Ritger, and R. D. Andrews, *J. Appl. Phys.*, **40**, 11, 4243 (1969).
367. Perepechko, I. I. and V. E. Sorokin, *Fizika Tverdogo Tela*, **13**, 3, 932 (1971).

368. Golub, P. D. and I. I. Perepechko, *Akustich. Zhur.*, 20, 1, 38 (1974).
369. Balagurov, B. Ya. and V. G. Vaks, *Zhur. Eksper. i Teoret. Fiz.*, 57, 11, 1646 (1969).
370. Sorokin, V. E. and I. I. Perepechko, *Vysokomol. Soedin.*, A, 16, 7, 1653 (1974).
371. Kawaguchi, T., *J. Appl. Polymer Sci.*, 2, 4, 56 (1959).
372. Golub, P. D. and I. I. Perepechko, *Akustich. Zhur.*, 19, 4, 619 (1973).
373. Reich, S. and A. Eisenberg, *J. Chem. Phys.*, 53, 7, 2847 (1970).
374. Flory, P. J., *Statistical Mechanics of Chain Molecules*, Wiley-Interscience, New York, 1969.
375. Perepechko, I. I. and P. D. Golub, *Mekhanika Polimerov*, 4, 749 (1973).
376. Golub, P. D. and I. I. Perepechko, in: *Some Problems of Teaching Physics at Higher and Secondary Schools*, BGPI, Barnaul, 1973 (in Russian).
377. Davidse, P. D., H. I. Waterman, and J. B. Westerdijk, *J. Polymer Sci.*, 59, 168, 389 (1962).
378. Perepechko, I. I. and L. A. Bodrova, *Vysokomol. Soedin.*, B, **10**, 3, 148 (1968).
379. Perepechko, I. I., V. A. Grechishkin, and L. G. Kazarian, *Akustich. Zhur.*, 16, 2, 223 (1970).
380. Perepechko, I. I. and P. D. Golub, *Mekhanika Polimerov*, 4, 604 (1973).
381. Sorokin, V. E. and I. I. Perepechko, *Mekhanika Polimerov*, 1, 18 (1974).
382. Sakurada, I., T. Ito, and K. Nakamae, *Khim. i Tekhn. Polimerov*, 10, 19 (1964).
383. Volkenshtein, M. V., *The Structure and Physical Properties of Molecules*, Izd. Akad. Nauk SSSR, 1955 (in Russian).
384. Matsuoka, S. and I. Ishida, in: *Transitions and Relaxations in Polymers*, ed. by R. Boyer, Interscience Publishers, 1966.
385. Golub, P. D. and I. I. Perepechko, *Vysokomol. Soedin.*, A, 16, 7, 1593 (1974).
386. Alers, G. A., in: W. P. Mason, (Ed.), *Physical Acoustics. Principles and Methods*, vol. III, part B. *Lattice Dynamics*. New York, Academic Press, 1965.
387. Leibfried, G. and W. Ludwig, in: F. Seitz and D. Turnbull (Eds.), *Solid State Physics*, vol. 12. *Theory of Anharmonic Effects in Crystals*, New York, Academic Press, 1961.
388. Lebedev, B. V., I. B. Rabinovich, and V. A. Budarina, *Vysokomol. Soedin.*, 9, 3, 488 (1967).
389. Urzendowski, S. R., A. H. Guenter, and J. R. Asay, *Am. Chem. Soc. Polymer Preprints*, 9, 1, 878 (1968).
390. Barker, R. E., *J. Appl. Phys.*, 34, 1, 107 (1963).
391. Lamberson, D. L., J. R. Asay, and A. H. Guenter, *J. Appl. Phys.*, 43, 3, 976 (1972).
392. Barker, R. E., *J. Appl. Phys.*, 38, 11, 4234 (1967).
393. Wada, Y. *et al.*, *J. Polymer Sci.*, A-2, 7, 1, 201 (1969).
394. Hartman, B. and J. Jarzynski, *J. Appl. Phys.*, 43, 11, 4304 (1972).

NAME INDEX

Numbers in parentheses are reference numbers and indicate that an author's work is referred to, although his name is not cited in the text. The full references are listed on pp. 277-286.

A

Airoldi, G., 203 (336)
Akheizer, A., 206, 207
Aklonis, J. J., 97 (158), 107 (158), 109
Akopian, V. B., 32
Allan, R. N., 125 (209), 126, 128, 138 (209), 140 (209), 272 (209)
Allen, P. S., 167, 170, 174
Aleksandrov, N. M., 147 (232)
Alers, G. A., 256 (386)
Amamiia, A., 160 (247), 161 (247)
Amatuni, A. M., 97
Anderson, A. C., 56 (96), 71
Anderson, O. L., 35 (61)
Andrews, R. D., 216 (366)
Armeniades, C. D., 182, 183 (272), 193 (268), 221 (268)
Aroms, F., 136
Arzhakov, S. A., 44 (78)
Asay, J. R., 262 (389, 391), 263 (389, 391), 264 (389, 391)
Athougies, A. D., 211 (357), 258 (357)

B

Baccaredda, M., 183 (274), 216 (365)
Baer, E., 182 (269), 185 (270, 308), 186 (269), 187 (269), 191, 192 (308), 193 (268), 194, 221 (268, 269, 270)
Bakeev, N. F., 44 (78)
Balagurov, B. Ya., 221 (369)
Baltes, H. P., 44 (75)
Barker, J. A., 92 (148)
Barker, R. E., 261 (392), 262 (390), 263, 265, 267
Barron, T. H., 85, 86
Barshtein, R. S., 203 (339, 340)
Bartenev, G. M., 19 (31), 179 (264), 180 (264)
Baur, H., 14, 21 (7), 270 (7)
Beck, D. L., 100 (168)
Becker, G. W., 203 (334)
Bergmann, K., 168
Berman, R., 56 (97, 98), 61 (97), 74, 75, 76, 77 (97), 271 (98)
Birks, J. B., 281 (192)
Bloembergen, N., 153
Bodrova, L. A., 184 (279), 238 (378)
Boerio, F. J., 187
Bohn, L., 190, 191 (306)
Bordoni, P. G., 183 (273)
Born, M., 7, 85
Boyer, R. F., 98 (164), 103, 104, 122, 184 (276), 286 (384)
Brandt, W., 90 (143), 92 (145)
Brown, R. G., 56 (95), 68, 69, 74, 187, 271 (95)
Brown, W., Jr., 118 (188), 121 (188)
Brown, W. B., 195 (312)
Budarina, V. A., 260 (388), 270 (388)

C

Callaway, J., 52 (86), 67
Campbell, G. A., 195 (312)
Carson, R. A. J., 125 (208), 126, 127, 132, 133, 134
Chang, G. K., 67
Chant, M. J., 125, 126, 127, 135, 136, 137 (205), 138 (205), 142 (205), 146, 272 (205)
Choy, C. L., 37 (66), 38, 39, 258 (66), 270 (66)
Chudnovsky, A. F., 48 (83), 52 (83), 53 (83)
Chujo, R., 155
Chung, C. I., 202, 203 (331)
Cieloszyk, G. S., 37 (67), 38, 57 (67), 76, 77 (67), 79 (67), 80 (67), 81 (67)
Clark, E. S., 102 (176), 186
Clough, S., 167, 170, 172 (256, 259), 174, 175 (256, 259)
Coffin, D. O., 56 (94), 71, 271 (94)
Cole, R. H., 118 (192), 121 (192)
Corruccini, R., 87 (129), 97 (129), 271 (129)
Crissman, J. M., 183, 185 (290), 196, 197, 198, 199, 202 (330), 204 (290), 205
Crist, B., 185

D

Dainton, F. S., 24, 25 (48), 33, 34, 37 (48), 270 (48)
Daney, D. E., 97 (161)
Das, T. P., 165 (250), 174 (250), 200 (250), 233
Davidse, P. D., 236
Debye, P., 4, 46 (79), 117 (186)
Dempsey, C. W., 21 (39), 31, 37 (39)
De Santis, P., 187
De Sorbo, W., 19 (36)
De Vos, W. J., 130 (216, 217)
Di Benedetto, A. T., 87, 88
Dillinger, J. R., 39, 40 (68, 69), 41 (68, 69), 42 (68), 43 (68, 73)
Dole, M., 19 (34), 100
Domehick, R., 136 (220)
Dreyfus, B., 65

E

Efros, A. L., 207, 221 (345)
Ehrenreich, H., 207
Eidelnant, M. P., 190 (305)
Eierman, K., 56 (101, 102), 57 (101), 57 (101, 108, 109), 58, 60 (108, 111, 112), 62 (111, 112, 113), 66, 71, 75, 77, 79, 81, 271 (101, 102)
Einstein, A., 2
Eisenberg, A., 198 (327), 199 (326), 200, 201 (326, 327), 229, 230
Elford, M. T., 53 (89)
Eucken, A., 18
Evans, D. M., 33, 34 (48), 37 (48)
Eyring, H., 121 (197), 169 (197)

F

Fehl, D. L., 39, 40 (68, 69), 41 (68, 69), 42 (68), 43 (68, 73)
Fernandes, N. C., 65
Ferry, J. D., 178 (263)
Fisher, E. W., 185
Flory, R. J., 87, 232 (374)
Flubacher, P., 35 (62)
Foster, E. L., 56 (98), 74 (98), 75 (98), 271 (98)
Fox, D., 284 (314)
Frenkel, Ya. I., 102
Friedman, E. A., 216 (366)
Fröhlich, H., 118 (189), 121
Frosini, V., 198, 199, 202, 203
Fujiwara, S., 160 (247), 161
Fulde, P., 43 (72)
Furukawa, G. T., 19, 21, 30, 102

G

Gall, W. G., 197
Garbuglio, C., 203 (336)
Garland, C. W., 25 (51)
Geil, P. H., 198 (324)
Genensky, S. M., 21
Gianella, V., 100
Giles, M. M., 57 (106), 70 (106), 71 (106)
Glasstone, S., 121 (197), 169 (197)
Gniewek, J. J., 87 (129), 97 (129), 271 (129)
Godovsky, Yu. K., 56 (93)
Golub, P. D., 211, 213 (356), 214 (356), 216 (363, 364), 218 (356, 368), 220 (356, 368), 226 (356, 368), 227 (368), 228 (372), 231 (372), 232 (375), 233 (375), 234 (375), 235 (375, 376), 238 (356), 241 (356, 368, 372, 375, 380), 249 (380), 250 (380), 252 (380), 254 (385), 256 (368, 372, 375, 376, 385), 259 (385), 262 (385), 263 (385), 264 (385), 273 (368, 372, 375), 274 (380)
Goodman, B. B., 57 (103)
Gorbatkina, Yu. A., 19 (31)
Gordon, J. E., 21 (39), 31, 37 (39)
Gotlib, Yu. Ya., 28, 29, 31, 32, 123
Gray, R. W., 185
Grechishkin, V. A., 238 (379)
Grigoriev, V. P., 154, 156
Grissom, D., 136
Grüneisen, E., 85
Guenter, A. H., 262 (389, 391), 263 (389, 391), 264 (389, 391)
Gupta, R. P., 162 (248)
Gurevich, V. L., 207, 221 (345)
Gutowsky, H. S., 164 (249), 165, 166, 167, 169, 170 (249), 174 (249), 198, 200, 229

H

Haldon, R. A., 97 (155, 156), 103, 104, 105, 267 (156)
Hansen, D., 62 (114), 65
Hara, T., 127, 137 (213), 141 (213), 142 (223)
Hartman, B., 233, 234
Hartwig, W. H., 136
Havlik, A. J., 87
Hayakowa, R., 185 (286)
Head, E. L., 87 (128), 97, 98, 99, 102, 103, 271 (128)
Hecht, C. E., 16, 17, 21
Heise, B., 30 (56)

Hellwege, K. H., 56 (101), 57 (101), 66 (101, 119), 77 (119), 271 (101)
Hershey, H. C., 97 (157), 98, 99 (157), 100 (157), 266 (157), 271 (157)
Heybey, O., 125 (210), 127, 135, 272 (210)
Hijmans, J., 87 (133)
Hill, N. E., 123
Hiltner, A., 182, 185 (270), 194, 221 (270)
Hiltz, A. A., 100 (168)
Ho, C. C., 62 (114)
Hoare, F. E., 33, 34 (48), 37 (48)
Hoff, E. A. W., 104 (179), 106 (179), 107 (179)
Hoffman, J. D., 121, 180, 184, (266)
Holland, V. F., 186 (292, 293)
Hopkins, I. L., 184 (280)
Hunt, R. G., 37 (66), 38, 39, 258 (66), 270 (66)

I

Illers, K. H., 184 (282), 185
Irvin, J. D., 142 (226)
Isaacs, L. L., 25 (51)
Ishida, I., 254 (384)
Ishida, Y., 123 (199), 203 (338)
Ishikawa, K., 88 (139, 141), 89 (141), 91 (141), 92 (141)
Ishinabe, T., 88 (139, 141), 89 (141), 91 (141), 92 (141)
Ito, T., 244 (382)

J

Jackle, J., 208 (352)
Jackson, W., 121 (196)
Janacek, J., 195 (311)
Jarzynski, J., 233, 234
Jenckel, E., 201 (328)
Jones, R. E., 67
Jura, G., 95 (152)

K

Kabanov, V. A., 44 (78)
Kabin, S. P., 127 (215)
Kajiama, T., 184 (277)
Kaneko, M., 190 (307)
Kapur, S., 195
Karasz, F. E., 19 (35), 281 (191)
Kargin, V. A., 44 (76)
Kawaguchi, T., 227
Kazarian, L. G., 238 (379)
Keesom, P., 19 (25)
Kerkjian, K., 184 (280)
Kevorkian, H. K., 20, 33, 100
Kilian, H. G., 30
King, G. J., 21 (38), 30, 102
Kirby, R. K., 101, 102
Kirgis, J. B., 97 (161)
Kirkwood, J. G., 92 (144)
Kitaigorodsky, A. I., 44 (76)
Kittel, C., 54, 82 (3), 83 (3)
Klein, R., 208 (350)
Klemens, P., 48 (81), 52 (81), 54, 62, 63, 64
Kline, D. E., 184, 201 (329)
Knappe, W., 56 (101), 57 (101), 66 (101), 271 (101)
Knox, J. R., 100 (168)
Koenig, J. L., 187
Kolarik, H., 195 (311)
Kolesov, V. P., 34 (59), 270 (59)
Kolouch, R. J., 56 (95), 68, 69, 74, 271 (95)
Konovalov, A. G., 190 (304)
Kontos, E. G., 100 (167)
Kosfeld, R., 166 (253), 167 (253, 257), 168 (253, 257), 169 (253), 170, 171 (253, 257), 172 (253, 257, 262), 173 (257), 175 (257), 176 (257)
Kosourov, G. I., 101 (172)
Kubo, R., 154 (239), 155
Kuffel, E., 125 (209), 126, 128, 138 (209), 140 (209), 272 (209)
Kvacheva, L. A., 157 (246), 188 (300), 238 (246)

L

Labes, M. M., 284 (314)
Laidler, K., 121 (197), 169 (197)
Lamberson, D. L., 262 (391), 263 (391), 264 (391)
Landau, L. D., 165 (252), 206, 208 (353), 209 (353)
Laquer, H. L., 87 (128), 96 (154), 97, 98, 99, 100 (128), 102, 103, 271 (128)
Lebedev, B. V., 260 (388), 270 (388)
Leibfried, G., 48 (82), 51 (82, 84), 83, 223 (82), 257 (387)
Leksina, I. E., 101, 102 (171)
Lifshitz, E. M., 165 (252), 208 (353), 209 (353)
Lifshitz, I. M., 14, 15, 24
Lindenmeyer, P. H., 186 (293)
Litt, M., 198 (323)
London, F., 90 (142)
Lösche, A., 147 (229)
Ludwig, W., 257 (387)

Lukyanov, I. A., 19 (31)
Lyubimov, A. N., 107 (185), 143 (185), 147 (185), 150 (185), 159 (185), 162, 164 (185), 167 (185), 172 (185)

M

McCall, D. W., 156
McCammon, R. D., 97 (159), 125 (159), 137, 142 (225), 143, 145, 183, 202, 272 (221, 225)
McConnell, P. M., 97 (161)
McCoskey, E., 21 (38), 30, 102
McCrum, N. G., 98 (163), 117 (163), 118 (163), 119 (163), 120 (163), 121 (163), 125 (163), 143 (163), 183 (163), 184 (163), 185, 188 (163), 189, 190 (163), 194, 195 (163), 197, 198
McCullough, J., 277 (29)
McKenna, L., 184 (277)
McKnight, N. J., 184 (277)
Madding, R. P., 43 (73)
Maklakov, A. I., 154, 156
Manaresi, P., 100
Mandelkern, L., 103, 184 (278), 185
Mandell, E. R., 171 (260)
Mansfield, P., 196 (319)
Maris, H. J., 208 (349)
Mark, P. C., 19 (34)
Martin, G. M., 195 (315)
Masaki, G., 43 (71)
Mason, W. P., 283 (280), 286 (386)
Mathes, K. N., 126, 127, 135, 136, 272 (212)
Mathot, V., 87 (130, 131)
Matochkin, V. S., 158 (183)
Matsik, F. J., 104 (180), 106 (180), 107 (180)
Marsuoka, S., 254 (384)
Maynard, R., 65
Meakins, R. J., 118 (193), 121 (193)
Melia, T. P., 19 (30), 33, 34 (48), 37 (48)
Mendelssohn, K., 19 (24)
Mijake, A., 154 (238), 155
Mikhailov, G. P. 127 (215), 190 (305)
Miki, K., 186 (291), 190
Miyazawa, T., 28
Mogilevsky, B. M., 48 (83), 52 (83), 53 (83)
Müller, F. H., 30 (56), 125 (210), 127, 135, 272 (210)
Muus, L. T., 102 (176)
Mylius, U., 166 (253), 167 (253, 257), 168 (253, 257), 169 (253), 170, 171 (253, 257), 172 (253, 257), 173 (257), 175 (257), 176 (257)

N

Nakamae, K., 244
Nanda, V. S., 87, 88 (138), 92 (147), 93 (147), 94 (147)
Navotki, K., 168
Nernst, W., 18
Newell, G. K., 22
Nichols, G. E., 19 (36)
Nicol, J., 57 (104)
Nishi, T., 185 (286)
Noer, R. J., 21 (39), 31, 37 (39)
Novikova, S. I., 101 (174), 102 (171)
Nowell, J. B., 195 (312)
Nozaki, M., 142 (224)

O

Odajima, A., 171 (222)
Oehme, F., 125 (203)
Ohzawa, Y., 188
Okamoto, S., 127 (214), 142 (224)
O'Reilly, J. M., 19 (35)
Orwoll, R. A., 87 (136)
Oskotsky, V. S., 52 (85)
Ozvold, M., 208 (347), 221 (347)

P

Pagliari, A., 203 (335), 204
Papir, Y. S., 182 (269), 185 (308), 186 (269), 187 (269), 191, 192 (308), 193, 195, 221 (269)
Papoular, M., 94 (149)
Passaglia, E., 20, 33, 100, 180, 184 (266), 195 (315)
Pastine, D. J., 94 (150), 95 (150, 151), 99 (151)
Paukov, I. E., 34 (59), 270 (59)
Paul, D. R., 88
Pauling, L., 134 (218)
Pechhold, W., 185, 186, 236
Peierls, R., 46 (80), 47
Perepechko, I. I., 43 (70), 44 (70), 68 (122), 98 (70), 118 (70), 119 (70), 122 (70), 124 (70), 143 (70), 157 (70, 246), 160 (70), 162 (70), 178 (70), 180 (70, 267), 183 (70), 184 (70, 279), 188 (70, 300, 301), 189, 190 (70), 191 (70), 193 (70), 194 (70), 198 (70), 203 (339, 340), 204 (70), 208 (70, 346, 354), 209 (70, 354), 210 (70), 211 (70), 213 (355, 356), 214 (355,

356), 216 (70, 361, 362, 363, 364), 217 (70, 122, 355, 367), 218 (122, 355, 356, 367, 368), 220 (70, 122, 356, 367, 368), 223 (122), 224 (70, 122, 370), 225 (70, 122), 226 (356, 368), 227 (368), 228 (367, 372), 231 (367, 372), 232 (370, 375), 234 (375), 235 (70, 370, 375, 376), 236 (70), 238 (70, 246, 356, 378, 379), 239 (70, 370), 240 (70), 241 (122, 356, 367, 368, 370, 372, 375, 380, 381), 243 (381), 249 (380, 381), 250 (380, 381), 252 (380), 255 (70, 385), 256 (70, 122, 367, 368, 370, 372, 375, 376, 385), 259 (70, 385), 262 (385), 263 (385), 264 (385), 265 (381), 273 (122, 367, 368, 370, 372, 375)
Peterlin, A., 185
Petersen, J., 203 (333, 337), 204
Pezzin, G., 203 (335, 336), 204
Phillips, W. A., 71 (123), 125 (207), 126, 130, 131, 132, 133, 134
Pirlman, N., 19 (25)
Ponomarev, Ya. G., 214
Popov, M. M., 19 (23)
Pound, R. V., 153
Powell, R. L., 56 (94), 71, 72, 73, 271 (94)
Powles, J. G., 164 (249), 165, 170 (249), 174 (249), 196 (319)
Prigogine, I., 87
Purcell, E. M., 153

R

Rabinovich, I. B., 260 (388), 270 (388)
Ränby, B., 203 (333, 337), 204
Read, B. E., 98 (163), 117 (163), 118 (163), 119 (163, 194), 120 (163), 121 (163, 194), 125 (163), 143 (163), 183 (163), 184 (163), 188 (163), 189, 190 (163), 194, 195 (163), 198 (163)
Reding, F. P., 100, 227 (165)
Rees, W., 14, 19 (33), 21 (40), 24, 26, 27 (52), 29, 30, 31, 32, 33, 35 (33, 52), 36, 37, 38 (33, 52), 43 (33, 52), 56 (40, 96, 99), 61 (99), 62 (115), 64, 66 (33), 67, 68, 71 (40), 72, 73, 74, 76, 77 (99), 78 (99, 115), 79, 81, 203, 255 (52), 258 (33), 270 (40), 271 (33, 40, 99)
Reich, S., 198 (327), 199 (326), 200, 201 (326, 327), 229, 230
Reiner, M., 117
Reneker, D. H., 186
Ritger, A. J., 216 (366)
Roberts, J. D., 147 (228)
Robinson, D. W., 104 (179), 106 (179), 107 (179)
Roe, J. M., 92 (147), 93 (147), 94 (147)
Rogers, Ch. E., 195
Rogers, S. S., 103
Rogers, W. M., 56 (94), 71, 271 (94)
Roinishvili, E. Yu., 32
Rose-Innes, A., 19 (28)
Rosenberg, H. M., 56 (98), 74 (98), 75 (98), 271 (98)
Rosenstock, H. B., 36 (64)
Roy, N. K., 56 (100)
Rumer, G., 206

S

Saba, R. G., 137 (221), 142 (225), 143, 145 (225), 179 (265), 180 (265), 182, 185 (265), 197 (265), 198 (265), 199 (265), 202, 205, 227 (265), 272 (221, 225), 274 (265)
Saito, N., 123, 124 (201)
Sakurada, I., 244
Salikhov, K. M., 123
Salinger, G. L., 37 (66, 67), 38, 39 (66), 57 (67), 76, 77 (67), 79 (67), 80 (67), 81 (67), 258 (66), 270 (66)
Samoilov, B. N., 101 (172)
Sauer, J. A., 104 (182), 179 (265), 180 (265), 182, 184, 185 (265, 290), 195 (316), 196 (290, 314), 197 (265, 290), 198 (182, 265, 290, 314), 199 (265, 290), 201 (329), 202 (330), 203 (331), 204 (290), 227 (265), 274 (265)
Sazhin, B. I., 127 (215), 281 (190)
Schatzki, T. F., 98, 107 (162), 121, 122, 184
Schell, W. J., 97 (158), 107 (158), 109
Schiller, P., 192 (310)
Schloemann, E., 51 (84)
Schmieder, K., 104 (181), 203
Scott, D., 277 (29)
Scott, R., 19 (26)
Scott, T. A., 57 (105), 70 (105), 71 (105), 271 (105)
Seeger, A., 192 (309, 310)
Seitz, F., 286 (387)

Shchegolev, I. F., 215
Shen, M. C., 95 (152), 104 (180), 106 (180), 107
Shetter, J. A., 57 (110)
Shimada, K., 142 (224)
Shimanouchi, T., 28
Shimizu, K., 211 (358)
Shinohara, K., 160 (247), 161 (247)
Shoulberg, R. H., 57 (110)
Shozo, T., 43 (71)
Siegel, K., 136
Simha, R., 87, 88 (138), 92, 93 (147), 94 (147), 97, 98, 99, 100, 103, 104, 105, 107 (158), 109, 266 (157), 267 (156), 271 (157)
Sinnott, K. M., 106, 171 (261), 183 (271), 184, 185, 196, 197, 202
Skripov, F. I., 147 (232), 147 (227)
Skuratov, S. M., 34 (59), 270 (59)
Slater, J. C., 92 (144)
Slichter, Ch. P., 147 (230)
Slichter, W. P., 100 (167), 138 (235), 147 (231, 233, 235), 156, 164 (231, 233, 235), 167 (231, 233, 235), 171 (260)
Slonim, I. Ya., 107 (185), 143 (185), 147 (185, 234), 150 (185), 159 (185), 162, 164 (185), 167 (185), 172 (185), 190 (304)
Slonimsky, G. L., 44 (76)
Smirnov, I. A., 52 (85)
Sochava, I. V., 23 (42), 24, 28, 29, 31, 32, 37, 38 (42, 65), 260 (65)
Somcynsky, T., 88 (138)
Sorokin, V. E., 68 (122), 211, 213 (355), 216 (361, 362), 217 (122, 355, 367), 218 (122, 355, 367), 220 (122, 367), 223 (122), 224 (122, 370), 225 (122), 228 (367), 231 (367), 232 (370), 233 (370), 235 (370), 239 (370), 241 (122, 367, 370, 381), 243 (381), 249 (381), 250 (381), 265 (381), 273 (122, 367, 370), 274 (381)
Startsev, O. V., 180 (267)
Stehling, F. C., 184 (278), 185
Stejskal, E. O., 165, 166, 167, 169, 170, 174 (251), 198, 200, 229
Stephens, R. B., 37 (67), 38, 57 (67), 76, 77 (67), 79, 80 (67), 81 (67)
Stockmayer, W. H., 16, 17, 21
Strelkov, P. G., 101
Strong, J. D., 104 (180), 106 (180), 107 (180)
Stryukov, V. B., 215
Swan, P. R., 100

T

Takeuchi, K., 127 (214)
Talun, G. G., 208 (348)
Tarasov, V. V., 8, 9, 10 (8), 11, 14 (8), 15, 259
Tasumi, M., 28
Tavkhelidze, N. N., 32
Terry, C., 57, (106), 70, 71
Tomita, K., 154 (239), 155
Trapeznikova, O. N., 23 (42), 24, 37, 38 (42)
Trappeniers, N., 87 (130, 131)
Tseng, T. P., 57 (104)
Tucker, J. E., 14, 21 (40), 24, 26, 29, 30, 31, 32, 33, 67, 68, 71 (40), 74, 270 (40), 271 (40)
Turnbull, D., 286 (387)

U

Urman, Ya. G., 190 (304)
Urzendowski, S. R., 262 (389), 263 (389), 264 (389)
Ushakov, L. A., 203 (339, 340)

V

Vaks, V. G., 221 (369)
Van de Voorde, M., 97 (160), 99 (160), 100 (160), 103, 271 (160)
Van Vleck, J. H., 150, 168, 173
Vincett, P. S., 125, 126, 129, 132, 136, 137, 272 (206)
Volger, J., 130 (216, 217)
Volkenshtein, M. V., 244 (383)
von Kármán, Th., 7, 85
Vosskötter, G., 172 (262)
Vrij, A., 87 (136)

W

Wada, Y., 185, 188, 202, 203, 264
Wagner, H., 43 (72)
Wagner, M., 52 (88), 53
Wall, R. A., 104 (182), 198 (182)
Walton, D., 52 (87)
Waterman, H. I., 236
Weissberger, A., 284 (314)
Westerdijk. J. B., 236
Weyman, H. D., 208 (351)
Wheatley, J. C., 56 (96), 71, 72, 73
White, G. K., 19 (27), 53 (89)
Wilhoit, R. C., 19 (32)
Wilkinson, R. W., 100
Willblown, A. H., 104 (179), 106 (179), 107 (179)
Williams, G., 98 (163), 117 (163), 118 (163), 119 (163, 194), 120 (163), 121 (163, 194), 125 (163), 143

(163), 180, 183 (163), 184 (163, 266), 188 (163), 189, 190, (163) 194, 195 (163), 198 (163)
Wolf, K., 203
Woodruf, T. O., 207
Woods, S. B., 53 (89)
Woodward, A. E., 104 (182), 106, 171 (222), 184, 185 (290), 196 (290, 314, 318), 197 (290), 198 (182, 290, 314), 199 (290), 202 (318, 330), 203, 204 (290), 205
Work, R. N., 97 (159), 125 (159), 137 (221), 142 (225, 226), 143, 145 (225), 272 (221, 225)
Worthington, A. E., 19 (34)
Wu, C. K., 95 (152)
Wunderlich, B., 14, 21 (7), 24, 26 (49, 50), 28, 122, 260, 270 (7)

Y

Yamafuji, K., 123
Yano, O., 203
Yasukawa, J., 190 (307)
Yeh, G. S. Y., 44 (77)

Z

Zakin, J. L., 97 (157), 98, 99 (157), 100 (157), 266 (157), 271 (157)
Zelenev, Yu. V., 179 (264), 180 (264)
Zeller, R. C., 35 (63)
Ziman, J. M., 54, 55, 63, 78 (92), 86 (127)
Zoller, P., 39, 40, (68, 69), 41 (68, 69), 42 (68), 43 (68)
Zyryanov, P. S., 208 (348)

SUBJECT INDEX

A

Absolute rate theory, 121, 127
Absorption coefficient, sound, 207, 216
Acoustical branch, 7, 17, 41, 42
Acoustical measurements, 211 *et seq.*
Acoustical properties, 206 *et seq.*
  and structure, 236 *et seq.*
Acoustic relaxation, 113
Acoustic spectroscopy, 178, 181
Activation energy, 119, 122, 124, 151, 217, 222 *et seq.*
Adiabatic bulk modulus, 211, 262
Adiabatic calorimeter, 18, 19
Amorphous polymers
  heat capacity, 34-44, 258
  thermal conductivity, 76-81
  thermal expansion, 86-94
Anharmonicity, 46, 83, 261, 265
Anharmonicity factor, 82, 83
Antiplasticization, 162
Arrhenius equation, 129
Asymmetric potential barrier, 232

B

Barker formula, 265, 266, 267
Bloembergen-Purcell-Pound theory, 153
Boltzmann constant, 1
Boltzmann distribution function, 82, 83
Boltzmann equation, 48, 207
Bordoni method, 183
Bordoni peaks, 192, 193
Born-Kármán theory, 7, 85
Bose-Einstein statistics, 47
"Bound" kink-defects, 187
Boyer model, 121
BPP theory, 153
Bridge circuits, 125
Bridgman relation, 265
Brillouin zone, 51
Buffer-rod method, 211, 212
Bulk modulus of elasticity, 241, 242

C

Calorimeter, 18
Cell model, 87, 88
Chain flexibility, 91
Chain interaction, 11 *et seq.*
Chang-Jones formula, 67, 70
Characteristic Debye temperature, 5
Characteristic Einstein temperature, 3
Chujo assumption, 155
Classical harmonic oscillators, 2, 3
Clausius-Mosotti equation, 111
Clough theory, 174, 175
Coherent phonons, 206, 207
Cohesive energy density, 88, 122
Collision, of phonons, 48
Complex compliance, 118
Complex dielectric constant, 113
Complex elastic modulus, 118, 178
Conformational kink-defects, 182, 185, 186, 187, 192, 193
Correlation frequency, 151
Correlation function, 151
Correlation length, 55
Correlation time, 151, 152
Correlation-time spectrum, 154, 155
Correlation-time spectrum density, 154, 155, 159
Coulomb interaction, 49
Crankshaft rotation, 98, 121, 122, 184
Cryostat, 213
Crystal lattice, 2
Crystalline polymers
  acoustical properties, 218 *et seq.*
  heat capacity, 23-34
  relaxation processes, 218-28
  thermal conductivity, 65-76
  thermal expansion, 94, 95
Crystallinity,
  and sound velocity, 236 *et seq.*
Cubic expansion coefficient, 60, see also Volume expansion coefficient

D

Deborah number, 117
Debye characteristic temperature, 5
Debye elastic waves, 8
Debye formula, 58, 117, 118
Debye function, 5
Debye one-dimensional function, 10
Debye's cube law, 6, 34, 35
Debye's theory, 4, 22, 35, 37, 38, 49, 119

Debye temperature, 255 *et seq.*
Debye two-dimensional function, 10
Debye waves, 11, 22
  scattering of, 54
Deformation polarization, 110
Deformation vibrations, 17, 29
Degree of crystallinity, 65, 66, 94
  and heat capacity, 26, 27
  and low-temperature plateau, 218
  and NMR linewidth, 155, 156
  and sound velocity, 236 *et seq.*
Devonshire potential, 92
Dielectric constant, 111, 114, 117, 118, 119
Dielectric loss tangent, 113
Dielectric measurements, 125
Dielectric properties, 126-46
  methods of investigation, 124, 125
  temperature dependence of, 118-20
Dielectric relaxation, 111, 113 *et seq.*
  mechanism of, 120-4
Dielectric relaxation time, 115 *et seq.*
Dielectric saturation, 129
Dielectrics
  electrical properties, 111
  thermal conductivity, 45 *et seq.*
Dilatometer, 96
Dipole moment, 110
Dislocation jogs, 182, 185, 186, 187, 193
Dislocation model, 193
Dispersion forces, 90
Dispersion law, 6, 14
Dissipation factor, 113
Distribution function, 48
Dulong-Petit law, 2, 23, 264
Dynamic compliance, 247
Dynamic elastic modulus, 178, 238, 241, 242, 243 *et seq.*
Dynamic mechanical properties, 178 *et seq.*
  effect of chemical constitution, structure and composition, 178-82
  methods of investigation, 183
Dynamic shear modulus, 15, 178, 179, 183, 209, 241, 249

E

Edge dislocations, 186, 187
Eierman diagram, 59
Eierman theory, 58, 59, 79
Einstein characteristic temperature, 3
Einstein function, 3
Einstein harmonic oscillator, 2, 38, 39, 40
Einstein's theory, 2-4
Elastic constant, 41
Elastic continuum, 4, 8, 9
Elastic correlation length, 63
Elastic flexural waves, 14
Elastic moduli, 15
Elastic scattering, 52
Elastic waves, 4, 5, 14
Electrical induction, 112
Electrical properties, 110-46
Electric displacement, 112, 113, 114, 118
Electric displacement vector, 113
Electric field strength, 112, 113, 118
Elementary thermal conductivity, 59
Elementary thermal resistance, 58, 59
Energy dissipation, 230
Energy levels, 165, 166
Energy of activation, *see* Activation energy
Energy transfer, 62
Epoxide resin
  acoustical properties, 228, 231
  dynamic elastic moduli, 245
  elastic parameters, 274, 275
  Poisson's ratio, 252
  ultrasonic velocity, 228, 273
Equations of state, 83-6
"Excess" heat capacity, 27, 35, 43

F

Flexural waves, 14
Force constant, 16, 123
Formaldehyde, 34
Fourier law, 45
Four-phonon processes, 51
"Free" kink-defects, 187
Fröhlich theory, 119

G

Genensky-Newell model, 21, 22
Grüneisen constant, 51, 85, 93, 207, 276
  determination of, 261 *et seq.*
Grüneisen relation, 85
Gyromagnetic ratio, 174

H

Hamiltonian, 49
Harmonic approximation, 49
Harmonic oscillators, 1 *et seq.*, 38, 39, 40, 85

Heat capacity, 1, 255, 258, 259, 260, 270
  at constant pressure, 20
  at constant volume, 1 *et seq.*
  Debye's theory, 4
  Einstein's theory, 2
  measurement of, 17-20
  molar, 1, 2, 23
  of amorphous polymers, 22, 34-44
  of crystalline polymers, 22, 23-34
  of solids, 1-8
  temperature dependence of 3, 4, 6, 7, 11 *et seq.*
Heat-capacity function, 12
Heat conduction, 45, 221
Heat flux, 45, 47
Heat flux density, 48, 209
Hecht-Stockmayer theory, 16, 17, 21, 28
Helmholtz free energy, 83, 84, 92, 209
Hexagonal lattice, 88, 89, 91, 92
Hoffman-Williams-Passaglia model, 180
Hooke's law, 1
Hosemann-Bonart model, 158, 238
Hysteresis processes, 233

I

Imaginary dielectric constant, 113
Incoherent phonons, 206
Inelastic tunnelling, 230
Interacting-chain model, 89
Intermolecular interaction, 16, 59, 243, 244, 246
Internal energy, 1, 4, 5, 6, 84
Intrinsic angular momentum, 147
Intrinsic magnetic moment, 147
Inverted torsion pendulum, 183
Ishinabe-Ishikawa theory, 88
Isothermal bulk modulus, 209
Isothermal compressibility, 20, 84, 261
Isotropic elastic continuum, 8

K

Kink-defects, 185, 186, 187, 192, 193
Kink-isomers, 186
Klemens theory, 63, 64, 67, 78
Kramers-Chandrasekhar equation, 124

L

Lamella thickness, 74
Landau-Rumer theory, 206
Lattice defects, 52
Lattice vibrations, 4, 7, 8, 47, 83, 84, 85, 86
Law of conservation of momentum, 50, 208
Law of linear continuum, 9, 11, 12
Lennard-Jones potential, 87, 89, 92, 124, 261
Lifshitz theory, 14
Linear expansion coefficient, 83, 93, 95 *et seq.*, 262, 271
Linear expansivity, 83
Local mode, 53, 123, 124
London equation, 90
"Longitudinal" Debye temperature, 14
Longitudinal phonons, 64
Longitudinal waves, 4, 5, 14, 219 *et seq.*
Long-wave acoustic phonons, 52
Loss factor, 178
Loss modulus, 178
Loss tangent, 113, 118, 178 *et seq.*
  frequency dependence of, 118
Low-temperature calorimetry, 18
Low-temperature plateau, 218 *et seq.*

M

Macroscopic electric field strength, 112
Magnetic field, 148
Magnetic field strength, 148
Magnetic moment, 147
Magnetic polarization, 153
Magnetization vector, 153
Mathieu equation, 134
Mean free path, of phonons, 46, 55, 68, 69, 206
Mechanical relaxation, 123, 178 *et seq.*
Methyl group
  re-orientation of, 166, 167, 172, 229
  tunnelling of, 167, 169, 170, 173, 175, 176, 198
Micro-Brownian segmental motion, 98, 171
Molar heat capacity, 1, 2, 23
Molar volume, 1
Molecular motion, 162, 163, 164, 178, 179
  mechanism of, 121, 122
Molecular polarizability, 110, 111
Molecular resonance phonon scattering, 53

N

Natural rubber
  thermal conductivity, 57, 58
Natural vibrations, 8 *et seq.*

Nearest-neighbour forces, 7
Network density, 159
NMR lineshape, 149
NMR linewidth, 150
  and cross-linking, 158-61
  and crystallinity, 155, 158-61
  and plasticizer concentration, 161-3
  and temperature, 156, 157
NMR spectra, 149, 150
Non-interacting chain theory, 11
"Normal" processes, 50, 206, 207, 221
Normal vibrations, 6, 7, 8, 85
  frequency spectrum, 6, 7
Nuclear magnetic resonance, 147 *et seq.*
  effect of structure and composition, 154 *et seq.*
  in polymers with methyl groups, 167-77
  second moment, 150, 151, 160
  spin-lattice relaxation, 153
Nylon 6, 34
  acoustical properties, 226, 227
  activation energy, 226, 227
  bulk modulus, 248, 249
  Debye temperature, 257, 272
  dynamic elastic moduli, 245
  elastic parameters, 275
  Grüneisen constant, 263, 276
  heat capacity, 34, 259, 270
  linear expansion coefficient, 266, 276
  low-temperature plateau, 218
  temperature transitions, 222
  ultrasonic velocity, 273
  Young's modulus, 243, 244
Nylon 6,6, 33, 138
  dielectric properties, 138, 272
  elastic parameters, 274, 275
  heat capacity, 33, 270
  linear expansion coefficient, 271
  loss peaks, 138, 139
  loss tangent, 138, 139
  thermal conductivity, 73, 74, 75, 271
Nylon 6,10
  acoustical properties, 226, 227, 238
  bulk modulus, 248, 249
  Debye temperature, 257, 272
  elastic parameters, 274, 275
  Grüneisen constant, 263, 276
  heat capacity, 259
  linear expansion coefficient, 266, 276
  low-temperature plateau, 218
  Poisson's ratio, 249, 250, 253
  temperature transitions, 222
  ultrasonic velocity, 273
  Young's modulus, 243
Nylon 7, 34
  acoustical properties, 226, 238
  activation energy, 226
  bulk modulus, 248, 249
  Debye temperature, 257, 272
  dynamic elastic moduli, 245
  elastic parameters, 274, 275
  Grüneisen constant, 276
  heat capacity, 34, 259, 270
  linear expansion coefficient, 266, 276
  low-temperature plateau, 218
  Poisson's ratio, 249, 250, 253
  temperature transitions, 222
  ultrasonic velocity, 226, 273
  Young's modulus, 243
Nylon 11, 139
  acoustical properties, 226, 238
  activation energy, 140, 226
  bulk modulus, 248, 249
  Debye temperature, 257, 272
  dielectric properties, 140, 141, 272
  dynamic elastic moduli, 245
  elastic parameters, 274, 275
  Grüneisen constant, 263, 276
  heat capacity, 259
  linear expansion coefficient, 266, 276
  loss peaks, 140, 141
  loss tangent, 140
  Poisson's ratio, 249, 252, 253
  temperature transitions, 222
  ultrasonic velocity, 218, 226, 273
  Young's modulus, 243
Nylon 12
  acoustical properties, 226, 227, 238
  activation energy, 226, 227
  bulk modulus, 248, 249
  Debye temperature, 257
  dynamic elastic moduli, 245
  elastic parameters, 274, 275
  Grüneisen constant, 263, 276
  linear expansion coefficient, 276
  temperature transitions, 222
  ultrasonic velocity, 218, 226, 273
  Young's modulus, 243

O

Oligomeric liquids, 87
One-dimensional continuum, 8, 9, 10, 22

One-dimensional harmonic oscillator, 1, 6
Onsager theory, 119
Optical branch, 7, 41
Orientational polarization, 110

P

Periodic harmonic processes, 210
Permanent dipoles, 110
Permittivity, 111
Phase shift, 54, 55
Phenomenological relaxation theory, 113, 221, 228, 239
Phenomenological theory, of sound propagation, 208-11
Phillips quantum model, 133
Phonon, 8
Phonon gas, 47
Phonon-phonon interaction, 49, 50, 62, 230
Phonon scattering, 51 *et seq.*, 62
Planck distribution function, 207
Planck formula, 2
Plasticized polymers, 161-3
Point defects, 52
Poisson's ratio, 241 *et seq.*, 249 *et seq.*
Polarizability, 110, 111
Polarization, 153
Polarization vector, 47, 110, 111
Polyamides
  acoustical properties, 226-8
  activation energy, 226, 227
  dielectric properties, 138-41
  dynamic elastic moduli, 245
  low-temperature plateau, 218
  mean free path of phonons, 73
  Poisson's ratio, 249 *et seq.*
  relaxation, 121, 138, 139, 140
  thermal conductivity, 73-5
  ultrasonic velocity, 217
Poly-*n*-butyl methacrylate
  linear expansion coefficient, 104
  temperature transitions, 106
Poly-*sec*-butyl methacrylate
  linear expansion coefficient, 105, 108
  temperature transitions, 106, 107
Poly-*tert*-butyl methacrylate
  linear expansion coefficient, 105, 108
Polycapramide
  acoustical properties, 238, 239
  dynamic mechanical properties, 194, 195
  Grüneisen constant, 263
  loss peaks, 194, 195
Polycarbonate
  acoustical properties, 228, 231
  activation energy, 173, 174
  Debye temperature, 257, 272
  dielectric properties, 272
  dynamic elastic moduli, 246
  elastic parameters, 274, 275
  Grüneisen constant, 263
  heat capacity, 270
  motion of methyl groups, 173, 174, 175
  NMR, 172-5
  Poisson's ratio, 251, 252
  second moment, 173, 174, 175
  tunnelling, 173, 174, 175
  ultrasonic velocity, 218, 273
Poly-*m*-chlorostyrene, 145
Poly-*o*-chlorostyrene, 41, 145
Poly-*p*-chlorostyrene, 145
Polycyclopentyl methacrylate
  linear expansion coefficient, 94
Poly-*n*-decyl methacrylate
  linear expansion coefficient, 105, 107, 108
Polyethylene, 23
  acoustical properties, 223, 224
  activation energy, 185
  amorphous, 23, 24, 25, 26, 27, 29, 35
  characteristic temperatures, 28, 29
  correlation frequency, 158
  crystalline, 23, 24, 25, 26, 27, 28
  Debye temperature, 257, 272
  degree of crystallinity, 24 *et seq.*
  density, 23
  dielectric constant, 127, 128
  dielectric properties, 127-35, 272
  dilatometric curve, 97, 98
  dynamic elastic moduli, 245, 246
  dynamic mechanical properties, 184-8
  elastic parameters, 274, 275
  glass-transition temperature, 98
  Grüneisen constant, 262, 263
  heat capacity, 23-9, 35, 259, 260, 270
  linear expansion coefficient, 97, 98, 99, 100, 271
  logarithmic decrement, 185, 186
  loss peaks, 98, 130, 134, 135, 182, 184, 185
  loss tangent, 127, 128, 129, 130, 133
  mean free path of phonons, 68, 69
  mechanical loss peaks, 185
  micro-Brownian motion, 98

Polyethelene
  NMR linewidth, 156, 157
  Poisson's ratio, 250, 251, 252
  potential energy, 132
  relaxations, 107, 121, 127 *et seq.*, 184, 185 *et seq.*
  sound velocity, 67, 157
  structural parameters, 68, 69
  temperature transitions, 97, 98, 222
  thermal conductivity, 60, 61, 66-71, 271
  thermal expansion, 97-100
  tunnelling, 130, 132, 133
  ultrasonic velocity, 217, 218, 219, 273
  Young's modulus, 157
Polyethylene terephthalate
  dielectric properties, 272
  elastic parameters, 174, 274, 275
  heat capacity, 32
  linear expansion coefficient, 104, 106
  mechanical loss peaks, 182, 193
  relaxations, 124, 187
  thermal conductivity, 60
Polyethyl methacrylate
  linear expansion coefficient, 104, 106, 108
Polyformaldehyde
  acoustical properties, 224-6
  Debye temperature, 257, 272
  dynamic mechanical properties, 189-94
  dynamic shear modulus, 190
  elastic parameters, 274, 275
  glass-transition temperature, 191
  heat capacity, 34, 259, 270
  logarithmic decrement, 189, 190, 192
  loss peaks, 189, 190, 191
  low-temperature plateau, 218
  low-temperature relaxation, 192
  Poisson's ratio, 252
  relaxations, 124, 187, 192, 193, 194
  segmental motion, 190
  temperature transitions, 222
  thermal conductivity, 60, 75, 271
  ultrasonic velocity, 273
  viscoelastic behaviour, 191
Poly-*n*-hexyl methacrylate
  linear expansion coefficient, 105, 108
Polyisobutylene
  NMR, 175-7
  rotation of CH_3 groups, 176
Polyisobutylene
  second moment, 175, 176, 177
  thermal conductivity, 57
  tunnelling, 176, 177
Polyisobutyl methacrylate
  linear expansion coefficient, 105, 108
  temperature transitions, 106, 107
Polymethyl acrylate
  activation energy, 172
  correlation frequency, 166, 172
  NMR, 171
  relaxations, 121
  second moment, 171
  tunnelling frequency, 172
Polymethyl methacrylate
  acoustical properties, 228, 229, 231
  activation energy, 197, 198
  amorphous, 76-81
  atactic, 37
  bulk modulus, 248, 249
  characteristic temperatures, 78
  correlation frequency, 166
  Debye temperature, 257, 272
  dielectric losses, 141, 142
  dynamic elastic moduli, 246
  dynamic mechanical properties, 197, 198
  elastic parameters, 274, 275
  Grüneisen constant, 263, 264, 276
  heat capacity, 35 *et seq.*, 259, 260, 270
  isotactic, 37
  linear expansion coefficient, 106, 108, 266, 271, 276
  loss tangent, 106, 141, 197
  mean free path of phonons, 78
  molecular parameters, 92
  NMR, 161-71
  potential barrier, 37, 170
  relaxations, 107, 180, 182
  rotation of methyl group, 37, 168, 169, 198
  second moment, 167, 168, 169, 170, 171
  syndiotactic, 37
  thermal conductivity, 57, 60, 61, 76-81, 271
  transverse vibrations, 78
  tunnelling, 169, 170, 198
  ultrasonic velocity, 273
  Young's modulus, 197, 243, 246
Poly-4-methyl pentene-1
  acoustical properties, 231
  bulk modulus, 248, 249
  Debye temperature, 272
  dynamic elastic moduli, 246

Poly-4-methyl pentene-1
  dynamic mechanical properties, 198-200
  elastic parameters, 274, 275
  Grüneisen constant, 263, 276
  heat capacity, 259, 260
  linear expansion coefficient, 266, 276
  loss tangent, 199
  Poisson's ratio, 249, 251, 253
  relaxations, 199
  second moment, 199
  spin-lattice relaxation time, 199
  thermal expansion coefficient, 105
  ultrasonic velocity, 273
  Young's modulus, 199, 243, 246
Poly-α-methylstyrene, 41
Poly-*o*-methylstyrene, 41
Poly-*n*-octyl methacrylate
  linear expansion coefficient, 105, 108
  molecular motion, 107
  temperature transitions, 106
Polyoxymethylene, *see* Polyformaldehyde
Polypropylene
  acoustical properties, 228, 231
  activation energy, 138, 196
  amorphous, 33
  atactic, 33, 57
  Debye temperature, 257, 272
  degree of crystallinity, 33
  dielectric constant, 137
  dielectric loss peaks, 137
  dielectric properties, 137, 272
  dynamic mechanical properties, 195-7
  elastic parameters, 274, 275
  glass-transition temperature, 100
  heat capacity, 33, 100, 259, 270
  isotactic, 33, 60, 137
  linear expansion coefficient, 100, 101, 271
  loss peaks, 195, 196
  loss tangent, 137, 196
  Poisson's ratio, 251, 252
  relaxations, 138, 182, 195
  temperature transition, 101
  thermal conductivity, 57
  thermal expansion, 100, 101
  ultrasonic velocity, 273
  volume expansion coefficient, 101
  Young's modulus, 196
Poly-*n*-propyl methacrylate
  linear expansion coefficient, 104, 108
  temperature transitions, 106
Polystyrene
Poly-*p*-propyl methacrylate
  linear expansion coefficient, 106
  acoustical properties, 232, 235
  activation energy, 142, 202, 203
  amorphous, 38
  atactic, 38
  bulk modulus, 248, 249
  Debye temperature, 257, 272
  dielectric constant, 142
  dielectric losses, 145
  dielectric properties, 142, 272
  dynamic mechanical properties, 201-3
  Einstein temperature, 40, 42
  elastic parameters, 274, 275
  Grüneisen constant, 263, 264, 276
  heat capacity, 35, 36, 38-44, 259, 260, 270
  linear expansion coefficient, 266, 271, 276
  loss modulus, 202
  loss tangent, 145
  molecular parameters, 92
  motion of phenyl group, 143
  potential energy, 143, 144
  relaxations, 142 *et seq.*
  relaxation peaks, 202, 203
  repeat unit, 42
  rotation of phenyl groups, 143
  shear modulus, 202, 203
  super-Debye heat capacity, 40, 43, 44
  thermal conductivity, 79, 80, 81, 271
  ultrasonic velocity, 273
  viscoelastic relaxation, 201-3
  Young's modulus, 243, 246
Polytetrafluoroethylene (Teflon), 29
  acoustical properties, 224
  Debye temperature, 31, 257, 272
  dielectric loss peak, 135, 136
  dielectric properties, 135, 136, 272
  dynamic elastic moduli, 245
  dynamic mechanical properties, 182, 188, 189
  elastic parameters, 274, 275
  frequency spectrum, 31
  heat capacity, 21, 30, 31, 32, 259, 260, 270
  linear expansion coefficient, 101, 102, 103, 266, 271
  logarithmic decrement, 189
  loss tangent, 136
  low-temperature plateau, 218
  mean free path of phonons, **72**

Polytetrafluoroethylene (Teflon)
  mechanical loss peaks, 188
  phase transition, 102
  Poisson's ratio, 252
  shear modulus, 189
  sound velocity, 238, 239
  specific heat, 30, 31
  temperature transitions, 101, 222
  thermal conductivity, 60, 66, 71-3, 271
  thermal expansion, 101-3
  ultrasonic velocity, 72, 217, 273
  vibrational spectrum, 32
  vibrations, 32
  Young's modulus, 243, 265
Polytrifluorochloroethylene, 32
  acoustical properties, 232, 235, 238, 239
  Debye temperature, 272
  density, 32
  elastic parameters, 274, 275
  heat capacity, 32, 33, 270
  linear expansion coefficient, 271
  Poisson's ratio, 252
  relaxations, 180
  thermal conductivity, 60
  ultrasonic velocity, 238, 239, 273
Polyvinyl acetate
  elastic parameters, 275
  relaxations, 182
Polyvinylalkyl esters
  linear expansion coefficients, 108
Polyvinyl chloride
  acoustical properties, 232, 234
  bulk modulus, 248, 249
  Debye temperature, 257, 272
  dynamic elastic moduli, 245
  dynamic mechanical properties, 203-5
  elastic parameters, 274, 275
  Grüneisen constant, 263, 276
  heat capacity, 259, 260, 270
  linear expansion coefficient, 266, 276
  loss maxima, 203, 204
  loss tangent, 204
  molecular parameters, 92
  Poisson's ratio, 249, 250, 253
  relaxations, 124, 203, 204, 205
  thermal conductivity, 57
  ultrasonic velocity, 273
  Young's modulus, 204, 205, 243, 246
Polyvinyl fluoride
  acoustical properties, 232
  bulk modulus, 248, 249
  Debye temperature, 257, 272
Polyvinyl fluoride
  dielectric properties, 272
  dynamic elastic moduli, 245
  elastic parameters, 274, 275
  Grüneisen constant, 263, 276
  heat capacity, 259
  linear expansion coefficient, 266, 276
  Poisson's ratio, 249, 250, 253
  ultrasonic velocity, 273
  Young's modulus, 243, 246
Polyvinylidene fluoride
  acoustical properties, 235
  Debye temperature, 257
  Grüneisen constant, 263
  low-temperature plateau, 218
  temperature transitions, 222
  ultrasonic velocity, 217
Potential barrier, 121, 122, 123, 165, 166, 167, 200, 201, 230
Potential energy, 49, 89, 120, 121, 122, 143, 144
Potential well, 165, 166
Principle of corresponding states, 87
Pseudo-momentum, 47, 49, 50
Pulse-phase method, 211, 212

Q

Quantum harmonic oscillator, 2, 3, 9
Quantum-mechanical tunnelling, 132, 164-7
Quantum model, 133
Quasi-elastic force, 82
Quasi-momentum, *see* Pseudo-momentum
Quasi-rotonic phonons, 43

R

Rayleigh scattering, 52
Real dielectric constant, 113
Reciprocal lattice, 50
Reduced Einstein temperature, 93
Reduced pressure, 91
Reduced volume, 91, 92
Reference temperature, 96
Relative permittivity, 113
Relaxation frequency, 124
Relaxation processes, 113 *et seq.*, 121, 122, 178, 179, 180, 181, 216 *et seq.*, 228 *et seq.*
Relaxation time, 111
Relaxation-time spectrum, 115, 116
Relaxation-time spectrum density, 211
Resonance method, 183
Resonance phonon scattering, 52, 53

Response equations, 209, 211
Retardation-time spectrum density, 211, 237
Rosenstock model, 36

S

Schatzki model, 98, 121, 122
Schering precision bridge, 125
Schrödinger equation, 134, 165
Second moment, 150, 151
  and structure and composition, 163, 164
  and temperature, 160
Secondary relaxation, 122
Secular equation, 6, 7, 16, 17
Selenium, thermal conductivity, 53, 79
Shear modulus, 15, 178, 179, 183, 209, 241, 249 K
Shear viscosity coefficient, 209
Shear waves, 219 *et seq.*
Simha-Boyer method, 103
Simha-Boyer rule, 104
Small-angle X-ray scattering, 68
Sound propagation, 206 *et seq.*
Sound velocity, 46, 216 *et seq.*, 255
  and crystallinity, 236 *et seq.*
  temperature dependence of, 218 *et seq.*, 256
Specific heat, 1, 207, 208, 255 *et seq.*
Specific volume, 209
Spin-lattice relaxation, 153
Spin-lattice relaxation time, 152, 163, 165
Static polarizability, 11
"Statistical" degree of crystallinity, 155
Stejskal-Gutowsky theory, 229
Stress tensor, 209
Structural scattering, 63, 67
Super-Debye heat capacity, 27, 35, 36, 43, 80
Supermolecular structure, 178

T

Tarasov theory, 8-14, 22, 24, 25, 28, 29, 37
T-cube law, 6
Teflon, *see* Polytetrafluoroethylene
Temperature transitions, 179
Tetragonal lattice, 90, 91, 92
Theory of non-interacting chains, 11
Thermal activation, 123, 169, 173, 175
Thermal conductivity, 45, 208
  and crystallinity, 61, 65, 66
  and orientation, 61
Thermal conductivity
  Debye formula, 46, 58
  effect of point defects, 52
  Eierman theory, 58, 59, 60, 79
  Klemens theory, 63, 64, 67, 78
  measurement of, 56
  of amorphous polymers, 57, 58, 59, 60, 61, 62, 76-81
  of crystalline polymers, 57, 60, 61, 65-76
  of dielectrics, 45-56
  of polymers, 56, 57 *et seq.*, 271
  temperature coefficient, 60
  temperature dependence of, 51
  theories, 62
  Ziman theory, 54, 55
Thermal cubic expansion coefficient, 60
Thermal exchange gas, 21
Thermal expansion, 82 *et seq.*
  of amorphous polymers, 86-94
  of crystalline polymers, 94, 95
  of solids, 82, 83
Thermal expansion coefficients, 97-109, 261 *et seq.*
  measurement of, 95-7
Thermal linear expansion coefficient, 83, 93, 95 *et seq.*, 262, 271
Thermal phonons, 206, 207
Thermal resistance, 58, 59, 60
Thermal volume expansion coefficient, 20, 83, 84, 85, 94, 95, 209
Thermophysical characteristics, 255 *et seq.*
Third power law, 6
Three-dimensional continuum, 8, 9, 12
Three-phonon interaction, 49, 50, 53
Torsional vibrations, 123, 124
Torsion pendulum, 183
Transverse phonons, 64, 68
Transverse rigidity, 14, 15
Transverse waves, 4, 5
Trioxane, 34
Tunnelling, 164-7, 200, 229 *et seq.*
Tunnelling frequency, 165, 167, 200
Tunnelling frequency modulation, 174
Two-dimensional continuum, 8, 9, 10, 22
Two-phonon interaction, 49

U

Ultrasonic phonons, 206
Ultrasonic velocity
  and relaxation processes, 216-26

Ultrasonic velocity
  measurement of, 211 *et seq.*
Ultrasonic wavelength, 206
Ultrasonic waves, 206
"Umklapp" processes, 50, 51, 207, 208, 221

V

Valence vibrations, 17, 29
Van der Waals forces, 11, 16, 59
Van Vleck theory, 150, 168, 173
Vibrational degrees of freedom, 9, 12
Vibrational energy, 10, 12
Vibrational frequency, 11 *et seq.*
Vibrational heat capacity, 10
Viscoelastic behaviour, 241 *et seq.*
Viscoelastic parameters, 241 *et seq.*
Viscoelastic relaxation, 200-5, 233
Volume expansion coefficient, 20. 83, 84, 85, 91, 209
Volume expansivity, 83

W

Wada hypothesis, 264, 265
Wave vector, 4, 47

Y

Young's modulus, 15, 183, 241 *et seq.*, 249
  and linear expansion coefficient, 265

Z

Zero-point energy, 84, 93
Ziman theory, 54, 55, 78

TO THE READER

Mir Publishers would be grateful for your comments on the content, translation and design of this book. We would also be pleased to receive any other suggestions you may wish to make.

Our address is:
Mir Publishers
2 Pervy Rizhsky Pereulok
I-110, GSP, Moscow, 129820
USSR

Printed in the Union of Soviet Socialist Republics